

# Exploring the Roles of CYCD3s and AINTÉGUMENTA in the Control of Plant Growth and Development

*Rico Randall*

School of Biosciences



Cardiff University

A thesis submitted in partial fulfilment of the degree of Doctor  
of Philosophy 2014

# Preface

## **DECLARATION**

This work has not been submitted in substance for any other degree or award at this or any other university or place of learning, nor is being submitted concurrently in candidature for any degree or other award.

Signed

Date 26<sup>th</sup> September 2014

## **STATEMENT 1**

This thesis is being submitted in partial fulfilment of the requirements for the degree of PhD.

Signed

Date 26<sup>th</sup> September 2014

## **STATEMENT 2**

This thesis is the result of my own independent work/investigation, except where otherwise stated. Other sources are acknowledged by explicit references. The views expressed are my own.

Signed

Date 26<sup>th</sup> September 2014

## **STATEMENT 3**

I hereby give consent for my thesis, if accepted, to be available online in the University's Open Access repository and for inter-library loan, and for the title and summary to be made available to outside organisations.

Signed

Date 26<sup>th</sup> September 2014

# Acknowledgements

I thank my primary supervisor Jim Murray for giving me the opportunity to work in his laboratory, and for assisting me throughout my project. As well as the advice and guidance for my research, I greatly appreciate the advice on making career choices and development. I thank Walter Dewitte, my second supervisor, for close project-related advice, and for a good sense of humour no matter what novel way to destroy an experiment I had discovered.

For experimental advice, I thank Celine Forzani, Simon Scofield, Jeroen Nieuwland and Angharad Jones. I hugely appreciate the technical assistance from Angela Marchbank and Jo Kilby. For help with bioinformatics I thank Alex Murrison. I cannot thank Patrick Hardinge for any technical help, but I appreciated his distractions in the forms of squash, snooker, camping and shooting very much. I thank Sonia Lopez de Quinto for taking the time to help me with Western Hybridisation experiments, even if they didn't make it into this thesis! I am grateful for fruitful discussions regarding my project with Wynand Van Der Goes Van Naters, my internal assessor. When I visited Yka Helariutta's lab in Helsinki, Mikko Herpola spent a lot of time teaching me techniques in histology, and told me where to go fishing. Also in Helsinki, Hanna Help taught me a lot in the lab and acted as my guardian angel during my time there. I am extremely grateful to Mikko and Hanna for making it such a pleasant trip. I also thank Yka for accommodating me and being very hospitable. I thank Vicky Buchanan Wollaston for hosting me in Warwick University, Claire Hill for arranging my visit and experiment and Peijun Zhang for showing me how to do it.

I thank my grandfather Ronald Wareham for teaching me the value of education and getting me this far. Finally, my most sincere gratitude goes to Emily Sornay, for putting up with my stress, helping me to make the right decisions and helping me with a lot of technical work in the lab.

# Exploring the roles of CYCD3s and AINTEGUMENTA in the Control of Plant Growth and Development

*Rico Randall*

## **Summary**

Regulation of higher plant growth and development involves the control of cell growth and division, since plant cells are immobile. A key point of plant cell cycle control is the G1 to S transition, which is promoted by CyclinD/CDK complexes. Several subgroups of D-type cyclins exist in higher plants, and the genes encoding these proteins appear to be under environmental and developmental regulation. In Arabidopsis, the *CYCD3* subgroup consists of three members. The roles that these genes play in growth and development are explored, and the interaction between these genes and other factors controlling plant growth and development are investigated.

A role for *CYCD3;1* and its putative regulator ANT in root auxiliary meristem development is shown. However, whilst *ant* and *cycd3;1* mutants shared some phenotypes, such as increased petal cell size, reduced leaf cell number and reduced root thickness, double mutants exhibited additive phenotypes, suggesting that there is not a strong regulation of *CYCD3;1* by ANT. Supporting this, a physical interaction between ANT and a putative ANT-binding site from the *CYCD3;1* promoter was not detected, and evidence of *CYCD3;1* transcription regulation by ANT was weak. Supporting an alternative hypothesis, evidence of coregulation of *ANT* and *CYCD3;1* by cytokinins in roots is provided. The expression of these genes in roots required cytokinins and appeared to be correlated.

Roles for all three *CYCD3*s and the *ERECTA* (*ER*) kinase in the regulation of primary vascular tissue development are described, and genetic evidence of a link between *CYCD3*s and *ER* is provided. These genes appear to be required for cell division events in the procambium lineage. Furthermore, *ER* was also found to regulate secondary growth. Thus five novel regulators of root development have been identified, and important knowledge regarding mechanisms of lateral aerial organ size control has been gained.

# Table of Contents

<b>Preface .....</b>	<b>ii</b>
<b>Abbreviations .....</b>	<b>x</b>
<b>Chapter One: Introduction .....</b>	<b>1</b>
<b>1.1 Plant Growth and Development .....</b>	<b>1</b>
1.1.1 The Embryo .....	1
1.1.2 Growth of the Root .....	4
1.1.3 Growth of the Shoot .....	6
<b>1.4 Regulation of the Plant Cell Cycle .....</b>	<b>8</b>
1.4.1 Mechanisms for Cell Cycle Control in Eukaryotes .....	9
1.4.2 The Cell Cycle in Plants .....	10
1.4.3 Plant Cyclins.....	13
<b>1.5 Control of Lateral Aerial Organ Size.....</b>	<b>16</b>
1.5.1 Leaf Development .....	16
1.5.2 Cell Division and Expansion in Leaf Growth .....	16
1.5.3 Control of Lateral Aerial Organ Growth Initiation and Growth by Auxins.....	19
1.5.4 Roles of Cytokinins, Giberellic Acid, Ethylene <i>and</i> Brassinosteroids in Lateral Aerial Organ Growth Control .....	20
1.5.5 Altered Cell Number and Endoreduplication in <i>shr</i> Leaves.....	22
1.5.6 Summary of Lateral Aerial Organ Growth Control.....	22
<b>1.6 Plant Vascular Tissue Development.....</b>	<b>22</b>
1.6.1 Primary Vascular Tissue Development .....	23
1.6.2 Secondary Vascular Tissue Development .....	23
<b>1.7 Regulation of Plant Vascular Tissue Development.....</b>	<b>26</b>
1.7.1 Interaction Between Auxin and Cytokinin Signalling During Plant Vascular Tissue Development.....	26
1.7.2 Auxin Phytohormones Control Vascular Cell Divisions and Differentiation .....	27
1.7.3 Regulation of Vascular Cell Divisions in Primary Growth by Cytokinins .....	29
1.7.4 Cytokinins Regulate Secondary Growth.....	29

1.7.5 Other Phytohormones Regulating Vascular Tissue Development ....	30
1.7.6 SHR and SCR regulate Radial Patterning in Roots .....	31
1.7.7 AHL Proteins Control the Boundary Between Xylem and Procambium Tissue in Young Roots .....	31
1.7.8 Similarities and Differences Between the WUS/CLV Signalling Mechanism in Shoot Meristem Development and the WOX4/TDIF Mechanisms Controlling Root Auxiliary Meristem Development.....	31
<b>1.8 The AINTEGUMENTA Transcription Factor .....</b>	<b>33</b>
1.8.1 The AP2/ERF Transcription Factor Family.....	33
1.8.2 Isolation and Early Investigations of the Functions of the <i>AINTEGUMENTA (ANT)</i> Gene .....	34
1.8.3 Transactivation Activity and DNA-binding Properties of <i>AINTEGUMENTA</i> .....	36
1.8.4 <i>AINTEGUMENTA</i> Controls Organ Growth via Regulation of Cell Division Activity.....	38
1.8.5 Functions of <i>AINTEGUMENTA</i> that Depend on other Proteins .....	38
1.8.6 The link between <i>ANT</i> and <i>CYCD3;1</i> .....	39
<b>1.9 Aims and objectives.....</b>	<b>40</b>
<b>Chapter Two: Materials and Methods .....</b>	<b>41</b>
<b>2.1 Plant Growth Conditions .....</b>	<b>41</b>
2.1.1. Plants in Soil.....	41
2.1.2. Seed Sterilization .....	41
2.1.3. <i>In vitro</i> Growth .....	41
2.1.4. Crossing Plants .....	42
<b>2.2 General DNA Techniques .....</b>	<b>42</b>
2.2.1 Arabidopsis Genomic DNA Isolation .....	42
2.2.2 Plasmid DNA Isolation.....	43
2.2.3 Isolation of DNA from Agarose Gels and PCR Reactions.....	43
2.2.4 Agarose Gel Electrophoresis.....	44
2.2.5 Determination of Nucleic Acid Concentration.....	44
2.2.6 Polymerase Chain Reaction (PCR).....	45
2.2.7 Digestion of DNA with Restriction Endonuclease Enzymes .....	51
2.2.8 Dephosphorylation of 5' Ends .....	51
2.2.9 Blunting Reaction .....	51
2.2.10 Ligation .....	51
2.2.11 TOPO®-TA Cloning (Invitrogen, USA).....	52

2.2.12 TOPO®-Blunt Cloning .....	52
2.2.13 BP and LR Reactions for Gateway Cloning .....	52
2.2.14 DNA Sequence Analysis .....	53
<b>2.3 General <i>Escherichia coli</i> Techniques.....</b>	<b>54</b>
2.3.1 <i>E. coli</i> Strains and Growth Conditions .....	54
2.3.2 <i>E. coli</i> Transformation .....	54
2.3.3 Transformant Selection .....	54
<b>2.5 Generation of Transgenic Arabidopsis Plants .....</b>	<b>55</b>
2.5.1 Agrobacterium Transformation .....	55
2.5.2 Transformation of Arabidopsis Plants .....	56
2.5.3 Recovery of Transgenic Plants .....	56
<b>2.6. Genotyping .....</b>	<b>56</b>
<b>2.7. Histological and Microscopical Analyses .....</b>	<b>57</b>
2.7.1 Preparation of Petals and Leaves .....	58
2.7.2 X-gluc Assay for $\beta$ -glucuronidase .....	58
2.7.3 Preparation of Root Sections .....	58
2.7.4 <i>In situ</i> hybridisation.....	59
2.7.5 Quantification of Cell File Number within the Primary Vasculature ...	60
<b>2.8. Flow Cytometry .....</b>	<b>61</b>
<b>2.9. RT-qPCR Analyses .....</b>	<b>61</b>
2.9.1. RNA Isolation .....	61
2.9.2 cDNA Synthesis .....	62
2.9.3. Quantitative PCR (qPCR).....	63
2.9.4. qPCR Data Analysis.....	64
<b>2.10. Yeast-one-hybrid (Y1H) Assays .....</b>	<b>64</b>
2.10.1 Yeast media .....	64
2.10.2. Yeast transformation .....	65
2.10.3. One-on-one Y1H .....	65
2.10.4. Y1H Screen .....	67
<b>2.11. Statistics .....</b>	<b>68</b>
<b>2.12. Bioinformatics .....</b>	<b>69</b>
<b>Chapter Three: Control of Lateral Aerial Organ Size by</b>	
<b>AINTEGUMENTA and CYCD3;1 .....</b>	<b>70</b>
Introduction .....	70
Aims & Objectives.....	74
<b>3. Results .....</b>	<b>75</b>

3.1. Generating the <i>ant-9 cycd3;1</i> double mutant .....	75
3.2. Relationship Between Cell Size and Petal Growth in <i>ant-9</i> , <i>cycd3;1</i> and <i>ant-9 cycd3;1</i> Mutants .....	78
3.3 Increased Petal Size is Correlated with Increased Cell Size within the <i>ant-9 cycd3;1</i> Mutant Population .....	81
3.4 Characterization of the <i>ant-GK</i> mutant .....	82
3.5 Comparison of Ler <i>ant</i> and <i>cycd3;1</i> Petal Phenotypes and <i>Col-0 ant</i> and <i>cycd3;1</i> Petal Phenotypes .....	84
3.6 Ploidy Levels in Cells of <i>ant</i> and <i>cycd3;1</i> Mutants .....	87
3.7 Leaf Size and Cell Number in <i>ant-9</i> and <i>cycd3;1</i> Mutants .....	89
3.8 CYCD3;1 Promoter Activity is Downregulated in <i>ant</i> Mutants but Transcript Levels are Not .....	93
3.9 Characterization of a Transgenic Line Expressing an ANT-GR Fusion Protein Under the 35S Promoter .....	97
<b>Discussion .....</b>	<b>106</b>
 <b>Chapter Four: CYCD3;1, AINTEGUMENTA and ER regulate root secondary growth .....</b>	
<b>Introduction .....</b>	<b>111</b>
<b>Aims &amp; Objectives .....</b>	<b>115</b>
<b>Results .....</b>	<b>116</b>
4.1 Secondary growth is reduced in the <i>cycd3;1</i> mutant.....	116
4.2 Expression Pattern of <i>CYCD3;1</i> in Roots During Secondary Growth	119
4.3 The Response of Secondary Growth to Cytokinins is Altered in <i>cycd3;1</i> Mutants.....	121
4.4 Correlation of <i>ANT</i> and <i>CYCD3;1</i> expression .....	123
4.5 <i>ANT</i> Regulates Secondary Growth .....	125
4.6 Expression of <i>CYCD3;1</i> in <i>ant</i> mutants.....	129
4.7 Genetic Interaction Between <i>ANT</i> and <i>CYCD3;1</i> .....	133
4.8 Regulation of <i>CYCD3;1</i> and <i>ANT</i> by Cytokinins .....	135
4.9 <i>ANT</i> is Required for Induction of the <i>pCYCD3;1:GUS</i> Reporter by Cytokinins .....	136
4.10 Other Potential Regulators of <i>CYCD3;1</i> Expression .....	139
4.11 The <i>ERECTA</i> gene is required for proper secondary growth.....	144
<b>Discussion .....</b>	<b>146</b>
 <b>Chapter Five: CYCD3s and ER Regulate Primary Development of the Vascular Tissue.....</b>	
	<b>156</b>

<b>Introduction .....</b>	<b>156</b>
<b>Aims &amp; Objectives .....</b>	<b>158</b>
<b>Results .....</b>	<b>159</b>
5.1 Roots Lacking Functional <i>CYCD3</i> Genes Have a Reduced Number of Cell Files within the Primary Stele .....	159
5.2 <i>Ler</i> Roots have a Reduced Number of Vascular Cell Files, and this Reduction is not Enhanced by Loss of <i>CYCD3</i> Genes .....	162
5.3 <i>ER</i> is Required for the Correct Number of Vascular Cell Files in the Root Meristem .....	163
5.4 <i>CYCD3</i> Expression is Unchanged in the <i>er-105</i> mutant .....	166
<b>Discussion .....</b>	<b>168</b>
<b>Chapter 6: Final Discussion.....</b>	<b>174</b>
6.1 Novel Roles for <i>CYCD3;1</i> in Arabidopsis Development & Cytokinin Signalling .....	174
6.2 Weakening the Link Between <i>AINTEGUMENTA</i> and <i>CYCD3;1</i> .....	175
6.3 Novel Roles for <i>ERECTA</i> in Root Radial Cell Divisions .....	177
6.4 Concluding Remarks and Future Directions .....	178
<b>Appendix.....</b>	<b>179</b>
<b>References.....</b>	<b>180</b>

# Abbreviations

<b><i>A. thaliana</i></b>	<i>Arabidopsis thaliana</i>
<b><i>A. tumefaciens</i></b>	<i>Agrobacterium tumefaciens</i>
<b>ABS</b>	ANT-binding sequence
<b>ACT</b>	<i>ACTIN</i>
<b>AD</b>	Activation domain
<b>AG</b>	Agamous
<b>AGL</b>	AG-like
<b>AHK</b>	Arabidopsis histidine kinase
<b>AHL</b>	AT-hook motif nuclear localized protein
<b>AHP</b>	Arabidopsis histidine phosphotransfer protein
<b>AIL</b>	Aintegumenta-like
<b>ANOVA</b>	Analysis of variance
<b>ANT</b>	Aintegumenta
<b>AP2</b>	Apetala 2
<b>APC</b>	Anaphase-promoting complex
<b>ARE</b>	Auxin response element
<b>ARF</b>	Auxin response factor
<b>ARGOS</b>	<i>Auxin-regulated gene controlling organ size</i>
<b>ARL</b>	Argos-like
<b>ARR</b>	Arabidopsis response regulator
<b>At</b>	<i>Arabidopsis thaliana</i>
<b>BA</b>	Brassinosteroid
<b>BD</b>	Binding domain
<b>Bp</b>	<i>Abies procera</i>
<b>CCD</b>	Charge-coupled device
<b>CDC25</b>	Cell division cycle 25
<b>CDK</b>	Cyclin-dependent kinase
<b>cDNA</b>	Copy DNA
<b>CEI</b>	Cortex-endodermis initial

<b>ChIP</b>	Chromatin immunoprecipitation
<b>CKX</b>	Cytokinin oxidase
<b>CLV</b>	CLAVATA
<b>cM</b>	Centimorgan
<b><i>Col-0</i></b>	<i>Columbia 0</i>
<b>CRE</b>	Cytokinin response
<b>CRN</b>	CORYNE
<b>CYCA</b>	Cyclin A
<b>CYCD</b>	Cyclin D
<b>CYP735A</b>	Cytochrome P450 monooxygenase
<b>d.f.</b>	Degrees of freedom
<b>DAG</b>	Days after germination
<b>DEL</b>	DP/E2F-like
<b>df</b>	Degrees of freedom
<b>DNA</b>	Deoxyribonucleic acid
<b>dNTP</b>	Deoxynucleotide triphosphate
<b>DP</b>	Dimerization partner
<b><i>E. coli</i></b>	<i>Escherichia coli</i>
<b>E2F</b>	E2 transcription factor
<b>ER</b>	Erecta
<b>ERF</b>	Ethylene response factor
<b>FIL</b>	Filamentous flower
<b>G1/G2</b>	Gap1/Gap2
<b>GA</b>	Giberellic acid
<b>GFP</b>	Green fluorescent protein
<b>GM</b>	Growth medium
<b>GR</b>	Glucocorticoid receptor
<b>GUS</b>	$\beta$ -glucuronidase
<b>H4</b>	Histone 4
<b>HDG</b>	Homeodomain group
<b>HMG</b>	High mobility group
<b>IAA</b>	Indole-3-acetic acid
<b>IPT</b>	Adenosine phosphate-isopentenyl transferase

<b>IPTG</b>	Isopropyl $\beta$ -D-1-thiogalactopyranoside
<b>KRP</b>	Kip-related protein
<b>LAO</b>	Lateral aerial organ
<b>LB</b>	Luria-Bertani
<i>Ler</i>	<i>Landsberg erecta</i>
<b>MP</b>	Monopteros
<b>mRNA</b>	Messenger RNA
<b>ORF</b>	Open reading frame
<b>PBS</b>	Phosphate-buffered saline
<b>PCR</b>	Polymerase chain reaction
<b>PIN</b>	Pin-formed
<i>pkc</i>	<i>protein kinase C</i>
<b>PLT</b>	Plethora
<i>pxy</i>	<i>phloem intercalated with xylem</i>
<b>QC</b>	Quiescent centre
<b>RAM</b>	Root apical meristem
<i>RAV</i>	<i>Related to ABI3/VP1</i>
<b>RB</b>	Retinoblastoma
<b>RBR</b>	Retinoblastoma-related
<b>RLK</b>	Receptor-like kinase
<b>RNA</b>	Ribonucleic acid
<b>rpm</b>	Revolutions per minute
<b>RT-qPCR</b>	Reverse transcription quantitative PCR
<b>S</b>	Synthesis phase
<i>S. cerevisiae</i>	<i>Saccharomyces cerevisiae</i>
<b>SAM</b>	Shoot apical meristem
	SKP, Cullin, F-box containing complex/Transport
<b>SCF<sup>TIR1</sup></b>	inhibitor response 1
<b>SCL</b>	Scarecrow-like
<b>SCR</b>	Scarecrow
<b>SD</b>	Synthetic defined
<b>SEM</b>	Standard error of the mean
<b>SHR</b>	Short root

<b>SSC</b>	Saline sodium citrate
<b>T-DNA</b>	Transfer DNA
<b>TAIR</b>	The Arabidopsis information resource
<b>TCP</b>	<i>Teosinte branched1, Cycloidea, and PCF</i>
<b>TDIF</b>	Tracheary element differentiation inhibiting factor
<b>TDR</b>	TDIF receptor
<b>TF</b>	Transcription factor
<b>TOR</b>	Target of rapamycin
<b>tZ</b>	Trans-zeatin
<b>uORF</b>	Upstream ORF
<b>UTR</b>	Untranslated region
<b>UV</b>	Ultra violet
<b>wol</b>	<i>wooden leg</i>
<b>WOX</b>	Wuschel-related homeobox
<b>WT</b>	Wild-type
<b>WUS</b>	WUSCHEL
<b>Y1H</b>	Yeast-one-hybrid
<b>YAB</b>	Yabby
<b>YFP</b>	Yellow fluorescent protein
<b>YPD</b>	Yeast extract peptone dextrose
<b>ZHD</b>	Zinc finger homeodomain

# Chapter One: Introduction

## **1.1 Plant Growth and Development**

---

This study investigates novel roles of a developmental transcription factor and a core cell cycle regulator in the regulation of plant growth and development. Further to this, a hypothesized interaction between these two factors is tested. In this introduction, an overview of plant growth and development will be given, before a more detailed description of the developmental processes investigated in this study. Radial growth of the root vascular tissue, petal growth and leaf growth are the developmental processes investigated in this study. This section will begin with embryogenesis, since the primary radial pattern of the vascular tissue is established during embryogenesis. Shoot and root growth will then be discussed. Both maintenance of the primary pattern of the vascular tissue and secondary vascular tissue development occur during root growth. Shoot growth involves the growth of lateral aerial organs such as leaves and petals.

### 1.1.1 The Embryo

Due to the absence of an ability of plants cells to migrate around the organism, plant growth and development is determined by cell division and its orientation, and cell growth and its polarity. Arabidopsis is the most commonly used model organism for studying higher plant development, due to its relatively small diploid genome, simple growth conditions and rapid life cycle (Koornneef and Meinke, 2010). It is also highly amenable to genetic manipulation.

As in other higher plants, the beginning of a new generation of an Arabidopsis plant results from the fertilization of an egg cell: the female gamete, by the sperm nucleus: the male gamete. The resulting diploid cell, the zygote, divides to derive a terminal cell and a basal cell (see Figure 1.1 for overview). The terminal cell divides to derive the embryo proper, and subsequent cell divisions determine the architecture of the embryo. In eudicots such as Arabidopsis, two cotyledon primordia are formed in the apical region of the embryo, before these grow and form the full-sized cotyledons. In the basal region of the embryo, a procambium that will later derive the vascular tissue is

formed. The formation of these different tissues in the correct parts of the embryo is highly dependent on the phytohormone auxin, and polar transport of this hormone in embryos is essential for correct development (Liu *et al.*, 1993; Friml *et al.*, 2003). The establishment of shoot and root apical meristems (SAM/RAM) occurs during embryogenesis. These meristems will provide the majority of cells for further plant growth and development, including those comprising tissues not present in the embryo.

In eudicots, the fully-developed embryo contains two cotyledons. A radical will form both the hypocotyl and the root (Leyser and Day, 2007). Seed maturation involves a decrease in metabolic activity and water content (Taiz and Zeiger, 2006). Seed dispersal and germination mechanisms differ from plant to plant, but in general imbibition, i.e. the uptake of water, and reactivation of metabolism occur with favourable environmental conditions. Once this occurs, germination occurs via the penetration of the radical through first the endodermis and then the testa (seed coat). The mechanisms driving radical emergence are still being investigated, although cell expansion and cell divisions in the RAM both seem to play roles (Chen and Bradford, 2000; Masubelele *et al.*, 2005b; Da Silva *et al.*, 2008).

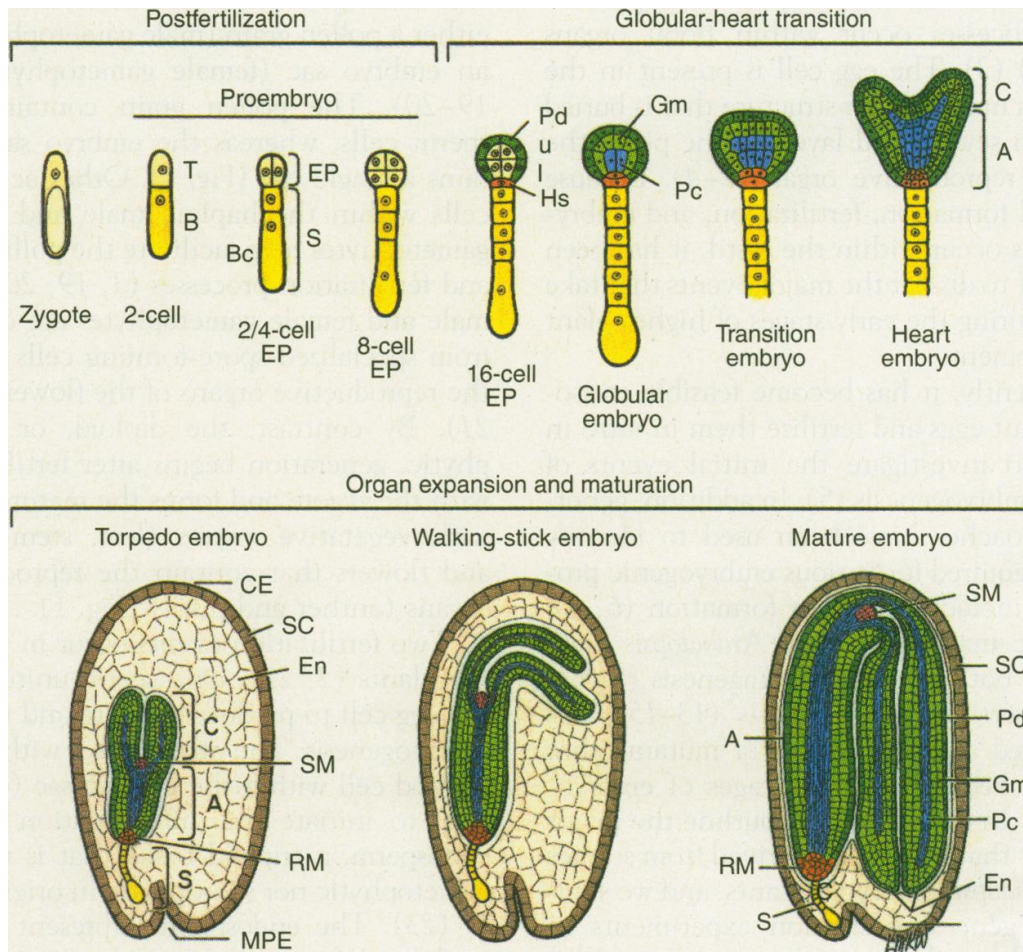


Figure 1.1: Overview of plant embryogenesis. From fertilization to the heart-stage embryo, the developing embryo alone is shown. From the torpedo stage onwards, the developing embryo is shown as part of the seed. The protoderm exists from the 16-cell stage onwards. In the globular embryo, the ground meristem and procambium have also been formed. By the heart stage, the cotyledons and embryo axis can be distinguished. At the torpedo stage, the shoot and root apical meristems can be identified. Embryo growth and maturation occur after this. T: terminal cell; B: basal cell; EP: embryo proper; S: suspensor; Bc: suspensor basal cell; Pd: protoderm; u: upper tier; l: lower tier; Hs: hypophysis; Pc: procambium; Gm: ground meristem; C: cotyledon; A: axis; MPE: micropylar end; CE: chalazal end; SC: seed coat; En: endosperm; SM: shoot meristem; RM: root meristem. From Goldberg *et al.* (1994).

### 1.1.2 Growth of the Root

Post-embryonically, *Arabidopsis* roots grow by cell division in the amplifying region of the RAM, and by cell expansion further away in the zone of cell expansion (Leyser and Day, 2007). Following cell expansion, cells mature, becoming specialized for their individual functions (see Figure 1.2 for overview). For example, some root epidermal cells develop into root hair cells that protrude from the root and absorb water and nutrients from the soil (Carol and Dolan, 2002). In seedlings, growth in roots serves to elongate the root. Thus most cell divisions are transversal: that is the newly built cell wall is perpendicular to the direction of root growth. However periclinal divisions, which are defined by the generation of a new cell wall parallel to the direction of root growth, do occur close to the quiescent centre (QC). For example, lateral root cap / epidermal initial cells undergo formal cell divisions, that is divisions that produce cells with distinct identities, to derive the respectful cells (van den Berg *et al.*, 1995).

As the roots grow older, periclinal cell divisions in the older parts of the root occur. Pericycle cells within the stele are primed by high auxin levels to divide periclinally after an initial asymmetric division (Dubrovsky *et al.*, 2008). Following this division event, these cells continue to divide, push their way through the outer cell layers of the root and eventually undergo cell divisions that produce a new root meristem that provides the cells for the growth of a lateral root (Figure 1.2B) (Malamy and Benfey, 1997).

In some plant species, such as *Arabidopsis*, the procambium cells within the stele also undergo periclinal cell divisions, which results in the formation of the cambium tissue (Zhang *et al.*, 2011a). This marks the beginning of secondary growth in roots, and continued proliferation of cambial cells results in thickening of the roots (Figure 1.2C). Secondary xylem and phloem develop from the cambium. Secondary xylem normally become highly lignified and are interesting from an economic perspective as this tissue is energy-rich (Novaes *et al.*, 2010).

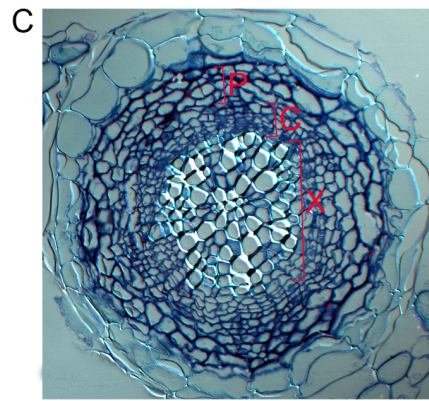
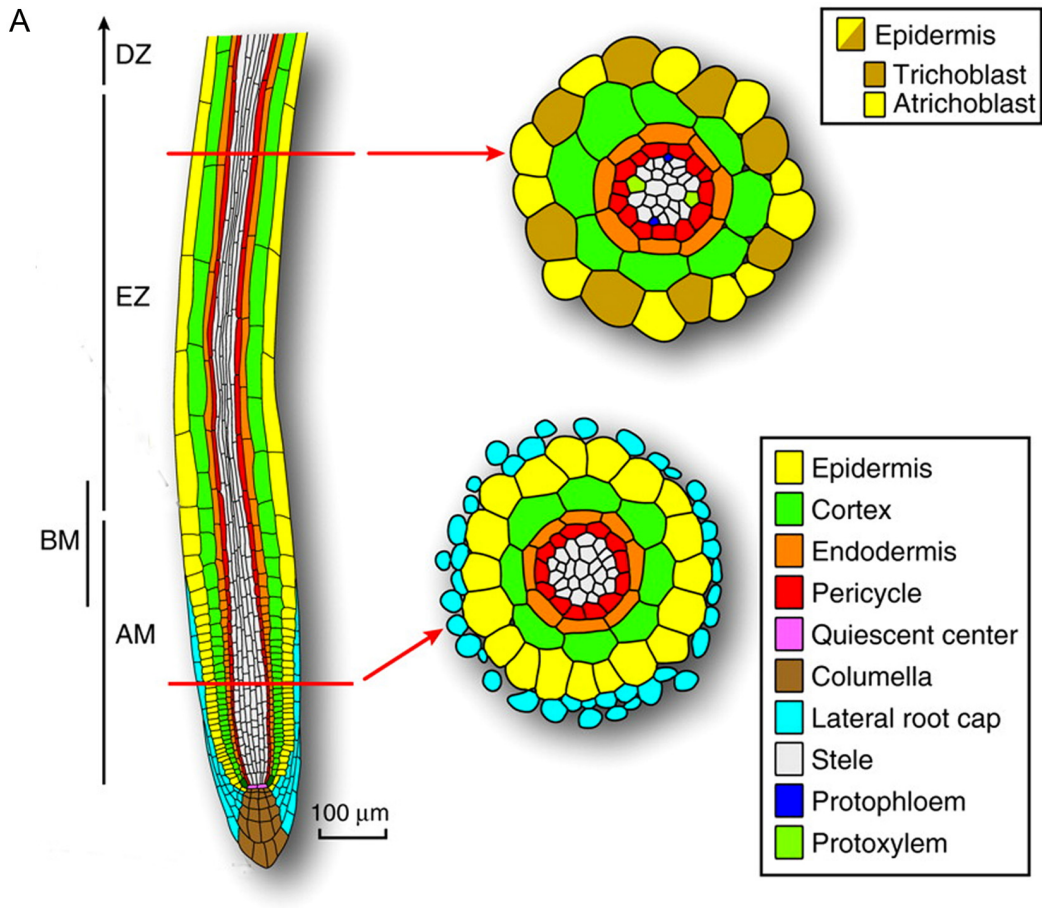


Figure 1.2: Arabidopsis root development. A) The Arabidopsis primary root. On the left is shown a longitudinal section showing the different cell files that exist in the root during primary growth. Cell division occurs in the apical meristem (AM), cell division slows down whilst cell elongation begins to occur in the basal meristem (BM), whilst cell elongation alone occurs in the elongation zone (EZ). The lower cross-section on the right shows the radial organization of the Arabidopsis cell files in the apical meristem. The upper cross-section shows the radial organization of the cell files in the elongation zone. At this stage, differentiation of cells can be observed, such as that of the protoxylem (green) and protophloem (blue). The positions of these cells give rise to the diarch symmetry seen in a mature root. Also shown are the alternative identities of root epidermal cells, either as trichoblasts that form root hairs, or atrichoblasts that do not. Adapted from Overvoorde *et al.* (2010). B) Picture of a lateral root emerging taken using light microscopy. The vasculature tissue is marked in blue using the activity of the *AINTEGUMENTA* promoter. C) Cross section of an Arabidopsis root showing secondary growth. The outer layers (epidermis, cortex and sometimes endodermis) are lost during secondary growth. The remaining tissues can be seen. Marked are the xylem cells (X), the cambium cells (C) and the pericycle cells (P).

### 1.1.3 Growth of the Shoot

Following germination, cell division in the SAM drives shoot growth, followed by cell expansion, as in roots (Leyser and Day, 2007). Some growth of the hypocotyl, the stem-like structure “underneath” the cotyledons, occurs, and this seems to be driven mainly by cell elongation (Gendreau *et al.*, 1997).

As the shoot grows, cells at the periphery of the SAM become primed by high auxin levels to undergo cell divisions that derive leaf primordia (Reinhardt *et al.*, 2000b; Reinhardt *et al.*, 2003). In *Arabidopsis*, these primordia are arranged in such a manner that an angle of  $137.5^\circ$  exists between each primordium and the next (Palauqui and Laufs, 2011). This category of phyllotaxis is that of spiral growth. Other patterns of phyllotaxis exist in other species. Polar transport and localized synthesis of auxin are required for correct phyllotaxis (Pinon *et al.*, 2013b; van Berkel *et al.*, 2013). Leaf growth then occurs, and is driven initially by cell division and later by cell elongation (Beemster *et al.*, 2006). The parts of the stem from which lateral aerial organs (LAOs) including leaves protrude are termed nodes, whilst parts of the stem between LAOs are termed internodes. This period of plant shoot growth makes up the vegetative growth phase.

At some point in a higher plant growth cycle, the transition from the vegetative phase to the reproductive phase is made (Figure 1.3). In *Arabidopsis*, this is seen as a rapid growth of the stem, often termed “bolting” (Bradley *et al.*, 1997). Instead of vegetative leaves, organ primordia now form new lateral stems, which have their own inflorescence meristems at the tips, so called since flowers originate from these (Leyser and Day, 2007). In most higher plant species, the formation of a new inflorescence meristem coincides with the development of a leaf immediately basipetally. Auxiliary shoots can also arise from buds developing in leaf axils, for example in the mature rosette of an *Arabidopsis* plant (Leyser and Day, 2007).

From inflorescence meristems, new primordia develop, and these form floral meristems. In *Arabidopsis*, cell proliferation within these floral meristems drives growth of a stem-like structure termed the petiole, which connects the newly developing flower to the plant (petioles also attach leaves to the plant) (Taiz and Zeiger, 2006). From floral meristems develop floral organs, which make up the four whorls of flowers (Coen and Meyerowitz, 1991). At the outside of the flower is normally found the sepal whorl, inside of that is found the petal

whorl, inside of that the stamen whorl and inside of that the carpel whorl. Whilst the four whorls are normally present, the numbers of organs within these whorls, as well as their morphology, vary greatly (Irish and Litt, 2005). Within the carpel and stamens gametogenesis occurs, producing the egg cells and sperm cells respectively.

Secondary growth also occurs in shoots and hypocotyls, and is essential for wood development in trees (Raven *et al.*, 2005). Once again, procambium cells are precursors to cambial cells. In shoots and hypocotyls, vascular tissue is often arranged in bundles surrounding the central pith (see Figure 1.4 for overview). Cambium cells within these bundles form the fascicular cambium. However, in aerial parts, parenchyma cells, which exist between the vascular bundles, are also precursors to cambium cells (Baucher *et al.*, 2007). These cambium cells form the interfascicular cambium. Once secondary growth has been underway for some time, the fascicular and interfascicular cambium merge. In woody plants, a peridermis usually forms on the outside of the shoot, forming the bark (Raven *et al.*, 2005).

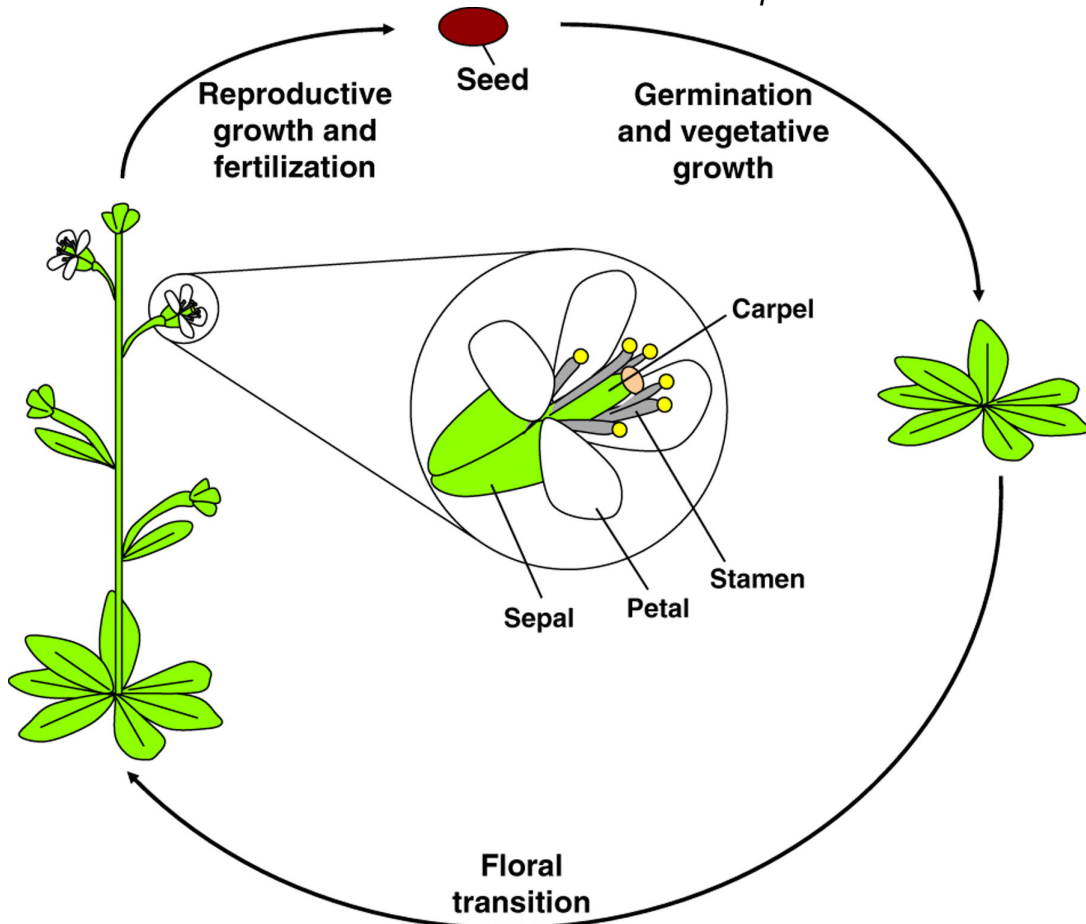


Figure 1.3: Overview of the Arabidopsis life cycle. Following germination, the young seedling grows and new leaves emerge and develop in the rosette. At some point, the floral transition is made, and the plant “bolts”, growing a new stem with an inflorescence meristem. From this emerge auxiliary stems and floral meristems, which give rise to the growth and development of flowers. The flower is composed of four whorls of organs consisting of:- the sepals, the petals, the stamen and the carpel. Self-fertilization in the ovule gives rise to the next generation of an Arabidopsis plant. From Liu *et al.* (2009).

#### 1.4 Regulation of the Plant Cell Cycle

---

The cell cycle is essential for plant growth and development. The number of cells, as well as the sizes of those cells, define the size of the organ. Since plant cells are immobile, cell division in specified orientations also influences tissue patterning and organ shape.

### 1.4.1 Mechanisms for Cell Cycle Control in Eukaryotes

The eukaryotic mitotic cell cycle consists of four phases that progress in the following order:- G1, a gap phase in which cells can remain (aka G0) in the absence of mitotic stimuli; S phase, during which cells replicate their DNA; G2, another gap phase, when cells grow; Mitosis, during which chromosomes are segregated, new nuclear envelopes are created, and cells divide in two. During the G1 phase, cells make the decision of whether or not to enter the cell cycle; if they do not, they enter the quiescent so-called G0 phase (Harashima *et al.*, 2013).

At the heart of eukaryotic cell cycle regulation are cyclin/Cyclin-dependent kinase (cyclin/CDK) complexes, CDKs being the catalytic partners (Murray, 2004). These cyclin/CDK complexes phosphorylate target proteins in order to promote cell cycle progression. For example, budding yeast G1 cyclin/CDK complexes phosphorylate Sic1, thus marking it for destruction (Schneider *et al.*, 1996). When active, Sic1 inhibits the expression of S-phase and mitotic cyclin-encoding genes (Tyers, 1996). In higher eukaryotes, cyclin/CDK complexes phosphorylate Retinoblastoma (RB) protein (Adams *et al.*, 1999), which plays a similar role to that of aforementioned yeast Sic1. Specifically, RB inhibits the activity of E2F transcription factors that when active induce the expression of genes required for S phase progression (Weintraub *et al.*, 1992).

In fission yeast, a single cyclin promotes both DNA replication and mitosis (Fisher and Nurse, 1996), leading to the suggestion that different levels of CDK activity promote the different transitions in the cell cycle (Stern and Nurse, 1996). During evolution, the numbers of cyclins and CDKs in a species' genome have generally increased (Murray, 2004). In higher eukaryotes, generally speaking, the G1 to S transition is controlled by cyclin Ds, S phase progression by E- and A-type cyclins, and mitosis by cyclin Bs (Strausfeld *et al.*, 1996; Murray, 2004). It has been suggested that the diversity of cyclins in complex organisms reflects the requirement for different levels of regulation of cell cycle activity in these organisms, as opposed to different cyclin/CDK complexes targeting different proteins (Murray, 2004). This is supported by the observation that mice expressing only a single D-type cyclin develop abnormally because the *CYCLIN* gene is not expressed in all tissues; thus

developmental regulation of cell cycle activity that appears to be aberrant in this mutant (Ciemerych *et al.*, 2002).

#### 1.4.2 The Cell Cycle in Plants

Plants are sessile organisms, and therefore have to respond to environmental stimuli and/or stresses physiologically, as they cannot move away from them. Another distinguishing attribute of plants is that the majority of their development occurs post-embryonically; plants grow new organs throughout their life cycle. Furthermore, plants can generate whole organisms from single differentiated cells, demonstrating a high level of totipotency (De Veylder *et al.*, 2007). It might therefore be expected that plants have developed unique aspects to their cell cycle control, as growth must be coordinated with these environmental stimuli and developmental programs. The effects of environmental stimuli on cell cycle activity have been shown in various ways (De Veylder *et al.*, 2007). For example, water stress reduces CDK activity and consequently cell cycle activity in wheat (Schuppler *et al.*, 1998). The very cell biology of higher plants is somewhat distinguished from that of lower eukaryotes and metazoans. Plant cells cannot move, they have rigid cell walls, the cells are connected in many cases, and plant cells often undergo endoreduplication: successive rounds of DNA replication in the absence of cell division.

With the above in mind, it is not surprising that higher plants have evolved a great number of unique factors regulating their cell cycle. For an overview of plant cell cycle regulation, see Figure 1.4. The plant homologue of Cdk1 is CDKA. CDKA/CyclinD complexes, plant cyclinDs being the plant homologues of animal CyclinDs, primarily control the G1 to S transition in plants (Zhao *et al.*, 2012). One of the major molecular mechanisms employed by CDKA/cyclinD to do this is proposed to be the phosphorylation of RBR (RB-related), the plant functional homologue of metazoan RB. Like in metazoans, plant RBR associates with and inhibits the activity of E2F/DP transcription factor complexes, which would otherwise induce the expression of S phase genes (Shen, 2002). Phosphorylation of RBR by CDKA/cyclinD is proposed to lead to the dissociation of the former from E2F/DP (Rossi and Varotto, 2002). The catastrophic consequences of loss of CDKA in plants have recently been demonstrated (Nowack *et al.*, 2012). These include failure to enter S phase and a loss of stem cells. Interestingly, RBR also appears to specifically regulate

asymmetric cell divisions in plants, via its association with SCR and SHR (Cruz-Ramirez *et al.*, 2012).

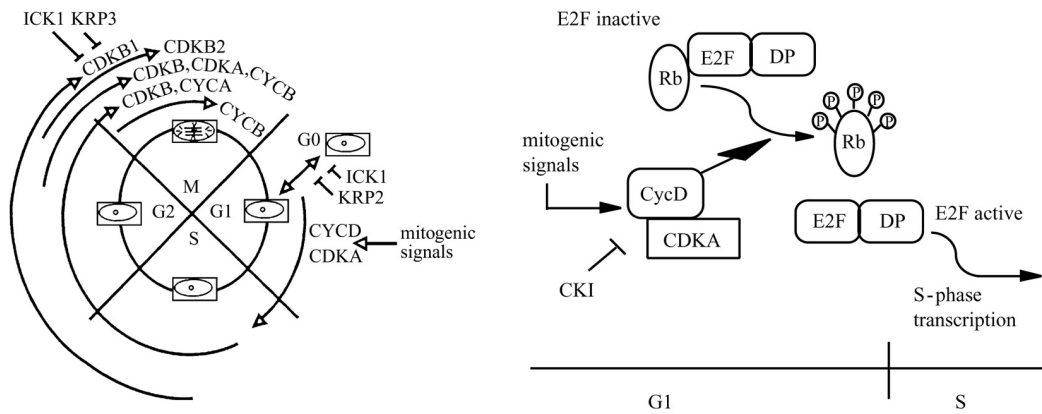


Figure 1.4: Overview of molecular regulation of the plant cell cycle. The mitotic plant cell cycle consists of four phase:- the G1 phase, which is named the G0 phase when internal and external signals do not give the go ahead for cell cycle progression; the S phase, during which DNA replication occurs; the G2 phase, during which cell growth occurs; M phase, mitosis, during which sister chromatids are separated and segregated and finally cell division occurs. Cyclin-D/CDKA complexes promote the G1 to S transition. They are activated by mitogenic signals but are inhibited by CKI and ICK/KRP proteins. S phase and G2 progression are promoted by both CDKA and the plant-specific CDKB proteins, in complexes with CyclinAs and CyclinBs. ICK/KRP proteins also inhibit the activity of these complexes. When not bound by RBR, typical E2F/DP transcription factor complexes promote the expression of genes required for S phase progression. Unphosphorylated RBR binds to these complexes to inhibit their activity. Phosphorylation of RBR by CyclinD/CDKA complexes causes RBR to dissociate from E2F/DP. Adapted from Oakenfull *et al.* (2002) .

CDKBs appear to be plant-specific, and are generally implicated in the regulation of mitosis (Endo *et al.*, 2012). However, specific developmental roles for CDKBs have been implicated from some experiments, such as the regulation of asymmetric cell divisions in stomata precursor cells (De Veylder *et al.*, 2007). Plants also appear to possess a unique group of atypical E2Fs: DELs (DP/E2F-like), which lack a transactivation domain, do not appear to bind RBR and harbour an extra DNA binding domain allowing them to bind to DNA without DP (Mariconti *et al.*, 2002). These E2Fs are proposed to repress gene expression.

In contrast to metazoans, within plants CDKA expression appears to be uniform throughout the cell cycle (Fobert *et al.*, 1996); how then is regulation of the G1 to S transition in plants fine-tuned to coordinate cell cycle activity with development and environmental changes? In metazoans, post-translational modification of CDKA by the inhibitory Wee1 kinase and the activating Cdc25 phosphatase offer an extra level of regulation (McGowan and Russell, 1993; Nilsson and Hoffmann, 2000). However, the roles of these kinases in plants remain unclear, as plant CDC25 appears to function as an arsenate reductase (Bleeker *et al.*, 2006), and the WEE1 kinase appears to be involved in the DNA damage checkpoint response, as opposed to normal cell cycle progression (Sorrell *et al.*, 2002; De Schutter *et al.*, 2007).

### 1.4.3 Plant Cyclins

Plants have evolved a great number of cyclins in comparison to the other kingdoms (Menges *et al.*, 2007), and these appear to be subjected to differential regulation during the cell cycle (Menges *et al.*, 2005) and development (Beemster *et al.*, 2005; Dudits *et al.*, 2011). In particular, higher plants have a large number of D-type cyclins (Figure 1.5), which can be split into six subgroups conserved in most species analysed (Menges *et al.*, 2007). Arabidopsis, for example, has ten D-type cyclins (Menges *et al.*, 2007). Perhaps this is how plants differentially regulate CDKA activity during the cell cycle and development. In Arabidopsis, there are ten *CYCD* genes split into seven subgroups (Menges *et al.*, 2007). The expression of these genes varies both anatomically and temporally. The reported different expression patterns of several *CYCDs* during seed development are a good example (Collins *et al.*, 2012).

In support of the hypothesis that D-type cyclins regulate CDKA activity in response to different stimuli, the Arabidopsis D-type cyclins appear to have differential roles. *CYCD2;1* and *CYCD4;1* are each required for effective lateral root formation, the former being regulated by auxin in the process, the expression of the latter dependent on sucrose levels (Nieuwland *et al.*, 2009; Sanz *et al.*, 2011). *CYCD6;1* appears to be involved in stimulating asymmetric cell divisions in CEI cells in response to high auxin levels (Cruz-Ramirez *et al.*, 2012). *CYCD7;1* may play roles in regulating cell division in the stomata cell lineage (Patell *et al.*, manuscript in preparation). The roles of different *CYCDs* in the root apex during germination appear to be separated temporally (Masubelele *et al.*, 2005a).

Arabidopsis *CYCD3s*, of which there are three, appear to play several roles in cell cycle regulation. Over a decade ago, their expression was observed to increase following exposure of cells to exogenous cytokinins (Riou-Khamlichi *et al.*, 1999). Later, analyses of the consequences of over-expression of *CYCD3;1* revealed some of the proteins' potential functions. In cell culture, *CYCD3;1* decreased the proportion of cells in the G1 phase, implying faster progression into S phase (Menges *et al.*, 2006). In plants, cell proliferation was enhanced, differentiation inhibited, and development perturbed (Dewitte *et al.*, 2003). Interestingly, cell sizes were reduced, hinting at a compensation mechanism, be it active or passive. In *cycd3* mutants, cells still progress through the cell cycle, but the mitotic window in developing lateral aerial organs is reduced in time, and SAM function is compromised (Dewitte *et al.*, 2007). Furthermore, cytokinin responsiveness in calli was reduced, and petal cells entered endocycles prematurely. Thus the *CYCD3s* appear to have specific roles in regulating the cell cycle during development, as opposed to general assistance in activating CDKA during the G1 to S transition. Indeed, the *CYCD3* promoters were not active ubiquitously, but in shoots were found to be active in distinct but overlapping expression domains in developing flowers (Dewitte *et al.*, 2007). The functions of *CYCD3s* in promoting cell proliferation and in linking cytokinin responses to cell cycle activity make them interesting candidates for molecular regulators of vascular tissue establishment and proliferation. Other than proteasome-dependent degradation of the *CYCD3;1* protein (Planchais *et al.*, 2004), little is known about the direct regulation of *CYCD3* expression.

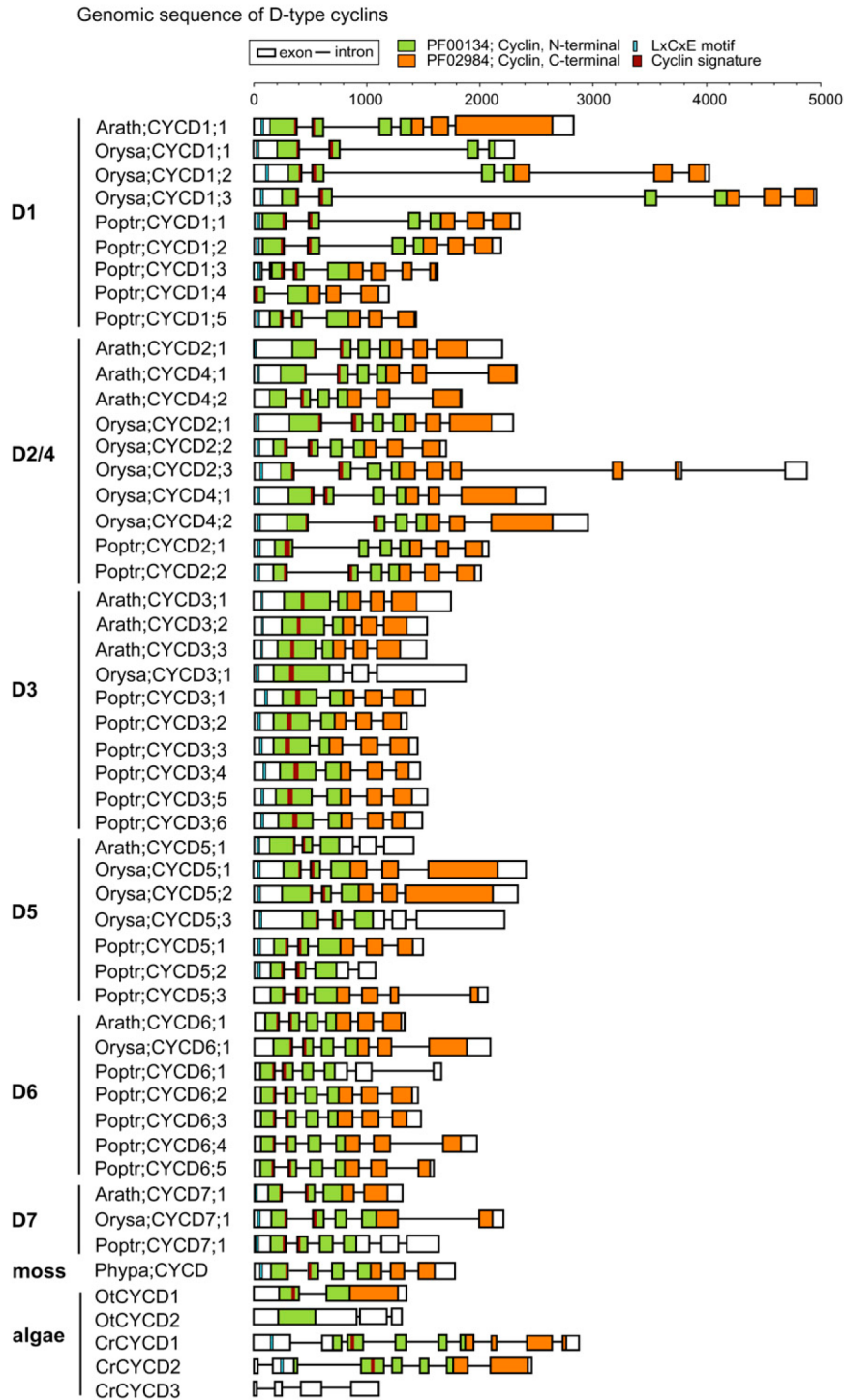


Figure 1.5: Genomic organization of 52 D-type cyclin genes in: *Arabidopsis thaliana* (Arath), a eudicot. *Oryza sativa* (Orysa), a monocot; *Poplar trichocarpa* (Poptr), a tree; *Physcomitrella patens* (Phypa), a moss; *Chlamydomonas reinhardtii* (Cr) and *Ostreococcus tauri* (Ot), two species of unicellular green algae. See legend at top for meanings of different colours. From Menges *et al.* (2007).

## 1.5 Control of Lateral Aerial Organ Size

---

The final size of higher plant lateral aerial organs (LAOs) varies greatly from species to species, is affected by environmental conditions and is of great importance to human beings, as this constitutes a great deal of either the food we eat, or the food for the food that we eat! The size of a plant organ is determined by both the number of cells constituting the organ, and by the sizes of those cells.

### 1.5.1 Leaf Development

LAO growth has been investigated extensively in leaves. Leaf development starts with initiation, which entails asymmetric division of cells at the periphery of the SAM, and proliferation of these cells to form leaf primordia (Donnelly *et al.*, 1999). Although phytohormones are known to signal initiation of leaf primordia outgrowth (Reinhardt *et al.*, 2000b), changes in cell shape caused by localised induction of *EXPANSIN* gene expression are sufficient to initiate leaf primordia that go on to form whole leaves (Pien *et al.*, 2001). Thus regulation of cell division by physical forces appears to be important in lateral aerial organ initiation. Leaf growth is then driven by cell division (see Figure 1.6 for overview). Finally, a mitotic arrest front initiates at the leaf tip, and spreads basipetally. A cell expansion phase follows this, and after this, cell number can be further increased by divisions of meristemoid cells in the epidermis, which belong to the stomata lineage of cells (Gonzalez *et al.*, 2012).

### 1.5.2 Cell Division and Expansion in Leaf Growth

The importance for cell division in achieving the correct final size of leaves has been demonstrated in the *struwwelpeter* mutant, in which cell number allocated to primordia is reduced, and the mitotic arrest front is initiated prematurely (Autran *et al.*, 2002). The leaves are smaller. *KLUH*, encoding the cytochrome P450 CYP78A5, also regulates leaf size via regulation of the duration of the mitotic window (Anastasiou *et al.*, 2007), as does the microRNA miR396 (Rodriguez *et al.*, 2010). Cell division rate can also influence final organ size. Leaves in which *APC10*, encoding a subunit of the anaphase-promoting

complex (APC), was overexpressed became larger than their *WT* counterparts (Eloy *et al.*, 2011). The APC complex mediates the ubiquitination of mitotic cyclins amongst other targets, and the degradation of these cyclins is required for entry into G1. Increased leaf size in *APC10* overexpressors was due to faster cell proliferation. Increased cell proliferation in the meristemoid cells can also increase leaf size, as demonstrated in the *peapod* mutant (White, 2006). Since this mutant also had reduced cell division in other so called dispersed meristematic cells, including procambium cells, the author proposed the existence of a second mitotic arrest front, regulated by *PEAPOD*.

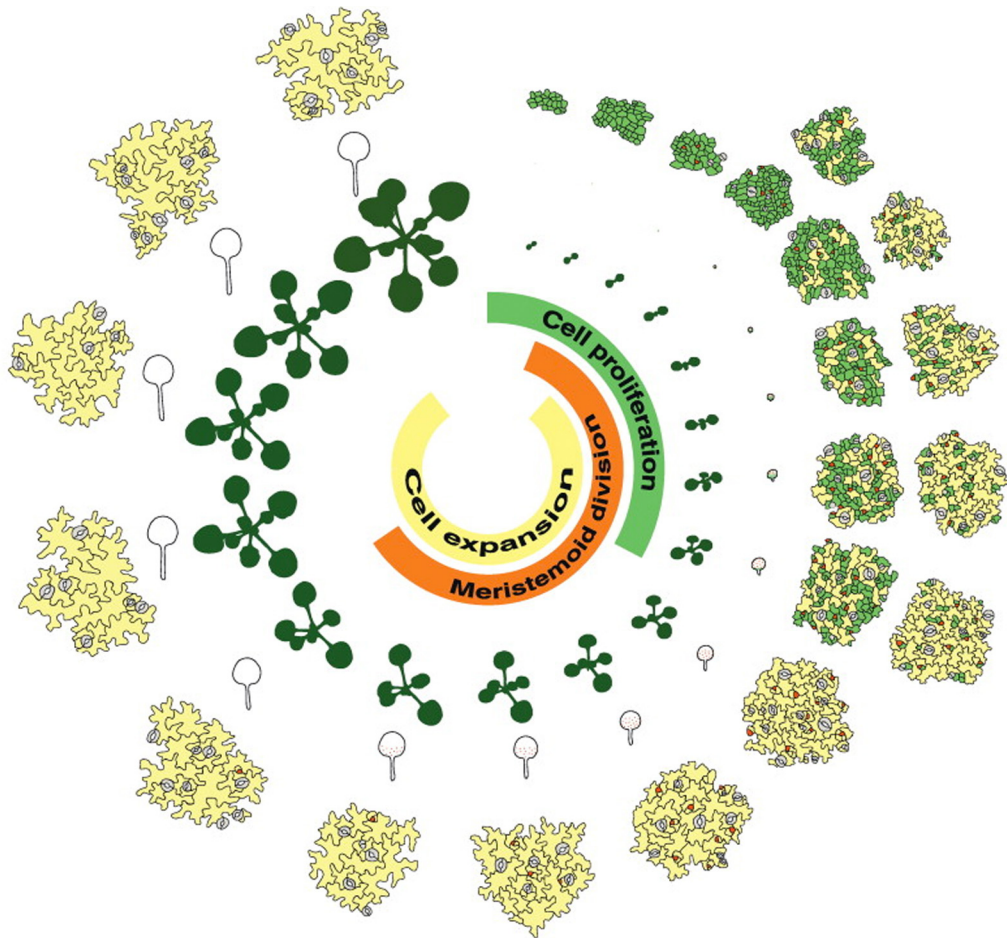


Figure 1.6: Arabidopsis leaf development. Developmental progression of rosette, whole leaf and leaf at cellular level are shown (at same developmental points). The pictures represent plants from four to twenty days old. Cells of the abaxial surface of the leaves are shown. Dividing cells in the primary division front are shown in green. Meristemoid cells, which continue to divide after the primary cell division front has ended, are shown in orange. Expanding cells are shown in yellow. These are “puzzle” shaped, which is the shape of differentiated leaf abaxial pavement epidermal cells. Adapted from Gonzalez *et al.* (2012).

Although the effects of cell expansion on organ size may be more limited than those possible with alterations in cell number, cell size does have an important effect on organ size, and appears to contribute significantly to the difference between petal and leaf size in *Arabidopsis* (Mizukami, 2001). Cell expansion requires the loosening of cell walls, *de novo* synthesis of cell wall components, and turgor pressure (Gonzalez *et al.*, 2012). Expansins are involved in cell expansion, and plants over-expressing an *EXPANSIN* gene have larger leaves containing larger cells (Cho and Cosgrove, 2000). Interestingly, it has more recently been shown that ectopic *EXPANSIN* expression can only influence leaf size if expressed during the middle stages of leaf growth, suggesting that there may be an interaction between cell division and growth during leaf growth (Sloan *et al.*, 2009). Repression of *EXPANSIN* expression leads to development of smaller leaves, although the cells within these leaves were larger than control leaf cells, indicating that cell number was reduced in these leaves (Sloan *et al.*, 2009). Other genes promoting cell expansion during leaf growth include *ARGOS-LIKE (ARL)* (Hu *et al.*, 2006), *TARGET OF RAPAMYCIN (TOR)* and *ZINC FINGER HOMEODOMAIN 5 (ZHD5)* (Gonzalez *et al.*, 2012). *TOR* was shown to regulate cell expansion via regulation of cell wall component biosynthesis (Ren *et al.*, 2012). The ploidy level of cells is correlated with their size (Kondorosi *et al.*, 2000), and has been shown to affect leaf size in *Lolium* (Sugiyama, 2005). It is thought that ploidy levels affect cell size by altering gene expression levels (Galitski *et al.*, 1999; Lee and Chen, 2001).

### 1.5.3 Control of Lateral Aerial Organ Growth Initiation and Growth by Auxins

Like root growth, lateral aerial organ growth control appears to be under complex control of phytohormones. Auxins appear to control the initiation of these organs, as well as their growth. Auxins are small molecules with an aromatic ring and a carboxylic acid group (Bartel, 1997). The most common naturally occurring auxin is indole-3-acetic acid (IAA) (Bartel, 1997). Auxin response factors (ARFs) bind to auxin response elements (AREs) when auxin is present and induce the expression of primary auxin-responsive genes downstream of these elements (Teale *et al.*, 2006). In the absence of auxin, Aux/IAA proteins bind to ARFs and inhibit their activity. Binding of auxin to the SCF E3 ubiquitin ligase SCF<sup>TIR1</sup> mediates ubiquitination of the Aux/IAA proteins

thereby marking them for proteasome-mediated degradation and activating ARFs (Teale *et al.*, 2006). In tomato and Arabidopsis, polar auxin transport is required for leaf and flower initiation, respectively, but also for the correct positioning of the primordia (Reinhardt *et al.*, 2000a). Live imaging has shown that lateral aerial organs initiate at sites of high auxin concentration, so-called auxin maxima, and that depletion of auxins in the regions between initiated primordia inhibits inappropriate primordia formation (Benkova *et al.*, 2003; Scanlon, 2003; Heisler *et al.*, 2005; Vernoux *et al.*, 2011).

The ways that auxins control organ growth and final size remain unclear, as there appear to be some inhibitory effects as well as some stimulating effects. Plants lacking the function of AUXIN-RESPONSE FACTOR 2 (ARF2), which is encoded by a primary auxin-responsive gene, have larger seeds, leaves and floral organs (Schruff *et al.*, 2006b). Plants lacking the function of auxin-inducible *AUXIN-REGULATED GENE CONTROLLING ORGAN SIZE* (ARGOS), however, have smaller aerial organs primarily due to reduced cell number (Hu *et al.*, 2003). Similarly, auxin-regulated *EBP1* that encodes the ERBB3 EPIDERMAL GROWTH FACTOR RECEPTOR BINDING PROTEIN positively regulates aerial organ size via cell number and expansion control (Horvath *et al.*, 2006). For plants to use auxin to control such a diversity of developmental processes, it is perhaps not so surprising that some of the functions of auxin signalling may counteract each other.

#### 1.5.4 Roles of Cytokinins, Gibberellic Acid, Ethylene and Brassinosteroids in Lateral Aerial Organ Growth Control

Cytokinins also control LAO size, but neither the significance nor the mechanisms behind this are yet clear. Several naturally occurring cytokinin molecules exist, zeatin being the most common in plants (Hirose *et al.*, 2008). Plant cytokinins derive from isopentenyl adenine (Hirose *et al.*, 2008). This molecule is created by adenosine phosphate-isopentenyl enzymes (Werner and Schmülling, 2009). Isopentenyl adenine is then converted to trans-zeatin by cytochrome P450 monooxygenase (CYP735A) enzymes (Werner and Schmülling, 2009). Cytokinin signalling occurs via a two-component signalling cascade. Cytokinins bind to AHK receptor molecules, which dimerise and then undergo autophosphorylation (Werner and Schmülling, 2009). The phosphoryl group is transferred to AHP proteins, which themselves

transfer the phosphoryl group to ARR proteins (Werner and Schmülling, 2009). Type-B ARRs can then transactivate cytokinin-responsive genes (Werner and Schmülling, 2009). Type-A ARRs lack a DNA binding domain and negatively regulate cytokinin signalling (Werner and Schmülling, 2009). The mechanisms proposed for this negative regulation include competition for phosphoryl groups and interaction with AHP proteins (To *et al.*, 2007). Cytokinin levels are negatively regulated by cytokinin oxidase (CKX) enzymes that inactivate cytokinins (Schmülling *et al.*, 2003). Plants lacking the function of two CKX genes have enhanced levels of active cytokinins, and have larger floral organs (Bartrina *et al.*, 2011). These mutants also have larger apical meristems, but the link between the meristem size and the organ size is yet to be established. However, increased degradation of cytokinins specifically in leaf primordia has shown that cytokinins are rate-limiting for leaf growth (Holst *et al.*, 2011).

Giberellic acid (GA) signalling regulates both cell division rates and the duration of the mitotic window, positively and negatively respectively, during leaf growth (Achard *et al.*, 2009). Thus altering GA levels has positive and negative effects on leaf size, potentially revealing a compensatory mechanism to counteract unwanted effects on cell proliferation during organ growth. GA has long been known to regulate organ size by promoting cell elongation (Gray, 1957). Additionally, GA is involved in orientating microtubules in elongating cells to coordinate the direction of elongation with the direction of organ growth (Shibaoka, 1994).

Plants with enhanced ethylene signalling have smaller organs due to reductions in both cell number and size, and plants with reduced ethylene signalling have larger organs (Ecker, 1995). On the other hand, in rose petals, ethylene can promote their size by promoting cell expansion (Liu *et al.*, 2013). Like auxins then, ethylene can have both positive and negative effects on LAO size.

Brassinosteroid-signalling mutants have smaller leaves due to reduced cell elongation (Szekeres *et al.*, 1996). Brassinosteroids may also influence cell proliferation rates, although to what extent this occurs remains unclear (Hu *et al.*, 2000; Nakaya *et al.*, 2002; Gonzalez-Garcia *et al.*, 2011). The expression of cell division markers was altered dramatically in brassinosteroid-insensitive mutants, implicating these hormones in the regulation of cell cycle activity (Gonzalez-Garcia *et al.*, 2011).

### 1.5.5 Altered Cell Number and Endoreduplication in *shr* Leaves

Many genes involved in the regulation of LAO size have been identified. Some genes involved in the regulation of developmental processes occurring in root growth also appear to have similar functions in the regulation of LAO growth. *SHR* is expressed in young leaves, and *shr* mutants have smaller leaves (Dhondt *et al.*, 2010a). This was not a secondary effect of altered root growth, as reversal of the root phenotype did not alter the shoot phenotype. Interestingly, *shr* leaves exhibited reduced cell number as well as reduced occurrence of endoreduplication. In *Antirrhinum majus formosa* mutant flowers, cell division is enhanced but cell expansion is reduced, revealing another compensatory mechanism to maintain correct aerial organ size (Delgado-Benarroch *et al.*, 2009).

### 1.5.6 Summary of Lateral Aerial Organ Growth Control

The huge numbers of roles of different hormones involved in the regulation of organ size are becoming well characterized, and many individual genes required for attainment of correct organ size are now known. To fully understand control of organ size, this information must be integrated, and systems biology must be employed to use the huge datasets now available in the public domain to explain how developmental and environmental signals are assimilated to fine-tune organ growth.

## **1.6 Plant Vascular Tissue Development**

---

Development of vascular tissue in higher plants involves developmentally coordinated regulation of cell division and its orientation in various contexts, such as during embryogenesis, lateral root formation and leaf vein development. This process is not only an excellent model for understanding control of cell division during development, but is important for water and nutrient transport through plants and plant strength and resilience in harsh conditions. For example, secondary xylem and cork cambium tissue form wood in trees (Chaffey *et al.*, 2002), which would not, at least on Earth, stand tall without it. Development of the vascular tissue of the *Arabidopsis thaliana* root is particularly amenable to investigation, as it is a well-developed experimental

model and the root is narrow, almost transparent and has a well-defined small number of cell files (Mahonen *et al.*, 2000).

### 1.6.1 Primary Vascular Tissue Development

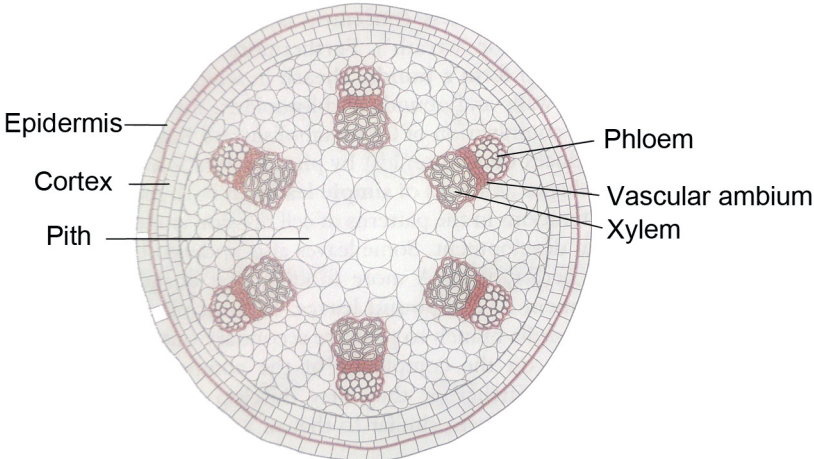
The vasculature of higher plants is characterized by two distinct developmental growth phases: primary and secondary growth (Figure 1,7). During primary growth, a well-defined cellular pattern within the vascular tissue is established (Bowman, 1993). The first step toward the creation of a radial pattern in *Arabidopsis* occurs at the dermatogen (16 cell-) stage of embryogenesis, when longitudinal divisions occur in the eight inner cells of the embryo. These cells will derive the ground tissue (cortex and endodermis) as well as the pluripotent procambium cells. The procambium cells divide and differentiate into the procambium, prophanloem, proxylem and pericycle cells by the torpedo stage (Bowman, 1993; Fosket, 1994), thus establishing the radial pattern of the stele tissue. This consists of a central axis of proxylem cells, flanked by the procambium cells, which are themselves flanked by prophanloem cells (Dolan *et al.*, 1993). A ring of pericycle cells surrounds all of these, thus completing the vascular cylinder. During early post-embryonic primary growth, this pattern remains unchanged, although cell differentiation does occur (Dolan *et al.*, 1993; Mahonen *et al.*, 2000), and roots and shoots elongate via anticlinal cell divisions (Fosket, 1994).

### 1.6.2 Secondary Vascular Tissue Development

Eudicots then progress into a secondary growth phase, which involves further periclinal procambial cell divisions that give rise to meristematic cambial cells (Miyashima *et al.*, 2013), themselves capable of differentiating into secondary xylem and phloem (Elo *et al.*, 2009; Groover and Spicer, 2010). Secondary growth is important for efficient water, nutrient and mineral transport, and is also required for wood formation in trees (Du and Groover, 2010). Like primary vascular tissue development, secondary vascular tissue development can be studied in *Arabidopsis* roots. As well as cambium establishment and proliferation, secondary growth involves secondary xylem formation. Secondary xylem, distinguished as either tracheary elements or xylem fibres, develop following cell elongation, cell wall deposition and programmed cell death

(Nieminen *et al.*, 2004). These cells have highly lignified thick cell walls (Taylor *et al.*, 2004) and are therefore energy-rich, contributing to the attractiveness of plants as renewable sources of biofuels (Ragauskas *et al.*, 2006; Pauly and Keegstra, 2008).

Primary development



Secondary Development

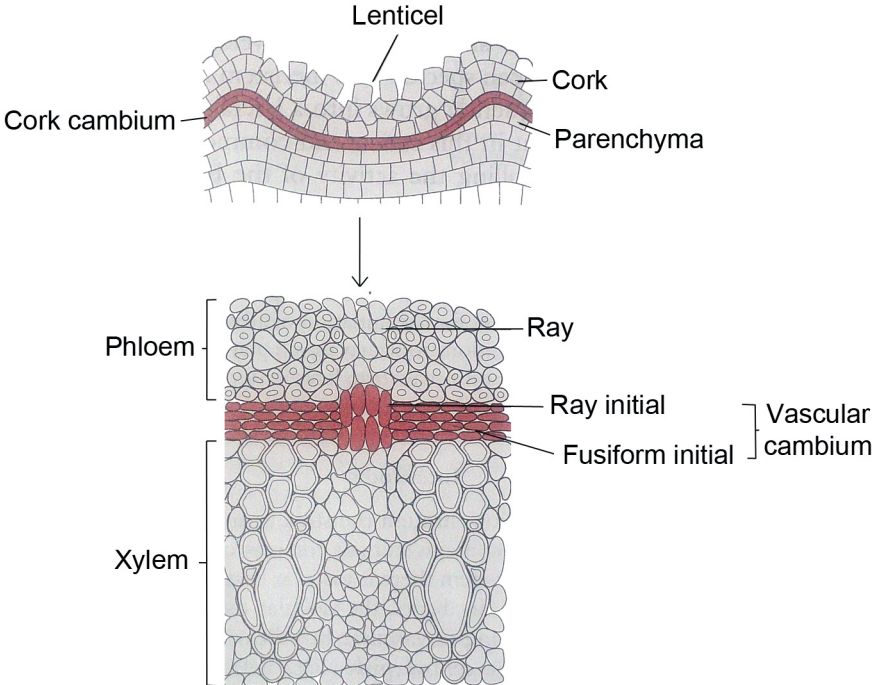


Figure 1.7: Radial development of a dicot shoot. A major difference from the radial organization of the root is that in the shoot, the pith is the central tissue of the stem (the vascular tissue takes the centre spot in the root). The vascular tissue is arranged in bundles in primary growth. Xylem cells are on the inside of these bundles, phloem cells are on the outside and cambium cells lie between. Outside of the pith is found first the cortex, then the tissue that will later form the cork cambium (red), then the epidermis. Secondary growth and development involve the proliferation of the cambium cells and the differentiation of these cells into secondary xylem and phloem. These secondary xylem cells become highly lignified in trees and form wood. Daughter cells of fusiform initials become randomly placed secondary xylem and phloem cells, whereas daughters of ray initials form secondary xylem and phloem rays that allow lateral conduction of water and nutrients. The parenchyma cells allow nutrient storage and gaseous exchange. The cork cambium provides cells for the cork cells that form a protective layer around the shoot, as well as the lenticels that ensure gaseous exchange between the plant and the atmosphere can take place. Modified from Leyser & Day (2007) .

## 1.7 Regulation of Plant Vascular Tissue Development

---

### 1.7.1 Interaction Between Auxin and Cytokinin Signalling During Plant Vascular Tissue Development

Cytokinin and auxin signalling are known to antagonise and/or agonise each other depending on the tissue and developmental context. For example, during early embryogenesis, auxins down-regulate cytokinin signalling in the hypophysis-derived basal cell via activation of the A-type *ARRs* *ARR7* and *ARR15* (Muller and Sheen, 2008). Type-A *ARRs* down-regulate cytokinin signalling to provide negative feedback following a cytokinin input (Gupta and Rashotte, 2012). The promoters of these genes contain putative auxin response elements, which were required for their induction by auxin, highlighting a direct interaction between auxin and cytokinin signalling. In vascular tissue development, both auxin and cytokinin appear to promote cell divisions to achieve the correct vascular cell file number. In primary growth, cytokinins in the phloem induce the expression of the polar auxin transporter gene *PIN7* (Bishopp *et al.*, 2011b). When cytokinin levels in the phloem are reduced, auxin distribution changes and protoxylem cell file patterning is altered. Cytokinins and auxins also interact to regulate the differentiation of vascular cells (Figure 1.8). Cytokinins up-regulate *PIN7* expression in procambium cells, which leads to an influx of auxin into the (pre-) protoxylem pole cells (Bishopp *et al.*, 2011a). In these cells, auxins induce *AHP6* expression. *AHP6* lacks a conserved histidine residue found in other AHP proteins, and is thought to be a pseudo-phosphohistidine transfer protein providing negative feedback in cytokinin signalling (Hwang *et al.*, 2002). Thus cytokinins direct auxins toward the protoxylem poles, where auxin down-regulates cytokinin signalling. This down-regulation is required for protoxylem differentiation.

### 1.7.2 Auxin Phytohormones Control Vascular Cell Divisions and Differentiation

Auxin phytohormones regulate vascular tissue patterning from early stages, and auxin-signalling output is high in the provascular tissue (Blilou *et al.*, 2005). *MONOPTEROS/ARF5* encodes an auxin-response factor (Hardtke and Berleth, 1998), and mutants lacking the function of this gene display defects in radial organization of embryonic tissue (Berleth and Jurgens, 1993), including reduced cell divisions in the provascular tissue (Hardtke and Berleth, 1998). *pin1* (*pin-formed 1*) mutants, that lack the function of a polar auxin transporter, display reduced growth of vascular tissue in inflorescence stems, highlighting the requirement for proper auxin transport and signalling for vascular tissue development later in plants during secondary growth (Galweiler *et al.*, 1998). Furthermore, cambium and phloem development is perturbed in *Populus* trees with reduced auxin signalling (Nilsson *et al.*, 2008b), confirming the role of auxin in promoting secondary growth.

As well as ensuring that the provascular cell divisions required for growth of this tissue occur, auxins are involved in the differentiation of vascular cells. The *LONESOME HIGHWAY* gene encoding a bHLH transcription factor is required for correct auxin transport and signalling, and for asymmetric cell divisions in embryos that derive vascular cells (Ohashi-Ito *et al.*, 2013).

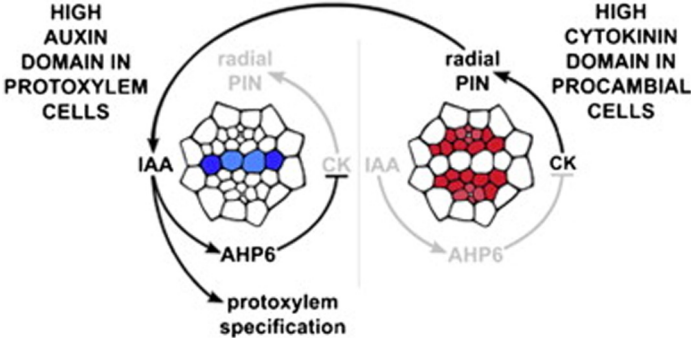


Figure 1.8: Cross-sections of the primary stele are illustrated, with the pericycle as the outermost cell type. The blue colours show high auxin levels in the protoxyle (dark blue) and metaxylem (lighter blue) on the left. High levels of auxin inhibit cytokinin signalling via activation of the pseudo phosphohistotransfer protein AHP6 and promote differentiation of xylem cells. High cytokinin levels in the procambium cells are shown in red on the right. High cytokinin levels inhibit differentiation and promote radial organization of the auxin efflux carrier PIN7, which assists the transport of auxin from the procambium to the xylem. This prevents inappropriate promotion of xylem differentiation by auxin in the procambium. From Bishopp *et al.* (2011a).

### 1.7.3 Regulation of Vascular Cell Divisions in Primary Growth by Cytokinins

Cytokinin phytohormones also play roles in the regulation of vascular tissue development. The *Arabidopsis wol* (*wooden leg*) mutant harbours a mutation in the procambium-expressed gene encoding the ARABIDOPSIS HISTIDINE KINASE 4 (CRE1/AHK4) cytokinin sensor (Suzuki *et al.*, 2001b; Yamada *et al.*, 2001; Mahonen *et al.*, 2006a). AHKs are cytokinin receptors whose activation results in activation of Arabidopsis response regulator (ARR) transcription factors via a phospho-relay loop involving Arabidopsis histidine phosphotransfer proteins (AHPs) (Ueguchi *et al.*, 2001; Yamada *et al.*, 2001; Hutchison *et al.*, 2006). The *wol* mutation prevents CRE1/AHK4 from binding to cytokinins (Yamada *et al.*, 2001), and confers constitutive phosphatase activity, thus creating a dominant negative mutant protein (Mahonen *et al.*, 2006b). *wol* embryos develop fewer procambial precursor cells, resulting eventually in exclusive differentiation of xylem cells (Scheres *et al.*, 1995b). Based on the anatomical analyses, it was concluded that this phenotype was due to the absence of a single cell division event around the embryonic torpedo stage (Scheres *et al.*, 1995b). During primary root growth, these mutants do not undergo periclinal cell divisions in the procambium, and thus have a narrower stele (Mahonen *et al.*, 2000). That this phenotype is due to reduced cytokinin signalling is supported by the demonstration of roots harbouring fewer procambium cell files when the *CYTOKININ OXIDASE 2* (CKX2) gene, encoding an enzyme that degrades cytokinins, is expressed specifically in the procambium using the *CRE1* promoter (Mahonen *et al.*, 2006a). Furthermore, *ahp* mutants harbour fewer vascular cells in roots undergoing primary growth (Hutchison *et al.*, 2006).

### 1.7.4 Cytokinins Regulate Secondary Growth

Cytokinins are becoming well known for their roles in the regulation of secondary growth, which is itself driven by cambium proliferation. Arabidopsis plants lacking four genes encoding isopentenyl transferase enzymes, which catalyse steps in *tz*-type and *iP*-type cytokinin synthesis, display reduced secondary growth in roots (Matsumoto-Kitano *et al.*, 2008). To confirm that this phenotype was due to a reduction in endogenous cytokinin levels, the mutants

were supplemented with exogenously applied *trans*-zeatin, a natural cytokinin. This rescued the phenotype, and at high levels induced secondary growth exceeding that seen in untreated *WT* plants. It could be clearly seen that increased secondary growth was associated with increased cell division, suggesting that cytokinins act, at least in secondary growth, via activation of cell division.

Vascular development in primary growth is easier to analyse in roots than in shoots, since the radial pattern varies less in roots. In *Arabidopsis* shoots, cytokinin signalling promotes at least secondary growth, since *ahk2;3* mutants display reduced radial cambium proliferation in shoots (Hejatko *et al.*, 2009). Cytokinins also promote secondary growth in Poplar tree stems, as transgenic poplar plants expressing *AtCKX2* under regulation of the cambium-specific *pBpCRE1* promoter have narrower stems with less cambium tissue (Nieminen *et al.*, 2008).

#### 1.7.5 Other Phytohormones Regulating Vascular Tissue Development

Auxins and cytokinins play many roles in higher plant vascular tissue development, with cytokinins in particular promoting vascular cell proliferation. However, other phytohormones also play roles, albeit more subtle roles, in this regulation. Gibberellins and ethylene promote cambium growth, and gibberellins and brassinosteroids promote phloem and xylem differentiation, respectively (Sehr *et al.*, 2010; Ursache *et al.*, 2013). In *Arabidopsis* stems, jasmonic acids stimulate specifically the growth of the interfascicular cambium (that between the vascular bundles) (Sehr *et al.*, 2010).

#### 1.7.6 SHR and SCR regulate Radial Patterning in Roots

Several proteins, especially transcription factors, have been identified as important regulators of vascular tissue development. In Arabidopsis, the transcription factors SHORT ROOT (SHR) and SCARECROW (SCR) are required for correct radial patterning in roots (Di Laurenzio *et al.*, 1996a; Helariutta *et al.*, 2000). *SHR* is expressed in the stele within the RAM, from where the protein moves toward the endodermis (Gallagher *et al.*, 2004). At the cortex/endodermis (CEI) initial cells, SHR encounters locally abundant SCR. Together these proteins induce asymmetric divisions in these cells to produce the cortex and endodermis cell files. More recently, it has been shown that SHR induces the expression of *CKX3* in the xylem poles during primary development, and thereby promotes xylem and xylem-associated pericycle differentiation (Cui *et al.*, 2011).

#### 1.7.7 AHL Proteins Control the Boundary Between Xylem and Procambium Tissue in Young Roots

Recently, two AT-hook proteins, encoded by *AT-HOOK MOTIF NUCLEAR LOCALIZED PROTEIN (AHL) 3* and *4*, were discovered to control the boundary between xylem and procambium tissue in roots during primary development (Zhou *et al.*, 2013). Specifically, these proteins appeared to down-regulate xylem differentiation in the procambium zone.

#### 1.7.8 Similarities and Differences Between the WUS/CLV Signalling Mechanism in Shoot Meristem Development and the WOX4/TDIF Mechanisms Controlling Root Auxiliary Meristem Development

Procambium and cambium cells are meristematic. Perhaps it is not surprising that some proteins controlling stem cell identity and function in shoots have homologues performing similar tasks in roots' axillary meristems. *WUSCHEL-RELATED HOMEODOMAIN 4 (WOX4)*, which encodes a homologue of the WUS transcription factor which maintains stem cell identity in the SAM (Laux *et al.*, 1996), is required for procambium development in both Arabidopsis and tomato (Ji *et al.*, 2010), but also promotes cambium growth (Suer *et al.*, 2011). The

promotion of cambium growth by WOX4 occurs at least in part by imparting auxin responsiveness to cambium cells (Suer *et al.*, 2011). In the SAM, *WUS* expression is restricted to the organizing centre by the CLAVATA (CLV) pathway (Brand *et al.*, 2000; Schoof *et al.*, 2000). Outside of the organizing centre, CLV3 peptide is secreted and activates the receptor-like kinases (RLKs) CLV1, CORYNE (CRN) and/or CLV2 to inhibit *WUS* expression (Durbak and Tax, 2011). In *Zinnia* cell cultures, the Arabidopsis peptide TRACHEARY ELEMENT DIFFERENTIATION INHIBITORY FACTOR (TDIF) has been documented as an inhibitor of xylem cell differentiation (Ito *et al.*, 2006). TDIF is a CLV3 orthologue, and binds to the RLK TDIF receptor (TDR), which belongs to the same subclass of proteins as CLV1 (Hirakawa *et al.*, 2008). In Arabidopsis, *tdr* loss-of-function mutants have fewer procambium cell files in hypocotyls (Hirakawa *et al.*, 2008). A *tdr* mutant has been isolated independently and was named *phloem intercalated with xylem (pxy)* as the boundaries between the different vascular tissues in stems were destabilized (Fisher and Turner, 2007). Thus a pathway regulating stem cell maintenance and function in the procambium and cambium containing paralogues of members of the SAM CLV pathway appears to exist, but the interactions within the pathway differ. Whilst CLV proteins in the SAM act by repressing cell division and promoting differentiation, TDIF/PXY is required for cell division and inhibits cell differentiation.

## 1.8 The AINTEGUMENTA Transcription Factor

---

### 1.8.1 The AP2/ERF Transcription Factor Family

Genes encoding proteins with APETALA 2 (AP2) DNA binding domains fall into three categories: those containing a single AP2 DNA-binding domain, the *ETHYLENE RESPONSE FACTOR* (ERF)-like genes, the *RAV* genes, containing a single AP2 domain and a different DNA-binding domain, and the AP2-like genes, such as *AP2* and *AINTEGUMENTA* (*ANT*) (Kim *et al.*, 2006) that encode floral homeotic proteins containing two AP2 domains. In *Arabidopsis*, there are 18 *AP2* genes, 122 *ERF* genes and 6 *RAV* genes (Nakano *et al.*, 2006). In general, *ERF*-like genes are thought to be predominantly involved in responses to biotic and abiotic stresses, whereas *AP2*-like genes are thought to regulate developmental processes. For example, *AP2* regulates floral meristem, flower and seed development (Jofuku *et al.*, 1994). Not much is known about *RAV* gene function, but early indications are that they are involved in mediating senescence (Woo *et al.*, 2010).

Homologues of the AP2 domain appear to be present in diverse species, such as cyanobacteria, a ciliate and even some viruses, but the functions of the domain within these species are also diverse (Kim *et al.*, 2006). *AP2/ERF* genes themselves appear to be unique to plants, and have been identified in monocot and eudicot angiosperms, gymnosperms, basal angiosperms and a moss (Jofuku *et al.*, 1994; Riechmann and Meyerowitz, 1998; Vahala *et al.*, 2001; Shigyo and Ito, 2004; Kim *et al.*, 2006). Outside of the AP2 domain, AP2 and ERF proteins show poor amino acid sequence conservation (Kim *et al.*, 2006), possibly reflecting their specialized individual roles.

A sub-category of AP2-like genes encoding proteins showing high amino acid sequence similarity with that of *ANT* have been designated *AINTEGUMENTA-LIKE/PLETHORA* (*AIL/PLT*) genes (Figure 1.9). These are expressed in young dividing tissues and appear to promote states of mitotic competence (Nole-Wilson *et al.*, 2005). Several *AIL/PLTs* respond to auxin in roots in a concentration-dependent manner (Aida *et al.*, 2004), providing a readout for the instructive auxin gradient. At high levels in the root tip, *AIL/PLTs* specify stem cell identity and maintenance (Galinha *et al.*, 2007). At lower levels in the meristem, these proteins promote mitotic activity (Galinha *et al.*, 2007). In

the transition and elongation zones, levels of AIL/PLTs must be sufficiently low for cell differentiation and elongation to occur (Galinha *et al.*, 2007). In the shoot, three members of this family, including ANT, promote apical meristem activity (Mudunkothge and Krizek, 2012b). AIL/PLTs also regulate phyllotaxis (Prasad *et al.*, 2011) and rhizotaxis (Hofhuis *et al.* 2014). These proteins appear to play roles both upstream (Pinon *et al.*, 2013a) and downstream (Hofhuis *et al.*, 2014) of auxin signalling in the regulation of these processes. Thus *ANT* and the *AIL/PLT* genes play diverse roles in the regulation of plant growth and development.

### 1.8.2 Isolation and Early Investigations of the Functions of the *AINTEGUMENTA (ANT)* Gene

The *ANT* gene was initially characterized independently in the laboratories of David Smyth and Robert Fischer, and the associated two pieces of work were co-published in a 1996 issue of *The Plant Cell* (Elliott *et al.*, 1996; Klucher *et al.*, 1996). A loss-of-function mutant that failed to develop integuments, and thus failed to complete megasporogenesis, was identified, and was thus given the name *aintegumenta* (Elliott *et al.*, 1996).

Once the gene was cloned and the sequence determined, it was found that *ANT* encoded a protein belonging to the APETALA2-like family of transcription factors. Observations of narrow floral organs of reduced number per plant were also made. Specifically, reduced numbers of sepals, petals and stamens developed in the mutant (Klucher *et al.*, 1996).

RNA *in situ* hybridization analysis indicated that, in shoots, *ANT* was strongly expressed in organ primordia, such as leaf, petal, stamen, sepal and ovule primordia. *ANT* mRNA was also detected, albeit less intensely, in the procambium tissue of floral buds (Elliott *et al.*, 1996). Thus it was proposed that *ANT* might have a general role in promoting organ primordia development. *ANT* was also identified in yeast as a gene that could complement the  $\Delta pkc1$  mutant (Vergani *et al.*, 1997). *Pkc1* is essential for cell growth in budding yeast (Heinisch *et al.*, 1999), but is also involved in regulating cytoskeleton and hence cell polarity (Mazzoni *et al.*, 1993) as well as cell wall integrity during osmotic stress (Paravicini *et al.*, 1992). Perhaps higher plant *ANT* regulates cell polarity during organ primordium development.

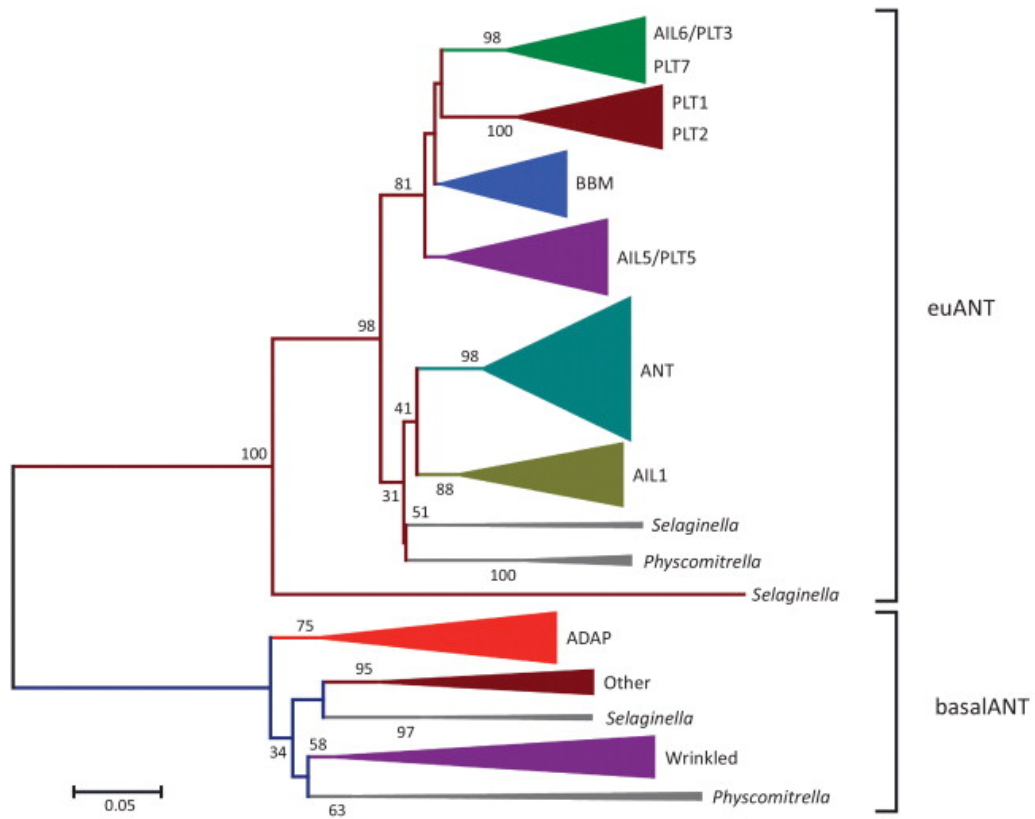


Figure 1.9: Evolution of the AIL/PLT family. A phylogenetic tree is shown. Numbers at nodes indicates bootstrap support values. The basal ANT clade does not appear to contain orthologues of Arabidopsis ANT. *Selaginella moellendorffii* and *Physcomitrella patens* are shown. eu: eudicot. From Horstman *et al.* (2014).

### 1.8.3 Transactivation Activity and DNA-binding Properties of AINTEGUMENTA

The expected DNA-binding activity of ANT was shown using gel mobility shift assays, and the optimal binding site for this activity determined (Nole-Wilson and Krizek, 2000). ANT has two AP2 binding domains (Figure 1.10), and each is involved in and required for binding of ANT to DNA (Nole-Wilson and Krizek, 2000). ANT appears to bind a DNA sequence different from the AT-rich sequence bound by APETALA2 (Dinh *et al.*, 2012). However, a proof-of-concept protein microarray study demonstrated specific *in vitro* binding of four other AP2-domain containing proteins to the ANT consensus sequence (Gong *et al.*, 2008). These were PLT2, BBM, WRI4 and AIL7/PLT7. Interestingly, these four AP2-domain-containing proteins are, phylogenetically, relatively closely related (Kim *et al.*, 2006).

Transactivation activity of ANT has been demonstrated in budding yeast (Vergani *et al.*, 1997; Krizek, 2003) as well as *in planta* (Krizek and Sulli, 2006). *In planta*, ANT induced expression of a reporter downstream of an optimal ANT-binding DNA sequence (Krizek, 2003). This is not therefore direct evidence of ANT transactivating native Arabidopsis genes. Expression of *AGAMOUS* (*AG*) is repressed redundantly by ANT and other AIL proteins, but no evidence of a direct link between ANT and *AG* was shown (Krizek *et al.*, 2000). A region of the ANT protein rich in serine/threonine, glutamine/aspartate and acidic amino acids was identified and shown to be essential for ANT-dependent transactivation. Thus this region likely contains a transactivation domain.

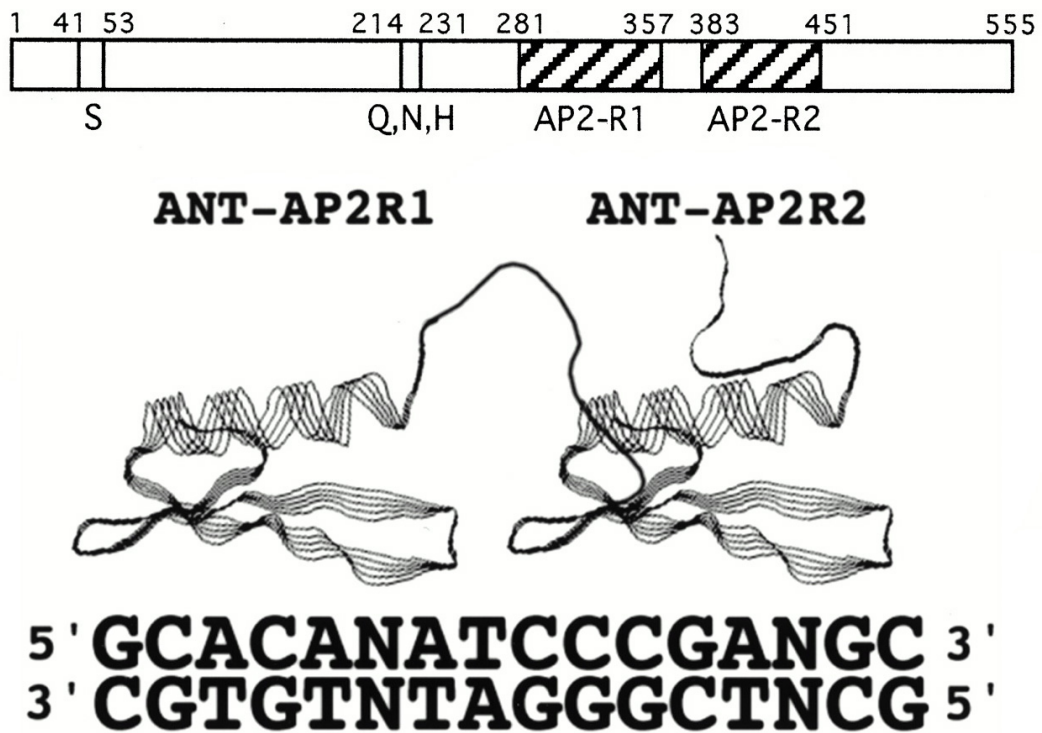


Figure 1.10: Schematic of ANT (top) and a model the AP2 DNA-binding domains of ANT binding to an optimal ANT-binding DNA sequence (Nole-Wilson and Krizek, 2000). The numbers (top) indicate the number of amino acids from the N terminus. Regions rich in acidic amino acids are indicated. Boxes with horizontal black lines indicate AP2 DNA binding domains. Models of these binding to an optimal ANT-binding DNA sequence are shown below. Adapted from (Nole-Wilson and Krizek, 2000).

#### 1.8.4 AINTEGUMENTA Controls Organ Growth via Regulation of Cell

##### Division Activity

Following the discovery that *ant* mutants fail to develop proper integuments, it was confirmed that ANT also regulates the growth of other lateral aerial organs. *ant-1* leaves and petals are smaller than those of *WT* plants (Mizukami and Fischer, 2000). Microscopical analyses showed that the mutant petals and leaves had fewer cells, but the cells were larger, once again highlighting the likelihood of a compensation mechanism in action when lateral aerial organ size control is perturbed. However, this compensation mechanism is not as strong as that seen in *cyd3;1* mutants, where organ size is fully compensated by cell enlargement (Dewitte *et al.*, 2007). Ectopic over-expression of *ANT* results in increased lateral aerial organ growth (Krizek, 1999; Mizukami and Fischer, 2000). Larger leaf growth in these transgenic plants was correlated with an increase in the length of the window of *CYCD3;1* and *CYCB1;1* expression, suggesting increased or prolonged cell cycle activity. In one these studies, vegetative organs such as leaves were unchanged, whereas floral organs were altered (Krizek, 1999). In this study, sepals had a greater number of cells, whilst petals, stamens and carpels had larger cells but an unchanged number. Thus the phenotype was attributed to either increased cell division or expansion in the associated organs. However, in the other study, leaves as well as floral organs were larger when *ANT* was over-expressed, and this was attributed to an increase in cell number, itself due to an increase in the duration of cell proliferation during organ growth, as opposed to an increase in the rate of cell proliferation (Mizukami and Fischer, 2000). The discrepancy between these two studies might be due to the fact that they were performed in different *Arabidopsis* ecotypes, namely *Landsberg erecta* and *Columbia-0* respectively. Regulation of leaf size by *ANT* was also suggested by the finding that the *grandifolia-D* mutants that have small leaves contain a chromosomal deletion in the region in which *ANT* resides (Horiguchi *et al.*, 2009). Intriguingly, this region also contains the *CYCD3;1* locus.

#### 1.8.5 Functions of AINTEGUMENTA that Depend on other Proteins

*ANT* appears to act redundantly with other AIL-proteins in the regulation of some developmental processes. *ANT* acts in combination with AP2 to repress

AG in second whorl flower cells, although later in petal development ANT acts independently to promote the identity of petal epidermal cells (Krizek *et al.*, 2000). ANT works with *FILAMENTOUS FLOWER (FIL)*, a YABBY gene, to promote adaxial-abaxial polarity in growing lateral organs (Nole-Wilson and Krizek, 2006). These were proposed to do this by up-regulating *PHABULOSA*, a HD-ZIP gene that specifies adaxial cell identity. Plants mutated for *AIL6/PLT3* and *ANT* have additive reductions in organ growth and number, but also have problems in floral organ positioning (Krizek, 2009). The *ant fil* and *ant ail6* mutants each had altered *APETALA3* expression, possibly contributing to the phenotypes. The *ant ail6* mutant also appeared to have altered auxin distribution in flowers, suggesting that ANT may be required for correct auxin transport. When auxin transport is altered, the severity of the *ant ail6* mutant is increased; flowers fail to initiate, suggesting that these genes do indeed interact with auxin transport and/or signalling (Krizek, 2011b; Krizek, 2011a). ANT appears to act redundantly with *AIL6* and *AIL7* to maintain SAM function, as triple mutants fail to produce new leaf primordia once a few have already been made, whereas the single mutants do not (Mudunkothge and Krizek, 2012a). Despite much being known regarding the roles of ANT, evidence for it transactivating target genes in plants is completely lacking.

#### 1.8.6 The link between ANT and *CYCD3;1*

That constitutive expression of ANT leads to maintenance of *CYCD3;1* expression in LAOs (Mizukami and Fischer, 2000) opens the possibility that ANT regulates the expression of *CYCD3;1*. Supporting this, an orthologue of ANT in *Poplar trichocarpa* directly regulates an orthologue of *CYCD3;1* in this species during adventitious root primordia formation (Rigal *et al.*, 2012). This would present the first known molecular link between ANT and cell division control, and the first known transcriptional regulator of *CYCD3;1*.

## 1.9 Aims and objectives

---

The aims of this study were as follows:

- Investigate the link between *ANT* and *CYCD3;1* and explore the roles played by these genes in the regulation of plant growth and development further. Only a small amount of indirect evidence suggesting that *ANT* regulates *CYCD3;1* expression exists in the literature, and no other putative targets of *ANT* have been identified. *ANT* has been shown to regulate cell number in plant organs, and *CYCD3;1* could provide the mechanism for this action. It is therefore important to determine whether or not this is truly the case. A genetic approach and molecular biology are utilized to investigate both the functional interaction between these genes and the physical interaction between *ANT* and *CYCD3;1*.
- Roles of *CYCD3s* in the regulation of cell proliferation during lateral aerial organ growth have been identified, but there exist no known roles for these genes in the root. Several genes regulating plant development in shoots have later been found to play similar roles in regulating root development, and *vice versa*. Another aim of this study was to explore the roles of these genes in the regulation of plant development further, and especially to identify any roles they might play in roots. As *CYCD3;1* appears to respond to cytokinin hormones (Riou-Khamlichi *et al.*, 1999), cytokinin-regulated developmental processes were focused upon.
- As some redundancy between the three *CYCD3* genes involved in the regulation of petal and leaf growth has been shown (Dewitte *et al.*, 2007), such redundancy within newly identified roles was also investigated.

# Chapter Two: Materials and

## Methods

### **2.1 Plant Growth Conditions**

---

All experiments with *Arabidopsis thaliana* plants were performed either in the *Col-0* (*Columbia-0*) or *Ler* (*Landsberg erecta*) ecotype backgrounds.

#### 2.1.1. Plants in Soil

Plants were grown in one of two plant growth rooms, which had controlled environments with 16 hours of light per 24 hours and were kept at 21°C. Plants were grown in a soil/sand mixture that had one part sand to every three parts soil. Plants were watered when needed which was typically once a week when young and twice a week following bolting.

#### 2.1.2. Seed Sterilization

Seeds to be grown *in vitro* were surface-sterilized to prevent contamination with bacteria or fungi. This was done by submerging the seeds in 2.5 mg/mL sodium dichloroisocyanurate dehydrate (Chlorifix, Bayrol, Germany) in 70% ethanol. Seeds were washed in ethanol three times, and were then dried in a sterile flow-hood before being added to plates.

#### 2.1.3. *In vitro* Growth

Seedlings were grown either on GM or GM roots media as indicated. GM media consisted of 1.5% sucrose, 4.4 g/L Murashige and Skoog medium (MS), 0.5 g/L 2-(N-morpholino) ethansulfonic acid (MES) buffer and 1% agar and was at pH 5.8. GM roots media was used for growing plants vertically with the roots on the surface of the media and contained 1.5% agar, 2.3 g/L MS and 0.75% sucrose.

Prior growth, seeds on plates underwent a stratification treatment that consisted of dark storage at 4°C for three days. For growing seedlings on antibiotic-containing media, seedlings were grown in a growth room with continuous light and a temperature maintained at 21°C. For experiments, seedlings were grown in a Percival growth cabinet (Percival Scientific Inc.) with 16-hour days (125  $\mu\text{mol m}^{-2} \text{s}^{-1}$  light) and a constant temperature of 25°C.

#### 2.1.4. Crossing Plants

To cross plants, the sepals, petals and stamens were removed from recipient flowers to emasculate them. This was performed on the three eldest unopened flowers of a stem. If pollen could be visualized on the stigma of the recipient, the flower was discarded. The pistils were left for two days, at which point pollen from the donor plant was added to them. This was done with forceps cleaned with ethanol to avoid contamination. Success was observed with the subsequent growth of siliques. The strategy for generating the *ant-9 cycd3;1<sub>Ler</sub>* double mutant is described in Chapter 3.

## **2.2 General DNA Techniques**

---

### 2.2.1 Arabidopsis Genomic DNA Isolation

Two techniques were used for the isolation of Arabidopsis genomic DNA. The first used the REExtract-N-Amp™ Plant PCR Kit (Sigma, USA). Green plant tissue was harvested using ethanol-cleaned forceps to avoid sample-to-sample contamination. 50  $\mu\text{L}$  of extraction solution was added to this, samples were vortexed briefly, and were then incubated at 95°C for ten minutes shaking at 300 rpm. Following this, the samples were placed on ice and 50  $\mu\text{L}$  of ice-cold dilution solution was added. Samples were vortexed briefly to mix these solutions. Samples were stored at 4°C. The second technique used for genomic DNA extraction was as follows. Green tissue was harvested as described above. Tissue was then subjected to grinding with a small pestle. 400  $\mu\text{L}$  of a DNA extraction buffer containing 200 mM Tris, 250 mM NaCl, 25 mM EDTA and 0.5% w/v SDS was added. Samples were briefly vortexed then centrifuged at 13000 rpm for one minute. 300  $\mu\text{L}$  of the supernatant was transferred to a new tube. To this was added an equal volume of ice-cold isopropanol for DNA

precipitation. Samples were incubated at RT for two minutes, before centrifugation at 13000 rpm for fifteen minutes. The supernatant was removed, the pellet resuspended in 70% v/v ethanol for washing and precipitation again followed by centrifugation at 13000 rpm for five minutes. The supernatant was removed and the pellets were dried with the tube lids open at room temperature for at least ten minutes to remove any remaining ethanol. The DNA was dissolved in 100  $\mu$ L 1X TE (10 mM Tris-HCl pH8.0, 1 mM EDTA) and stored at 4°C.

### 2.2.2 Plasmid DNA Isolation

Plasmid DNA was isolated using one of two commercial kits: the Wizard® Plus SV Miniprep kit from Promega or the QIAprep® Miniprep kit from Qiagen. For either, bacteria were grown overnight in 2 mL cultures at 37°C shaking at 200 rpm. Cells were pelleted by centrifugation at 4500 rpm for four minutes. For either kit, cells were resuspended in a resuspension solution. For the Promega kit, cells were lysed with a cell lysis solution, then an alkaline protease solution was added to remove proteins. For the Qiagen kit, these two processes were achieved with a single buffer. In each case, a neutralization solution was added, and samples were subjected to centrifugation at 13000 rpm for ten minutes. The supernatant was added to a silica membrane column that retains DNA. Samples in columns were washed with an ethanol-containing wash solution at least twice. Columns were incubated at 70°C for five to eight minutes in fresh tubes to remove any remaining ethanol. DNA was eluted using 1X TE buffer. Samples were stored at -20°C.

### 2.2.3 Isolation of DNA from Agarose Gels and PCR Reactions

DNA fragments, either for cloning or sequencing purposes, were extracted from agarose gels (see 2.2.4 for agarose gel electrophoresis) or PCR reactions using the Macherey-Nagel Nucleospin® Gel and PCR Clean-up kit according to the manufacturer's instructions. To remove pieces of agarose gel containing a DNA fragment of interest, the gel was placed on a blue light illuminator and DNA was visualized through an orange semi-transparent filter. The use of blue light instead of UV minimizes the chances of mutations occurring in the DNA. DNA fragments were excised with clean scalpel blades. For every 100 mg of gel in a

tube, 200  $\mu$ L of buffer NTI was added. Samples were incubated at 50°C for five to ten minutes until the gel had dissolved. The solution was then added to a column containing a silica membrane. For extractions of DNA fragments of interest from PCR reactions, NTI buffer twice the volume of the PCR was added to the PCR. This solution was then added to a column. For agarose gel and PCR extractions, the columns were placed in collection tubes and unwanted solutions and compounds were removed by centrifugation at 11000 *g* for 30 s. Samples were washed with an ethanol-containing wash solution twice. The membrane was dried by centrifugation at 11000 *g* for one minute. DNA was eluted with buffer NE (5 mM Tris/HCl pH 8.5).

#### 2.2.4 Agarose Gel Electrophoresis

Unless stated otherwise, agarose gels were made with 1% w/v agarose in 1X TAE (40 mM TrisAcetate, pH 8.0 and 2 mM Na<sub>2</sub>EDTA). SafeView Nucleic Acid Stain (NBS Biologicals, UK) was used to stain nucleic acids. 5  $\mu$ L of this was added per 100 mL of molten 1X agarose. Samples were added to wells in solution with 1X loading buffer that consisted of 5% v/v glycerol and 0.04% w/v bromophenol blue (1  $\mu$ L of a 6X buffer was added per 5  $\mu$ L nucleic acid solution). To estimate the sizes of nucleic acid fragments, the DNA ladder SmartLadder (Eurogentec) was added to the gel as specified by the manufacturer. Electrophoresis was carried out with a constant voltage between 80V and 100V applied using a BioRad Power Pack 300. Nuclei acids were visualized under UV light with a U:genius (Syngene) transilluminator connected to an integrated camera to acquire gel images.

#### 2.2.5 Determination of Nucleic Acid Concentration

For estimations of DNA concentrations when the DNA of interest was a fragment, band intensity on an agarose gel was compared to the intensity of SmartLadder bands that contain DNA of concentrations specified by the Manufacturer (Eurogentec). For the determination of nucleic acid concentration more precisely, a NanoDrop-1000 spectrophotometer was used (ThermoFisher Scientific, USA). This instrument measures the absorbance of a solution at 260 nm to determine the concentration of nucleic acid. The instrument also measures the absorbance of the solution at 280 nm since proteins, phenol and other

contaminants usually absorb light of this wavelength. A 260/280 absorbance ratio of 1.8 or higher is considered to represent a DNA sample of high quality, whilst a ratio of 2.0 or higher is considered to represent an RNA sample of high quality.

### 2.2.6 Polymerase Chain Reaction (PCR)

All PCR reactions were performed in a Mastercycler Pro Thermocycler (Eppendorf AG, Hamburg). Unless specific primers had to be used, for example at the start codon of a gene of interest, PCR primers (Table 2.1) were designed using the Primer3 tool embedded in MacVector Software (USA). Primers were designed to be between eighteen and 25 nucleotides long, when tails were not required, to have a minimal GC content of 45% when possible, and a minimal melting temperature ( $T_m$ ) of 55°C. The software selected primers based on minimal probability of the formation of secondary structures and primer dimers when primers were in pairs. When DNA sequences greater than 1 kb were to be amplified for cloning purposes, the Phusion High-Fidelity DNA polymerase (Finnzymes, ThermoScientific, USA) was used. To amplify sequences of less than 1 kb for cloning, or for other purposes, one of three DNA polymerase enzyme kits were used:- Qiagen Taq PCR Master Mix Kit (Qiagen, Netherlands), GoTaq® (Promega, USA) or REDExtract-N-Amp™ Tissue PCR Kit (Sigma-Aldrich, USA). The protocols for these enzymes are listed below.

#### **Phusion High-Fidelity DNA Polymerase**

The Phusion High-Fidelity DNA polymerase enzyme is a *Pyrococcus*-like enzyme that has a claimed error rate of  $4.4 \times 10^{-7}$ , making it suitable for high-accuracy cloning. PCR reactions with this enzyme were performed in a 50 µL volume typically containing 1X HF reaction buffer, 200 µM of each dNTP (no dUTP), 0.5 µM each primer, 2 µL template DNA and one unit of enzyme. If reactions were unsuccessful, the GC buffer was used in the place of the HF buffer and DMSO was added at 3%. MilliQ ultrapure water was used to make up the volume to 50 µL. Typical reaction conditions contained an initial 30 s denaturation step at 98°C, then 30 cycles of: denaturation at 98°C for 10 s, annealing for 30 s and extension at 72°C. The annealing temperature was calculated using the Finnzymes  $T_m$  calculator (<http://www.thermoscientificbio.com>). Extension was carried out for 30 s/kb. A

final extension step at 72°C for ten minutes was then carried out. Complete reactions were kept at 4°C.

**Qiagen Taq PCR Mastermix, GoTaq® PCR Master Mix and REExtract-N-Amp™ Tissue PCR Kit**

All enzymes are provided as 2X mixes. PCR reactions were typically performed in a 20 µL volume. The final reaction mixture contained 0.2 µM of each primer, 2.5 units of *Taq* DNA polymerase, 1X reaction buffer, 200 µM of each dNTP (excluding dUTP) and 1 µL DNA template. The final volume was made up to 20 µL using MilliQ ultrapure water. Typical cycling conditions were: initial denaturation at 94°C for three minutes; 30 cycles of:- denaturation at 94°C for 30 s, annealing for 30 s and extension at 72°C for one min/kb; final extension at 72°C for ten minutes. The annealing temperature was determined using the Sigma-Aldrich Tm calculator ([www.sigmaaldrich.com](http://www.sigmaaldrich.com)). Complete reactions were kept at 4°C.

Table 2.1: List of all primers used in this study.

<b>Primer name</b>	<b>Sequence (5' – 3')</b>	<b>Purpose</b>
ANTfwd	agatcccaacggattcaaacagc	Genotyping for ANT or ant-GK allele in ant-GK segregating populations.
ANTrev(1021)	gggctcatggataagctcag	Genotyping for ANT allele in ant-GK segregating populations.
GKLB	atattgaccatcatactcattgc	Genotyping for ant-GK allele in ant-GK segregating populations
ANTex2fwd	cactgagcttatccatgag	Genotyping for ANT allele in ant-9 segregating populations.
ANTgenotrev2	ccatgaagattgaagtggtacttacc	Genotyping for ANT or ant-9 allele in ant-9 segregating populations.
ACEL2	cgtatcggtttctgattaccgtatt	Genotyping for ant-9 allele in ant-9 segregating populations.
ANT_RT3f	catcaccagcatggaagg	qPCR of ANT transcripts.
ANT_RT3r	agtattcctgacgacaatgc	qPCR of ANT transcripts.
D3;1rt-F	gcaagttgatccctttgacc	qPCR of CYCD3;1 transcripts.

D3;1rt-R	cagcttggactgtcaacga	qPCR of CYCD3;1 transcripts.
D3;1longRT_f2	ctctcccctgctaagctaacc	qPCR of putative longer species of CYCD3;1 transcripts.
D3;1LONGRT_R2	ttcctcctccgaatcg	qPCR of putative longer species of CYCD3;1 transcripts.
pANT-ANTcod_fwd	cgccaaagcggccgccccgggatgaagtcttttgtgataatgatg	Amplification of the ANT coding sequence.
GlyLnk-GR-ANTcod_rev	tgctgaaccgcctccacgcgtagaatcagcccaagcagc	Amplification of the ANT coding sequence.
ANTcod-GlyLnk-GR_fwd	cgtaggagcggttcagcaagaaaaaatcaaagggattc	Amplification of the GR domain sequence.
pGREEN35STn-GR_rev	atggccgtctagttatctagattatcatttttgatgaaacagaagc	Amplification of the GR domain sequence.
CYCD3;1-IS-F1	tccaatttcgttcgtagacc	Amplifying the template for transcription of CYCD3;1 RNA probe 1.
CYCD3;1-IS-R1	tctgtaaaccgatgcggtcc	Amplifying the template for transcription of CYCD3;1 RNA probe 1.
CYCD3;1-IS-F1T7	ggatcctaatacgcactactatagggaggtccaatttcgttcgtagacc	Transcription to produce sense CYCD3;1 RNA probe 1.
CYCD3;1-IS-R1T7	ggatcctaatacgcactactatagggaggtctgtaaaccgatgcggtcc	Transcription to produce anti-sense CYCD3;1 RNA probe 1.
CYCD3;1-IS-F2	tgccgcagctacatgatgc	Amplifying the template for transcription of CYCD3;1 RNA probe 2.

Chapter Two: Materials & Methods

CYCD3;1-IS-R2	ctcattctctcagctcctc	Amplifying the template for transcription of CYCD3;1 RNA probe 2.
CYCD3;1-IS-F2T7	ggatcctaatacagactcactatagggagggtccgcagctaccatgatgc	Transcription to produce sense CYCD3;1 RNA probe 2.
CYCD3;1-IS-R2T7	gggatcctaatacagactcactatagggagggtcattctctcagctcctc	Transcription to produce anti-sense CYCD3;1 RNA probe 2.
CYCD3;1-IS-F3	ccaccgtctcctcctctctg	Amplifying the template for transcription of CYCD3;1 RNA probe 3.
CYCD3;1-IS-R3	tatggagtggctacgattgc	Amplifying the template for transcription of CYCD3;1 RNA probe 3.
CYCD3;1-IS-F3T7	ggatcctaatacagactcactatagggaggccaccgtctcctcctctg	Transcription to produce sense CYCD3;1 RNA probe 3.
CYCD3;1-IS-R3T7	ggatcctaatacagactcactatagggagggtatggagtggctacgattgc	Transcription to produce anti-sense CYCD3;1 RNA probe 3.
attB1-pD3;1-frag1	ggggacaagttgtacaaaaaagcaggcttcttctgttccagggtcc	Amplification of fragment 1 of pCYCD3;1 for GW cloning and Y1H screen.
attB2-pD3;1-frag1	ggggaccactttgtacaagaaagctgggtgatgattatacggcgataag	Amplification of fragment 1 of pCYCD3;1 for GW cloning and Y1H screen.
attB1-pD3;1-frag2	ggggacaagttgtacaaaaaagcaggcttgtcatcatcctcttgag	Amplification of fragment 2 of pCYCD3;1 for GW cloning and Y1H screen.

*Chapter Two: Materials & Methods*

attB2-pD3;1-frag2	ggggaccactttgtacaagaaagctgggtatggttttacgtttgcttttac	Amplification of fragment 2 of pCYCD3;1 for GW cloning and Y1H screen.
attB1-pD3;1-frag3	ggggacaagttgtacaaaaaagcaggctcacacatttaataaaaaata aag	Amplification of fragment 3 of pCYCD3;1 for GW cloning and Y1H screen.
attB2-pD3;1-frag3	ggggaccactttgtacaagaaagctgggttggtgggggactaaactcaag	Amplification of fragment 3 of pCYCD3;1 for GW cloning and Y1H screen.
UGT85A1_rtF	aatgagagaaaaggcggtag	qPCR of UGT85A1 transcripts.
UGT85A1_rtR	tcctgtgattttgtcccaa	qPCR of UGT85A1 transcripts.

### 2.2.7 Digestion of DNA with Restriction Endonuclease Enzymes

All restriction enzymes were from New England Biolabs (NEB; USA). Reactions were typically in 20  $\mu$ L volumes, and contained: 0.1 – 4  $\mu$ g DNA, 1X buffer, 1X NEB bovine serum albumin (BSA) when required, 1 – 5 units enzyme/ $\mu$ g DNA and MilliQ ultrapure water. When larger volumes were used, concentrations stayed the same. Reactions were incubated at 25°C or 37°C, depending on the enzyme, for at least two hours. When necessary and possible, enzymes were inactivated as instructed by NEB.

### 2.2.8 Dephosphorylation of 5' Ends

When plasmids were digested with a single enzyme so that DNA fragments could be inserted, the plasmids 5' ends were dephosphorylated using the shrimp alkaline phosphatase enzyme (SAP; Promega). The reaction mixture contained 10 – 20  $\mu$ L of digested vector, 1  $\mu$ L SAP, 1X reaction buffer and water. The total reaction volume was 30  $\mu$ L. The reaction was incubated at 37°C for fifteen minutes. The enzyme was then inactivated at 65°C for fifteen minutes.

### 2.2.9 Blunting Reaction

When DNA fragments were to be cloned into vectors with blunt ends, for example using the pCR-Blunt® vector (Invitrogen, USA), the ends of the fragments to be inserted were blunted using the T4 DNA polymerase (NEB, USA). This enzyme exhibits 3' – 5' exonuclease activity, and so cleaves any 3' overhang and fills in any 5' overhang. The reaction was performed with one unit of enzyme per  $\mu$ g DNA and 1X T4 DNA polymerase buffer. This reaction was incubated at 12°C for fifteen minutes. The reaction was stopped by adding EDTA to a final concentration of 10 mM and incubating the reaction at 75°C for twenty minutes.

### 2.2.10 Ligation

Other than for TOPO® cloning, DNA fragments were ligated into vector backbones using the T4 DNA ligase enzyme (NEB, USA). A typical ligation

reaction contained 6  $\mu\text{L}$  of the vector backbone, 2  $\mu\text{L}$  of the fragment to be inserted (or the same volume of water in a negative control), 1  $\mu\text{L}$  of enzyme and 1  $\mu\text{L}$  of the reaction buffer. Molar quantities of vector and insert were added at ratios between 1:1 and 1:3 for vector:insert, respectively, and therefore the volumes of vector and insert were sometimes different from above. The reaction was incubated at 16°C for one hour or 4°C overnight. When ligated products were not to be used for transformation immediately, they were stored at -20°C.

#### 2.2.11 TOPO®-TA Cloning (Invitrogen, USA)

TOPO®-TA cloning takes advantage of the 3' A overhang left on DNA amplicons by *Taq* DNA polymerase. Invitrogen supply a vector named pCR2.1, which is pre-digested to leave two ends with 3' T overhangs. These ends are covalently linked to the topoisomerase 1 enzyme from the *Vaccinia* virus, which ligates the fragment to be inserted to the vector backbone. For a typical TOPO®-TA reaction, 4  $\mu\text{L}$  PCR product was added to 1  $\mu\text{L}$  salt solution and 1  $\mu\text{L}$  pCR2.1 vector. The reaction was incubated at RT for 30 minutes, and was then kept on ice prior to transformation.

#### 2.2.12 TOPO®-Blunt Cloning

TOPO®-Blunt cloning allows quick insertion of blunt-ended PCR products into the pCR-Blunt II-TOPO® vector. The principals are the same as those for 2.2.11, other than the ends of the linearized vector and insertion fragment having no overhangs, but the reaction is slightly different. A typical reaction contained 1  $\mu\text{L}$  linearized vector, 1 – 5  $\mu\text{L}$  PCR product, 2  $\mu\text{L}$  ligation buffer and MilliQ ultrapure water to 10  $\mu\text{L}$ . Reactions were incubated at 16°C for one hour. Reactions were kept on ice prior to transformation.

#### 2.2.13 BP and LR Reactions for Gateway Cloning

Invitrogen Gateway® cloning uses site-specific recombination based on a system from the bacteriophage lambda to insert DNA fragments into vectors, and if wished to assemble multiple fragments at once. Recombination occurs between *att* sites, which can be added to the ends of PCR products via primer tails, but are also present in sub-cloning vectors that your fragment/s of

interest can be inserted into via other means. Gateway sub-cloning vectors are called donor vectors (pDONR). These contain *attP* sites. Addition of *attB* sites to a DNA fragment allows the insertion of the fragment into the donor vector. The *att* sites are then changed and are called *attL* sites. The vector is then called an entry vector (pENTR), and recombination can occur between the *attL* sites in this vector and the *attR* sites in a destination vector (pDEST). The destination vector is the final vector that will be used for plant or yeast transformation purposes (in this study). To carry out BP and LR recombination reactions, the BP and LR clonase enzyme mixes (Invitrogen, USA) were used, respectively. A BP recombination reaction contained the following: 20 – 50 fmoles of *attB* PCR product (1 – 7  $\mu$ L), 1  $\mu$ L of the pDONR vector that is supplied at 150 ng/ $\mu$ L, 2  $\mu$ L BP clonase enzyme mix (added last) and 1X TE buffer pH 8.0 to a final volume of 8  $\mu$ L. The reaction was incubated at 25°C for one hour. To inactivate the enzymes, 1  $\mu$ L of 2  $\mu$ g/ $\mu$ L proteinase K solution was added and the reactions were incubated at 37°C for ten minutes. 1  $\mu$ L of the reaction was used for *E. coli* transformation. The LR reaction was as above other than that 10 fmoles of the entry clone and 20 fmoles of the destination vector were used, the LR clonase enzyme mix was used in place of the BP mix, and the reaction was incubated at 25°C for 16 hours or overnight.

#### 2.2.14 DNA Sequence Analysis

All DNA sequences were obtained via an external service that used the ABI3730XL Sequencing Analyser of MWG Eurofins, (London, UK). Samples were prepared as specified by the provider of this service; typically 15  $\mu$  L of sample containing 50 ng/ $\mu$ L of DNA was sent. This service employs Sanger sequencing (Sanger *et al.*, 1977). Analyses of chromatograms were performed using MacVector software (MacVector, Inc., USA) or Sequencher 4.0 software (Gene Codes Corporation, USA). The identity of sequences was analysed using the NCBI Blast tool via <http://blast.ncbi.nlm.nih.gov> or <https://www.arabidopsis.org>.

## 2.3 General *Escherichia coli* Techniques

---

### 2.3.1 *E. coli* Strains and Growth Conditions

For standard procedures, DG1 *E. coli* cells (Eurogentec, Belgium) were used. For the transformation of Gateway® products, OneShot TOP10 (Invitrogen, USA) cells were used. Empty Gateway® vectors contain the lethal *ccdB* gene that is removed or inactivated during recombination. To grow cells with these empty vectors, *ccdB* survival cells (Invitrogen, USA) were used. *E. coli* were grown at 37°C, either on solid LB media (5 g/L yeast extract, 100 g/L bacto-tryptone, 10 g/L NaCl and 15 g/L bacto-agar, pH7.0) or in LB liquid broth (LB media lacking bacto-agar). Liquid cultures were shaken at 200 rpm.

### 2.3.2 *E. coli* Transformation

Chemically competent *E. coli* were used for plasmid transformation. Typically 1 - 2 µL DNA was added to the cells on ice, and the cells were incubated with this DNA, on ice, for 5 – 30 minutes. Cells were then heat-shocked at 42°C for 40 s. Cells were recovered on ice for 5 min, and were incubated with 250 µL LB broth for 1 hour at 37°C shaking at 200 rpm. 50-200 µL of cells were added to LB plates containing appropriate selection agents and were incubated overnight at 37°C.

### 2.3.3 Transformant Selection

Transformants were selected on LB media containing appropriate antibiotics. Antibiotics were used at the following concentrations: Kanamycin 50 µg/mL; zeocin 25 µg/mL; ampicillin 50 µg/mL. Products of Gateway® reactions underwent additional selection via the *ccdB* gene, which kills the cell when present. This gene is displaced by recombination. The products of TOPO®-Blunt ligation reactions underwent a similar selection, in which the sequence distance between a *PLac* promoter and the *ccdB* gene is increased when a fragment is inserted into the vector, so that expression of *ccdB* no longer occurs. This selects against recircularised vectors. The products of TOPO®-TA reactions were selected via a blue-white assay as well as on antibiotics. DNA fragments are inserted between the *PLac* promoter and the *lacZα* gene,

disrupting expression of the gene. X-gal assays were performed by spreading 32  $\mu\text{L}$  of 25 mg/mL X-Gal dissolved in dimethylformamide (DMF) and 20  $\mu\text{L}$  of 200mg/mL IPTG onto the LB media prior to spreading the cells onto it. IPTG activates the *Plac* promoter and X-gal is a substrate of the *lacZ $\alpha$*  product. Expression of the *lacZ $\alpha$*  gene resulted in the colonies turning blue after overnight growth at 37°C. White colonies were therefore considered to be true positives. To check that colonies contained the correct DNA insertion, colony PCR was performed initially. This was done by adding a small amount of *E. coli* cells to a PCR reaction containing primers specific for the insertion. Plasmids were extracted from colonies that yielded correctly sized amplicons, and restriction enzyme digestions that could distinguish between the vectors with and without the correct insertion were used for confirmation. Ultimately, plasmids were sent for sequencing to ensure that the sequence was correct.

## 2.5 Generation of Transgenic Arabidopsis Plants

---

Arabidopsis plants were transformed using the GV3101 strain of *Agrobacterium tumefaciens* (Agrobacterium) that contains the pMP90 Ti plasmid and a rifampicin resistance gene on one of its chromosomes. The floral dip method (Clough and Bent, 1998) was employed.

### 2.5.1 Agrobacterium Transformation

1  $\mu\text{L}$  of plasmid was added to electrocompetent cells that had been thawed on ice, and this solution was added to an electroporation cuvette that had been chilled on ice. A voltage of 2.4 kV was briefly applied to the cells using an electroporation apparatus (BioRad, USA). 1 mL of LB broth was added to the cells, and they were transferred to a 1.5 mL tube for recovery at 28°C for 2 hours shaking a 200 rpm. Cells were then spread onto LB agar plates containing 20  $\mu\text{g}/\text{mL}$  gentamycin to select for the pMP90 plasmid, 50  $\mu\text{g}/\text{mL}$  rifampicin to select against other bacteria and the selective agent required to select for the binary vector. Plates were incubated at 28°C for 2 days. Colonies were checked for the presence of the binary vector by colony PCR as in 2.3.3.

### 2.5.2 Transformation of Arabidopsis Plants

Plants for transformation were grown in pots with five plants per pot. Following bolting, the primary stems were cut to promote the growth of auxiliary stems and the presence of a greater number of flowers. Plants were used for transformation 10-12 days after cutting. 5 mL LB broth containing 20 µg/mL gentamycin, 50 µg/mL rifampicin and another selective agent for the binary vector was inoculated with a single colony of *Agrobacterium*. Cultures were incubated at 28°C for 24 hours shaking at 200 rpm. 1 mL of this culture was then used to inoculate 200 mL of the same media, and this was incubated for 24 hours. Cells were pelleted by centrifugation at 4500 rpm for 5 minutes. The supernatant was discarded and cells were resuspended in infiltration medium (5% sucrose, 0.05% silwet) to an OD<sub>600</sub> of 0.8. Plants were dipped into this solution for 30-60 s and were kept in dark moist conditions overnight by placing plastic bags over them. Following this, plants were grown under normal conditions for 2-3 weeks.

### 2.5.3 Recovery of Transgenic Plants

The untransformed seeds of the plants in 2.5.2 are termed T0s, whereas those that were transformed are termed T1s. To identify the T1s, the seeds were surface sterilized and placed on GM media containing the appropriate selective agent for the marker on the inserted T-DNA fragment as well as 200 µg/mL cefotaxime to kill any remaining *Agrobacteria* on the seeds. Plants with hygromycin resistance were identified by the growth of true leaves following 10-12 days of growth on media with 50 µg/mL hygromycin. Those with kanamycin resistance grew greener and faster than those without, as did those with phosphinothricin (PPT) resistance. This was visible after 7-10 days of growth. Kanamycin and PPT were used at 50 µg/mL and 15 µg/mL, respectively. Resistant seedlings were transferred to soil.

## **2.6. Genotyping**

---

*ant* homozygous plants are female sterile, and so must be obtained from the offspring of a heterozygous parent i.e. segregating populations. In any

experiment where *ant* mutants were used for analyses, plants were genotyped. DNA was extracted from plants as described in 2.2.1. Two PCR reactions were performed per plant, one to detect the presence of the *ANT* allele, and one to detect the presence of the *ant* allele. See Table 2.1 for primer sequences. For *ant-9* genotyping, the *ANT* allele was detected using primers flanking the site of the Ac transposon insert (ANTgenotrev2 & ANTex2fwd). The *ant-9* allele was detected using one primer for the left border of the Ac transposon (ACEL) and one 3' of the insert within the *ANT* gene (ANTgenotrev2). The following PCR reaction was performed using either set of primers: initial denaturation at 94°C for 3 min, followed by 35 cycles of [94°C for 1 min, 52°C for 1 min, 72°C for 1 min], and finally a 10 min elongation step of 72°C. For *ant-GK* genotyping, the *ANT* allele was detected using primers flanking the site of the T-DNA insert (ANTfwd & ANTrev(1021)). The *ant-GK* allele was detected using one primer for the left border of the T-DNA insert (GKLB) and one 3' of the insert within the *ANT* gene (ANTfwd). A PCR with the same cycling conditions as those above but with an annealing temperature of 55°C was used. DNA samples which yielded a product when using the *ANT*-specific primers but not using the *ant*-specific primers were assumed to come from *ANT* homozygotes, and samples which yielded a product when using *ant*-specific primers but not *ANT*-specific primers were assumed to come from an *ant* homozygote. PCR genotyping using the same PCR parameters as for *ant-9* genotyping was used to screen for *cycd3;1* mutants during the generation of plants containing *ant-9* and *cycd3;1* alleles on the same chromosome. The following primers were used for the mutant allele: genoD3-1F & SUNDA\_DS5. genoD3-1F & genoD3-1R were used for the *WT* allele.

## 2.7. Histological and Microscopical Analyses

---

Unless stated otherwise, light microscopy was performed either with a Leica SP5 compound microscope (Leica, Germany), or a Zeiss AX10 ImagerM1 (Zeiss, Germany) coupled with an AxioCam MRc5 camera. Confocal microscopy was performed using a Zeiss LSM 7 (Zeiss, Germany) line scanning confocal microscope.

### 2.7.1 Preparation of Petals and Leaves

Petals were fixed and cleared in a solution of 10% acetic acid, 50% methanol overnight. They were then incubated for at least an hour in 80% chloral hydrate. To identify the third leaf of a plant, a piece of cotton was tied around the leaf when it was between 3 and 8 mm long. Leaves were fixed and cleared by overnight incubation in 100% methanol followed by incubation in 60% lactic acid. Petals and leaves were mounted on microscope slides in the same solutions they came from.

### 2.7.2 X-gluc Assay for $\beta$ -glucuronidase

To assay for  $\beta$ -glucuronidase activity, samples were first incubated in 90% acetone for 15 min to increase the permeability of cell membranes. Samples were then washed in 100 mM sodium phosphate (NaPi) buffer pH7. Samples were incubated in the following reagent for 16 hours: 1mg mL<sup>-1</sup> 5-bromo-4-chloro-3-indolyl-beta-D-glucuronic acid cyclohexylammonium salt (X-Gluc) dissolved in dimethyl formamide, 0.5 mM K-ferrocyanide, 0.5 mM K-ferricyanide, 0.01% polyoxyethylene sorbitan monolaurate, all dissolved in 100 mM NaPi buffer pH7. Following the 16-hour incubation, samples were incubated in 100% methanol to clear tissue. Signal was assessed by eye using a Leica MZ 16F binocular microscope, and pictures were taken using the Leica DFC42 DC camera.

### 2.7.3 Preparation of Root Sections

Cross-sections of roots were created by embedding in plastic and sectioning with a microtome. Initially, plant root material was fixed in a fixative of 1% v/v glutaraldehyde, 4% v/v formaldehyde and 100 mM NaPi buffer (pH7.2). Roots were kept in this fixative for three hours at RT or longer at 4°C. Next, the roots were dehydrated with an ethanol series. This started with incubation in 10% ethanol, then went through steps of 30%, 50%, 70%, 96% and two 100% ethanol steps. Each step was 30 minutes long. The first step of plastic embedding was then performed. The roots were incubated in 50% ethanol in a solution of basic resin and 1% w/v hardener powder from the Technovit® 7100 embedding kit (Heraeus Kulzer, Germany). Infiltration of the roots with the resin was aided by placing them in a vacuum for one minute. The roots were left in

this solution for at least 1.5 hours. Next, this solution was replaced with the basic resin and 1% w/v hardener powder alone. The roots were subjected to a vacuum for one minute again. The roots were left in this solution for at least 1.5 hours. The roots needed to be orientated so that they could be cut later at a specific angle (perpendicular to the direction of root growth). Roots were placed in shallow chambers. These were created by adhering double-sided sticky tape either side of an overhead projector transparency sheet (3M, USA), cutting a square hole (roughly 15 x 7 mm) through all layers, and then attaching another transparency sheet to one side. A solution of basic resin, 1% w/v hardener powder and 6% v/v hardener liquid was added to them. A plastic cover was placed on top of the chamber, since air inhibits the hardening process. Once hard, flat pieces of plastic containing roots were cut with a scalpel blade, to remove rectangular slices in which one edge is perpendicular to the direction of root growth. These slices were then piled atop one another, with the edges perpendicular to the root pushed flush against the side of a square petri dish. The slices were stuck together using the solution of basic resin, 1% w/v hardener powder and 6% v/v hardener liquid. This created stacks of roots all orientated in the same direction. These stacks were placed with the roots facing downwards into moulds, which were filled with the embedding solution containing hardener liquid. Three days later, the newly formed blocks of plastic were glued to wooden cylinders, using Superglue, whose size was compatible with the microtome attachment. A Leica microtome with T-95 disposable blades was used for sectioning this material. For secondary growth analysis, sections of 3 µm were taken. For *GUS* expression detection, sections of 7 µm were taken. For analysis of the primary meristem, 5 µm sections were taken. Sections were placed on Superfrost slides (Fisher Scientific, USA). Non-*GUS*-stained samples were stained with 1% w/v toluidine blue (Fisher Scientific, USA) in 0.5% w/v sodium tetraborate ("borax").

#### 2.7.4 *In situ* Hybridisation

This procedure was conducted in the laboratory of Yka Helariutta in Helsinki University, Finland. All solutions were made with DEPC-treated water. Cut root tissue was fixed in 4% paraformaldehyde, washed in 100 mM phosphate-buffered saline (1X PBS) and embedded in 1% SeaKem LE-agarose (Lonza, Switzerland) for tissue orientation. Tissue was then dehydrated in an ethanol series, and cleared with 100% xylene. The sample was embedded in molten

Histoplast (paraffin; Thermo Scientific, USA), and oriented and set in blocks. Sections were taken with a Leica microtome using Leica 819 disposable blades. Sections were then cleared further with xylene, and rehydrated with an ethanol series. Samples were treated with 0.85% NaCl, then 0.2 M HCl, then washed in 2X SSC (300 mM sodium chloride, 30 mM trisodium citrate, pH7.0). Proteins were degraded and removed by incubation with proteinase K (Thermo Scientific, USA) in 100 mM Tris pH7.5, 50 mM EDTA followed by washes in 1X PBS. 0.85% NaCl treatment was repeated, and then samples were dehydrated using another ethanol gradient series. Prehybridisation and hybridisation occurred in a formamide atmosphere. Prehybridisation and hybridisation buffers contained formamide, salts, Denhart's blocking agent (1% Bovine Serum Albumin, 1% ficoll and 1% polyvinylpyrrolidone in water), tRNA and RNase inhibitor. T7 in vitro transcription was used to produce sense and antisense DIG-labelled RNA probes, which were used in hybridisation. Template DNA containing the *CYCD3;1* coding sequence was used to create a template with sites at the ends recognised by the T7 DNA-dependent RNA polymerase. Three antisense and three sense probes were created, each corresponding to non-overlapping sequences in *Arabidopsis* to *CYCD3;1*. Primers used to create templates for these probes are listed in Table 2.1. Primer pairs share the same number. Primers with T7 tails are indicated. For each pair, one primer would have a T7 tail whereas the other would not. If a forward primer contained a T7 tail, the template would be used to create an antisense probe, and vice versa. RNA synthesis was performed using the Roche DIG RNA labelling kit (cat. no. 1 175 025). Probes were added at two concentrations: 0.25 and 0.5 µg/mL/kB. Post-hybridisation, slides were washed in 5 x SSC in 50% formamide. RNase treatment was performed with a solution of 10 µg/mL RNase A, 0.5 M NaCl, 10 mM Tris pH8.0 and 5 mM EDTA. Further washes with 0.5 x SSC/50% formamide then 1 x PBS were performed. An anti-digoxigenin-alkaline phosphatase-conjugate was used, with FastRed as a substrate (Roche), for detection of the probe.

### 2.7.5 Quantification of Cell File Number within the Primary Vasculature

To count the number of cell files within the vasculature of the primary meristem, optical transverse sections of 5 DAG (days after germination) roots at the position of the seventh cortical cell were visualized with a Zeiss LSM 710 confocal microscope coupled with a CCD camera. Roots were fixed in a solution

of 50% methanol and 10% acetic acid, and were then incubated in 1% periodic acid. Roots were stained with a solution of 2% W/V sodium metabisulphate, 6 mM HCl and 0.1 mg/mL propidium iodide. Samples were mounted in chloral hydrate solution.

## **2.8. Flow Cytometry**

---

The CyStain UV Precise P kit (Partec, Japan) was used for nuclei extraction and DNA staining. Arabidopsis petals were cut into thin pieces using a razor blade repeatedly at different angles, in an empty petri dish. 100  $\mu$ L of nuclei extraction solution was added to the tissue, rinsed over it repeatedly and passed into a tube through a filter that removed plant tissue. The remaining plant tissue in the petri dish was rinsed with another 100  $\mu$ L nuclei extraction buffer, which was again passed through a filter into the tube. To stain DNA, 1 mL of DNA staining solution was added and the solutions were mixed. The solution was then analysed in a Partec CyFlow Space instrument (Partec, Japan), using the FL2 channel for laser excitation at 375 nm. Liquid was passed through the machine at 1  $\mu$ L/s and the gain was set to 384. Histograms were created in Cyflogic software (CyFlo Ltd, Finland).

## **2.9. RT-qPCR Analyses**

---

### **2.9.1. RNA Isolation**

Due to the abundance of RNase enzymes, care was taken throughout this procedure to avoid RNase contamination. Gloves were always worn, and clean autoclaved 1.5 mL tubes and pipette tips were used. All centrifugation was performed at 4°C. Any water used was ultrapure MilliQ. RNA was extracted from plants using the phenol-containing TriPure isolation reagent (Roche, Switzerland). All equipment coming into contact with the plant tissue before the addition of this reagent was kept cold using liquid nitrogen. Between 100 mg and 500 mg of plant tissue was used for RNA extraction. Plant tissue was frozen with liquid nitrogen, and was subsequently ground, either using a porcelain pestle and mortar, or a smaller plastic pestle and a 1.5 mL tube. Ground tissue

was sometimes frozen at  $-80^{\circ}\text{C}$  prior to the remainder of the extraction protocol. 1 mL of TriPure reagent was added to each sample, and the sample was allowed to thaw. Once thawed, this mixture was mixed by inversion and incubated at room temperature for five minutes or more. 200  $\mu\text{L}$  of ice-cold chloroform was next added, and the sample was mixed thoroughly and incubated on ice for 15 minutes, with occasional mixing. Following this, the sample was centrifuged at  $12000 \times g$  for 15 minutes. This resulted in phase separation, with DNA and protein being in the lower, coloured organic phase, and RNA being in the upper colourless aqueous phase. The upper phase was transferred to a new tube, and an equal volume of ice-cold isopropanol was added to this to precipitate the RNA. The samples were mixed by inverting several times, and were incubated for at least ten minutes on ice. To pellet the RNA, the samples were centrifuged at 14000 rpm for ten minutes. The supernatant was discarded and the sample was washed by resuspension in 70% ethanol and centrifugation at 14000 rpm for five minutes, twice. To remove all ethanol, samples were air-dried for at least five minutes. RNA was dissolved in 100  $\mu\text{L}$  water. Some contaminating DNA can remain at this point, and this can affect qPCR results. To remove any remaining DNA, the Ambion® DNA-free kit (Life Technologies, USA) was used. 11  $\mu\text{L}$  of the 10X DNase buffer and 1  $\mu\text{L}$  of the DNase were added to each sample, and the mixture was incubated at  $37^{\circ}\text{C}$  for one hour. To inactivate the DNase, which would otherwise interfere with cDNA synthesis and qPCR, 11  $\mu\text{L}$  of the Ambion® DNase inactivation reagent was added. Samples were mixed and incubated at RT for five minutes. Samples were centrifuged at  $10000 \times g$  for two minutes. This causes the inactivation reagent to separate into a lower phase. The upper phase was transferred to a new tube.

### 2.9.2 cDNA Synthesis

One of two commercial kits was used for cDNA synthesis.

#### **Ambion RETROscript® (Life Technologies, USA) cDNA synthesis kit**

0.5-1.0  $\mu\text{g}$  of RNA was added to 2  $\mu\text{L}$  oligod(T) and MilliQ ultrapure water was used to make the volume up to 12  $\mu\text{L}$ . To denature the RNA, this mixture was incubated at  $85^{\circ}\text{C}$  for five minutes. The mixture was then allowed to cool on ice to allow the annealing of oligod(T) primers to mRNA poly(A) tails. The following cDNA synthesis reaction components were then added:- 4  $\mu\text{L}$  dNTP mix, 2  $\mu\text{L}$

10X reaction buffer, 1  $\mu\text{L}$  RNase inhibitor and 1  $\mu\text{L}$  MuMV RTase. The reaction was mixed and incubated at 42°C for one hour. To inactivate the RTase enzyme, the reaction was then incubated at 95°C for 5-10 minutes. The total volume was made up to 400  $\mu\text{L}$ . Samples were stored at -20°C.

**RevertAid® (ThermoScientific, USA) cDNA synthesis kit**

0.5-1.0  $\mu\text{g}$  RNA was added to 2  $\mu\text{L}$  50  $\mu\text{M}$  oligod(T) and MilliQ ultrapure water was used to make the volume up to 12.5  $\mu\text{L}$ . This mixture was incubated at 65°C for five minutes then chilled on ice. The following components were then added:- 4  $\mu\text{L}$  5X reaction buffer, 0.5  $\mu\text{L}$  RiboLock® RNase inhibitor, 2  $\mu\text{L}$  dNTP mix and 1  $\mu\text{L}$  RevertAid RTase. The reaction was incubated at 42°C for one hour. Enzyme inactivation was by incubation at 70°C for 10 minutes. 100  $\mu\text{L}$  of water was added for dilution.

2.9.3. Quantitative PCR (qPCR)

One of two commercial kits was used for qPCR. The first was the ABsolute QPCR SYBR Green Master Mix (Thermo Scientific, USA). This 2X master mix contains all of the reagents required for qPCR, including DNA polymerase and SYBR Green I dye that fluoresces when bound to double-stranded DNA, bar the template and primers. The second kit was the pPCRBIO SyGreen master mix (PCR Biosystems Ltd, UK), which is also a 2X master mix and contains components similar to those of the other kit. For either of these kits, qPCR reactions were performed in 10  $\mu\text{L}$  volumes in a Rotorgene 6000 light-cycler (Qiagen, USA). 5  $\mu\text{L}$  of the master mix was added to 2.5  $\mu\text{L}$  of a working primer stock containing 1.25  $\mu\text{M}$  of each primer and 2.5  $\mu\text{L}$  of template cDNA. Reaction conditions for the Absolute QPCR SYBR Green master mix were as follows: initial denaturation and enzyme activation at 95°C for 15 min, followed by 45 cycles of [95°C 30s, 55°C for 30s, 72°C for 30s] and a final elongation step at 72°C for 90s. Reaction conditions were as follows for the pPCRBIO SyGreen mix: initial denaturation at 95°C for 2 min, followed by 45 cycles of [95°C for 5s, 60°C for 30s]. The DNA polymerase enzyme in the pPCRBIO SyGreen mix is optimized for activity at 60°C; hence the primer annealing stage and elongation stage are amalgamated. For both reagents, melt curve analysis was performed following qPCR. This is done to determine whether or not different products are present in the reaction at the end of qPCR, since altered length and/or nucleotide composition change the melting temperature of the dsDNA molecule.

This is visualized by the machine as a loss of fluorescence. This also allowed the comparison of the products in the samples and the no template controls, to ensure that product specific to the target was the primary product in the samples. A melt curve was generated by increasing the temperature from 72°C to 95°C in incremental 5s steps rising 1°C each. When new primers were used, the products were also visualized using gel electrophoresis to ensure that there were not similar products in reactions containing sample and no template controls.

#### 2.9.4. qPCR Data Analysis

The number of cycles taken for logarithmic amplification to occur was determined using the Rotor-Gene software (Qiagen, USA). Transcript levels were normalized to those of *ACT1N2*, which were detected using the same reaction conditions and primers ssACT2rtF & ssACT2rtR. mRNA levels were quantified using the  $2^{-(\Delta\Delta C(T))}$  method (Livak and Schmittgen, 2001).

### **2.10. Yeast-one-hybrid (Y1H) Assays**

---

#### 2.10.1 Yeast media

YPD solid media consisted of: 20g glucose (added and dissolved first), 20g peptone, 10g yeast extract and 18g agar. This was all dissolved and autoclaved in 1L water.

YPDA solid media consisted of the same ingredients as YPD as well as 100mg adenine.

SD solid media consisted of 26.7g minimal SD base (added and dissolved first) and 18g agar dissolved in 1L water plus the following quantities of drop-out supplements for the respective medias:- 0.69g leucine drop-out supplement for SD-leu; 0.74g tryptophan drop-out supplement for SD-trp; 0.64g leucine/tryptophan drop-out supplement for SD-leu-trp.

All liquid media was made with the above ingredients minus agar at the same concentrations.

### 2.10.2. Yeast transformation

1 mL YPD/A media was inoculated with yeast colonies, vortexed for five minutes to remove any clumps and transferred to 50 mL YPD/A in a flask. This culture was grown overnight shaking at 250 rpm at 30°C until an OD<sub>600</sub> of 1.5 or greater was achieved, representing a stationary phase culture. 30 mL of this culture was transferred to a flask containing 300 mL YPD. If the new OD<sub>600</sub> was less than 0.2, more of the starter culture was added. This culture was incubated for three hours at 30°C shaking at 230 rpm. The culture was transferred to 50 mL tubes and cells were pelleted by centrifugation at 1000 x *g* for five minutes. The supernatant was discarded and the cells were resuspended in sterile 1X TE buffer. All of the cells were pooled into one 50 mL tube with a final volume of 25-50 mL. Cells were pelleted once again by centrifugation at 1000 x *g* for five minutes. The supernatant was discarded, and cells were resuspended in a solution of 1X TE and 100 mM LiAc. 0.1 µg of the DNA to be transformed and 0.1 mg of Salmon sperm DNA (Sigma-Aldrich, USA), which had been boiled for ten minutes then cooled on ice for five minutes, were mixed together in a fresh 1.5 mL tube. 0.1 mL of the yeast cells were added to each such tube, as was 0.6 mL of a sterile solution of 40% polyethylene glycol (PEG) 4000 (Sigma-Aldrich, USA), 1X TE and 100 mM LiAc. This mixture was vortexed for 10 s and incubated at 30°C for 30 minutes shaking at 200 rpm. 70µL 100% DMSO was added, and the cells were subjected to a heat shock by transferring them to a 42°C heat block for 15 minutes. Cells were chilled on ice for two minutes and by centrifugation at 14000 rpm for 10 s. The supernatant was carefully removed. Cells were resuspended in water, and the cell suspension was spread on agar plates containing selective agents or lacking amino acids for selection of the DNA of interest. Plates were incubated at 30°C for two to three days or until colony growth was visible. Colonies were restreaked onto fresh selective plates, and new colonies were used for the Y1H assays.

### 2.10.3. One-on-one Y1H

#### **Yeast transformation**

The Y1H assay was done with the assistance of Emily Sornay (Cardiff, UK). Strains containing the *LacZ* reporter downstream of the optimal ANT-binding sequence (ABS) (Nole-Wilson and Krizek, 2000), a sequence from *pCYCD3;1*

or no sequence were created initially. The optimal ABS is GCACGTTTCCATAG, and is flanked by CTGTAA at the 5' end and ACCAAGT at the 3' end. The putative ANT-binding sequence from *pCYCD3;1* is GCACGTTTCCATAG and is flanked by the same sequences at the same relative positions. Yeast of the YM4271 strain (*MATa*, *ura3-52*, *his3-200*, *ade2-101*, *ade5*, *lys2-801*, *leu2-3, 112*, *trp1-901*, *tyr1-501*, *gal4D*, *gal8D*, *ade5::hisG*) were transformed with linearized *pLacZi* vectors. The *NcoI* restriction enzyme was used for the digestion. The resulting DNA can undergo homologous recombination at the *URA3* locus, which results in the integration of a functional *URA3* gene, thus restoring uracil prototrophy. Thus transformants were selected for on media lacking uracil. These YM4271 transformants containing the reporters were then transformed with pGAD424 vectors containing *ANT* or a dominant negative form of *ANT* (*ANT*<sub>Δ281-357</sub> that exhibits DNA-binding activity but no transactivation activity (Krizek and Sulli, 2006)).

#### **X-gal assay**

Yeast colonies from the transformation were streaked onto fresh selective plates. After two days of growth, these plates were replica plated onto SD agar plates (2.10.1) containing 80 mg/L X-gal and 1X NaPi buffer, pH 7.0. These plates were then incubated at 30°C for 4-6 days, and the plates were checked regularly for the development of a blue colour.

#### 2.10.4. Y1H Screen

##### Yeast Transformation

For transformation of yeast with the pHISLEU2 vector containing the *CYCD3;1* promoter fragments (2.4), yeast of the haploid Y187 strain (*MAT $\alpha$* , *ura3-52*, *his3-200*, *ade2-101*, *trp1-901*, *leu2-3*, 112, *gal4 $\Delta$* , *met-*, *gal80 $\Delta$* , *MEL1*, *URA3::GAL1<sub>UAS</sub>-GAL1<sub>TATA</sub>-lacZ*; Clontech, USA) was used. Transformation of yeast with the transcription factor library was carried out at Warwick University by Peijun Zhang, in the haploid AH109 strain (*MAT $\alpha$* , *trp1-901*, *leu2-3*, 112, *ura3-52*, *his3-200*, *gal4 $\Delta$* , *gal80 $\Delta$* , *LYS2 : : GAL1<sub>UAS</sub>-GAL1<sub>TATA</sub>-HIS3*, *GAL2<sub>UAS</sub>-GAL2<sub>TATA</sub>-ADE2* *URA3 : : MEL1<sub>UAS</sub>-MEL1<sub>TATA</sub>-LacZ MEL1*; Clontech, USA). In both cases, YPDA media was used.

##### Y1H Assay

Day 1: Cultures of the yeast containing the transcription factor library were set up in Warwick University by Peijun Zhang. This was done in three 96-well plates with 2.2 mL-deep wells. 96-well plates containing glycerol stocks of the yeast were kept at -80°C. To inoculate new cultures for the assay, these stock plates were removed from -80°C and placed on ice. A sterile 96-prong hedgehog was used to scratch cells from the surface and to transfer these cells to the new plates, which were then placed into a 30°C incubator shaking at 900 rpm.

Day 4: For each of the three yeast strains containing the *CYCD3;1* promoter fragments, a 10 mL SD-leu culture was inoculated with fresh colonies. These cultures were incubated at 30°C overnight shaking at 200 rpm.

Day 5: Yeast containing the transcription factors were mated with the yeast containing the promoter fragments. This was done on YPDA plates without any selection. Using an 8-well pipette, 3  $\mu$ L of promoter fragment-containing yeast culture from each well was spotted onto YPDA plates, in a similar 96-spot format. These spots were allowed to dry, before 3  $\mu$ L of transcription factor-expressing yeast from each well was spotted on top. The spots were again allowed to dry, and were then incubated overnight at 30°C.

Day 6: The YPDA plates from day 5 were replica plated onto SD-leu-trp plates with or without 3-amino-1,2,4-triazole (3-AT) to select for yeast in which the Arabidopsis transcription factor was binding to the *CYCD3;1* promoter fragment. These plates were incubated at 30°C overnight.

Day 7: To remove leftover yeast from the YPDA plates, a piece of sterile filter paper was pressed against each plate. Plates were incubated at 30°C for three days.

Day 10: Yeast were scored for growth to identify those which expressed a transcription factor that bound to a *CYCD3;1* promoter fragment. Pictures of yeast plates were obtained using a digital scanner. From each position that yeast were growing substantially, five colonies were taken and spread in patches on fresh selective plates (SD-leu-trp). These plates were incubated at 30°C overnight.

### **Identification of transcription factors**

To identify the transcription factors that bound to *CYCD3;1* promoter fragments, yeast colony PCR with the Qiagen Taq PCR Mastermix (2.2.6.) was performed. A small amount of yeast was smeared onto the bottom of a 200 µL PCR tube, and this tube was placed in a microwave at full power for one minute. The tube was immediately cooled on ice, and the PCR master mix was added. Primers used were SABR150 and SABR4506, which flank the transcription factor insertion site in the pDEST22 vector. PCR products were sent to MWG (Eurofins MWG, Germany) for direct sequencing using the SABR150 primer. Returned sequences were analysed using the NCBI Blast tool to obtain the identity of the transcription factor (Chapter 4).

### **2.11. Statistics**

---

Student's t-tests were performed in Microsoft Excel 2011 (Microsoft, USA), were two tailed and assumed unequal variance. One-way ANOVA analysis was performed in GraphPad Prism 6 (GraphPad software Inc., USA). The Sidak test was used for multiple comparisons. Multiplicity adjusted P values (Wright, 1992) are given. In the text, mean values  $\pm$  standard errors are given. Pearson's correlation tests were performed in R (open-source software; [www.r-project.org](http://www.r-project.org)), and  $r^2$  values are given.

## **2.12. Bioinformatics**

---

Arabidopsis gene sequences were obtained from The Arabidopsis Information Resource ([www.arabidopsis.org](http://www.arabidopsis.org)). For correlation analyses, a list of Arabidopsis transcription factors was obtained from the Database of Arabidopsis Transcription Factors (<http://datf.cbi.pku.edu.cn>). Gene expression data was obtained from Genevestigator software (NEBIOM AG, Switzerland). Blast searches were performed via the NCBI BLAST tool, using the nucleotide collection database ([blast.ncbi.nlm.nih.gov/Blast.cgi](http://blast.ncbi.nlm.nih.gov/Blast.cgi)). The program was optimized for highly similar sequences (megablast).

# Chapter Three: Control of Lateral

## Aerial Organ Size by

### AINTEGUMENTA and CYCD3;1

#### **Introduction**

---

In separate studies, Klucher *et al.* (1996) and Elliott *et al.* (1996) identified *aintegumenta* mutants and showed that the transcription factor encoded by this gene was required for proper integument development and hence megasporogenesis. Development of floral organs of the outer three whorls was also perturbed in these mutants (Elliott *et al.*, 1996; Klucher *et al.*, 1996). It was not until later, however, that pleiotropic roles for *ANT* in the regulation of LAO (Lateral Aerial Organ) growth were documented (Krizek, 1999; Krizek *et al.*, 2000; Mizukami and Fischer, 2000).

In these studies, it was found that plants lacking functional *ANT* developed smaller leaves and petals than did their WT counterparts. Krizek (1996) found that *ant-5*, *ant-6*, *ant-8* and *ant-9* mutants, which are all of the *Ler* ecotype, had smaller petals and often other floral organs than *Ler* WT plants. In the same study it was also shown that over-expression of *ANT*, using the constitutively active 35S promoter from the Cauliflower Mosaic Virus, led to the development of larger petals, sepals, stamens and carpels and hence larger flowers than normal (Krizek, 1999). Consistent with these roles, *in situ* hybridization showed the presence of *ANT* mRNA in various tissues within young flowers, but expression was reduced as the flowers aged (Krizek, 1999).

To investigate the mechanism by which *ANT* regulates organ size, scanning electron micrographs were used to measure cell size in 35S:*ANT* floral organs (Krizek, 1999). Larger cells were observed in the over-expressers than were in *WT* plants. It was also shown that in 35S:*ANT* plants, the floral meristem was not larger than that of *WT* plants, suggesting that an increased number of cells

### Chapter Three: *ANT* & *CYCD3;1* and Organ Size

being recruited from the floral meristem to the organ primordia was not the cause of enlarged organs (Krizek, 1999). Expression of the histone gene *H4* was used as a marker of cell cycle activity to examine enhanced cell cycle activity in the over-expressers. *In situ* hybridization did not reveal any difference in expression between *Ler* WT and *35S:ANT* flowers (Krizek, 1999). It was therefore suggested that *ANT* regulates cell size to regulate organ size. However, this study focused on the over-expresser rather than the mutants. This therefore does not directly address what causes reduced organ size when the function of *ANT* is lost, and is not necessarily a direct reflection of the mechanism by which *ANT* normally acts.

Whilst Krizek *et al.* (1999) investigated the phenotypes of *ant* mutants and over-expresser in the *Ler* ecotype, Mizukami & Fisher (2000) analysed the consequences of reducing and increasing functional *ANT* expression in the *Col-0* ecotype. The *ant-1* mutant, which was originally isolated in the *WS* ecotype but was backcrossed four times to the *Col-0* ecotype, was used as a loss-of-function mutant. *ANT* was once again expressed constitutively using the *35S* promoter. In this study, the effects of altered *ANT* expression in leaves were also investigated. *ant-1* mutants had smaller petals and leaves than their WT counterparts (Mizukami and Fischer, 2000). Over-expressers had greater rosette and flower mass, and over-expression of *Arabidopsis thaliana* *ANT* in tobacco increased seed size in this organism. Mizukami & Fisher were also interested in the mechanism by which *ANT* regulates lateral aerial organ (LAO) size. They showed that petals of *35S:ANT* plants contained cells of unchanged size, and hence cell density was also unchanged in these petals. From this it can be deduced that cell number must have been increased, and indeed this was the case. In *ant-1* mutant petals, cell size was increased, as opposed to decreased. Cell density and number were decreased, indicating that reduced petal size in this mutant was due to a reduction in cell number. The increase in cell size is likely to be part of a known compensation mechanism buffering changes to LAO size (Tsukaya, 2008).

Mizukami & Fisher did not simply quantify organ size and cell number and size in mature petals; they also performed these analyses on younger petals. They found the phenotype to be reduced or absent in the younger petals, and in the over-expresser changes in cell number did not occur in the early stage of petal development (Mizukami and Fischer, 2000). Changes in organ size only occurred when there was a change in cell number and *vice versa*. This

### Chapter Three: *ANT* & *CYCD3;1* and Organ Size

led the authors to conclude that *ANT* regulated LAO size by regulating the so-called mitotic window, a period of time during LAO growth during which cell proliferation can occur, and not the rate of cell proliferation. This is in agreement with the conclusion made by Krizek *et al.* (1999), based on observations of *H4* expression, that cell cycle activity was not enhanced in *35S:ANT* flowers.

It was hypothesized that *ANT* must be regulating the maintenance of cell cycle activity to determine the size of the mitotic window during LAO growth (Mizukami and Fischer, 2000). To test this hypothesis, the expression of the cell cycle marker *CYCD3;1* was analysed using semi-qPCR in mature leaves and young floral buds from *WT* plants and *35S:ANT* plants (Mizukami and Fischer, 2000). *CYCD3;1* expression was undetectable in mature *WT* leaves, but was observed in *35S:ANT* leaves of the same age. However, whilst *CYCD3;1* expression was detected in *WT* young floral buds, it was expressed at a similar level in the *35S:ANT* buds. Thus *ANT* did appear to be maintaining cell cycle activity but was not increasing its rate, at least not to an observable level (Mizukami and Fischer, 2000). It is notable however that expression of *CYCD3;1* was not reported in *ant* loss-of-function mutants.

The mechanism by which cell expansion is utilized to compensate for reduced final organ size in *ant* mutants is not understood. Cell size increase is often associated with increases in ploidy levels, the number of genome copies within each cell nucleus (Kondorosi *et al.*, 2000). Ploidy level increase is normally driven by endoreduplication in Arabidopsis. Endoreduplication is the replication of nuclear DNA without subsequent cell division (Kondorosi *et al.*, 2000). Following the S phase of the cell cycle, the cells progress straight back into the G1 phase instead of the G2 and M phases. Each time this happens, genome content, or ploidy, doubles. Plants cells can go through several rounds of endoreduplication. In hypocotyls, GA and ethylene promote both endoreduplication and cell elongation (Gendreau *et al.*, 1999). Leaf trichome cells normally have a ploidy level of 32C (Hulskamp *et al.*, 1994), meaning 32 copies of each chromosome, instead of the diploid level of 2C found in young cells. Several studies have shown that cell cycle proteins are required for proper control of endoreduplication. For example, *CYCA2;3*, a cyclin promoting S phase progression, inhibits endoreduplication in young tissues (Imai *et al.*, 2006). TCP (TEOSINTE BRANCHED1, CYCLOIDEA, and PCF) transcription factors generally promote organ maturation and endoreduplication (Martín-Trillo and Cubas, 2010), and TCP15 has been shown to bind directly to the *CYCA2;3*

### *Chapter Three: ANT & CYCD3;1 and Organ Size*

and *RBR* promoters (Li *et al.*, 2012b). E2FA proteins, which promote the S phase of the cell cycle, have been shown to promote cell division or endoreduplication depending on whether or not they are bound by RBR (Magyar *et al.*, 2012). This opens the possibility that *CYCD3;1* might regulate endoreduplication via phosphorylation of RBR when bound to CDKA kinases. Indeed, organs lacking all three *AtCYCD3* genes have higher ploidy levels (Dewitte *et al.*, 2007).

## Aims & Objectives

---

To determine whether or not an interaction between ANT and *CYCD3;1* might be involved in the regulation of LAO size, an *ant-9 cycd3;1* double mutant was generated and the LAO phenotypes of this genotype were compared to those of *ant-9* and *cycd3;1* single mutants. Since ANT and *CYCD3;1* loci are physically linked on Arabidopsis chromosome four (TAIR), the linkage distance between these two loci was also determined to aid in the generation of any future mutant combinations. Specifically, the interaction between these two genes in petals and leaves was to be addressed.

As there were some differences in the conclusions made by Krizek *et al.* (1999) and Mizukami & Fisher (2000) regarding the mechanism of ANT action, the clarification of this mechanism was sought. Krizek *et al.* (1999) used *ant* mutant alleles in the *Ler* ecotype, whereas Mizukami and Fisher (2000) used an allele originally isolated in the *WS* ecotype but backcrossed to *Col-0* for their study. Clarification of the mechanism by which ANT acts was carried out by re-analyzing the phenotype of the *ant-9* mutant, and by analyzing the phenotype of the novel *ant-GK* mutant. This second allele was isolated in the *Col-0* ecotype and was used in this background. The *ant-GK* allele is available publically but has not been characterized to the author's knowledge. Therefore, this allele was to be characterized in this study.

There appears to be a compensation mechanism occurring in *ant* mutants leading to increased cell size, and such an increased cell size has also been observed in *cycd3;1* mutants (Dewitte *et al.*, 2007). Increased ploidy levels have been associated with increased cell size (Sugimoto-Shirasu and Roberts, 2003). The hypothesis that increased ploidy levels mediated this size increase was to be tested using flow cytometry.

No direct targets of AtANT have yet been identified. To allow for such targets to be searched for in future studies, a genetic construct that can be used for microarray analyses and chromatin immunoprecipitation (ChIP) studies was constructed. Following the introduction of this construct into plants, the phenotypic and molecular consequences of the expression of this construct were investigated.

### 3. Results

---

#### 3.1. Generating the *ant-9 cycd3;1* double mutant

To explore the possibility that ANT regulates *CYCD3;1* expression as a means of regulating cell proliferation during LAO development, the genetic interaction between the two loci was investigated. Since the *ant-9* allele has been used in several investigations of ANT function, this allele was utilised. Furthermore, the only characterized *cycd3;1* loss-of-function mutant allele was originally isolated in the *Ler* ecotype (Dewitte *et al.*, 2007), and the *ant-9* allele has also been characterized in this ecotype (Krizek, 2009).

The *ant-9<sub>Ler</sub>* mutant was crossed to the *cycd3;1<sub>Ler</sub>* mutant, and the genotypes of the F2 progeny were established. *ant-9* plants contain an insertion of the maize Ac transposon within the second intron of ANT (Elliott *et al.*, 1996). The *ant-9* allele was originally isolated in the C24 ecotype but the mutant was backcrossed to *Ler* and made homozygous for the *er* allele (Elliott *et al.*, 1996). These mutants fail to develop integuments, and this phenotype is complemented by ectopic expression of *ANT* (Elliott *et al.*, 1996). Full-length *ANT* transcripts are absent in the *ant-9* mutant (Elliott *et al.*, 1996). The *cycd3;1* allele contains a Ds insertion in the first exon, and was originally isolated in the *Ler* ecotype. qPCR confirmed that the respective full length transcripts were absent in this mutant (Dewitte *et al.*, 2007), as were transcripts containing the LxCxE motif that is required for binding to RBR protein (Dewitte *et al.*, 2007). An *ant-9 cycd3;1* double homozygous mutant was not obtained, probably due to the close proximity of these two loci (1.38 MB). When the proportion of the chromosome this distance represents is used to crudely estimate the proportion of the genetic map distance of the chromosome represented by this physical distance ([www.arabidopsis.org](http://www.arabidopsis.org)), a recombination frequency between the two loci of 11% is expected (Figure 3.1). A recombination event in *ant-9/ant-9 x cycd3;1/cycd3;1* F1s is required so that the *ant-9* and *cycd3;1* alleles are recombined on the same chromosome. To screen for mutants which have undergone such recombination events, the F1 was generated by crossing an *ant-9/ant-9* homozygous plant as a pollen donor with a *cycd3;1/cycd3;1* plant as female (Figure 3.1). The F1s were screened to confirm the presence of both mutant alleles by PCR, and were then back-crossed (as pollen donors) to *WT* plants (as pollen acceptors, B0s; Figure 3.1). B1s (offspring of F1 x B0 cross)

### Chapter Three: *ANT* & *CYCD3;1* and Organ Size

were then screened for the presence of both *ant9* and *cycd3;1* alleles by PCR (see Chapter Two). Any B1 plant possessing both alleles must have received them from an F1 gamete that harbours them on the same chromosome, since the *WT* B0 could only produce gametes with *WT* alleles. Such plants were identified. Out of 51 plants, six were homozygous for both *ANT* and *CYCD3;1* (*WT*) alleles, five were heterozygous for both loci, twenty were heterozygous for *CYCD3;1* but homozygous for *ANT*, and 20 were heterozygous for *ANT* but homozygous for *CYCD3;1*. A Chi squared test shows that B1s possessing both alleles occurred at a frequency significantly different from that expected if the two loci are not genetically linked, one in four ( $X^2 = 6.3$ ,  $df = 1$ ,  $P = 0.01$ ). The frequencies of these plants observed were not significantly different from that expected if the two alleles are genetically linked by a distance of 11 cM ( $X^2 = 0.07$ ,  $df = 1$ ,  $P = 0.78$ ) (Figure 3.1).

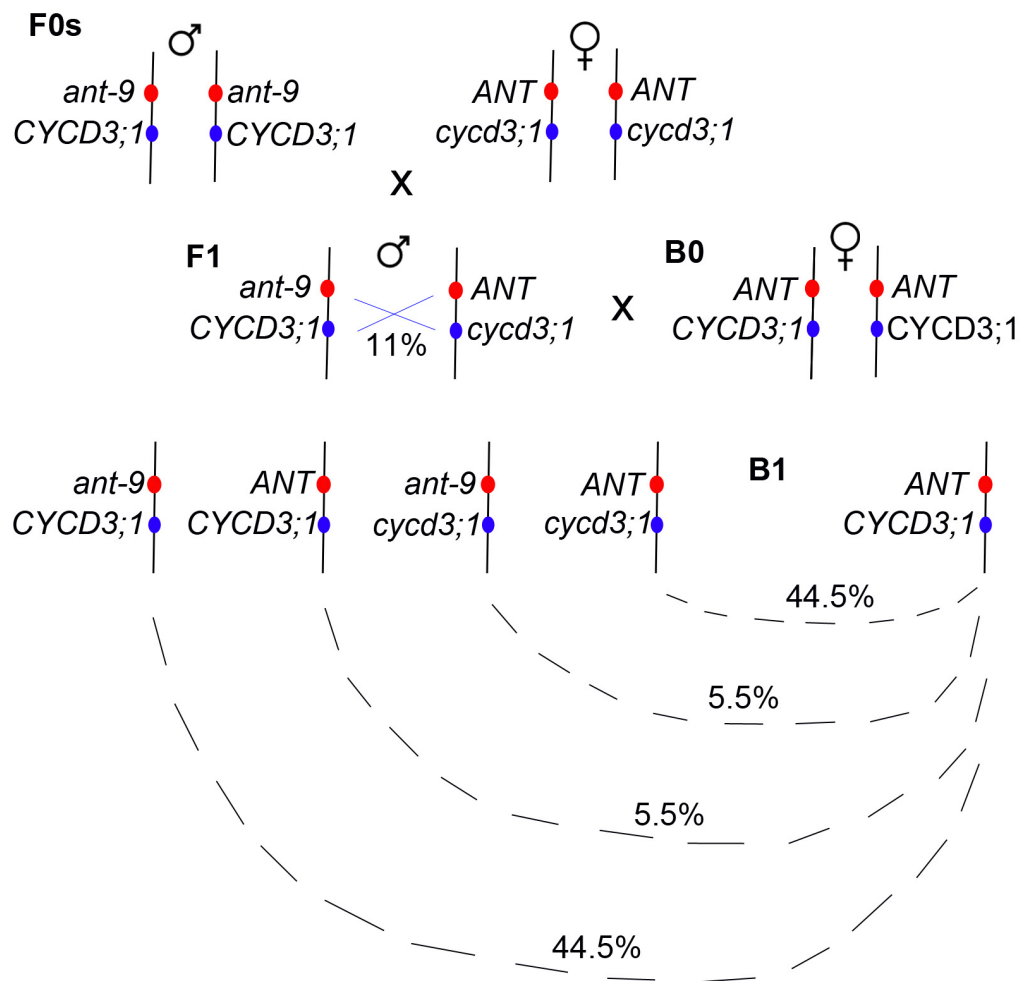


Figure 3.1: Generation of the *ant-9 cycd3;1* double mutants. Positions on chromosomes are not to scale. Expected crossover frequency ([www.arabidopsis.org](http://www.arabidopsis.org)) in F1s is indicated with blue cross. Expected occurrences of progeny of the backcross of the indicated genotypes are shown in black.

### 3.2. Relationship Between Cell Size and Petal Growth in *ant-9*, *cycd3;1* and *ant-9 cycd3;1* Mutants

B2 seeds co-segregating for *ant-9* and *cycd3;1* alleles, together with *WT<sub>Ler</sub>* and single mutants, were used to grow plants for analysis of petal size and cellular composition (Figure 3.2). Mean adaxial surface area of *WT<sub>Ler</sub>* petals was  $2.02 \pm 0.04$  mm<sup>2</sup>. Surface area of *ant-9<sub>Ler</sub>* petals was  $1.36 \pm 0.04$  mm<sup>2</sup>. This is a 33% reduction in surface area, and is statistically significant (one-way ANOVA,  $p < 0.0001$ , d.f. = 89) (Figure 3.2A,C,F). The mean surface area of *WT<sub>Ler</sub>* adaxial petal epidermis cells was  $188.9 \pm 4.3$  μm<sup>2</sup>. Cell surface area in *ant-9<sub>Ler</sub>* petals was  $252.3 \pm 3.8$  μm<sup>2</sup>, representing a 34% increase that was statistically significant (one-way ANOVA,  $p < 0.0001$ , d.f. = 804) (Figure 3.2B,D,G). This demonstrates partial compensation of the organ size phenotype via cell expansion. Petal epidermal cell numbers comprising the adaxial surface were inferred and estimated by dividing matched petal size by cell size. *ant-9<sub>Ler</sub>* petals contained an estimated  $5407 \pm 273$  epidermal cells, whereas *WT<sub>Ler</sub>* petals contained  $10654 \pm 477$  of these cells. *ant-9<sub>Ler</sub>* petals therefore contained 49% of the cells contained in *WT<sub>Ler</sub>* petals, showing that *ant-9<sub>Ler</sub>* petals are smaller than their *WT<sub>Ler</sub>* counterparts due to a reduced number of cells (one-way ANOVA,  $P < 0.0001$ , d.f. = 68) (Figure 3.2E).

Surprisingly, *cycd3;1<sub>Ler</sub>* petals were larger than *WT<sub>Ler</sub>* petals. Whilst the mean adaxial surface area of *WT<sub>Ler</sub>* petals was  $2.02 \pm 0.04$  mm<sup>2</sup>, that of *cycd3;1<sub>Ler</sub>* petals was  $2.789 \pm 0.05$  mm<sup>2</sup>. This is a statistically significant increase in petal adaxial surface area of 38% (one-way ANOVA,  $P < 0.0001$ , d.f. = 89) (Figure 3.2A,C,G). Whilst *WT<sub>Ler</sub>* epidermal cells had a mean surface area of  $188.9 \pm 4.3$  μm<sup>2</sup>, that of *cycd3;1<sub>Ler</sub>* petals was  $247.6 \pm 3.65$  μm<sup>2</sup>. This represents a statistically significant increase in cell surface area of 31% (one-way ANOVA,  $p < 0.0001$ , d.f. = 804) (Figure 3.2B,D,G). The percentage increase in cell size is similar to the percentage increase in petal adaxial surface area, suggesting that the former accounts for the latter. Accordingly, cell number in the adaxial epidermis was similar in *WT<sub>Ler</sub>* ( $10654 \pm 471$ ) and *cycd3;1<sub>Ler</sub>* ( $11197 \pm 306$ ) petals (one-way ANOVA  $q = 1.656$ ,  $P = 0.65$ , d.f. = 68) (Figure 3.2E). The *ant-9<sub>Ler</sub>* and *cycd3;1<sub>Ler</sub>* mutants share the cell size aspect of the petal phenotype, but they do not, in this study, share the cell number phenotype, nor the organ size phenotype.

### Chapter Three: ANT & CYCD3;1 and Organ Size

To investigate the interaction between these two loci in petal development, analyses of double mutants were performed. The mean adaxial surface area of *ant-9 cycd3;1<sub>Ler</sub>* petals was  $1.587 \pm 0.07 \text{ mm}^2$ , which is 21% smaller than the *WT<sub>Ler</sub>* value and is statistically significant (one-way ANOVA,  $p < 0.0001$ , d.f. = 89). However, the surface area of these petals was 17% larger than that of *ant-9<sub>Ler</sub>* petals (one-way ANOVA,  $P = 0.03$ , d.f. = 89) (Figure 3.2A,C,G). Cell size in *ant-9 cycd3;1<sub>Ler</sub>* double mutants was even larger than that observed in either single mutant at  $375.9 \pm 7.3 \mu\text{m}^2$ , 98% larger than *WT<sub>Ler</sub>* cells (one-way ANOVA,  $P < 0.0001$  and d.f. = 804 in each case) (Figure 3.2B,D,G). Thus the increased cell size phenotype appeared to be additive, suggesting independent action of each gene in control of petal adaxial epidermal cell size. Estimated cell number in *ant-9<sub>Ler</sub>* mutants was  $5407 \pm 273$ . Estimated cell number in *ant-9 cycd3;1<sub>Ler</sub>* double mutants was  $4467 \pm 224$ , 17% less than that of *ant-9<sub>Ler</sub>* mutants, although this difference did not appear to be statistically significant (one-way,  $P = 0.1$ , d.f. = 68) (Figure 3.2E). This suggests that the partial compensation of the petal size phenotype in *ant-9* mutants by the loss of functional *CYCD3;1* is due to an increase in cell size.

Chapter Three: ANT & CYCD3;1 and Organ Size

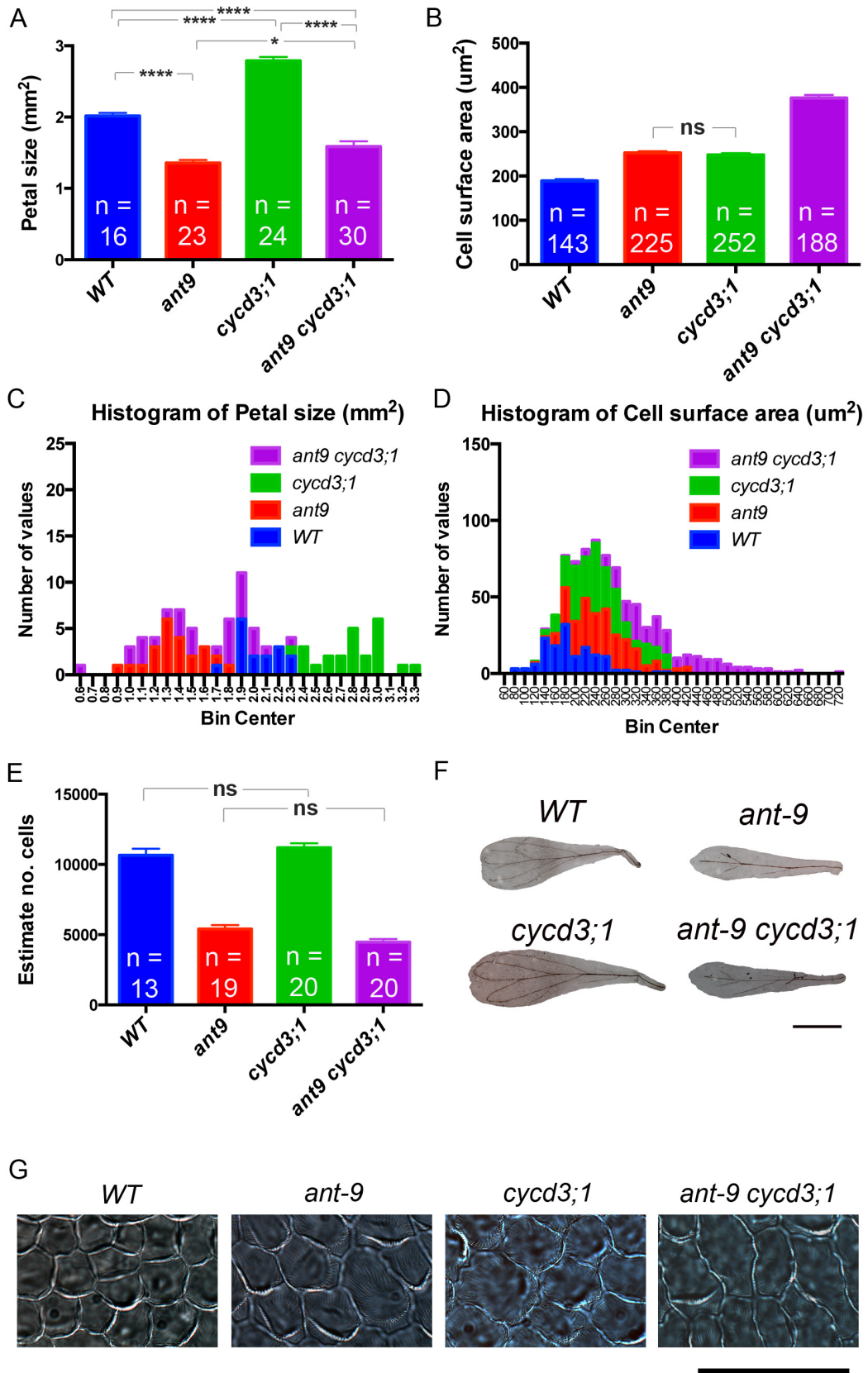


Figure 3.2: Petal phenotypes of *ant-9<sub>Ler</sub>*, *cyd3;1<sub>Ler</sub>* and *ant-9 cyd3;1<sub>Ler</sub>* mutants. A) Mean petal size. Error bars represent SEM. B) Mean petal cell size. Error bars represent SEM. C-D) Histograms showing petal and cell size data. E) Cell number estimated by dividing petal size by cell size. F) Pictures of petals. Scale bar represents 1 mm. G) Petal adaxial epidermal cells. Scale bar represents 50  $\mu\text{m}$ . For B & D, all comparisons of means via t tests generated P values < 0.0001 other than where stated (ns). For all graphs, \*\*\*\* : P<0.0001; \* : P<0.05; ns : P>0.05.

3.3 Increased Petal Size is Correlated with Increased Cell Size within the *ant-9 cycd3;1* Mutant Population

The range of petal sizes in *ant-9 cycd3;1<sub>Ler</sub>* mutants appeared to be greater than that in any other genotype (Figure 3.2C), as did the range of cell size (Figure 3.2D). This suggested that some petals in the double mutants were becoming much bigger due to increases in mean cell size within those petals. Plotting cell size against petal size indicated that this indeed seemed to be the case, as the two variables correlated positively with one-another in this genotype (Figure 3.3) ( $r = 0.63$ ,  $r^2 = 0.40$ ,  $P = 0.0027$ ). No such correlation was observed in other genotypes (Figure 3.3) ( $r^2 < 0.05$  and  $P > 0.4$  in each case).

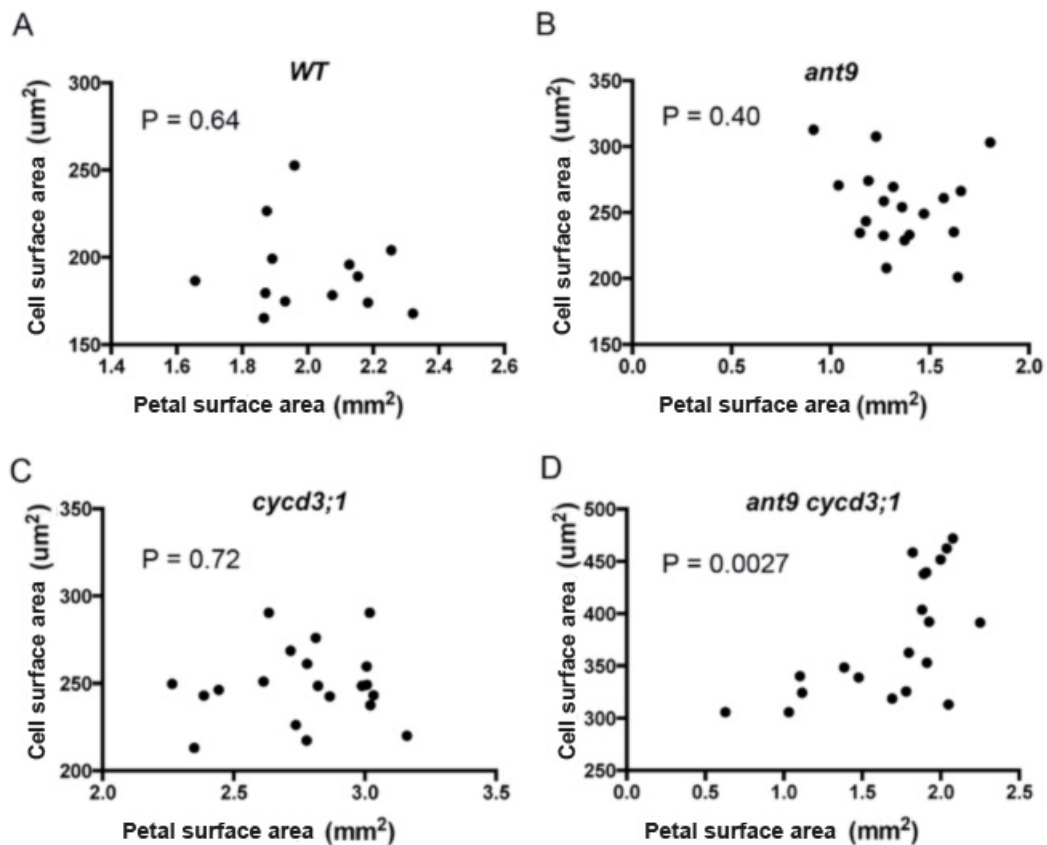


Figure 3.3: Cell size is correlated with petal size in *ant-9 cycd3;1<sub>Ler</sub>* double mutants. Each point represents the average adaxial epidermal cell size (y axis) of a particular petal, the size of which is plotted against (x axis). Thirteen pairs of data (i.e. from the same petal) are shown for *WT<sub>Ler</sub>* (top left), nineteen for *ant-9<sub>Ler</sub>*, twenty for *cycd3;1<sub>Ler</sub>* and twenty for the *ant-9 cycd3;1<sub>Ler</sub>* double mutant.

### 3.4 Characterization of the *ant-GK* mutant

To analyse the phenotype of a *Col-0* ecotype *ant* loss-of-function mutant, an *ant-GK* allele was chosen as a potential mutant and was characterized. The *ant-GK* allele TAIR accession number is 1006453905, and the GABI-KAT identification code is GK-874H08-026466.

Genotyping *ant-GK<sub>Col-0</sub>* mutants by PCR was initially unsuccessful. The possibility of this being due to incorrect primers being used, as a result of an incorrect location of T-DNA insertion being listed on [www.arabidopsis.org](http://www.arabidopsis.org), was investigated, and found to be the case. Using a genomic primer further upstream in the *ANT* gene, a PCR product was obtained and sequenced, and it was found that the T-DNA insertion was in the second exon of *ANT* (Figure 3.4A). This is upstream of the sequences encoding the AP2 DNA-binding domains (Figure 3.4A). qPCR analysis was used to determine whether or not *ANT* transcripts were produced in this line. qPCR with primers in the 3' end of the *ANT* gene (GABI-KAT) indicated a ~ 28-fold increase in mRNA levels (Figure 3.4B). However, using primers flanking the T-DNA insertion site, qPCR analysis indicated that full-length *ANT* transcripts were at ~ 0.1 WT levels (Figure 3.4C). Correlating with this, plants had the characteristic flowers with small organs (Figure 3.4D) of other *ant* mutants. No seeds were obtained from homozygous *ant-GK<sub>Col-0</sub>* mutants, demonstrating the female sterility caused by the loss of functional *ANT*.

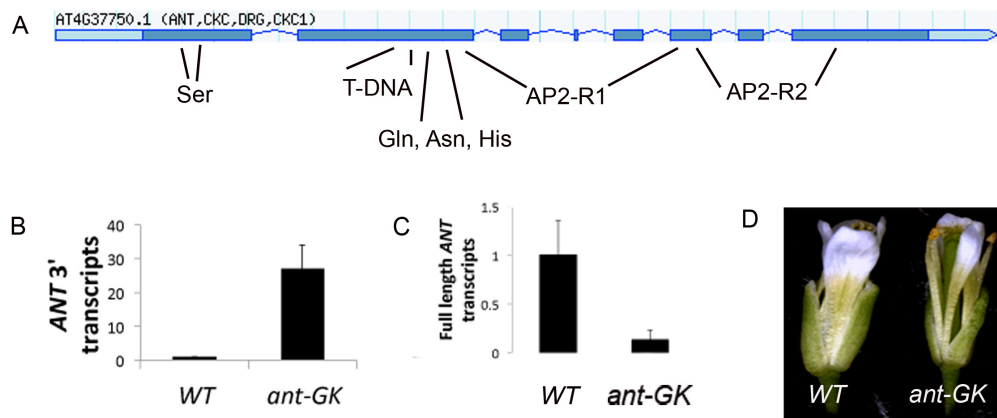


Figure 3.4: The *ant-GK* allele. A) Structure of the *ANT* gene ([www.arabidopsis.org](http://www.arabidopsis.org)) is shown, along with important motifs within the protein and the site of the GABI KAT 5149 bp T-DNA insertion. *ANT* transcripts determined by qPCR using primers at the 3' end of the *ANT* gene (B) and primers flanking the T-DNA insertion site (C). Transcript levels were normalized to those of *ACT2*. D) WT and *ant-GK*<sub>Col-0</sub> flowers.

### 3.5 Comparison of Ler *ant* and *cycd3;1* Petal Phenotypes and *Col-0 ant* and *cycd3;1* Petal Phenotypes

A reduction in cell number in *cycd3;1<sub>Col-0</sub>* mutants was reported by Dewitte *et al.* (2007), and was not observed in this study. Therefore, the analysis of petal size, cell size and cell number was repeated to confirm these results. Mean petal surface area in *WT<sub>Ler</sub>* plants was  $1.704 \pm 0.053 \text{ mm}^2$ , whereas that of *cycd3;1<sub>Ler</sub>* plants was  $2.248 \pm 0.064 \text{ mm}^2$  (Figure 3.5A,D). This represents a 32% increase in petal surface area (one-way ANOVA,  $P < 0.0001$ , d.f. = 24). Mean cell surface area in *WT<sub>Ler</sub>* petals was  $205.2 \pm 4.419 \mu\text{m}^2$ , whereas that of *cycd3;1<sub>Ler</sub>* petals was  $246.4 \pm 5.269 \mu\text{m}^2$  (Figure 3.5B,D), a 20% increase (one-way ANOVA,  $P < 0.0001$ , d.f. = 1136). Estimated cell number in *WT<sub>Ler</sub>* petals was  $8403 \pm 276$ , whereas that in *cycd3;1<sub>Ler</sub>* petals was  $9293 \pm 302$  (Figure 3.5C). Although this shows an increase of 11%, this increase was not statistically significant (one-way ANOVA,  $P = 1.5$ ).

In the previous study (Dewitte *et al.*, 2007), the *cycd3;1* mutant used was backcrossed to *Col-0 WT* plants twice, meaning that the plants would be expected to carry 25% of the *Ler* genetic material from the original mutant plant. Although the *er* allele is not present in the backcrossed *cycd3;1<sub>Col-0</sub>* mutant (Walter Dewitte, personal communication), other polymorphisms in the *Ler* background could affect the phenotype observed.

To confirm that the *cycd3;1* mutant backcrossed to *Col-0* does develop petals with a reduced number of cells, this analysis was repeated. Mean cell number in *WT<sub>Col-0</sub>* petals was  $9458 \pm 313$ , compared to  $9025 \pm 295$  cells in *cycd3;1<sub>Col-0</sub>* petals. This 5% decrease (Figure 3.5C) was not statistically significant (one-way ANOVA,  $P = 0.91$ , d.f. = 176). Mean cell surface area in *WT<sub>Col-0</sub>* petals was  $176.0 \pm 3.638 \mu\text{m}^2$ , whereas that in *cycd3;1<sub>Col-0</sub>* petals was  $214.2 \pm 4.450 \mu\text{m}^2$  (Figure 3.5B,D). Thus cell size was increased by 22% in the *cycd3;1<sub>Col-0</sub>* mutant (one-way ANOVA,  $P = 0.001$ , d.f. = 1136). Since cell number was not significantly changed in this mutant, whilst cell size was, petal size was expected to change. Mean *WT<sub>Col-0</sub>* petal surface area was  $1.625 \pm 0.037 \text{ mm}^2$ , whilst surface area of *cycd3;1<sub>Col-0</sub>* petals was  $1.899 \pm 0.032 \text{ mm}^2$  (Figure 3.5A,D), a 17% increase (one-way ANOVA,  $P < 0.0001$ , d.f. = 191). The results obtained in this study do not support the reduction in petal cell number observed by Dewitte *et al.* (2007). This could be due to the experiments being performed in

### Chapter Three: ANT & CYCD3;1 and Organ Size

different locations and/or by different persons (Prior experiments performed in Cambridge, these experiments performed in Cardiff University growth rooms). The results here show that *cycd3;1* mutants in the *Ler* or (predominantly) *Col-0* ecotype grow petals containing cells larger than those found in *WT* petals, and that this cell size increase increases final organ size.

In this experiment, the *ant-9 cycd3;1<sub>Ler</sub>* mutant did not show a suppression of the *ant-9<sub>Ler</sub>* petal size phenotype as large as that seen in the prior experiment (compare Figure 3.2A with Figure 3.5A). However, partial suppression of the phenotype was observed (Figure 3.5A & D). Mean petal surface area in *ant-9 cycd3;1<sub>Ler</sub>* petals was  $1.162 \pm 0.027 \text{ mm}^2$ , which is 15% greater than that of *ant-9<sub>Ler</sub>* mutants. However, this difference was not statistically significant (one-way ANOVA,  $p = 0.13$ , d.f. = 191). Mean cell surface area in *ant-9 cycd3;1<sub>Ler</sub>* mutants was  $374.7 \pm 9.629 \text{ }\mu\text{m}^2$ , 52% greater than that of *cycd3;1<sub>Ler</sub>* mutants (one-way ANOVA,  $p < 0.0001$ ) and 12% greater than that of *ant-9<sub>Ler</sub>* mutants (one-way ANOVA,  $p = 0.0002$ , d.f. = 1136). Therefore an additive increase in petal cell size was observed in the double mutant (Figure 3.5B & D). These data are not suggestive of a functional interaction between *ANT* and *CYCD3;1* in the regulation of petal size, but do suggest that the two genes may be part of independent pathways regulating cell size.

*Col-0* and *Ler* plants have different growth characteristics (Alonso-Blanco and Koornneef, 2000). Different *ant* LAO phenotypes have been observed in separate studies (Krizek, 1999; Mizukami and Fischer, 2000). However, no direct comparisons between mutants in different ecotypes have been made. The petal phenotypes of *ant-9<sub>Ler</sub>* and *ant-GK<sub>Col-0</sub>* plants were analysed and compared. As discussed (3.2), the *ant-9<sub>Ler</sub>* mutant had smaller petals due to a reduction in cell number. Like *ant-9<sub>Ler</sub>* mutants, *ant-GK<sub>Col-0</sub>* mutant petals were smaller than those of *WT* control plants (*Col-0* in this case), having a mean adaxial surface area of  $0.900 \pm 0.025 \text{ mm}^2$ , representing a 45% reduction (Figure 3.5A,D; One way ANOVA  $p < 0.0001$ , d.f. = 28). *ant-GK<sub>Col-0</sub>* petals also contained fewer cells than *WT<sub>Col-0</sub>* petals (Figure 3.5C; One way ANOVA,  $p < 0.0001$ , d.f. = 28). *ant-GK<sub>Col-0</sub>* petals were estimated to contain  $3792 \pm 126$  adaxial epidermal cells, 60% fewer than *WT<sub>Col-0</sub>*. Cell surface area in *ant-GK<sub>Col-0</sub>* mutants was  $236.7 \pm 5.040 \text{ }\mu\text{m}^2$ , representing an increase of 35% (Figure 3.5B,D; One way ANOVA,  $p < 0.0001$ , d.f. = 153), indicating the presence of a compensation mechanism like that observed in *Ler* plants.

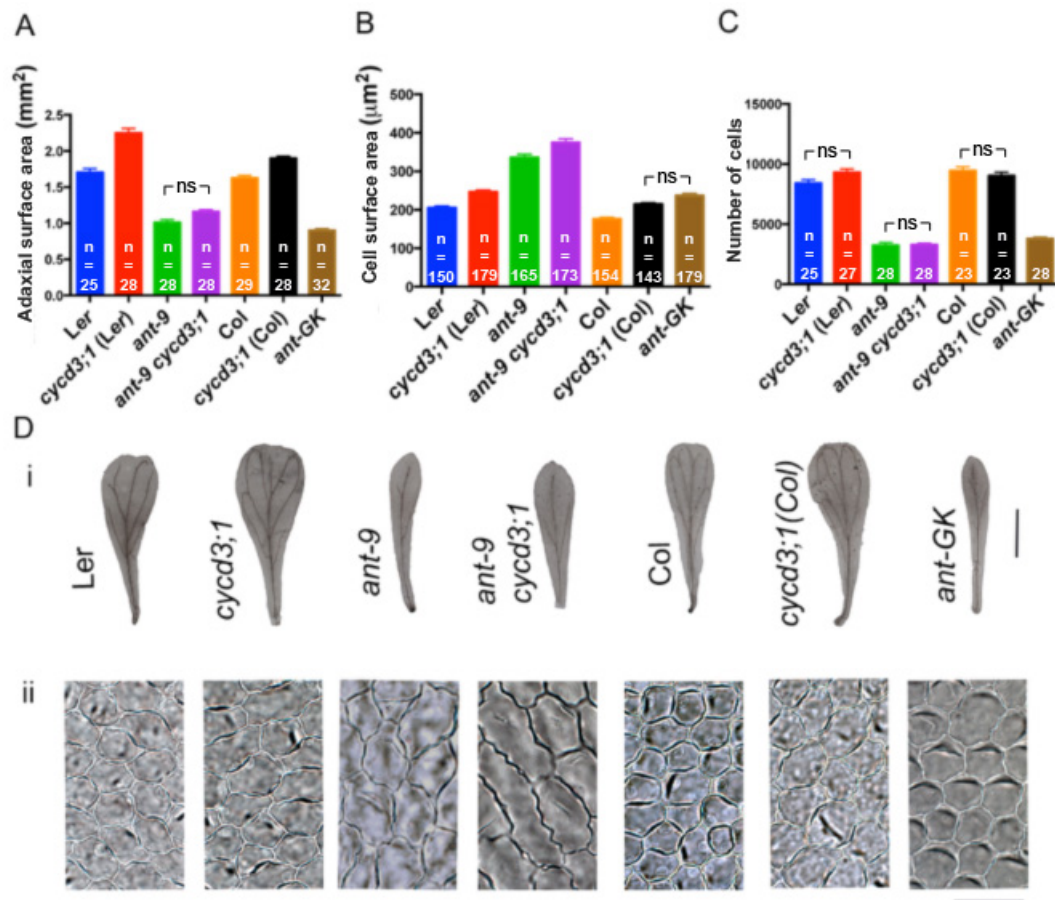


Figure 3.5: Petal phenotypes of *ant-9<sub>Ler</sub>*, *cycd3;1<sub>Ler</sub>* and *ant-9 cycd3;1<sub>Ler</sub>* mutants in the Ler background and *ant-GK<sub>Col-0</sub>* and *cycd3;1<sub>Col-0</sub>* mutants in the Col-0 background. A) Mean petal adaxial surface area. B) Mean petal cell surface area. Error bars represent SEM. C) Cell number estimated by dividing petal size by cell size. For A-C, ns :  $p > 0.05$ . For all other intra-ecotype comparisons between means,  $p < 0.001$ . D) (i) Pictures of petals. Scale bar represents 0.5 mm. (ii) Pictures of adaxial epidermis cells of petals. Scale bar represents 50 µm.

### 3.6 Ploidy Levels in Cells of *ant* and *cycd3;1* Mutants

A cell size increase potentially forming part of a compensation mechanism was observed in *ant* and *cycd3;1* loss of function mutant petals. To investigate the possibility that the compensation of cell size in *ant-9<sub>Ler</sub>*, *cycd3;1<sub>Ler</sub>* and *ant-9 cycd3;1<sub>Ler</sub>* mutants was associated with increases in ploidy level, flow cytometry was used to quantify the ploidy levels in petals of these plants (Figure 3.6). *WT<sub>Ler</sub>* petals contained mostly 2C cells, as seen previously in petal tips (Hase *et al.*, 2005). However, a small proportion of cells had a genome content of 4C, and fewer cells were detected that were 8C and 16C (Figure 3.6A). This indicates that petal cells do endoreduplicate, but although all care was taken to use only petal material for analyses, it is of course possible that there is a small amount of contamination from other floral organs. *cycd3;1<sub>Ler</sub>* mutants in the *Ler* ecotype showed a similar pattern (Figure 3.6B), although the 4C peak was relatively higher, an observation similar to that made by Dewitte *et al.* (2007) in the *cycd3;1-3<sub>Col-0</sub>* triple mutant. This might represent cells in the G2 phase of the cell cycle, but equally those cells might be in the G1 phase of the first round of endoreduplication. Whichever is the case, this might contribute to the increase in cell size observed in this mutant. In contrast, the *ant-9<sub>Ler</sub>* petal cells seemed to have the same ploidy levels in the same proportions as those of *WT<sub>Ler</sub>* plants (Figure 3.6C). The *ant-9 cycd3;1<sub>Ler</sub>* mutant showed a distribution of genome content similar to that in the *cycd3;1<sub>Ler</sub>* mutant, i.e. a 4C content higher than that in WT (Figure 3.6D). This is probably caused by the loss of *cycd3;1* in this double mutant. The ploidy levels of *cycd3;1<sub>Col-0</sub>* mutant petals in the *Col-0* background were also analysed and compared to those of *WT<sub>Col-0</sub>* petals. In this ecotype, ploidy levels did not appear to be affected by the loss of functional *CYCD3;1*, and both genotypes showed a distribution pattern similar to that observed in *WT<sub>Ler</sub>* petals (Figure 3.6E & F).

That the petal cell size phenotype of *ant-9<sub>Ler</sub>* and *cycd3;1<sub>Ler</sub>* mutants is additive suggests that this increase is occurring via independent mechanisms. The observation of a ploidy level increase in *cycd3;1<sub>Ler</sub>* mutants but not in *ant-9<sub>Ler</sub>* mutants is consistent with this conclusion. Since higher ploidy was not seen in the *cycd3;1<sub>Col-0</sub>* mutant in the *Col-0* background, cell size increase here may be occurring via a different mechanism, perhaps the same that is occurring in the *ant-9<sub>Ler</sub>* mutant. It would be interesting to see whether or not an additive phenotype would exist in an *ant cycd3;1* double mutant in the *Col-0* background.

Final organ size is highly important for plants. For example, leaves must be large enough to carry out photosynthesis optimally. It might be expected that there are several mechanisms in place to correct for reduced cell proliferation or expansion, and if one of these does not occur in one genotype then another might be initiated. Indeed, several categories of organ size compensation mechanisms have been observed, some of these involving endoreduplication and others not (Cookson et al., 2006; Ferjani et al., 2007; Fujikura et al., 2007).

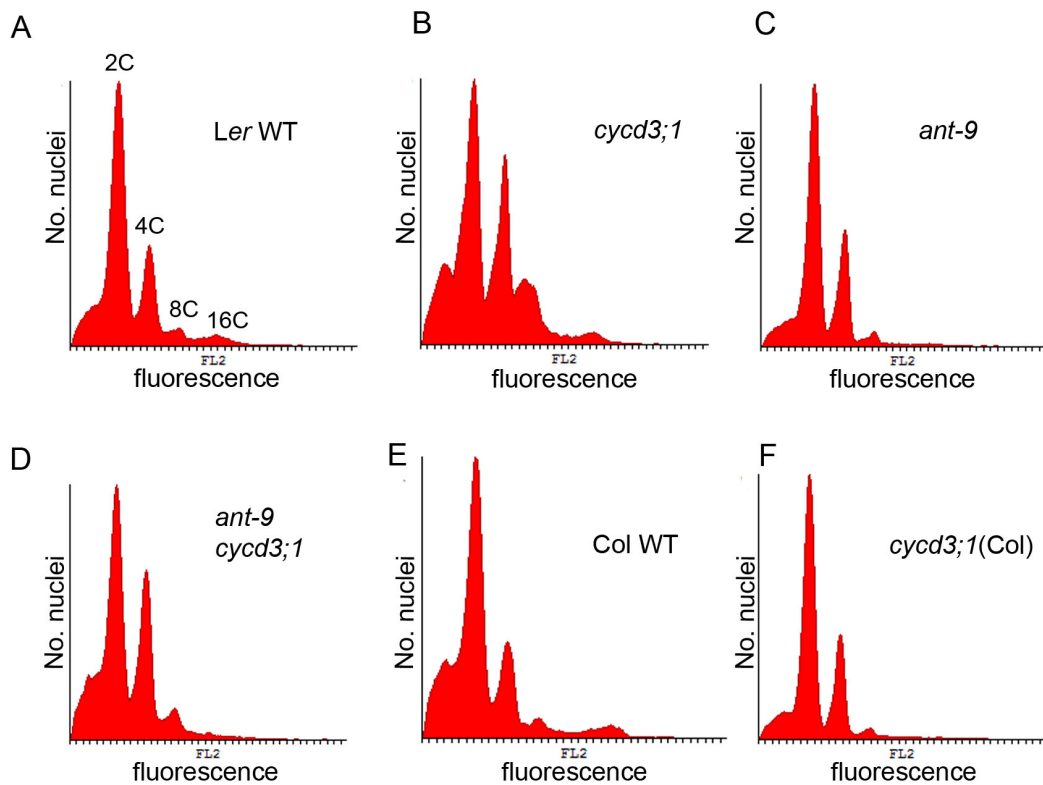


Figure 3.6: Cell ploidy distributions in petals from mature open flowers of *WT<sub>Ler</sub>* (A), *cycd3;1<sub>Ler</sub>* (B), *ant-9<sub>Ler</sub>* (C), *ant-9 cycd3;1<sub>Ler</sub>* (D), *WT<sub>Col-0</sub>* (E) and *cycd3;1<sub>Col-0</sub>* (F) plants. Data are shown in histograms. The x axis shows relative fluorescence values, whilst the the y axis shows the number of nuclei with that particular fluorescence level. In A, peak• representing 2C, 4C, 8C and 16C nuclei are indicated.

### 3.7 Leaf Size and Cell Number in *ant-9* and *cycd3;1* Mutants

As well as petal size, *ANT* regulates leaf size (Mizukami and Fischer, 2000). Mutants lacking all three Arabidopsis *CYCD3*s have leaves with reduced numbers of cells, but cell expansion in this mutant is sufficient to compensate any reduction in final leaf size that might occur otherwise (Dewitte *et al.*, 2007).

To investigate the functional interaction between *ANT* and *CYCD3;1* in leaf growth, leaf size and cell density was quantified in *WT<sub>Ler</sub>*, *ant-9<sub>Ler</sub>*, *cycd3;1<sub>Ler</sub>* and *ant-9 cycd3;1<sub>Ler</sub>* mutants. Since leaves of different ages in Arabidopsis vary in size, the third true leaf of each plant was analysed. This is the first non-juvenile true leaf (first there are the two cotyledons then two juvenile leaves that emerge opposite one another and perpendicular to the cotyledons). The leaves were marked by tying cotton around the petiole whilst they were emerging, and were harvested once the bolts of the plants were between 2 cm and 7 cm high. Mean adaxial surface area of the third leaf of *WT<sub>Ler</sub>* plants was  $75.61 \pm 4.39$  mm<sup>2</sup>, whilst that of *ant-9<sub>Ler</sub>* plants was  $52.94 \pm 3.02$  mm<sup>2</sup> (Figure 3.7A,D). This is a 30% reduction (one-way ANOVA,  $p = 0.02$ , d.f. = 87). This phenotype is in agreement with the published *ant* loss-of-function mutant phenotype (Mizukami and Fischer, 2000). The mean surface area in *cycd3;1<sub>Ler</sub>* mutants was  $73.51 \pm 2.98$  mm<sup>2</sup> (Figure 3.7A,D), similar to that of *WT<sub>Ler</sub>* plants (one-way ANOVA,  $p = 1.00$ , d.f. = 87). Mean surface area in the *ant-9 cycd3;1<sub>Ler</sub>* double mutant was  $37.94 \pm 2.30$  mm<sup>2</sup> (Figure 3.7A,D). Although this represents a 28% reduction from *ant-9<sub>Ler</sub>* single mutants, this reduction was not found to be statistically significant (one-way ANOVA,  $p = 0.12$ , d.f. = 87). Therefore, a synergistic interaction may occur between *ANT* and *CYCD3;1* in leaf growth, but this needs to be confirmed.

Interestingly, the *cycd3;1<sub>Col-0</sub>* mutant leaves in the *Col-0* background were smaller than *WT<sub>Col-0</sub>* leaves (Figure 3.7A,D). Whilst mean surface area in *WT<sub>Col-0</sub>* leaves was  $117.1 \pm 4.08$  mm<sup>2</sup>, that of *cycd3;1<sub>Col-0</sub>* leaves was  $100.3 \pm 3.42$  mm<sup>2</sup>, representing a 14% decrease (One way ANOVA,  $p = 0.01$ , d.f. = 87). *WT<sub>Col-0</sub>* leaves were larger than *WT<sub>Ler</sub>* leaves (Figure 3.7A,D; One way ANOVA,  $p < 0.0001$ , d.f. = 87). It might be possible that *CYCD3;1* plays a role downstream of some factor in the *Ler* ecotype, perhaps ER, in regulating leaf growth. Thus in the *Ler* ecotype this pathway may already be perturbed, and loss of functional *CYCD3;1* may make no further difference.

### Chapter Three: ANT & CYCD3;1 and Organ Size

Cell density was also calculated in these mutants, to assess whether or not this was being affected and whether or not this might be the factor leading to the reduction in leaf size in *ant-9<sub>Ler</sub>* and *cycd3;1<sub>Col-0</sub>* mutants. Mean cell density was  $758 \pm 40$  cells/mm<sup>2</sup> in *WT<sub>Ler</sub>* leaves, whereas it was  $540 \pm 15$  in *ant-9<sub>Ler</sub>* leaves (Figure 3.7B). This is a 29% reduction (one-way ANOVA,  $J = 0.0001$ , d.f. = 85), and means that there is an increase in cell size (Figure 3.7E). Therefore, like in *ant* petals, the third leaf in *ant-9<sub>Ler</sub>* mutants is smaller due to a reduction in cell number and not in cell size. Estimation of cell number using these organ size and cell density measurements confirms this conclusion (Figure 3.7C). *WT<sub>Ler</sub>* leaves contained  $58212 \pm 3731$  palisade mesophyll cells on average, whereas *ant-9<sub>Ler</sub>* leaves contained  $29147 \pm 1127$  of these cells (Figure 3.7C). This is a 50% reduction in cell number (one-way ANOVA,  $J < 0.0001$ , d.f. = 87). Cell size is increased in the *ant-9<sub>Ler</sub>* mutant (Figure 3.7E), revealing a compensation mechanism regulating final leaf size. In the *cycd3;1<sub>Ler</sub>* mutant, a mean cell density of  $771 \pm 34$  cells/mm<sup>2</sup> was similar to that of *WT<sub>Ler</sub>* leaves (one-way ANOVA,  $J = 1.0$ , d.f. = 85; Figure 3.7B & C). The mean estimated cell number in this mutant was  $56165 \pm 1200$ , again similar to *WT<sub>Ler</sub>* cell number (one-way ANOVA,  $J = 1.0$ , d.f. = 87; Figure 3.7C). Cell size in the *cycd3;1<sub>Ler</sub>* mutant appeared similar to cell size in *WT<sub>Ler</sub>* leaves (Figure 3.7E). Therefore, the *cycd3;1<sub>Ler</sub>* mutant had no observable phenotype in leaves. In *ant-9 cycd3;1<sub>Ler</sub>* double mutants, cell density was  $686 \pm 33.23$  cells/mm<sup>2</sup> (Figure 3.7B). This is similar to the cell density of *WT<sub>Ler</sub>* leaves (one-way ANOVA,  $J = 0.6$ , d.f. = 85; Figure 3.7B). Therefore, *CYCD3;1* is limiting for the reduction in cell density occurring in the absence of functional ANT. This is a surprising result as it implies a role for *CYCD3;1* in increasing cell size in *ant* leaves, whilst *CYCD3;1* has previously been shown to decrease cell size when ectopically expressed (Dewitte *et al.*, 2003). *CYCD3;1* would appear to function differently under different circumstances. The result does however explain why *ant-9 cycd3;1<sub>Ler</sub>* leaves are smaller than *ant-9<sub>Ler</sub>* leaves, as they will be expected to contain fewer cells that are smaller than those of *ant-9<sub>Ler</sub>* leaves. Double mutant leaves were estimated to contain  $25382 \pm 1349$  cells (Figure 3.7C), which is indeed a value similar to that in *ant-9<sub>Ler</sub>* single mutants (one-way ANOVA,  $J = 1.0$ , d.f. = 87).

Mean cell density in *WT<sub>Col-0</sub>* leaves was  $699 \pm 15$  cells/mm<sup>2</sup>, whilst that in the *cycd3;1<sub>Col-0</sub>* mutant was  $658 \pm 24$  cells/mm<sup>2</sup>, a similar density (Figure 3.7B; one-way ANOVA,  $J = 0.7$ , d.f. = 85). Since *cycd3;1<sub>Col-0</sub>* leaves were smaller than their *WT<sub>Col-0</sub>* counterparts (Figure 3.7A), it can therefore be inferred that they were smaller due to a reduction in cell number, and indeed estimated cell number

### Chapter Three: ANT & CYCD3;1 and Organ Size

in this mutant was less than that in *WT<sub>Col-0</sub>* leaves (Figure 3.7C). In *WT<sub>Col-0</sub>* leaves, mean cell number was  $81601 \pm 3111$  cells, whereas *cycd3;1<sub>Col-0</sub>* mean cell number was  $65978 \pm 3033$  cells, a 19% reduction (one-way ANOVA,  $P = 0.0003$ , d.f. = 87). As expected, cell size appeared to be similar in *WT<sub>Col-0</sub>* and *cycd3;1<sub>Col-0</sub>* leaves (Figure 3.7E).

These results show a reduction in leaf size and cell number in the *cycd3;1<sub>Col-0</sub>* mutant, but not in the *cycd3;1<sub>Ler</sub>* mutant. *WT<sub>Col-0</sub>* leaves were larger than *WT<sub>Ler</sub>* leaves (Figure 3.7A,D; one-way ANOVA,  $P < 0.0001$ , d.f. = 87) and contained a greater number of cells (Figure 3.7C; one-way ANOVA,  $P < 0.0001$ , d.f. = 87). Cell number in *WT<sub>Ler</sub>* and *cycd3;1<sub>Col-0</sub>* leaves was similar (Figure 3.7C; one-way ANOVA,  $P = 0.8$ , d.f. = 87), opening the possibility that something missing in the *WT<sub>Ler</sub>* might be in the same pathway regulating leaf cell number as *CYCD3;1*.

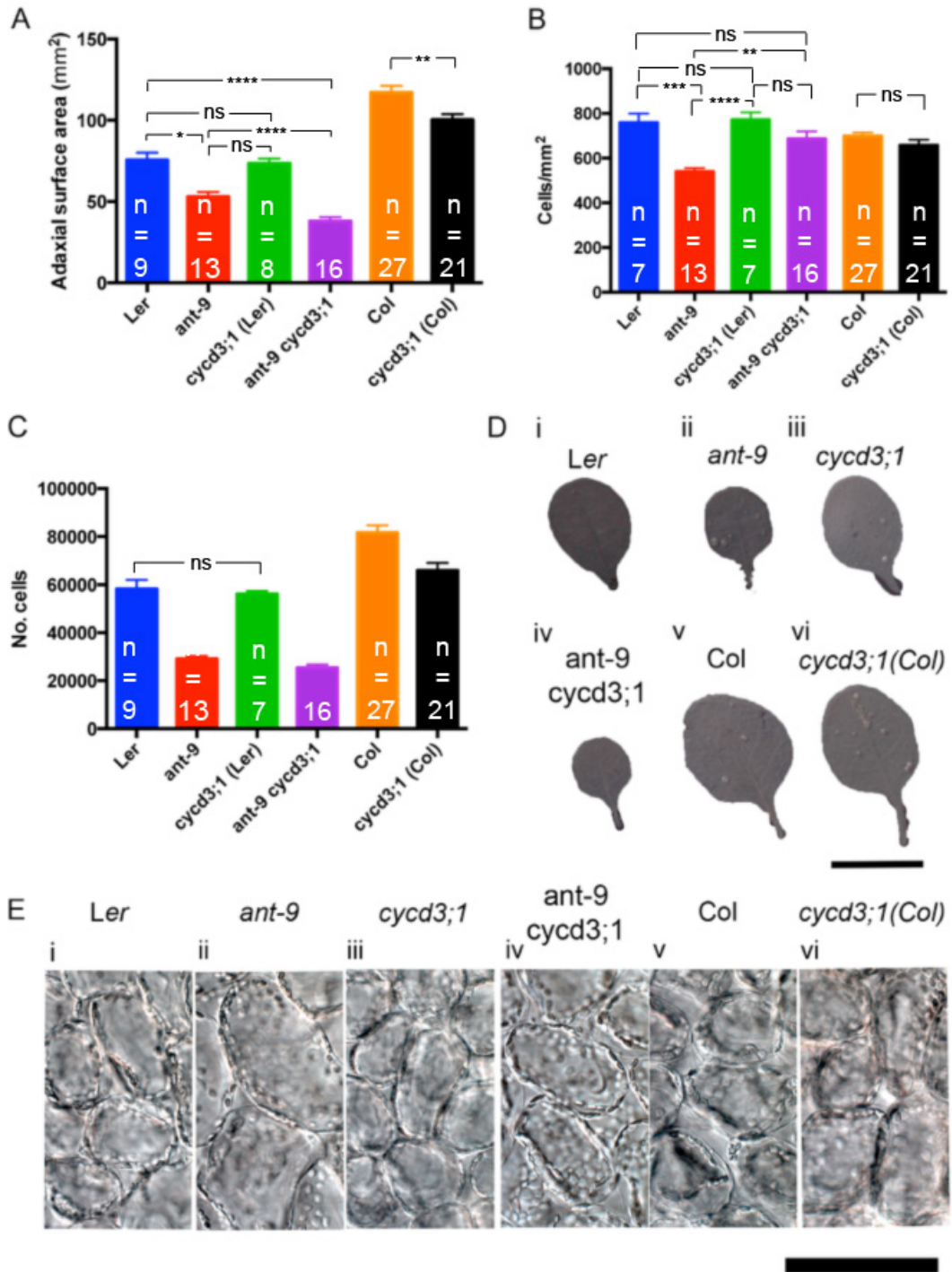


Figure 3.7: Leaf phenotype of *ant*<sub>Ler</sub>, *cycd3;1*<sub>Ler</sub> and *ant cycd3;1*<sub>Ler</sub> double mutants in the *Ler* background and the *cycd3;1*<sub>Col-0</sub> mutant in the *Col-0* background. All analyses were performed on the third leaf of plants when the bolt was between 2 cm and 7 cm high. A) Mean adaxial surface area. Error bars represent SEM. B) Mean palisade mesophyll cell density. Error bars represent standard deviation. C) The numbers of palisade mesophyll cells on the adaxial surface of leaves were estimated by multiplying cell density by leaf adaxial surface area. Data are shown as means and error bars represent SEM. D) Leaves of *WT*<sub>Ler</sub> (i), *ant-9*<sub>Ler</sub> (ii), *cycd3;1*<sub>Ler</sub> (iii), *ant-9 cycd3;1*<sub>Ler</sub> double mutants (iv), *WT*<sub>Col-0</sub> (v) and the *cycd3;1*<sub>Col-0</sub> mutant (vi) plants. \*\*\*\*:  $p < 0.0001$ ; \*\*\*:  $p < 0.001$ ; \*\*:  $p < 0.01$ ; \*:  $p < 0.05$ . In C, all comparisons between means yielded  $p$  values  $< 0.0001$ , other than where indicated (ns). ns:  $p > 0.05$ .

### 3.8 CYCD3;1 Promoter Activity is Downregulated in *ant* Mutants but Transcript Levels are not

To test the hypothesis that ANT regulates *CYCD3;1* expression, a *pCYCD3;1:GUS<sub>Ler</sub>* reporter line (Dewitte *et al.*, 2007) was crossed with the *ant-9<sub>Ler</sub>* mutant (Chapter 2). This reporter informs of the activity of the *CYCD3;1* promoter. *pCYCD3;1:GUS* plants express a construct containing the 1 kb of sequence upstream of the *CYCD3;1* ATG codon upstream of the *uidA* gene (hereafter referred to as *GUS*). This reporter has been described previously (Riou-Khamlichi *et al.*, 1999). As *ant/ant* mutants are female sterile, subsequent experiments were performed using F3 seeds which were homozygous for the *pCYCD3;1:GUS<sub>Ler</sub>* construct but segregated for the *ant-9* allele. In *pCYCD3;1:GUS<sub>Ler</sub>* shoots, GUS activity was detected in leaf primordia and hydathodes (Figure 3.8A). However, in the *ant-9<sub>Ler</sub>* mutant background, whilst GUS activity remained detectable in the hydathodes, none was detected in leaf primordia (Figure 3.8A). This suggests that ANT regulates the expression of *CYCD3;1* by modulating the activity of its promoter. To confirm this result, a *pCYCD3;1:GUS-GFP<sub>Col-0</sub>* reporter line was crossed with an *ant* GABI-KAT (*ant-GK<sub>Col-0</sub>*) mutant, both of which are in the *Col-0* background as opposed to the *Ler* background (see Chapter 2), and the experiment was repeated as above. *pCYCD3;1:GUS-GFP* plants express a gene encoding a GUS-GFP fusion under regulation of the 1 kb of sequence upstream of the *CYCD3;1* ATG codon. GUS activity was detected in the leaf primordia in the *WT<sub>Col-0</sub>* background (Figure 3.8B) but not in the *ant-GK<sub>Col-0</sub>* background, again demonstrating a requirement of the *CYCD3;1* promoter used in this assay for the presence of functional ANT.

That *CYCD3;1* promoter activity is reduced in *ant* mutants does not necessarily mean that native *CYCD3;1* is downregulated in these mutants. qPCR analyses of RNA extracted from *ant-9<sub>Ler</sub>* shoots showed no downregulation of *CYCD3;1* transcript levels when compared to *WT<sub>Ler</sub>* shoots (Figure 3.8C). This suggests that ANT is not rate-limiting for expression of endogenous *CYCD3;1*.

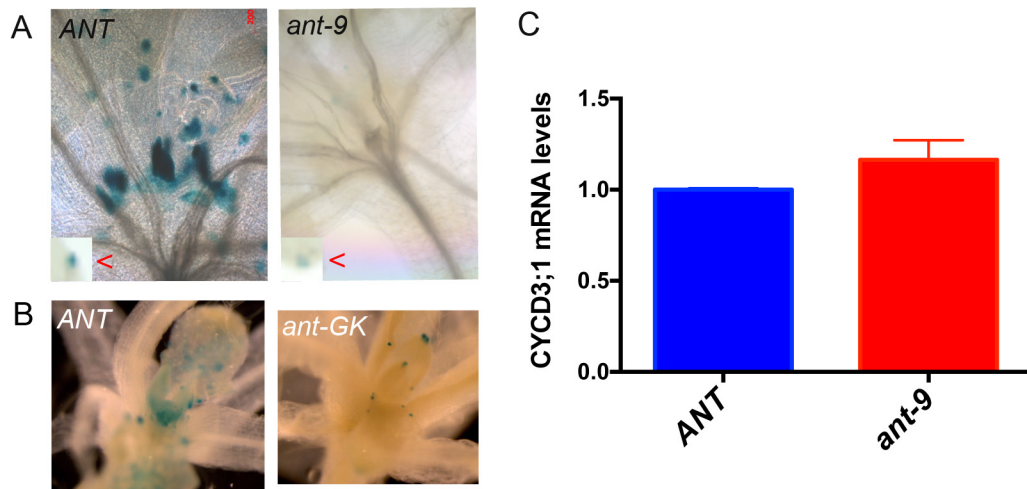


Figure 3.8: *CYCD3;1* expression in *WT* and *ant* loss-of-function mutant shoots. Pictures of plants were taken around the region of the SAM. A) *CYCD3;1* promoter activity represented by the *pCYCD3;1:GUS<sub>Ler</sub>* reporter in *ANT<sub>Ler</sub>* and *ant-9<sub>Ler</sub>* shoots. Insets show expression in hydathodes (red arrows), demonstrating that the GUS assay was functional in both cases. B) *CYCD3;1* promoter activity represented by the *pCYCD3;1:GUS-GFP<sub>Col-0</sub>* reporter in *ANT<sub>Col-0</sub>* and *ant-GK<sub>Col-0</sub>* shoots. C) *CYCD3;1* transcript levels relative to those of *ACT2*. Mean expression levels from three technical replicates are shown. Error bars represent s.d. RNA was extracted from pooled shoots for each sample to obtain an average from the population.

To confirm this result, the experiment was repeated with the *ant-GK<sub>Col-0</sub>* mutant (Figure 3.9). There appeared to be a slight reduction in *CYCD3;1* mRNA levels in *ant-GK<sub>Col-0</sub>* plants, specifically a reduction of 22% (Figure 3.9A). To confirm that the primers used for qPCR analyses were specific for *CYCD3;1* transcripts, they were used to measure *CYCD3;1* mRNA levels in *WT<sub>Ler</sub>*, *cycd3;1<sub>Ler</sub>* (Dewitte *et al.*, 2007) and *p35S:CYCD3;1<sub>Ler</sub>* (Dewitte *et al.*, 2003) plants. Transcript levels appeared to be absent in the loss-of-function mutant, and increased over 50-fold in the over-expresser (Figure 3.9B), indicating that the primers are appropriate for detection of *CYCD3;1* transcripts specifically. Agarose gel electrophoresis was employed to analyse qPCR products, and a single product of the expected size (Chapter 2) was obtained when *WT<sub>Ler</sub>* cDNA was used as a template, whereas a smaller product likely representing primer-dimers was obtained when water was used as a template (Figure 3.9C). The primer-dimer template was amplified logarithmically at a very late stage in the qPCR (36 cycles versus 21 cycles for amplicon from *CYCD3;1* cDNA), and this is therefore unlikely to make any significant contribution to transcript level values obtained.

The results from these two experiments are not apparently consistent, since qPCR shows no or little change but the reporter showed a dependence on *ANT*. One possible explanation for the discrepancy is that the *CYCD3;1* promoter used is not sufficient to provide a faithful representation of the gene's expression pattern.

There is another interesting possibility. Within the *CYCD3;1* 5' untranslated region (UTR) lie two sequential upstream open reading frames (uORFs) (Figure 3.9D). uORFs are known to disrupt the translation of downstream ORFs in eukaryotes, since the ribosome translates them, and dissociates from the mRNA once it reaches the stop codon (Gopfert *et al.*, 2003; Nishimura *et al.*, 2005b; Medenbach *et al.*, 2011). The presence of uORF stop codons can also disrupt gene expression by initiating nonsense-mediated mRNA decay, since the stop codon can be read as a premature stop codon, a warning to the cell that a mutation has happened (Saul *et al.*, 2009). It is possible that *ANT* initiates transcription downstream of these uORFs, producing an mRNA molecule lacking the ATG codons of these uORFs, possibly lacking both of them completely. To test this hypothesis, qPCR analyses using different primer pairs were used (Figure 3.9D; see Chapter 2). To analyse total *CYCD3;1* transcript levels, the primers used previously were used. These bind at the 3' end of the

### Chapter Three: ANT & CYCD3;1 and Organ Size

ORF (Figure 3.9D), and the results have been discussed. To examine differences in the levels of the putative distinguished longer transcript levels i.e. those containing the uORFs, primers indicated in Figure 3.9D (P3 & P4) were used. Once again a small reduction in transcript levels of 25% in the *ant-GK<sub>Col-0</sub>* RNA was detected (Figure 3.9A), confirming the results obtained with the 3' primers.

Taken together, these results suggest that the activity of the *CYCD3;1* promoter depends on the presence of functional ANT, whereas *CYCD3;1* mRNA levels either do not or do to a lesser extent.

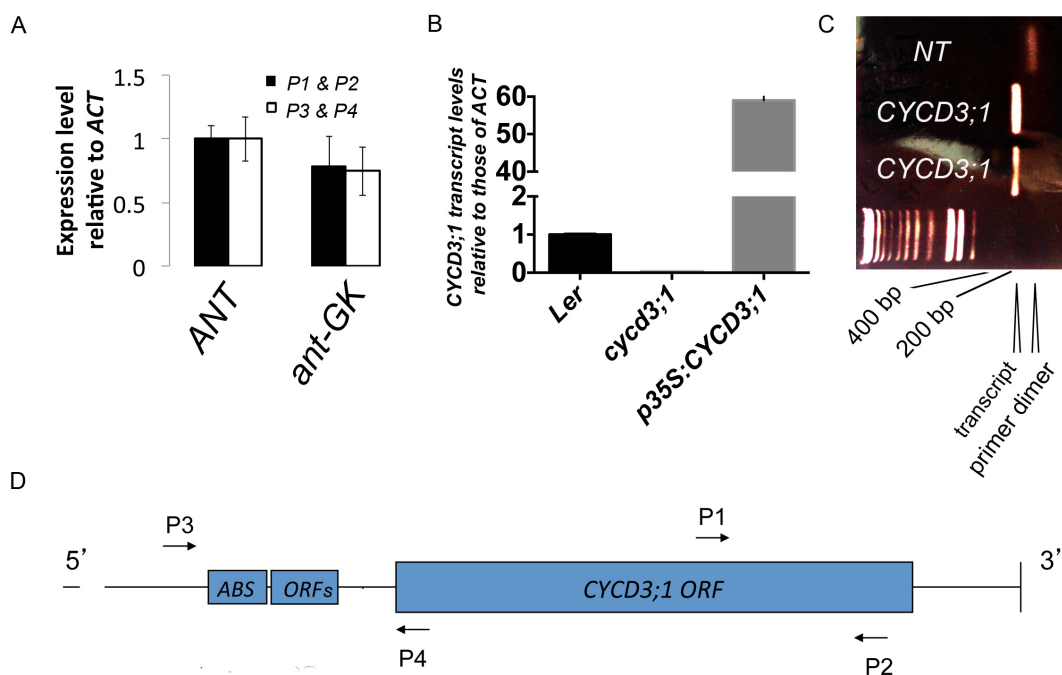


Figure 3.9: *CYCD3;1* transcript levels are similar in *ANT<sub>Col-0</sub>* and *ant-GK<sub>Col-0</sub>* plants. A) qPCR in *ANT<sub>Col-0</sub>* and homozygous *ant-GK<sub>Col-0</sub>* plants using primers in the 3' end of *CYCD3;1* and primers overlapping with the 5' UTR (D). Error bars represent s.d. from three individual plants. B) qPCR on pooled RNA from multiple *WT<sub>Ler</sub>*, *cycd3;1<sub>Ler</sub>*, or *35S:CYCD3;1<sub>Ler</sub>* plants. Error bars represent s.d. from three technical replicates. All transcript levels were normalized to those of *ACT2*. C) Results of agarose gel electrophoresis showing the qPCR products of two independent reactions containing *WT<sub>Ler</sub>* DNA and one containing water in place of template. D) Structure of *CYCD3;1* mRNA ([www.arabidopsis.org](http://www.arabidopsis.org)), showing the putative ANT-binding site (ABS), the localization of the small uORFs, the *CYCD3;1* ORF and the binding sites for the primers used for qPCR.

### 3.9 Characterization of a Transgenic Line Expressing an ANT-GR Fusion Protein Under the 35S Promoter

For future studies to determine whether ANT regulates the expression of *CYCD3;1*, and to identify other targets of ANT, an inducible over-expresser of ANT with an epitope tag could be employed. So that this might be possible, a genetic construct containing the *ANT* coding sequence upstream of the rat glucocorticoid receptor (GR) domain and downstream of the constitutively active 35S promoter was created (Figure 3.10). Plants expressing this construct could be used for microarray analysis and ChIP to identify putative direct targets of ANT. The metazoan GR domain anchors proteins in the cytoplasm thus excluding them from the nucleus and preventing them from physically interacting with target genes (Galigniana *et al.*, 1998). Steroid hormones release the domain from the cytoplasm and allow it to enter the nucleus. This system works analogously in plants when the GR domain is fused to other proteins, and the addition of the steroid hormone dexamethasone to plant cells causes cytoplasm-anchored protein-GR fusion molecules to enter the nucleus (Lloyd *et al.*, 1994).

The sequence for the GR domain was amplified by PCR using a vector containing this sequence along with a lysine linker from Alexander Murrison (Cardiff, UK). The primers used were ANTcod-GlyLnkGR\_fwd and pGREEN35STn-GR\_rev. An *MluI* site was added to the 5' end using the appropriate primer tail. The PCR product was cloned into a pCR-Blunt vector via a TOPO® reaction. The pCR-Blunt vector containing the GR domain was sequenced, and the results aligned with the *Rattus norvegicus* sequence from which the GR domain sequence derives. The fragment had the correct sequence, and was inserted in the reverse orientation. The *ANT* coding sequence was amplified by PCR using *WT<sub>Col-0</sub>* cDNA as a template. The primers used were pANT-ANTcod\_fwd and GlyLnk-GR-ANTcod\_rev. An *MluI* site was added to the 3' end. The PCR product was inserted into the pCR-Blunt vector via a TOPO® reaction. This fragment had the correct sequence and was also inserted in the reverse orientation. These vectors were each digested with the *MluI* restriction enzyme. In the pCR-Blunt vector containing the *ANT* coding sequence, two *MluI* sites were present downstream of the *ANT* insertion. Therefore, digestion with *MluI* opened up the vector immediately downstream of

the *ANT* coding sequence. In the pCR-Blunt vector with the *GR* domain insertion, two *MluI* sites flanked the insertion. Therefore digestion with *MluI* cleaved the *GR* fragment from this vector. This fragment was inserted downstream of the *ANT* coding sequence via a ligation reaction. The resulting *ANT-GR* sequence was confirmed to be in frame via sequencing. The binary vector pGREENII0229 containing a *YFP* gene downstream of a 35S promoter and upstream of a 35S terminator sequence was obtained from Celine Forzani (Cardiff, UK). A *NotI* site is present between the 35S promoter and the *YFP* sequence, and an *SpeI* site lies between the *YFP* gene and the 35S terminator. This vector and the pCR-Blunt vector containing the *ANT-GR* fusion were digested with *NotI* and *SpeI*. This excised the *ANT-GR* fusion and the *YFP* sequences from these vectors, respectively. The *ANT-GR* fusion was gel-eluted, as was the pGREENII0229 backbone, and the former was inserted into the latter via a ligation reaction. Thus the pGREENII0229 binary vector containing the *ANT-GR* fusion downstream of the 35S promoter and with a 35S terminator was obtained. The DNA between the left and right borders was sequenced and sequence analysis confirmed that it was correct.

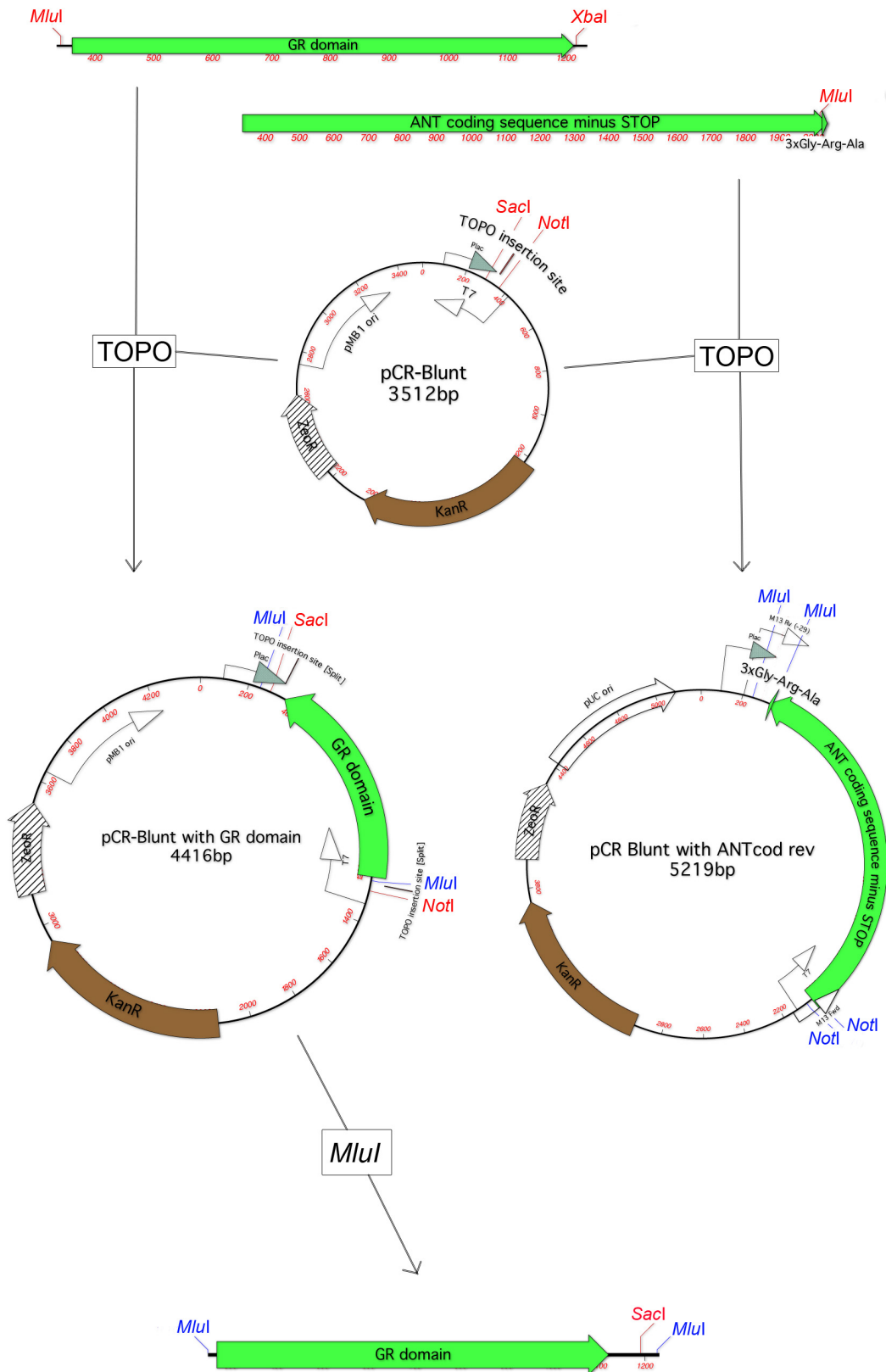
T1 plants from T0s (untransformed recipient plants) transformed with the vector containing the 35S:*ANT-GR* construct were originally selected on antibiotics, but were subsequently screened by PCR to confirm the presence of the transgene. A T1 plant showing over-expression of *ANT* was identified using qPCR on floral tissue-derived cDNA (Figure 3.11A) and T3 seeds of this line were screened by antibiotic resistance to find a population in which all individuals were homozygous for 35S:*ANT-GR*.

To measure *ANT* expression levels in this line, T3 seedlings were grown *in vitro* on GM roots media in long day conditions (see Chapter 2) and RNA was extracted from roots and shoots separately (Figure 3.11A). *ANT* expression was upregulated ~ 13-fold in roots and ~15-fold in shoots. When the plants were grown on media containing 30µM dexamethasone, expression was reduced to ~ 7-fold that of *WT<sub>Col-0</sub>* in roots and ~ 6-fold that of *WT<sub>Col-0</sub>* in shoots (Figure 3.11A). This suggests that negative feedback is occurring; perhaps *ANT* negatively regulates its own expression.

To check whether or not the fusion protein in this transgenic line was translated and functional, flowering plants were sprayed with 30µM dexamethasone. Whilst control 35S:*ANT-GR<sub>Col-0</sub>* plants sprayed with a mock solution senesced after approximately six weeks, with barely any new flowers

emerging from the shoot apex (Figure 3.11B), *35S:ANT-GR<sub>Col-0</sub>* plants grown alongside these sprayed with dexamethasone continued to develop new flowers, and silique growth appeared to be inhibited (Figure 3.11B). Delayed flower growth and female sterility have been observed in over-expressers of *ANT* (Krizek, 1999). Thus these results are consistent with those observed by Krizek *et al.* (1999) with a different genetic construct. Increases in the numbers of rosette leaves in *35S:ANT-GR<sub>Col-0</sub>* plants grown *in vitro* on media containing dexamethasone were also observed (Figure 3.11C), possibly reflecting a delay in the transition from the vegetative phase of development to the reproductive phase.

### Chapter Three: ANT & CYCD3;1 and Organ Size



# Chapter Three: ANT & CYCD3;1 and Organ Size

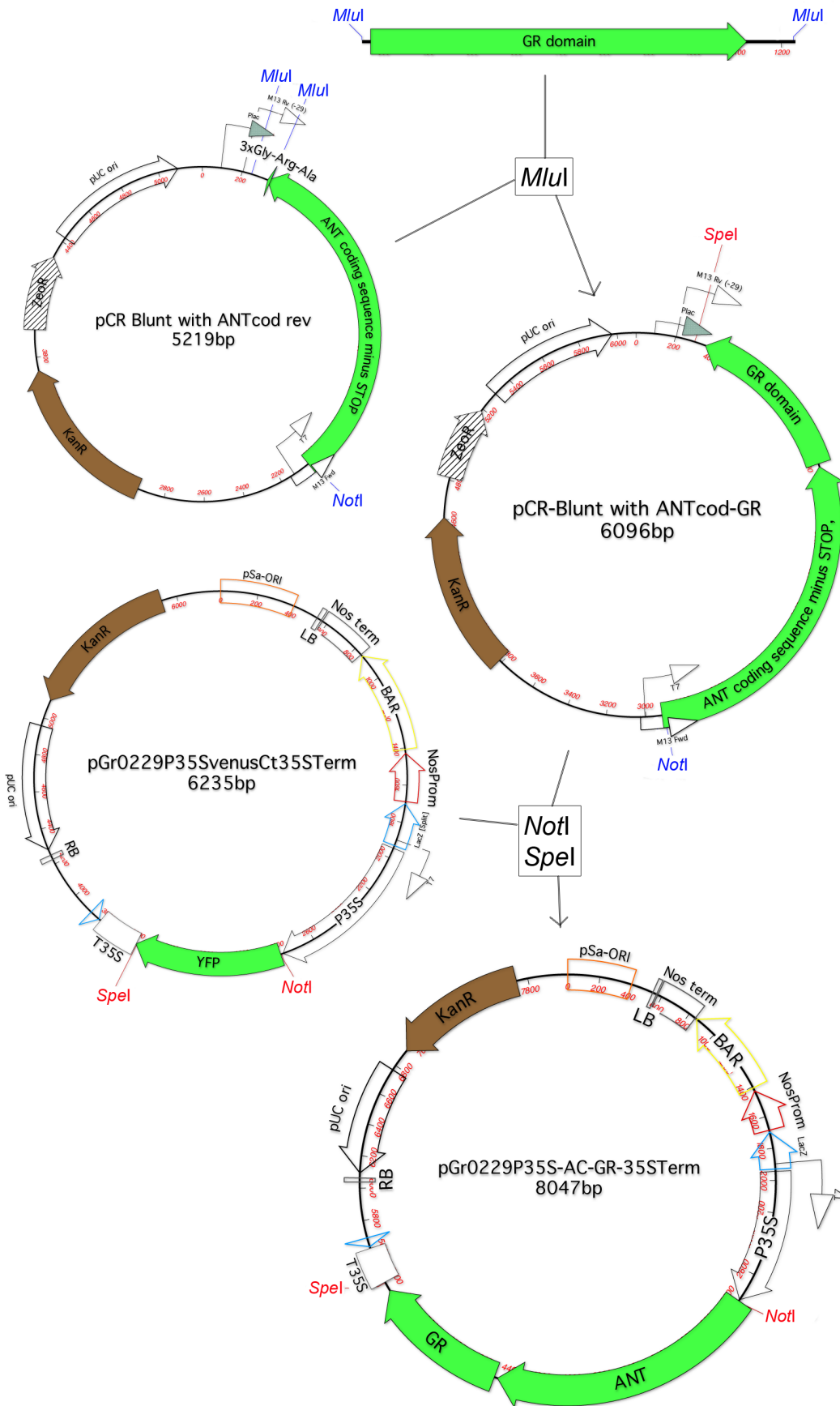


Figure 3.10: Steps involved in the construction of the *p35S:ANT-GR* vector. Restriction sites in red indicate those that only occurred once in a vector. Those in blue represent sites that occurred more than once in a vector. Boxes outside of vector maps indicate reactions. Ori: origin of replication. KanR: Kanamycin resistance marker gene for bacteria. ZeoR: Zeocin resistance marker gene for bacteria. BAR: phosphinothricin resistance marker gene for plants. NosTerm: *NOPELINE SYNTHASE* terminator sequence. LB and RB: Left and right borders of *Agrobacterium* T-DNA, respectively.

Since ANT regulates petal size and cell size, these parameters of LAO growth were analysed in *35S:ANT-GR<sub>Col-0</sub>* plants. Analyses were performed on petals extracted from stage 15 (mature) flowers (Smyth *et al.*, 1990). Petals of *35S:ANT-GR<sub>Col-0</sub>* plants sprayed with dexamethasone were larger than equivalent plants sprayed with a mock solution (Figure 3.11C). Petals of *35S:ANT-GR<sub>Col-0</sub>* plants sprayed with the mock solution had a mean adaxial surface area of  $1.596 \pm 0.048 \text{ mm}^2$ , whilst plants of the same genotype sprayed with the dexamethasone solution had a mean surface area of  $2.527 \pm 0.133 \text{ mm}^2$ , representing a 58% increase (Figure 3.11D,E; one-way ANOVA,  $p < 0.0001$ , d.f. = 30). *WT<sub>Col-0</sub>* plants sprayed with the mock solution had a mean adaxial surface area of  $1.469 \pm 0.036 \text{ mm}^2$ , whilst plants of the same genotype sprayed with the dexamethasone solution developed petals with a mean surface area of  $1.807 \pm 0.031 \text{ mm}^2$ . Therefore, *WT<sub>Col-0</sub>* plants also responded to dexamethasone with an increase in petal size (one-way ANOVA,  $p = 0.02$ , d.f. = 30), but in this case it was a smaller increase of 23% (Figure 3.11D,E).

Microscopical analysis of petal cells was performed to determine the cause of increased petal size in the transgenic line when induced. In *35S:ANT-GR<sub>Col-0</sub>* plants sprayed with dexamethasone, mean petal adaxial epidermis cell surface area was  $193.2 \pm 6.008 \text{ }\mu\text{m}^2$ . In plants of the same genotype sprayed with a mock solution, mean cell surface area was  $139.2 \pm 4.544 \text{ }\mu\text{m}^2$ . Thus spraying the plants with dexamethasone resulted in a 39% increase in cell surface area (one-way ANOVA,  $p < 0.0001$ , d.f. = 179; Figure 3.11F), suggesting that this might be the factor driving petal size increase. However, since flowering plants were used, these petals may have already progressed through the mitotic window, and induction of the fusion protein may therefore have only targeted cell expansion. ANT is known to affect cell expansion under some circumstances (Krizek, 1999). Moreover, the increase in petal adaxial surface area in *35S:ANT-GR<sub>Col-0</sub>* plants sprayed with dexamethasone was 58%, therefore cell expansion cannot solely account for the increase in petal size. Mean adaxial cell surface area in *WT<sub>Col-0</sub>* plants sprayed with dexamethasone was  $126.2 \pm 4.418 \text{ }\mu\text{m}^2$ . That of *WT<sub>Col-0</sub>* plants sprayed with a mock solution was a similar  $126.7 \pm 4.676 \text{ }\mu\text{m}^2$  (one-way ANOVA,  $p = 1.0$ , d.f. = 179). Since *WT<sub>Col-0</sub>* petals displayed a 23% increase in size following treatment with dexamethasone, and there is no observable cell size increase, petal size increase must be due to an increase in cell number. This suggests that in the *35S:ANT-GR<sub>Col-0</sub>* plants, petal cell size increase is driven by increases in cell expansion mediated by ANT, but also by increases in cell number as a consequence of exposure to dexamethasone.

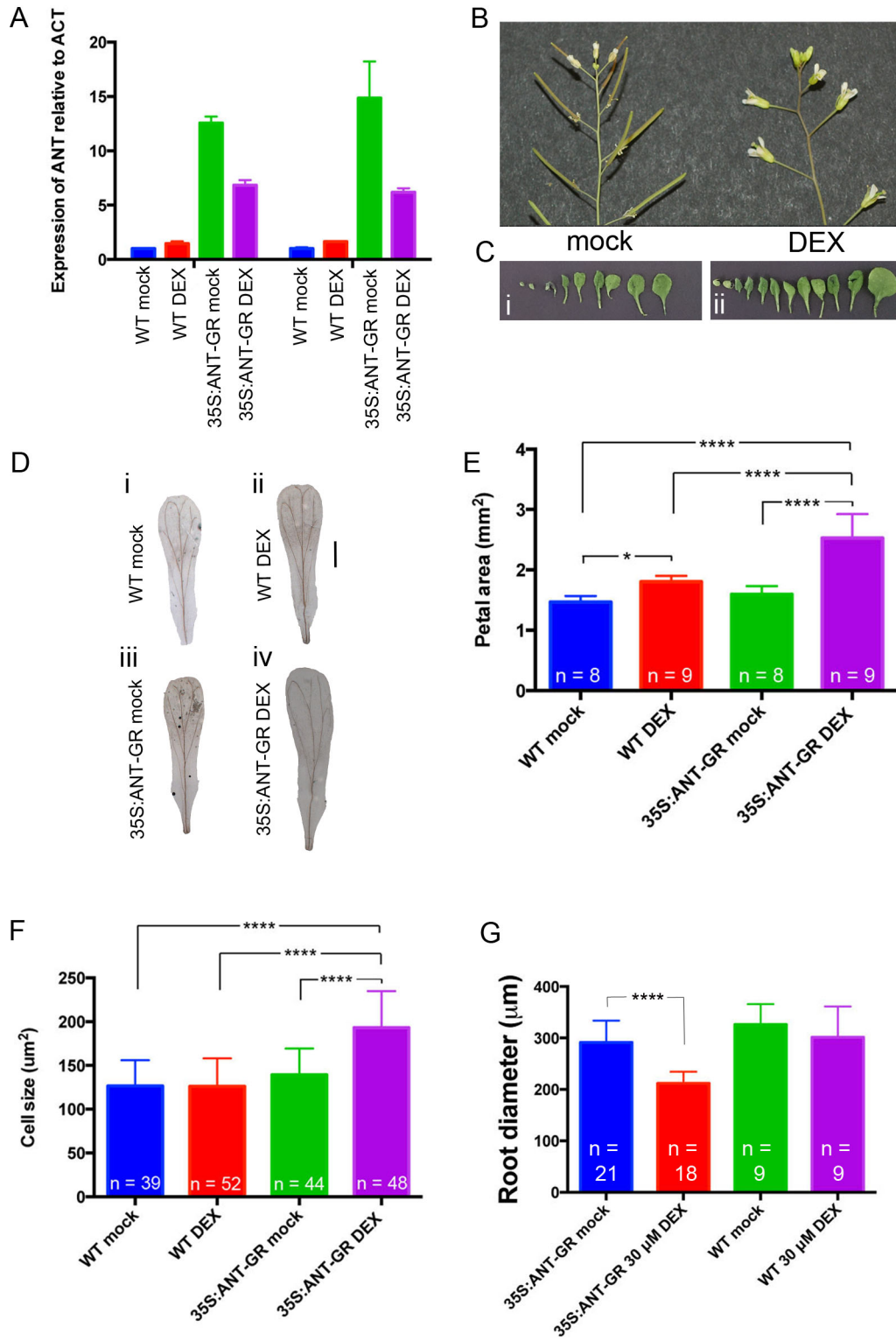


Figure 3.11: Characterization of the *35S:ANT-GR<sub>Col-0</sub>* transgenic line. A) qPCR analysis of *ANT* expression in *WT<sub>Col-0</sub>* plants and *35S:ANT-GR<sub>Col-0</sub>* plants grown for two weeks on GM roots media. Analysis was performed on shoots and roots separately. Expression levels are relative to those of *ACT2*. Error bars represent standard deviation from three technical replicates. Each sample contained roots or shoots from several plants to get an average from the population. B) Shoots of *HÍ ÛKÇP VËÖÛ* plants grown in soil were sprayed either with water or a water solution containing 30 µM dexamethasone. Pictures of the primary shoots were taken two weeks later. C) Seedlings were grown on GM media for 18 days and the leaves were taken off. Leaves are shown from smallest (left) to largest (right). As in B), *HÍ ÛKÇP VËÖÛ* plants grown on media without dexamethasone are shown on the left (i), and plants of the same line grown on media containing 30 µM dexamethasone are shown on the right (ii). D) Petals from plants sprayed either with water or 30 µM dexamethasone are shown. Plants were grown in soil and petals were taken one week after spraying. Analysis was performed on *Y VÇÔ[ ]ËD* (i-ii) and *HÍ ÛKÇP VËÖÛ* plants (iii-iv). E) Mean adaxial surface area of the petals described in (D). F) Mean surface area of cells of petals described in (D). G) Mean root diameter of plants grown on GM roots for two weeks. Error bars in (E-G) represent standard deviation. In all graphs,  $\chi^2$  values from t tests are presented as \* < 0.05, \*\* < 0.01, \*\*\* < 0.001, \*\*\*\* < 0.0001.

There is evidence for ANT acting as a regulator of secondary growth in roots (Chapter 4). To further characterize the *35S:ANT-GR<sub>Col-0</sub>* line, root diameter was measured in *35S:ANT-GR<sub>Col-0</sub>* plants grown vertically on media containing dexamethasone. *WT<sub>Col-0</sub>* roots did not appear to respond to dexamethasone, those sprayed with a mock solution having a mean root diameter of  $326.0 \pm 13.28 \mu\text{m}^2$  and those sprayed with dexamethasone having a mean root diameter of  $301.6 \pm 20.02 \mu\text{m}^2$  (one-way ANOVA,  $J = 0.58$ , d.f. = 53; Figure 3.11G). *35S:ANT-GR<sub>Col-0</sub>* roots were thinner when grown with the hormone (Figure 3.11G). Transgenic roots sprayed with a mock solution had a mean diameter of  $291.4 \pm 9.268 \mu\text{m}^2$ , whereas those sprayed with dexamethasone had a mean diameter of  $211.8 \pm 5.394 \mu\text{m}^2$ , representing a 27% decrease (one-way ANOVA,  $p < 0.0001$ , d.f. = 53). Anatomical analyses would need to be performed to determine the cause of this decrease. As ANT regulates cell proliferation, it might be that these roots contain many small cells that have failed to enlarge.

To further address the hypothesis that ANT regulates *CYCD3;1* expression, *CYCD3;1* transcript levels were measured in *35S:ANT-GR<sub>Col-0</sub>* plants grown on dexamethasone. An increase in *CYCD3;1* transcript levels of 43% was observed in induced shoots, but the variation among biological replicates was too great to confirm this (Figure 3.12A). Once ANT has been induced in plants for several days, molecular feedback might act to alter expression levels of *CYCD3;1* expression. To check whether or not this might be the case, 12 DAG *35S:ANT-GR<sub>Col-0</sub>* plants were incubated in 30 $\mu\text{M}$  dexamethasone, and *CYCD3;1* expression was monitored by sequential RNA extractions and subsequent qPCR over a 24 hour time course (Figure 3.12B). In both mock treated samples and samples with dexamethasone, *CYCD3;1* expression appeared to drop to around half the level of that in plants before incubation with any solution (Figure 3.12B). This happened as early as two hours, and these levels were maintained for the remainder of the experiment. These plants were undergoing a stress, as they were bathed in solution, and so this stress may have been the cause of *CYCD3;1* downregulation. None the less, no relative increase of *CYCD3;1* expression was observed in the plants incubated with dexamethasone.

The *35S:ANT-GR<sub>Col-0</sub>* line needs further characterization before use for microarray and ChIP experiments, to confirm that the protein is indeed capable of inducing the expression of targets. This is difficult at present, as no targets of ANT have been identified. Use of the transgenic line harbouring a reporter with the optimal ANT-binding site might be helpful (Krizek and Sulli, 2006).

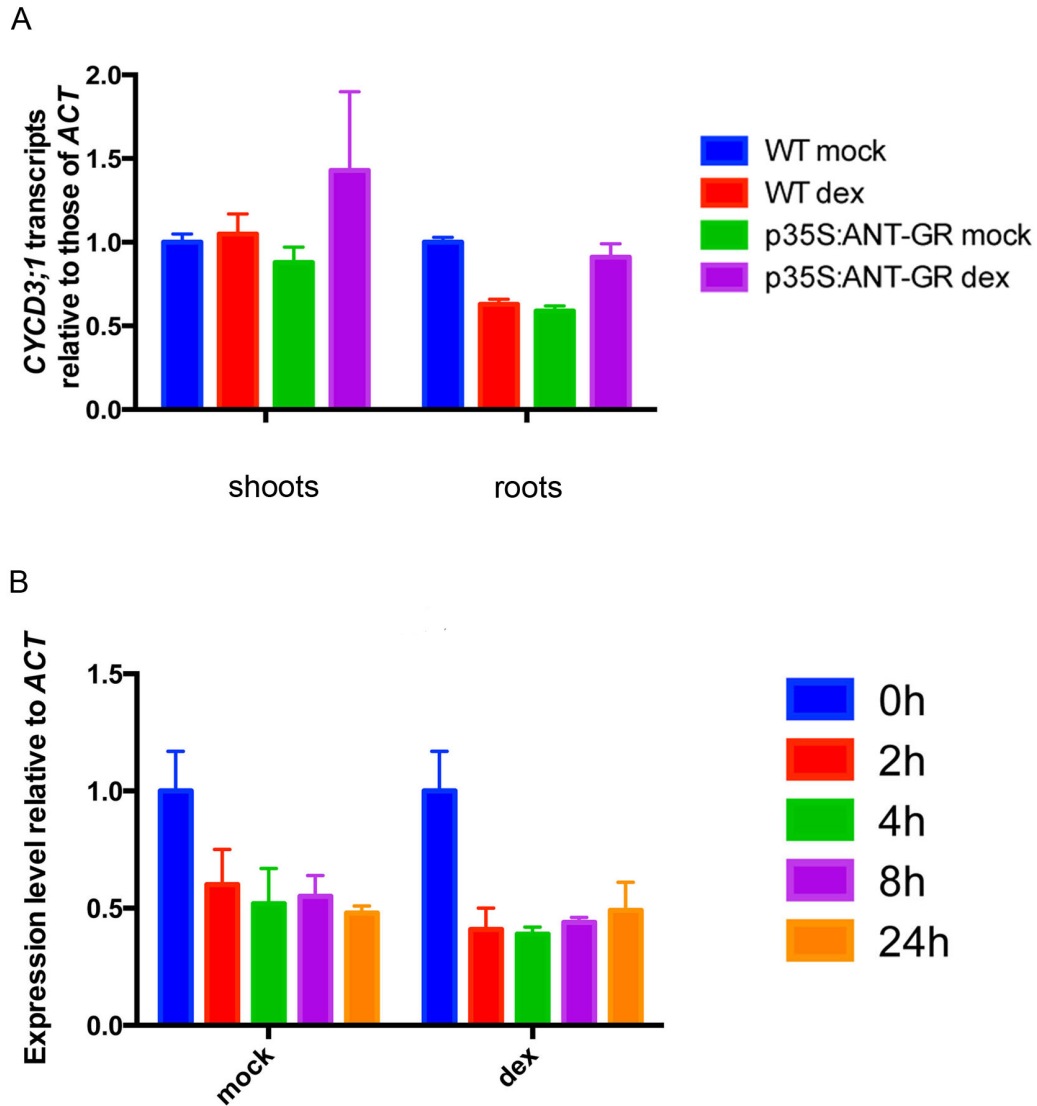


Figure 3.12: qPCR analysis of *CYCD3;1* expression following the induction of the ANT-GR fusion protein with dexamethasone. A) RNA was extracted from shoots or roots, as indicated, of two week-old plants grown on 30  $\mu$ M dexamethasone or media containing a mock solution. Error bars represent standard deviation of three technical replicates. Each sample was produced from RNA extracted from several roots or shoots. *ACT2* was used as a reference gene for normalization of data. B) RNA was extracted from whole seedlings, grown for two weeks on GM, then incubated with 30  $\mu$ M dexamethasone or a mock solution, at the time points after start of incubation indicated. *35S:ANT-GR<sub>Col-0</sub>* plants were used for this experiment. Error bars represent standard deviation of three technical replicates. Each sample was produced from RNA extracted from several seedlings.

## Discussion

---

*ANT* is now a well-established regulator of LAO growth. In their investigation of the mechanisms by which *ANT* regulates final LAO size, Mizukami & Fisher showed that *ANT* regulates the length of the mitotic window during which cell proliferation can occur during LAO growth (Mizukami and Fischer, 2000). They also showed that ectopic constitutive expression of *ANT* caused ectopic expression of *CYCD3;1* in mature leaves. However, it remained unknown whether or not this was a result of direct regulation of *CYCD3;1* expression by *ANT*. It might be that the identity of cells in leaves ectopically expressing *ANT* was such that *CYCD3;1* expression was part of the gene expression profile of those cells.

In this study, the functional interaction between these two genes was investigated in petals and leaves as models of LAOs. As part of this, the phenotypes of the *ant* and *cycd3;1* loss-of-function single mutants were reanalysed. As reported previously (Mizukami and Fischer, 2000), *ant* mutant petals were smaller than *WT* petals, and this was due to a reduction in cell number. Cell size was increased in these mutants, reflecting a compensation mechanism regulating LAO size. *cycd3;1* mutant petals had numbers of cells similar to those of *WT* petals in both *Ler* and *Col-0* backgrounds. As this does not agree with results obtained by Dewitte *et al.* (2007), the experiment was repeated, and the results of the second experiment in this study agreed with those of the first. Therefore, under the conditions used in this experiment, *CYCD3;1* does not appear to regulate cell number in petals. It might be that cell number in petals was affected by the different growth conditions experienced by the plants in different laboratories. As observed by Dewitte *et al.* (2007), cell size was increased in *cycd3;1* mutants. Thus *CYCD3;1* might play some role linking cell division and cell expansion in petals.

*ant* leaves were also smaller than *WT* leaves, and like petals had a reduced number of cells that were larger than their *WT* counterparts, consistent with a compensation mechanism counteracting reductions in cell number in plant LAO size control (Horiguchi and Tsukaya, 2011). At least in this case, the mechanisms of petal size control seem to be similar to the mechanisms of leaf size control. In *Ler*, *cycd3;1* mutants had no observable leaf phenotype. Perhaps in this this genetic background *CYCD3;2* and *CYCD3;3* are redundantly regulating LAO cell number and compensate for the loss of

functional *CYCD3;1*. However, in the *Col-0* ecotype, *cycd3;1* leaves were smaller than *WT* leaves, and this was due to a reduced number of cells. Thus something, or many things, in either the *Col-0* ecotype or the *Ler* ecotype, appears to have an epistatic interaction with *CYCD3;1*. However, since the *cycd3;1* mutant in the *Col-0* background was derived by crossing its original isolate in the *Ler* ecotype, it still contains DNA sequence from *Ler*, which could have an independent effect on leaf cell number. Therefore, to confirm that *CYCD3;1* does regulate leaf cell number in the *Col-0* background, an independent *cycd3;1* allele must be obtained in this background. Unfortunately the insertion in *Ler* is the only one known. One way to do this would be by using the new directed genome editing technology involving the CRISPR/Cas system adapted from the bacterial immune system (Belhaj *et al.*, 2013). Alternatively, a rescue construct expressing *CYCD3;1* might be employed in an attempt to restore organ size and cell size/number.

To investigate the functional interaction between *ANT* and *CYCD3;1*, the petals of double *ant-9 cycd3;1* loss-of-function mutants in the *Ler* background were analysed. This revealed an epistatic interaction between *ANT* and *CYCD3;1*, as loss of functional *CYCD3;1* partially suppressed the phenotype of the *ant-9<sub>Ler</sub>* mutant. This was due to an additive cell size increase from both mutant alleles. This does not support the hypothesis that *ANT* regulates the expression of *CYCD3;1*, but neither does it disprove it, as *ANT* is likely to be regulating the expression of many other genes involved in petal development, and *CYCD3;1* is likely to have other regulators. Thus whilst some functions of each protein could be shared, each is likely to have other independent functions.

Cell size increase was therefore a phenotype shared by *ant* and *cycd3;1* mutants in petals. In *ant-9 cycd3;1* double mutants, this cell size phenotype was additive. Thus at least some of the roles of *ANT* and *CYCD3;1* in the regulation of petal cell size appear to be exclusive to one factor or the other. Due to the additivity of this phenotype, petal size was actually increased in *ant-9 cycd3;1* mutants compared to *ant-9* single mutants.

The results obtained here also suggested that leaf size reduction in *ant-9* mutants was enhanced by the homozygous presence of the *cycd3;1* allele. Although this enhancement was not deemed as statistically significant at a P value of 0.12, use of a larger sample size in future experiments might reveal this phenotype unambiguously. If this is the case, this would suggest that in *ant-9* mutants, *CYCD3;1* is preventing a further reduction in cell number, thus

revealing a role for *CYCD3;1* in regulating leaf cell number in the *Ler* ecotype as well as the *Col-0* ecotype independently of ANT.

Since all mutant combinations contained petals composed of larger cells, the hypothesis that ploidy increase and/or endoreduplication was occurring to drive this increase in size in some or all of these mutants was tested. Endoreduplication entails replication of nuclear DNA without subsequent cell division. Cells progress from the G2 phase to the G1 phase, and the process can repeat itself several times. *ant-9<sub>Ler</sub>* mutants showed a ploidy distribution similar to that in *WT<sub>Ler</sub>*: most cells appeared to have a genome content of 2C. *cycd3;1* single and *ant-9 cycd3;1* double mutants showed a relative increase in ploidy content. *cycd3;1<sub>Ler</sub>* and *ant-9 cycd3;1<sub>Ler</sub>* mutant petals contained a larger proportion of cells with 4C DNA content than *WT<sub>Ler</sub>* or *ant-9<sub>Ler</sub>* petals. *cycd3;1-3* mutant petals also have cells with greater ploidy levels (Dewitte *et al.*, 2007). This shows that *CYCD3;1* is keeping cells in the G1 phase of the mitotic cell cycle. In *cycd3;1* mutants, the cells might be in the G2 phase of the mitotic cell cycle, or they might be in the G1 phase of the first endocycle, as the genome content would be 4C in both cases (Larkins *et al.*, 2001). Arabidopsis cells increase in size throughout the cell cycle (Schiessl *et al.*, 2012). Endoreduplication is also normally associated with increases in cell size (Sugimoto-Shirasu and Roberts, 2003). The Arabidopsis E2F/RBR complex is a target of CyclinD/CDK complexes (Oakenfull *et al.*, 2002). Overlaps in expression changes in plants with altered *E2FA* or *CYCD3;1* expression have been shown, enforcing the idea that these genes act in a common pathway (de Jager *et al.*, 2009). E2F binding-motifs are present in the promoters of two genes that regulate the onset of endocycles, *CCS52A1* and *CCS52A2*, and downregulation of *E2FA* expression leads to increases in the expression of these genes and premature endocycle onset (Magyar *et al.*, 2012). Perhaps *CYCD3;1* acts in this pathway to regulate the initiation of endocycling. Therefore increased ploidy level may be at least partially contributing to the increase in cell size in the *cycd3;1<sub>Ler</sub>* mutants.

A cell cycle inhibitor, KRP1, has been shown to alter endoreduplication in leaf trichomes when mis-expressed, demonstrating effects of cell cycle regulators on ploidy level (Schnittger *et al.*, 2003b). However, this cell cycle inhibitor reduced ploidy levels, implying that increasing cell cycle activity might in fact increase ploidy levels. KRP1 was shown to interact with a CDKA/*CYCD3;1* complex (Schnittger *et al.*, 2003b), and ectopic expression of *CYCD3;1*

suppressed the *KRP1* mis-expression phenotype. However, ploidy levels in *CYCD3;1* mis-expressers were not quantified. Ectopic expression of *E2FA* and *DPA*, the products of which form a complex promoting S phase progression via transcriptional activation, promotes cell proliferation, but when expressed in cells already endoreduplicating, promotes additional rounds of endoreduplication (De Veylder *et al.*, 2002). Therefore the effects of altering the activity of cell cycle proteins have on endoreduplication might depend on the initial ploidy status of the cells. On the other hand, altering *CYCD3* expression has previously been shown to alter the stage at which petal cells initiate endocycles (Dewitte *et al.*, 2007). In conclusion, endoreduplication may be initiated in *cycd3;1* mutant petals, and this may lead to an increase in cell size, but it is equally possible that *cycd3;1* mutant cells remain in the G2 phase of the cell cycle as opposed to the G1 phase.

The increase in cell size observed in the *ant-9<sub>Ler</sub>* mutant appears to be independent of endoreduplication. Reduction in LAO size by shading and water deficit also reduces cell number, whilst cell size is increased without any change in ploidy distribution (Cookson *et al.*, 2006). The mechanism driving cell expansion as part of a compensation mechanism might not involve cell cycle activity or endoreduplication. Alternatively, loss of functional *ANT* might lead to early differentiation and cell expansion of LAO cells. Supporting such a role for *ANT* in regulating cell differentiation initiation, over-expression of *ANT* using the 35S promoter appears to suppress senescence in flowers. High cytokinin levels also delay flower senescence (Gan and Amasino, 1995); perhaps this occurs in part via activation of *ANT*. In the *cycd3;1<sub>Ler</sub>* mutant, cell size increase is not part of a compensation mechanism, as in this mutant, petals do not have a reduced number of cells compared to *WT<sub>Ler</sub>* plants. The increase in cell size might instead be due to a change in endoreduplication. Since the mechanisms in cell size increase in *ant-9<sub>Ler</sub>* and *cycd3;1<sub>Ler</sub>* mutants appear to be different, it is not surprising that the cell size phenotype in the double mutant is additive.

A more direct approach to testing the hypothesis that *ANT* regulates the expression of *CYCD3;1* was employed. Using the *pCYCD3;1:GUS<sub>Ler</sub>* reporter line, *CYCD3;1* expression was detected in leaf primordia of plants with a *WT<sub>Col-0</sub>* *ANT* allele, whereas none was detected in *ant-9<sub>Ler</sub>* loss-of-function mutants. This was confirmed in the *Col-0* ecotype with an independent reporter and the novel *ant-GK<sub>Col-0</sub>* allele. However, qPCR analysis showed similar levels of *CYCD3;1* transcripts in *ant* mutants and *WT* plants. The *pCYCD3;1:GUS<sub>Ler</sub>* experiment

demonstrates a requirement of *CYCD3;1* promoter activity of the presence of functional ANT. It is possible that this promoter activity does not faithfully represent the expression pattern of the gene; other regulatory sequences may be required. Another hypothesis was tested, that the GUS protein levels might be reduced in the *ant* mutant whilst the transcript levels are not. This might then be true of the *CYCD3;1* gene and protein. This hypothesis came from the observation that two uORFs are present in the *CYCD3;1* 5' UTR. This UTR is also in the *CYCD3;1* promoter fragment used for the GUS assay, as the promoter used was the sequence 1kb upstream of the *CYCD3;1* start codon. uORFs are abundant in higher plant 5' UTRs (Tran *et al.*, 2008) and can inhibit translation of mRNAs (Saul *et al.*, 2009; Medenbach *et al.*, 2011). Such uORFs are present, for example, in the promoter of *MP*, a gene highly important in auxin signalling. These uORFs in the (*MONOPTEROS*) *MP* 5' UTR have been shown do inhibit *MP* expression at the translational level (Nishimura *et al.*, 2005a). However, qPCR using primers specific for a putative *CYCD3;1* transcript longer than the active form and containing uORFs did not reveal a difference in the abundance of this transcript species in the *ant* mutant.

Taken together, these results do not suggest that ANT significantly regulates the expression of *CYCD3;1*, although it might play a role in expression from the promoter in the absence of downstream elements. However, further research is needed to rule this out with certainty.

# Chapter Four: *CYCD3;1*, *AINTEGUMENTA* and *ER* Regulate Root Secondary Growth

## **Introduction**

---

Roles for *CYCD3;1* in the regulation of root development have, to the authors knowledge, not been reported to date. However, *CYCD3;1* is a target of cytokinin signalling (Riou-Khamlichi *et al.*, 1999), and given secondary growth of roots is regulated by cytokinins (Matsumoto-Kitano *et al.*, 2008), it was considered that this developmental program might involve *CYCD3;1*.

Post-embryonic primary root growth involves principally transversal cell divisions, whereas secondary thickening, a developmental process occurring in older root tissue, involves periclinal cell divisions. Procambial cells are activated and begin to divide periclinally, eventually assuming the identity of cambial cells, which proliferate to drive thickening (Miyashima *et al.*, 2013). It is this cell proliferation that is thought to be regulated by cytokinins (Matsumoto-Kitano *et al.*, 2008; Nieminen *et al.*, 2008).

In most monocots, growth ceases with that of the primary tissues (Spicer and Groover, 2010). Whilst there are some exceptions, such as palms that develop thick stems through primary growth alone (Tomlinson, 2006), stem and/or root thickening normally require secondary radial growth i.e. the growth of new tissues. Secondary growth occurs in lateral meristems, namely the vascular cambium and the cork cambium (Raven *et al.*, 2005). Growth in these meristems tends to occur during favourable environmental conditions, and in perennial plants this growth pattern gives rise to the appearance of growth rings (Begum *et al.*, 2013).

In shoots, the vascular cambium cells can normally be split into two cell-types: the fusiform initial cells and the ray initial cells (Raven *et al.*, 2005). Since

during secondary growth the direction of growth is perpendicular to that of primary growth, periclinal cell divisions are now defined as those parallel to the stem or root surface. Periclinal divisions of ray and fusiform initial cells produce secondary phloem and xylem cells. The daughter cells on the inside of the shoot or root cambium differentiate into xylem, whereas those on the outside differentiate into phloem. Differentiation of xylem tends to be more common than that of phloem (Raven *et al.*, 2005), and the highly lignified xylem cells form wood. Many peripheral phloem cells such as companion cells are in fact crushed by secondary growth. Since the xylem tissue becomes larger, the circumference of the vascular cambium has to increase to accommodate it. This is achieved via anticlinal divisions of the cambium cells (Raven *et al.*, 2005). Within trees, all tissue outside of the vascular bundle forms part of the bark.

As mentioned, secondary growth also occurs in the cork cambium of woody plants. The cork cambium is often derived from the cortex cells, but can derive from different cell types (Neuhaus, 2013). For example, when a thin layer of oak tree bark is peeled, the cells underneath derive a new cork cambium (Neuhaus, 2013). This process is used to grow cork for commercial use. The cork cambium provides an air-tight layer in the bark. However, plants need to undergo gas exchange, and to allow this to occur, the cork cambium cells are interspaced with gas-permeable lenticels (Raven *et al.*, 2005). Together, the cork cambium and lenticels (phellogen), and two other tissues, the phelloderm and phellem, form the periderm. The periderm often replaces the cortex and endodermis as a boundary on the outside of the shoot, as the cortex and endodermis are normally sloughed off during secondary growth (Raven *et al.*, 2005).

Secondary growth also occurs in roots, and is similar; both mechanistically and anatomically, to that in shoots. One major difference, however, is that whilst vascular tissue in shoots develops in separate vascular bundles surrounding a central pith, the vascular tissue of roots is normally found in one vascular cylinder, the stele, which is the centre-most structure of the root. In plants that undergo secondary growth, this developmental process begins in the roots in tissue that has ceased to elongate (Raven *et al.*, 2005). Meristematic procambium cells, which lie between the primary phloem and xylem, divide periclinally to produce cambium cells. However, another process unique to roots is the formative periclinal divisions of pericycle cells, which also contributes to the provision of cambium cells (Raven *et al.*, 2005). Subsequent

cambium growth increases the gap between the phloem and xylem. The remainder of secondary growth in roots is similar to that in shoots, the epidermis and cortex are sloughed off, and formation of the periderm occurs.

Several studies have shown that secondary growth occurs in the *Arabidopsis* shoot, including the hypocotyl, and the root (Nieminen *et al.*, 2004; Lens *et al.*, 2012). This has led to yet another use of *Arabidopsis* as a model plant: to model secondary growth and wood formation. One study has demonstrated that there is sufficient xylem tissue in *Arabidopsis* shoots to conduct hydraulic conductivity measurements and to explore the risk of cavitation caused by perturbations to metabolite levels (Tixier *et al.*, 2013). The inflorescence stems of *Arabidopsis* contain ray cells, display intrusive cambium growth and have stacked cambium cells such as those found in trees (Mazur and Kurczynska, 2012). Due to its small size, *Arabidopsis* has been a favourable model of secondary growth, for example in the dynamic analysis of vascular tissue growth in hypocotyls, an analysis that would otherwise be difficult with large tissue sections (Sankar *et al.*, 2014). Secondary growth also occurs in the *Arabidopsis* root, and this tissue has been used to model secondary growth (Zhang *et al.*, 2011a).

Several phytohormones regulate secondary growth (Groover and Robischon, 2006). Relatively high concentrations of auxin are found in the cambium of hybrid aspen trees (Tuominen *et al.*, 1997), and decreased auxin signalling in hybrid aspen leads to reduced cambial cell division activity as well as reduced secondary xylem formation (Nilsson *et al.*, 2008a). Application of auxin to hybrid aspen trees stimulates cambium growth, and this stimulation is enhanced when combined with GA treatment (Bjorklund *et al.*, 2007). Little is known regarding the molecular targets of auxin signalling in cambium growth, although evidence is emerging that *WOX4* might be one of them (Suer *et al.*, 2011). PXY, a protein originally known for its role in establishing the boundary between the phloem and xylem tissues (Fisher and Turner, 2007), appears to regulate secondary growth upstream of *WOX4* (Etchells *et al.*, 2013), but also interacts with ethylene signalling in the regulation of this developmental process (Etchells *et al.*, 2012).

Matsumoto-Kitano *et al.* (2008) revealed the importance of cytokinins in vascular cambium growth in *Arabidopsis*. *Arabidopsis* plants lacking four cytokinin biosynthesis genes displayed reduced root secondary growth, and external application of a natural cytokinin to these plants restored root thickness (Matsumoto-Kitano *et al.*, 2008). Cytokinins also appear to regulate secondary

growth in two tree species: *Populus trichocarpa* and *Betula pendula* (Nieminen et al., 2008). Cytokinin levels were reduced in these trees via expression of an *Arabidopsis* cytokinin-oxidase gene, the product of which degrades cytokinins, in the cambium (Nieminen et al., 2008). These trees displayed reduced secondary growth. In this study, relatively high expression of cytokinin-responsive genes was shown in *WT* cambium tissue (Nieminen et al., 2008). The targets of cytokinin signalling in cambium growth are yet to be identified.

## Aims & Objectives

---

The hypothesis that *CYCD3;1* acts downstream of cytokinin signalling to regulate secondary growth was tested in this study. Since redundancy between the three *CYCD3* genes has been shown (Dewitte *et al.*, 2007), analysis of secondary growth in the *cycd3;1-3* triple mutant was performed, to determine whether loss of *CYCD3;2* and *CYCD3;3* enhanced any phenotype observed in the *cycd3;1* mutant. A dose response curve measuring root thickness following application of various concentrations of cytokinin was obtained for WT roots and *cycd3;1* roots, to identify a functional link between cytokinin signalling and *CYCD3;1*.

The expression pattern of *CYCD3;1* in roots is unknown, and this was explored, as expression of *CYCD3;1* in the root tissue is a prerequisite to it playing a role there. To do this, promoter lines were employed, and an *in situ* hybridisation experiment was carried out to test the faithfulness of the *CYCD3;1* reporters. Gene expression correlation analysis was used to identify a putative regulator of *CYCD3;1* in roots, *AINTEGUMENTA (ANT)*. Following this, the interaction between *ANT* and *CYCD3;1* in secondary growth was investigated. The roles *ANT* plays in regulating secondary growth were also analysed, as was the regulation of *ANT* by cytokinins. The final objective was to generate a list of other potential regulators of *CYCD3;1* expression by using a yeast-one-hybrid assay to identify transcription factors that can bind to the *CYCD3;1* promoter.

## Results

---

### 4.1 Secondary growth is reduced in the *cycd3;1* mutant

To test for potential roles of CYCD3s in secondary growth, the diameter of 15 DAG *cycd3;1<sub>Ler</sub>* and *cycd3;1-3<sub>Ler</sub>* roots was measured, within 1 cm of the root-hypocotyl junction, as an indicator for secondary thickening (Figure 4.1A,B). *cycd3<sub>Col-0</sub>* loss-of-function mutants have previously been described (Dewitte *et al.*, 2007). The *cycd3;2* allele contains a T-DNA insertion in the first exon, and was originally isolated in the *Col-0* ecotype. The *cycd3;1* and *cycd3;3* alleles contain Ds insertions in their first exons, and were originally isolated in the *Ler* ecotype. qPCR confirmed that the respective full length transcripts were absent in these mutants, as were transcripts containing the LxCxE motif that is required for binding to RBR protein (Dewitte *et al.*, 2007). These alleles were therefore considered to be null alleles (Dewitte *et al.*, 2007). Mean *WT<sub>Ler</sub>* root diameter was  $179.2 \pm 3.2 \mu\text{m}$ . In *cycd3;1<sub>Ler</sub>* mutants, mean root diameter was  $154.7 \pm 4.1 \mu\text{m}$ , representing a 14% reduction from *WT<sub>Ler</sub>* levels that was statistically significant (one-way ANOVA,  $p < 0.0001$ , d.f. = 120). In *cycd3;1-3<sub>Ler</sub>* triple mutants mean root diameter was  $148.9 \pm 4.2 \mu\text{m}$ , representing a similar reduction from *WT<sub>Ler</sub>*, 17%, that was statistically significant (one-way ANOVA,  $p < 0.0001$ , d.f. = 120). Whilst *cycd3;1-3* root diameter was 4% less than *cycd3;1<sub>Ler</sub>* root diameter, this difference was not statistically significant (one-way ANOVA,  $p = 0.55$ , d.f. = 120). This data shows that CYCD3;1 is required for proper secondary thickening, and suggests that neither CYCD3;2 nor CYCD3;3 are significantly involved in the regulation of this process. In agreement with this, neither the *CYCD3;2* nor the *CYCD3;3* transcriptional reporters appear to be highly active in root tissue undergoing secondary growth (Shunsuke Miyashima, unpublished data).

To confirm this result, transverse cross-sections of 6 week-old roots of *WT<sub>Ler</sub>* and *cycd3;1<sub>Ler</sub>* plants were taken, and the cross-sectional area of the stele determined (Figure 4.1C,D). Since secondary growth occurs in two dimensions, this analysis is more powerful than measuring root diameter, a two-dimensional parameter. The cross-sectional area of *WT<sub>Ler</sub>* roots was  $38071 \pm 1959 \mu\text{m}^2$ . Mean cross sectional area of *cycd3;1<sub>Ler</sub>* roots was  $26554 \pm 1765 \mu\text{m}^2$ , 30% less than *WT<sub>Ler</sub>* (Student's t test,  $p < 0.0001$ , d.f. = 62). Visual analysis suggested

that *cycd3;1<sub>Ler</sub>* roots contained fewer cambium cells than their *WT<sub>Ler</sub>* counterparts (Figure 4.1D), consistent with CYCD3;1 acting to regulate cell proliferation.

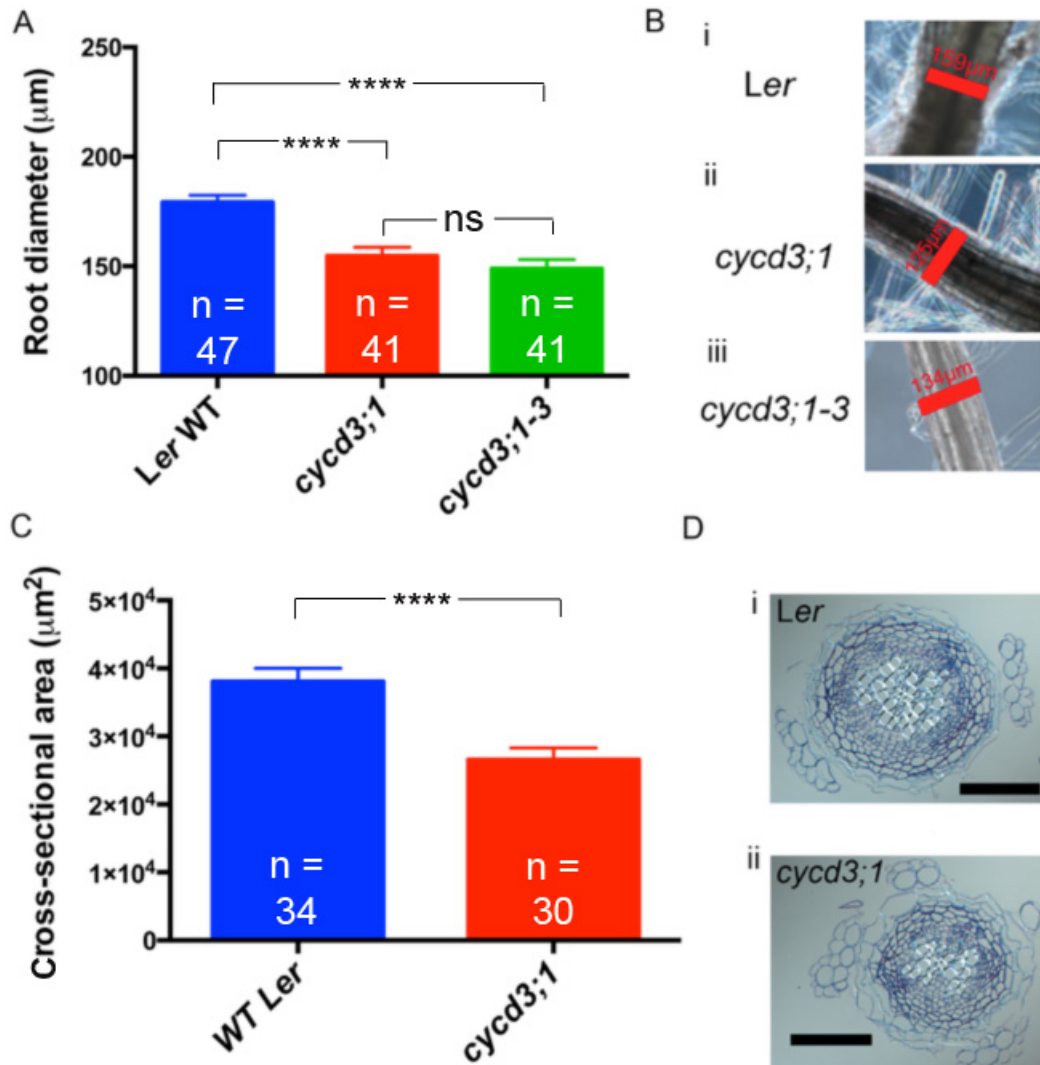


Figure 4.1: Secondary growth is reduced in *cycd3;1<sub>Ler</sub>* mutants. A) Mean diameter of two week-old *WT<sub>Ler</sub>*, *cycd3;1<sub>Ler</sub>* and *cycd3;1-3<sub>Ler</sub>* roots. Error bars represent SEM. B) Pictures of 2 week-old *WT<sub>Ler</sub>* (i), *cycd3;1<sub>Ler</sub>* (ii) and *cycd3;1-3<sub>Ler</sub>* (iii) roots. C) Mean cross-sectional area of the oldest part of 6 week-old *WT<sub>Ler</sub>* and *cycd3;1<sub>Ler</sub>* roots. Error bars represent SEM. D) Tangential cross-sections of *WT<sub>Ler</sub>* (i) and *cycd3;1<sub>Ler</sub>* (ii) roots. Sections were taken within 1 cm of the root-hypocotyl junction. Toluidine-blue staining was used to shown cell walls. Scale bars represent 100 µm. \*\*\*\*:  $p < 0.0001$ . ns:  $p > 0.05$ .

## 4.2 Expression Pattern of *CYCD3;1* in Roots During Secondary Growth

If *CYCD3;1* functions within the vascular tissue undergoing secondary growth, it is expected that the gene will be expressed within this tissue. *CYCD3;1* promoter activity was analysed using a *pCYCD3;1:GUS-GFP* construct in the *Col-0* background, and a *pCYCD3;1:GUS* construct within the *Ler* background. In eight-day old roots, *pCYCD3;1:GUS-GFP* activity was observed in the oldest part of the *Col-0* root, was weaker in younger parts, and was apparently absent in the youngest parts (Figure 4.2A). This gradient of expression is similar to that of the primary cytokinin reporter *ARR5* that responds to cytokinins in the cambium (Appendix). Thus the *CYCD3;1* promoter appears to be most active in vascular tissue undergoing secondary growth. To determine in which cell type the promoter is active, 14 DAG *pCYCD3;1:GUS-GFP<sub>Col-0</sub>* roots were subjected to a GUS assay, and were then embedded in plastic and sectioned. Activity was observed primarily in the outer vascular cells (Figure 4.2B).

*CYCD3;1* promoter activity was also assessed in the *Ler* background. In this case, activity was again observed within the stele of older parts of roots (Figure 4.2D). Promoter:reporter constructs may not reflect the true expression profile of a gene of interest. To confirm that *CYCD3;1* is expressed within the stele of roots undergoing secondary growth, *in situ* hybridisation on sectioned 14 DAG *Ler* roots was used. An antisense *CYCD3;1* probe produced signal within the cambium, but it appeared to be localized to the phloem poles (Figure 4.2Ci). A sense probe did not produce such a signal, although some weaker dark patches could be observed at random zones around the stele periphery (Figure 4.2Cii). Therefore, the promoter:reporter analyses and *in situ* hybridisation analyses do not agree completely. They do nonetheless both suggest expression within the stele. Since *in situ* hybridisation on root tissue undergoing secondary growth has not been published to this date, it is not known whether it is possible to obtain signal in all of the tissue within the sections, using the method employed.

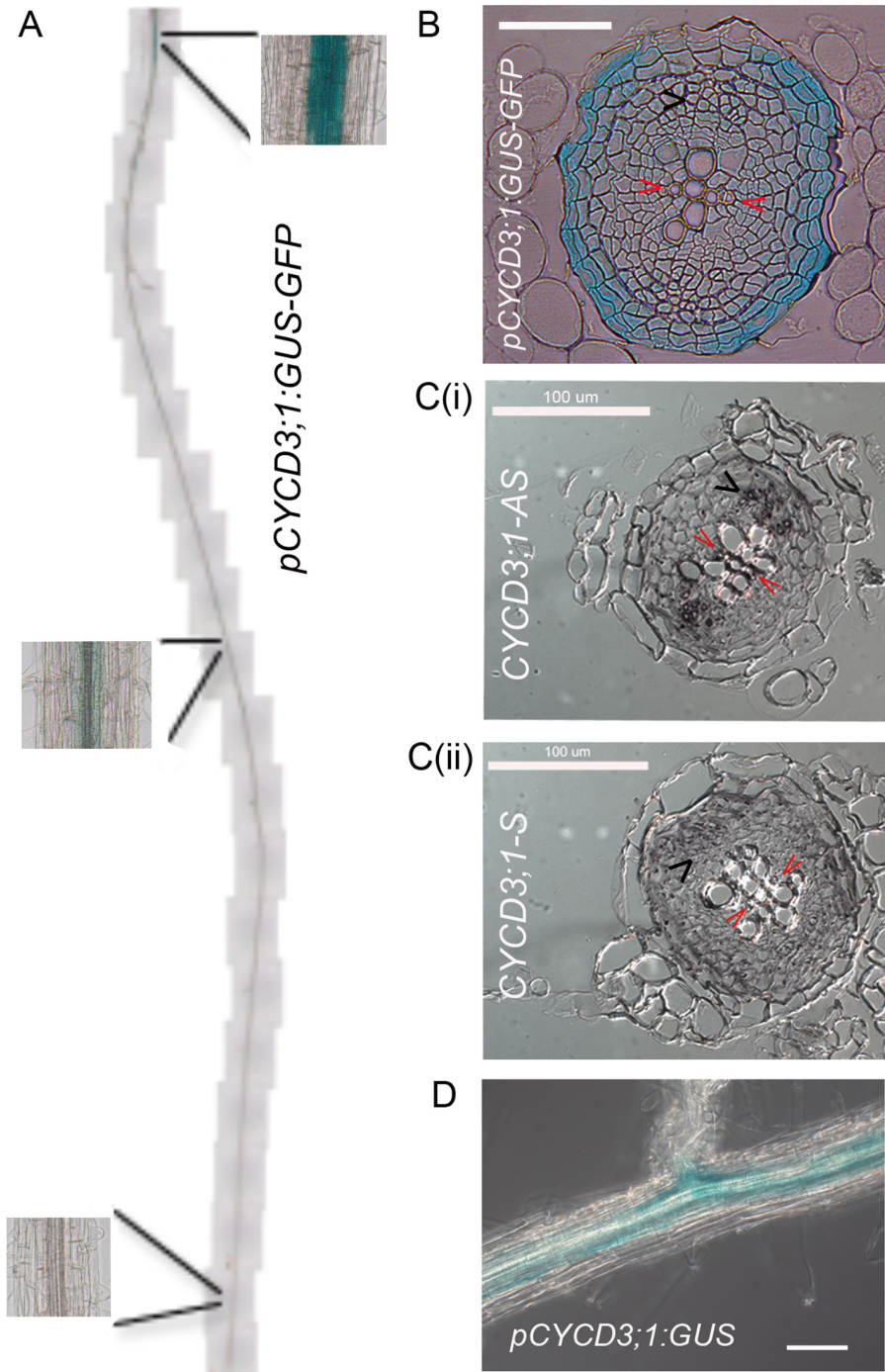


Figure 4.2: *CYCD3;1* is expressed in the vascular tissue of roots undergoing secondary growth. A) Results of a GUS assay resulting in a blue reaction product on an 8 DAG root expressing the *pCYCD3;1:GUS-GFP* construct in the *Col-0* background. The oldest part of the root is at the top. B) Cross section of a 14 DAG *Col-0* root expressing *pCYCD3;1:GUS-GFP* at the oldest part of the root shows activity in the outer stele. C) *in situ* hybridisation for *CYCD3;1* mRNA in cross-sections of the oldest part of 14 DAG *Ler* roots, using an anti-sense probe (i) and a sense probe (ii). In B & C, red arrows point along the primary xylem axis, which is perpendicular to the phloem poles indicated by the black arrows. D) GUS assay on a 14 DAG root expressing the *pCYCD3;1:GUS* construct in the *Ler* background. All scale bars represent 100  $\mu\text{m}$ .

### 4.3 The Response of Secondary Growth to Cytokinins is Altered in *cycd3;1* Mutants

*CYCD3;1* responds to cytokinins, in terms of transcriptional activity, in cell culture and *in planta* (Riou-Khamlichi et al., 1999), and cytokinins are key regulators of secondary growth (Matsumoto-Kitano et al., 2008). To investigate the part that *CYCD3;1* might play in cytokinin-induced secondary growth, the response of roots to a range of concentrations of the natural cytokinin, trans-zeatin (tZ), was measured in *WT<sub>Ler</sub>* and *cycd3;1<sub>Ler</sub>* roots (Figure 4.3). To do this, plants were initially grown for 11 days without additional cytokinin and were then transplanted onto mock treatment plates or plates with the cytokinin concentrations indicated (Figure 4.3A) and grown for 14 days. On media without cytokinins, *cycd3;1<sub>Ler</sub>* roots were narrower than *WT<sub>Ler</sub>* roots (Figure 4.3A). This remained the case when low amounts (< 200 ng/mL) of cytokinin were added, but the thickness of *WT<sub>Ler</sub>* and *cycd3;1<sub>Ler</sub>* roots was similar following addition of 200 and 500 ng/mL tZ (Figure 4.3A). A non-linear regression curve fitted to the data illustrates this phenomenon (Figure 4.3B). These concentrations have been shown to have an effect on secondary growth previously (Matsumoto-Kitano et al., 2008). This shows that *CYCD3;1* is not essential for cytokinin-induced secondary growth. However, given that *CYCD3;1* is rate limiting for radial root growth at cytokinin concentrations below 200 ng/mL, *CYCD3;1* does contribute to the cytokinin response. Cytokinin signalling output might be reduced in *cycd3;1<sub>Ler</sub>* mutants, but higher input can compensate for this, indicating that several pathways operate at the interface with the core cell cycle machinery.

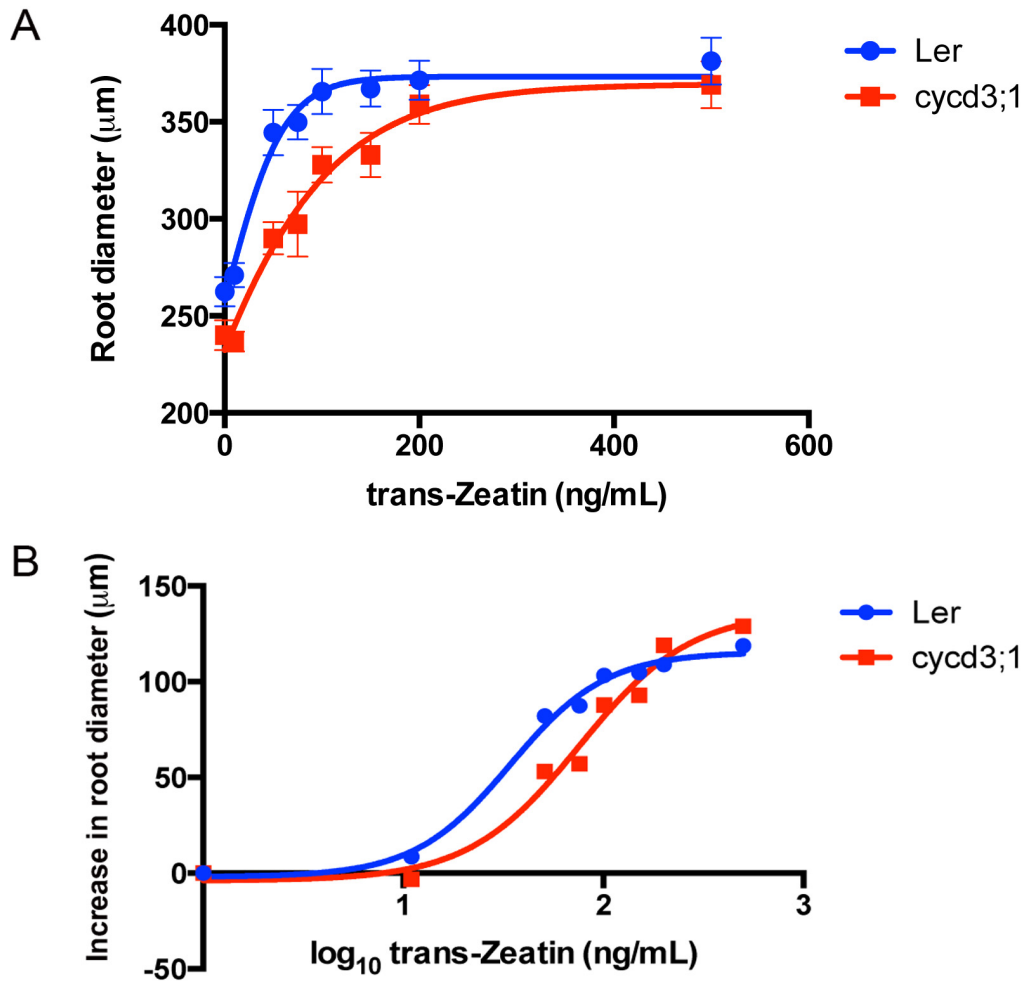


Figure 4.3: Secondary growth of  $WT_{Ler}$  and  $cycd3;1_{Ler}$  roots following treatments with different concentrations of supplemental cytokinin (trans-zeatin). A) Root diameter following 25 days of growth, 14 of which were on media with the indicated concentrations of additional cytokinin. Error bars represent SEM. B) Differences between the mean root diameter for the cytokinin concentrations indicated and that of those on the control plates with no additional cytokinin.

#### 4.4 Correlation of *ANT* and *CYCD3;1* Expression

To determine what upstream factors might activate *CYCD3;1* in older root tissues to promote secondary thickening, Pearson's correlation tests were used to identify genes which may be co-expressed with *CYCD3;1*. Multiple tests were carried out using expression data from all microarray experiments on roots available via Genevestigator (<https://www.genevestigator.com/gv/>), to test for the positive correlation of expression of D-type cyclins with that of any transcription factors analysed in the experiments (list of Arabidopsis transcription factors obtained from <http://datf.cbi.pku.edu.cn>). The expression of *AINTEGUMENTA* (*ANT*), a gene encoding an AP2-domain transcription factor (Elliott *et al.*, 1996; Klucher *et al.*, 1996), was correlated most highly with that of *CYCD3;1* (Table 4.1). Previous studies have shown that ectopic expression of *ANT* in leaves leads to ectopic expression of *CYCD3;1* (Mizukami and Fischer, 2000), and the gene's promoter is active in the root vascular tissue during secondary thickening (4.2). Furthermore, a sequence ~ 200 bp upstream of the *CYCD3;1* start codon, 5'-GCACGTTTCCATAGAG-3' (Annette Alcasabas, unpublished data), closely matches the optimal ANT-binding site 5'-gCAC(A/G)N(A/T)TcCC(a/g)ANG(c/t)-3'. *ANT* is therefore a good candidate regulator of *CYCD3;1* expression during secondary thickening.

Table 4.1: Pearson's correlation tests for the correlation of the expression of D-type cyclin genes with that of transcription factors. Data was obtained from Genevestigator. Probe sets used in microarray experiments are rarely if ever fully comprehensive with regard to the Arabidopsis genome, and only genes available on probe sets used in microarray experiments submitted to Genevestigator can be used for analysis. Data was selected from experiments on root tissue only.  $r^2$  values are shown. Data was sorted from highest to lowest correlation with the expression of *CYCD3;1*. At4g37750 represents *AINTEGUMENTA*.

	<i>CYCD1;1</i>	<i>CYCD2;1</i>	<i>CYCD3;1</i>	<i>CYCD3;2</i>	<i>CYCD3;3</i>	<i>CYCD4;1</i>	<i>CYCD4;2</i>	<i>CYCD5;1</i>	<i>CYCD6;1</i>
At4g37750	0.003	0.007	0.559	0.031	0.228	0.098	0.000	0.046	0.321
At3g06740	0.000	0.186	0.362	0.222	0.218	0.206	0.001	0.034	0.191
At1g31320	0.066	0.018	0.361	0.003	0.078	0.039	0.008	0.007	0.097
At1g16530	0.011	0.009	0.325	0.005	0.134	0.022	0.018	0.023	0.224
At5g60690	0.035	0.065	0.325	0.000	0.002	0.000	0.010	0.007	0.020
At1g32240	0.000	0.007	0.303	0.128	0.088	0.046	0.043	0.001	0.214

#### 4.5 ANT Regulates Secondary Growth

To initially explore the possibility that ANT regulates secondary growth and *CYCD3;1* expression, the expression of two promoter-reporter constructs were used to infer *ANT* expression in roots. The first is a GUS reporter. The *pANT:GUS<sub>Ler</sub>* reporter contains 6.2 kb of sequence 5' of the *ANT* start codon upstream of the *GUS* reporter (Krizek, 2009). Relatively strong expression of the *pANT:GUS<sub>Ler</sub>* reporter was observed in the stele of two-week old roots (Figure 4.4Ai), consistent with the hypothesis that ANT has a role in regulating secondary growth. In the youngest part of these roots, relatively weak *pANT:GUS<sub>Ler</sub>* expression was detected, and none was detected in the cells surrounding the QC (Figure 4.4Aii). This expression pattern is consistent with that observed with a *pANT:GFP<sub>Col-0</sub>* reporter (Anakaiso Elo, unpublished data). The other reporter used was a *pANT:Histone-YFP<sub>Col-0</sub>* reporter. The *pANT:histone-YFP<sub>Col-0</sub>* reporter was constructed in pKGWFS7 (Karimi *et al.*, 2002), contains 5175 bp of sequence upstream of the *ANT* start codon and was kindly gifted by Yka Helariutta (Helsinki, Finland). The histone domain of the protein expressed from this reporter causes the fusion protein to become nuclear-localized. A cellular localization of YFP fluorescence expected for a nuclear-targeted protein was observed (Figure 4.4B). This expression was detected in cells of the stele (Figure 4.4B), but not in the xylem cells, which are probably dead at this developmental stage.

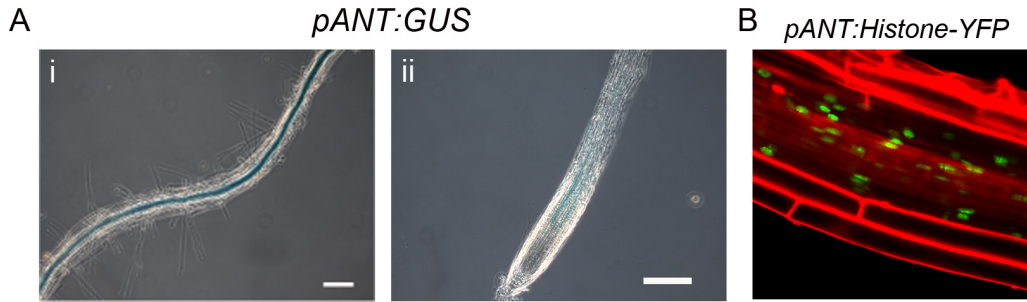


Figure 4.4: *ANT* is expressed in the root stele. A) Activity of the *ANT* promoter represented using a *pANT:GUS<sub>Ler</sub>* reporter line. Scale bars represent 200  $\mu$ m. (i) Old part of a 14 DAG root. GUS activity can be seen in the vascular tissue. (ii) RAM of a two week-old root. A relatively small amount of GUS activity can be seen in the central region of the root, in two strands. No activity is detected in the QC region. B) Activity of the *ANT* promoter presented using a *pANT:Histone-YFP<sub>Col-0</sub>* reporter. Laser scanning confocal microscopy was performed on propidium-iodide-stained roots. The picture is of the oldest part of a two week-old root. YFP signal is detected in the nuclei of vascular cells within the stele.

To test whether or not ANT is required for proper secondary growth, secondary growth was measured in *WT* and *ant* roots. Since the reporter analyses were performed in the *Col-0* background, the phenotype of the *ant-GK* mutant, also in the *Col-0* background, was analysed (Figure 4.5A,B). Mean cross-sectional area of *ant-GK<sub>Col-0</sub>* roots undergoing secondary growth was  $38271 \pm 4022 \mu\text{m}^2$ , whereas that of *WT<sub>Col-0</sub>* roots was  $71573 \pm 6473 \mu\text{m}^2$ . This reduction of secondary growth in *ant-GK<sub>Col-0</sub>* roots equated to 47% (one-way ANOVA,  $p < 0.0001$ , d.f. = 63). Visual analysis suggested that the *ant-GK<sub>Col-0</sub>* roots had fewer vascular cell files than *WT<sub>Col-0</sub>* roots (Figure 4.5B). Secondary growth was also measured in the *cycd3;1* mutant in the *Col-0* background. Mean cross-sectional area of *cycd3;1<sub>Col-0</sub>* roots was  $40677 \pm 3150 \mu\text{m}^2$ , 43% less than that of *WT<sub>Col-0</sub>*, and this difference was statistically significant (one-way ANOVA,  $p < 0.0001$ , d.f. = 63). Thus the phenotype of the *cycd3;1* mutant was similar to that of the *ant-GK* mutant in the *Col-0* background (Figure 4.5A,B; one-way ANOVA,  $p = 0.91$ , d.f. = 63). This is consistent with ANT regulating secondary growth via regulation of *CYCD3;1* expression.

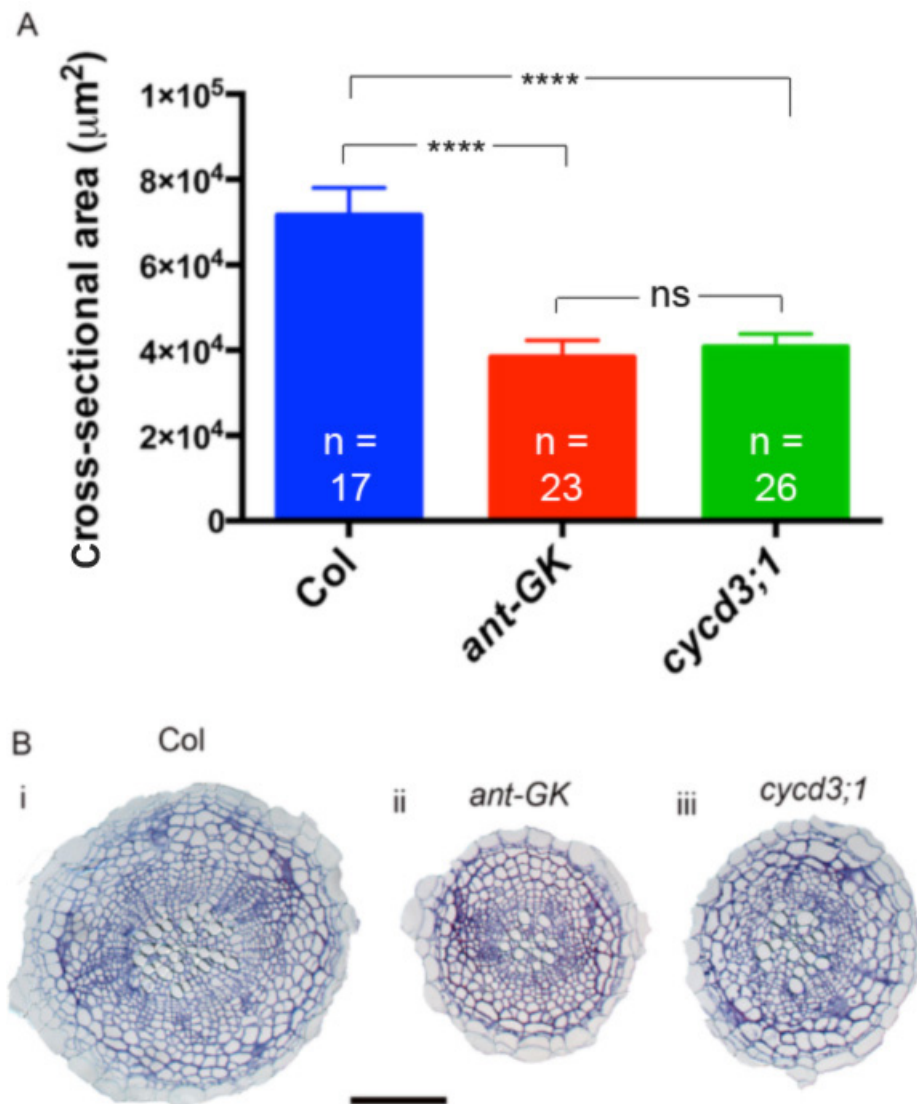


Figure 4.5: ANT regulates secondary growth. A) Mean cross-sectional area of  $WT_{Col-0}$ ,  $ant-GK_{Col-0}$  and  $cycd3;1_{Col-0}$  roots. Note that the  $cycd3;1$  allele was used in the  $Col-0$  background. Error bars represent SEM. B) Tangential cross-sections of  $WT_{Col-0}$  (i),  $ant-GK_{Col-0}$  (ii) and  $cycd3;1_{Col-0}$  (iii) roots. Sections were taken within 1 cm of the root-hypocotyl junction. Scale bar represents 100  $\mu\text{m}$ .

\*\*\*\*:  $p < 0.0001$ ; ns:  $p > 0.05$ .

#### 4.6 Expression of *CYCD3;1* in *ant* mutants

In Chapter 3, reduced *CYCD3;1* promoter activity was observed in *ant* mutant shoot organs. As a means of testing whether or not ANT might regulate the expression of *CYCD3;1* in roots, activity of the *CYCD3;1* promoter was assayed in *WT* roots and *ant* loss-of-function mutant roots (Figure 4.6). As *ant* mutants are female-sterile, experiments were performed on genotyped F3 seedlings, derived from a cross between a *CYCD3;1* reporter line and an *ant* mutant, that were homozygous for the reporter construct but segregated for the *ant* allele. Relatively strong *pCYCD3;1:GUS* expression was observed in *Ler* roots (Figure 4.6Ai), whereas no expression was detected in *ant-9<sub>Ler</sub>* roots (Figure 4.6Aii). This suggests that functional ANT is required for *CYCD3;1* promoter activity, and possibly expression, in roots. To confirm this result, the same experiment was performed with the *pCYCD3;1:GUS-GFP* reporter, created in the *Col-0* ecotype, in the *ant-GK<sub>Col-0</sub>* mutant (Figure 4.6B). Expression was detected in both *ANT<sub>Col-0</sub>* and *ant-GK<sub>Col-0</sub>* roots, at similar levels (Figure 4.6Bi & ii). This result is inconsistent with that obtained for the *ant-9<sub>Ler</sub>* allele. Since these reporter lines were created independently, it might be that they respond differently to the loss of functional ANT. Alternatively, since the experiments were performed in different ecotypes, it might be the case that in the *Ler* ecotype, ANT is required for *CYCD3;1* promoter activity, whereas it is not required in the *Col-0* ecotype.

To confirm that *CYCD3;1* expression is downregulated in *ant-9<sub>Ler</sub>* roots, qPCR analysis was performed in *ANT<sub>Ler</sub>* and *ant-9<sub>Ler</sub>* roots to quantify *CYCD3;1* expression. At 14 DAG, a time point during which *pCYCD3;1:GUS* expression was downregulated in *ant-9<sub>Ler</sub>* mutants (Figure 4.6A), *CYCD3;1* transcript levels were similar in *ANT<sub>Ler</sub>* and *ant-9<sub>Ler</sub>* roots (Figure 4.6C, top). *CYCD3;1* transcript levels were also unchanged in 6 week-old *ant-9<sub>Ler</sub>* roots (Figure 4.6C, bottom), ruling out the possibility that ANT is required to maintain *CYCD3;1* expression at the transcriptional level, rather than to activate it. Therefore the *Ler pCYCD3;1:GUS* reporter does not faithfully reflect native *CYCD3;1* expression at the transcriptional level. A hypothesis that ANT regulates *CYCD3;1* expression post-transcriptionally was tested in Chapter 3, but evidence supporting this hypothesis was not obtained. The reduction of *pCYCD3;1:GUS* expression in *ant-9<sub>Ler</sub>* mutants may represent a small part of *CYCD3;1* expression that is dependent on ANT.

To check whether or not expression of the endogenous *CYCD3;1* gene is downregulated in *ant-GK<sub>Col-0</sub>* mutants, qPCR analysis of *CYCD3;1* expression was performed on *Col-0 WT* and *ant-GK<sub>Col-0</sub>* root RNA-derived cDNA. *CYCD3;1* transcript levels in *ant-GK<sub>Col-0</sub>* roots were  $84 \pm 23\%$  those of *WT* roots (Figure 4.6D). Thus there might be a small downregulation of *CYCD3;1* transcript levels in *ant* mutants in the *Col-0* background. Since *pCYCD3;1:GUS-GFP* expression was difficult to compare quantitatively between the *Col-0 WT* and *ant-GK<sub>Col-0</sub>* mutant roots via the GUS assay, qPCR of *GFP* expression in these roots was used to check whether or not the expression of this reporter reflected expression of endogenous *CYCD3;1*. Indeed, expression levels of *GFP* were downregulated to a similar extent,  $76 \pm 26\%$  those of *WT<sub>Col-0</sub>* levels (Figure 4.6D). This suggests that the *Col-0 CYCD3;1* reporter is faithful to endogenous *CYCD3;1* expression, and is consistent with there being a small downregulation of *CYCD3;1* expression in *ant-GK<sub>Col-0</sub>* mutants. However, this downregulation might be an indirect consequence of the *ant-GK* mutation, as *ant-GK<sub>Col-0</sub>* roots might contain less of the tissue in which *CYCD3;1* is expressed; whether this is the case needs to be confirmed.

To check whether or not this downregulation of *CYCD3;1* levels in *ant-GK<sub>Col-0</sub>* mutants might be due to direct binding of ANT to the *CYCD3;1* promoter, a yeast-one-hybrid assay was undertaken (Figure 4.6E). An expression vector expressing ANT that has previously been shown to bind to the optimal ANT-binding site (ABS) was used (Figure 4.7), as was a reporter plasmid containing this ABS and the *LacZ* reporter (Krizek and Sulli, 2006). Whilst yeast expressing ANT but containing an empty reporter construct did not display any transactivation of *LacZ*, yeast containing the reporter downstream of three copies of the optimal ABS did (Figure 4.6E). A dominant-negative ANT protein that can bind to DNA but lacks transactivation activity was not capable of inducing this expression, at least to detectable levels (Figure 4.6E), demonstrating that ANT is responsible for this transactivation. When the putative ABS from the *CYCD3;1* promoter was used in place of the optimal ABS, no transactivation was observed (Figure 4.6E). Therefore, it does not appear that, at least in yeast, ANT can bind to the *CYCD3;1* promoter and induce downstream gene expression.

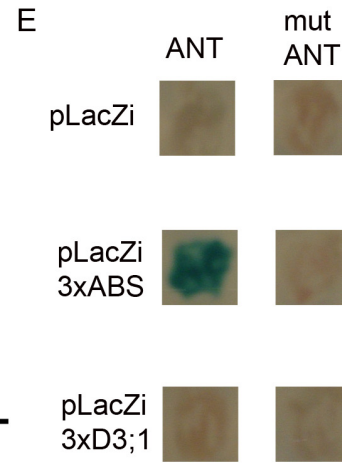
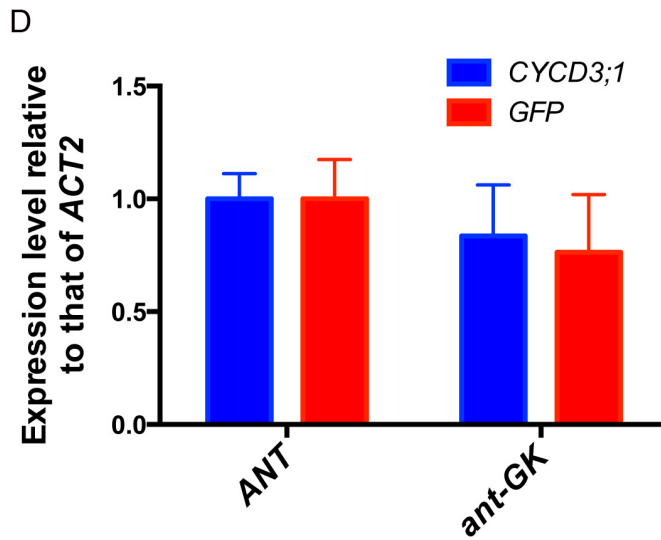
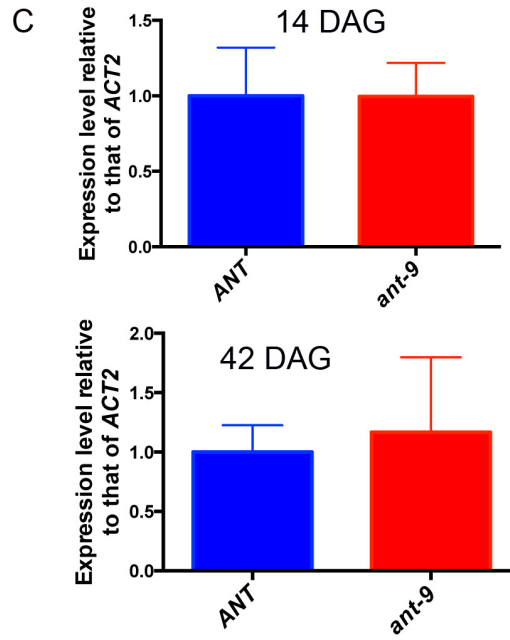
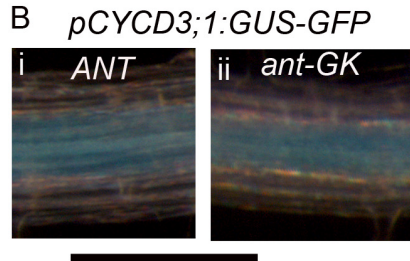
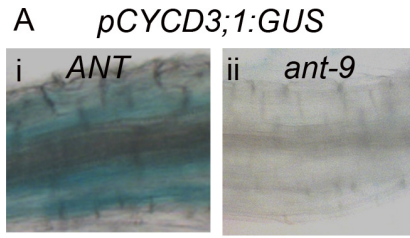


Figure 4.6: Molecular interaction between ANT and *CYCD3;1*. A) Expression of the *pCYCD3;1:GUS* reporter detected via a GUS assay in the *WT<sub>Ler</sub>* background (i) and the *ant-9<sub>Ler</sub>* mutant background (ii). Pictures were taken of the oldest part of two week-old roots. B) Expression of the *pCYCD3;1:GUS-GFP* reporter detected via a GUS assay in the *WT<sub>Col-0</sub>* background (i) and the *ant-GK<sub>Col-0</sub>* mutant background (ii). Pictures were taken of the oldest part of two week-old roots. In both A & B the scale bar represents 200  $\mu$ m. C) qPCR analysis of *CYCD3;1* expression in six week-old *ANT<sub>Ler</sub>* and *ant-9<sub>Ler</sub>* roots. Error bars represent standard deviation from three biological replicates. D) qPCR analysis of *CYCD3;1* and *GFP* expression in 16 day-old *ANT<sub>Col-0</sub> pCYCD3;1:GUS-GFP* and *ant-GK<sub>Col-0</sub> pCYCD3;1:GUS-GFP* roots. Error bars represent standard deviation from four biological replicates, each of which was from eight individual roots. E) Yeast-one hybrid testing the binding of ANT to a putative ANT-binding site in the *CYCD3;1* promoter. An X-gal assay was performed. A yeast expression vector expressing the ANT protein was used on the left, another expressing a dominant-negative ant protein was used on the right. The pLacZi reporter vector was either empty (top), contained three copies of the optimal ANT-binding site (middle) or three copies of the putative ANT-binding site in the *CYCD3;1* promoter. The yeast-one-hybrid assay was undertaken with the assistance of Emily Sornay.

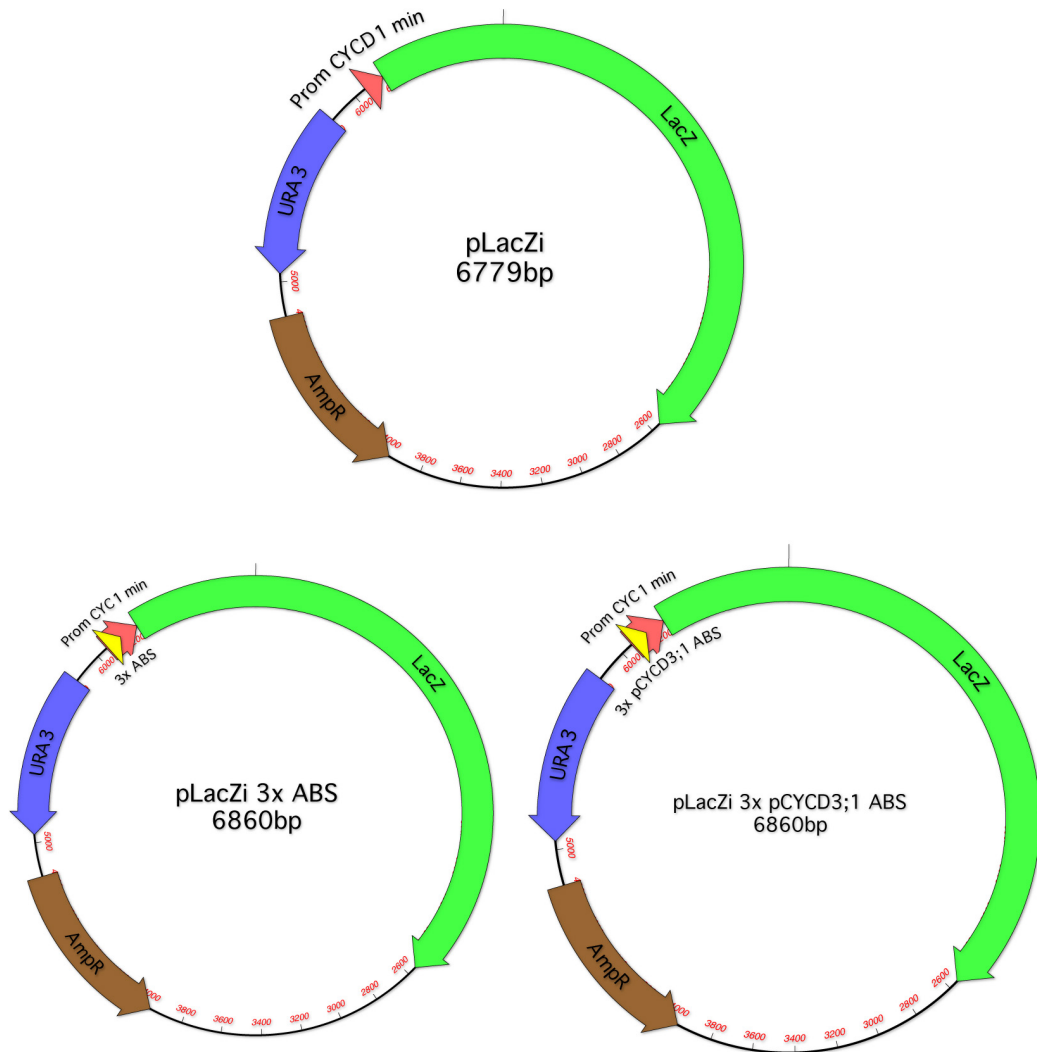


Figure 4.7: Vectors used in one-on-one yeast-one-hybrid assay. One vector contains no promoter elements upstream of the *LacZ* gene other than the yeast minimal *CYC1* promoter. Another contains three copies of the optimal ANT-binding site. The third contains three copies of a putative ANT-binding site in the *CYCD3;1* promoter.

#### 4.7 Genetic Interaction Between *ANT* and *CYCD3;1*

To further explore the interaction between *ANT* and *CYCD3;1*, their genetic interaction was analysed. This was achieved by looking at the secondary growth phenotype in *ant-9 cycd3;1* double mutants along side the respective single mutants (in *Ler*). Root cross-sectional area was  $38040 \pm 2654 \mu\text{m}^2$  in *WT\_{Ler}* (Figure 4.8A-B). In *cycd3;1\_{Ler}* roots, cross-sectional area was  $28654 \pm 2108 \mu\text{m}^2$ . This represents a 25% reduction that is statistically significant (one-way ANOVA,  $p = 0.03$ , d.f. = 144). *ant-9\_{Ler}* cross-sectional area was  $33531 \pm 3919 \mu\text{m}^2$ , 12% less than that of *WT\_{Ler}* roots. This difference was not statistically significant (one-way ANOVA,  $p = 0.66$ , d.f. = 144). Cross-sectional area of *ant-9 cycd3;1\_{Ler}* roots was  $18880 \pm 1521 \mu\text{m}^2$  (Figure 4.8A-B), a 50% drop from *WT\_{Ler}* that was statistically significant (one-way ANOVA,  $p < 0.0001$ , d.f. = 144). This is greater than the sum of the reductions in mean cross-sectional area in *cycd3;1\_{Ler}* and *ant-9\_{Ler}* roots (25% + 12% = 37%), and the differences between the double mutant and the *cycd3;1\_{Ler}* and *ant-9\_{Ler}* single mutants were significantly different (one-way ANOVAs;  $p = 0.04$  and  $p = 0.004$  respectively, d.f. = 144). This indicates a synergistic relationship between *CYCD3;1* and *ANT* in the regulation of root secondary growth. Visual analyses suggest that the phenotypes in all of these mutants are due to reduced cell number (Figure 4.8B).

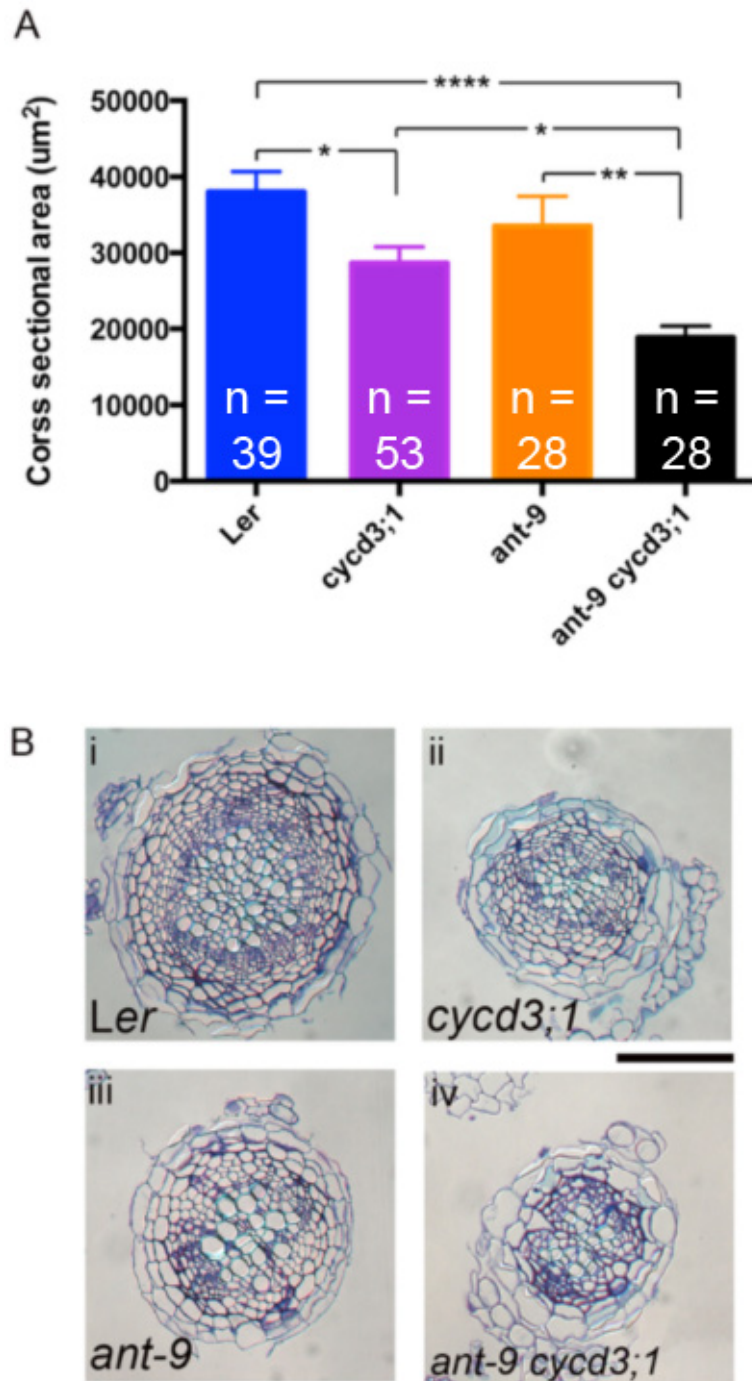


Figure 4.8: The secondary growth phenotype in *cycd3;1<sub>Ler</sub>*, *ant-9<sub>Ler</sub>* and *ant-9 cycd3;1<sub>Ler</sub>* mutants. A) Mean cross-sectional area of the oldest part of 30 day-old roots. Note that this experiment was performed with the *cycd3;1* mutant in the *Ler* background. Error bars represent SEM. B) Tangential cross-sections of roots in A. Sections were taken within 1 cm of the root-hypocotyl junction. Scale bare represents 100  $\mu$ m. \*\*\*\*: ] <0.0001; \*\*: ] <0.01; \*: ] <0.05.

#### 4.8 Regulation of *CYCD3;1* and *ANT* by Cytokinins

Application of cytokinins to cells in culture induces the expression of *CYCD3;1* (Riou-Khamlichi *et al.*, 1999). Application of cytokinins to plants induces the expression of *CYCD3;1* in the SAM (Riou-Khamlichi *et al.*, 1999). This work demonstrates that *CYCD3;1* is involved in the regulation of cytokinin-mediated secondary growth. To test the hypothesis that *CYCD3;1* expression is regulated by cytokinins in the vascular cambium, *CYCD3;1* transcript levels were measured in plants ectopically overexpressing the cytokinin oxidase gene *CKX1* (Werner *et al.*, 2001). This line contains a construct containing the full-length *CKX1* gene under regulation of the 35S promoter, and is from the pBINHygTx vector. The enzyme encoded by this gene oxidises cytokinins, thereby inactivating them. Demonstrating the requirement for cytokinins for proper secondary growth, 35S:*CKX1*<sub>Col-0</sub> roots were narrower than their *WT*<sub>Col-0</sub> counterparts (Figure 4.9A). If *CYCD3;1* is part of the cytokinin signalling mechanism that contributes to cambium proliferation, when this process is reduced in plants with less active cytokinins, such as 35S:*CKX1*<sub>Col-0</sub> roots, the expression of *CYCD3;1* might also be expected to be reduced. This was indeed the case (Figure 4.9B). *CYCD3;1* transcript levels in 35S:*CKX1*<sub>Col-0</sub> roots were reduced to 14 ± 6% those observed in *WT*<sub>Col-0</sub> roots.

*ANT* expression was highly correlated with that of *CYCD3;1*, and *ant* mutants have a similar phenotype to that of *cycd3;1* mutants in secondary growth. Therefore *ANT* might be expected to be subject to the same sort of regulation as *CYCD3;1*. This was the case: in 35S:*CKX1*<sub>Col-0</sub> roots *ANT* transcript levels were 9 ± 3% those of *WT*<sub>Col-0</sub> roots (Figure 4.9B). These results show that both *ANT* and *CYCD3;1* are regulated by cytokinins in roots undergoing secondary growth.

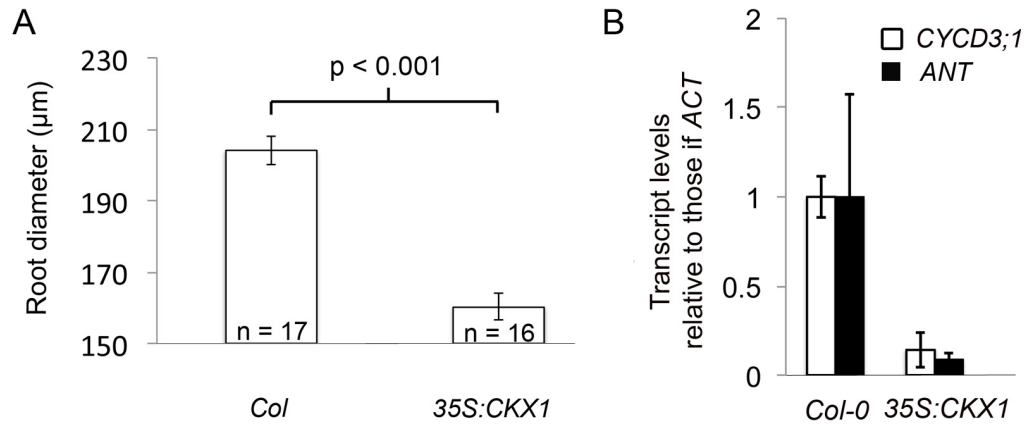


Figure 4.9: *ANT* and *CYCD3;1* expression are downregulated in roots with reduced cytokinin signalling. A) Root diameter in two week-old *WT*<sub>Col-0</sub> and *35S:CKX1*<sub>Col-0</sub>. Error bars represent SEM. B) qPCR analyses of *CYCD3;1* and *ANT* transcript levels in *WT*<sub>Col-0</sub> and *35S:CKX1*<sub>Col-0</sub> roots. Transcript levels were normalized to those of *ACT2*. Error bars represent standard deviation based on three biological replicates.

#### 4.9 *ANT* is Required for Induction of the *pCYCD3;1:GUS* Reporter by Cytokinins

Since *ANT* appears to be regulated by cytokinins, and *CYCD3;1* promoter activity appears to be dependent on *ANT* in the *Ler* ecotype, any activity of the *CYCD3;1* promoter induced by cytokinins in this ecotype might be anticipated to be dependent on *ANT*. To test this, two-week old *pCYCD3;1:GUS* roots, of the *ANT*<sub>Ler</sub> and *ant-9*<sub>Ler</sub> backgrounds, were treated with supplemental trans-zeatin for 24 hours (Figure 4.10). To confirm whether cytokinin treatment was sufficient to induce target genes, roots expressing *GFP* under regulation of the promoter of the primary cytokinin response gene, *ARR15*, were also treated. *pARR15:GFP*<sub>Col-0</sub> roots did not show signal within the RAM when no additional cytokinin was provided (Figure 4.10A). However, following treatments with 100 ng/mL and 1000 ng/mL tZ, signal was detected in this region (Figures 4.10C,D). In the *ANT*<sub>Ler</sub> background, *pCYCD3;1:GUS*<sub>Ler</sub> activity was detected weakly in the oldest part of the root when no supplemental cytokinin was provided (Figure 4.10E). Activity increased with a 10ng/mL tZ treatment, and became more evident with 100 and 1000 ng/mL treatments (Figures 4.10F-H). In the *ant-9*<sub>Ler</sub> mutants, on the other hand, activity was not observed with any treatment. Therefore, *ANT* appears to be required for cytokinin-induced *CYCD3;1* promoter

activity in *Ler*. As shown in Figure 4.6, this reporter does not appear to faithfully represent *CYCD3;1* transcript abundance. Therefore, this data does not show that induction of *CYCD3;1* expression by cytokinins is dependent on ANT, only that a small part of the regulation of *CYCD3;1* expression by cytokinins might be.

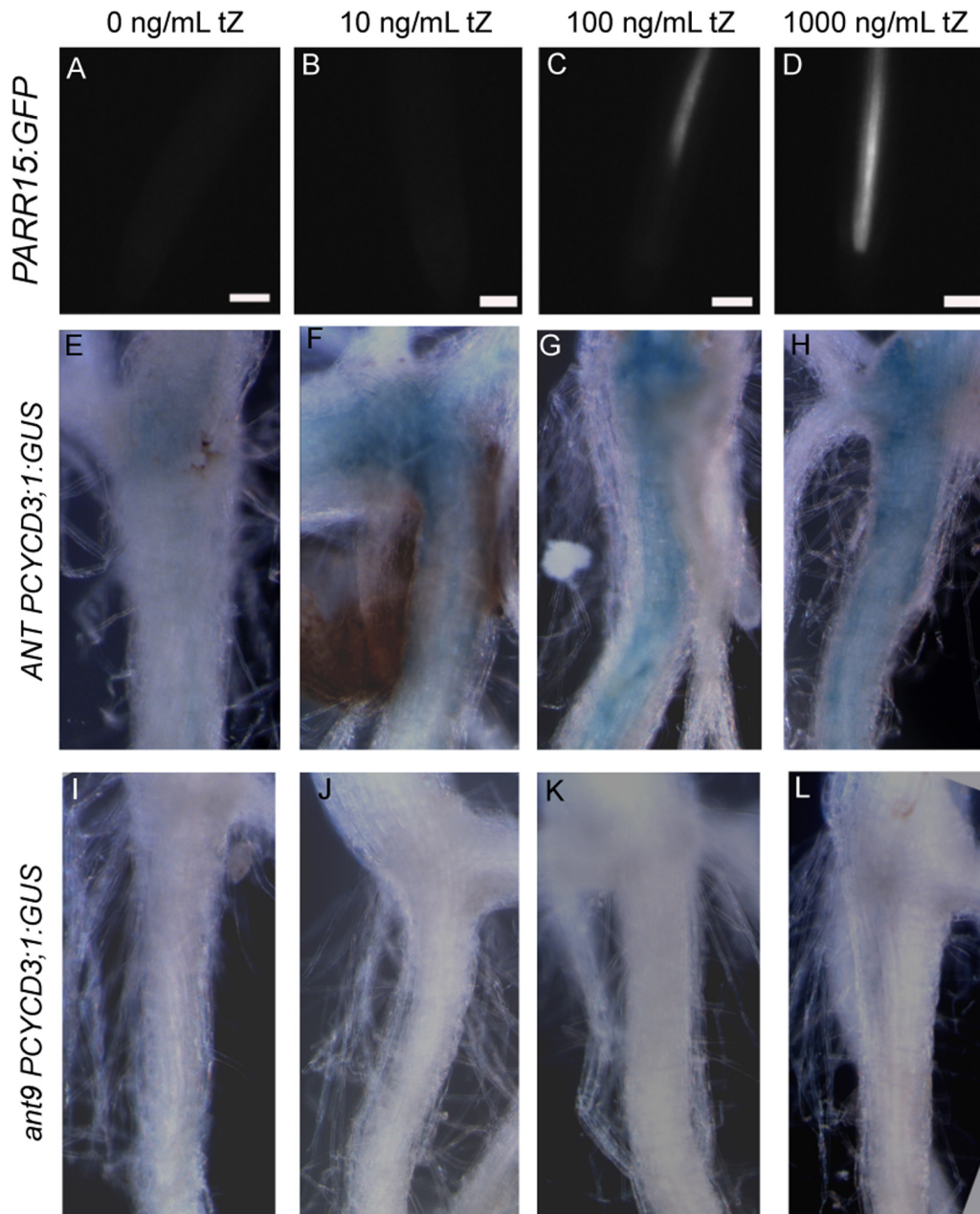


Figure 4.10: Induction of *CYCD3;1* promoter activity requires ANT. Trans-zeatin cytokinins were added to plants at the concentrations indicated, following a growth period of 2 weeks, in a water solution for 24 hours. A-D) Expression of the *pARR15:GFP<sub>Col-0</sub>* cytokinin primary response reporter following treatments with the concentrations of cytokinins shown. Pictures of the RAM were taken. Scale bar represents 100  $\mu\text{m}$ . E-I) Activity of the *pCYCD3;1:GUS<sub>Ler</sub>* reporter following indicated cytokinin treatments in *ANT<sub>Ler</sub>* and *ant-9<sub>Ler</sub>* plants.

#### 4.10 Other Potential Regulators of *CYCD3;1* Expression

To identify other potential regulators of *CYCD3;1* expression, a yeast-one-hybrid screen was undertaken. A library of yeast strains expressing Arabidopsis transcription factors were mated with reporter vectors containing three partially overlapping fragments of the *CYCD3;1* promoter (the 1 kb of sequence upstream of the ATG codon). To generate the three *CYCD3;1* promoter fragments (Figure 4.11), PCR was performed using *WT<sub>Col-0</sub>* genomic DNA as a template and the following primer pairs:- attB1-pD3;1-frag1 and attB2-pD3;1-frag1; attB1-pD3;1-frag2 and attB2-pD3;1-frag2; attB1-pD3;1-frag3 and attB2-pD3;1-frag3 (Chapter 2). As the names suggest, the primers included *att* sites at the 5' ends so that PCR products could be integrated into Gateway® vectors. These PCR products were purified via a PCR purification (2.2.3.) and integrated into pDONR/Zeo donor vectors via a BP reaction. The resultant vectors were sequenced to confirm that the correct insertions had integrated. The recombination between the *attB* and *attP* sites created *attL* sites in the newly formed entry vectors (pENTR). The promoter fragments were then transferred from these entry vectors to the pHISLEU2GW yeast-compatible destination vector via an LR reaction. DNA sequencing was used to confirm that the destination vectors contained the correct insertions.

Histidine auxotrophy/prot[rophy was used for selection of yeast colonies in which a transcription factor was binding to the *CYCD3;1* promoter fragment whilst exhibiting transactivation activity via the GAL4 yeast transactivation domain (see Chapter Two for further details). Colonies were screened by PCR with primers flanking the insertion site of the Arabidopsis transcription factor in the expression vector, and PCR products were sequenced. Sequences were entered into BLAST (NCBI) to identify the corresponding genes. Whilst 3-AT was used to select for strong expression of the reporter gene, all colonies growing on media lacking histidine were screened to identify potential targets. The relative strength of binding and transactivation activity in yeast may not reflect those properties in Arabidopsis.

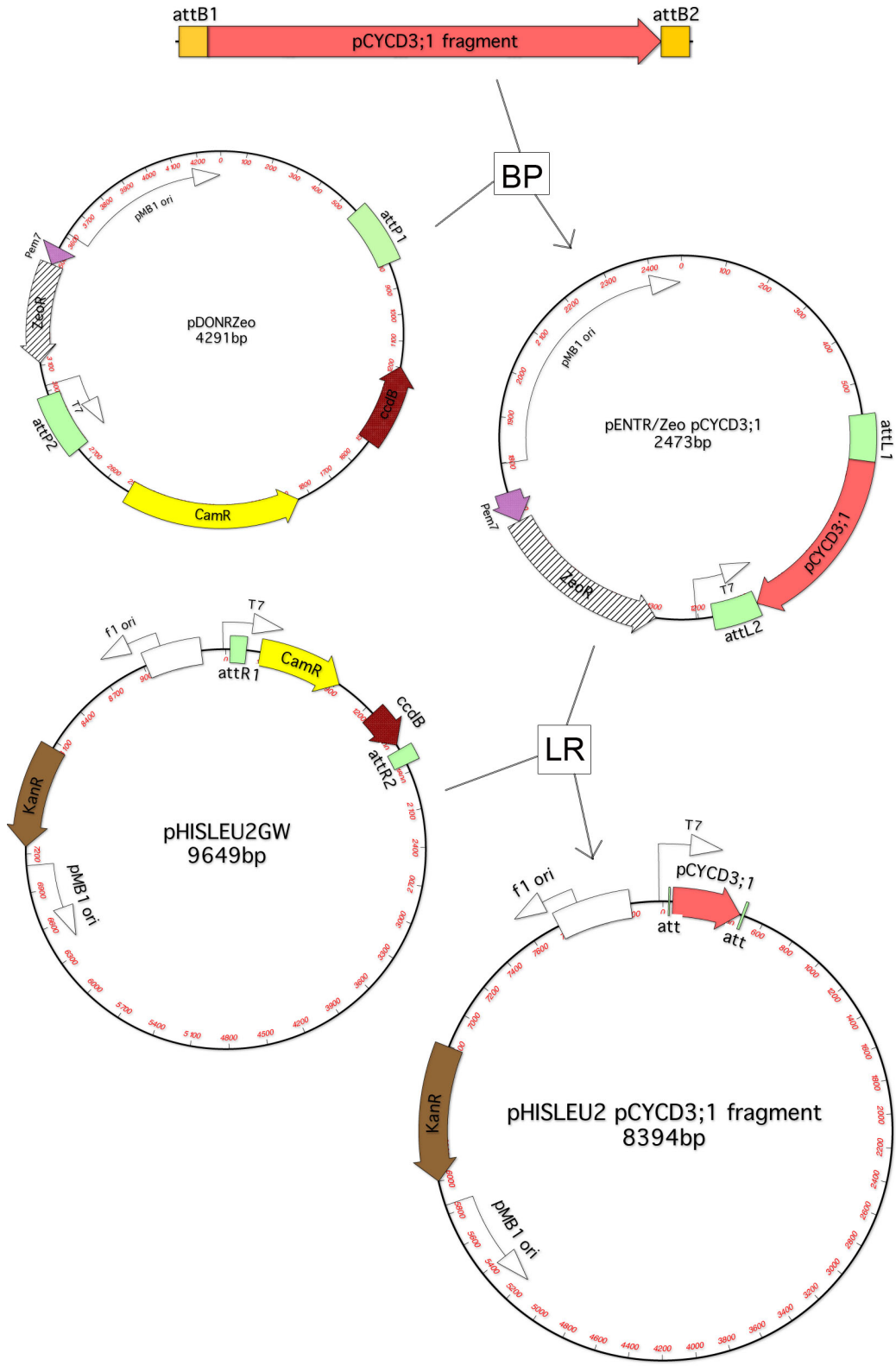


Figure 4.11: Steps involved in the construction of the reporter vectors for the Y1H screen searching for *Arabidopsis* transcription factors that bind the *CYCD3;1* promoter. This scheme applies to the three overlapping fragments of the *CYCD3;1* promoter. *att* recombination sites are indicated. ori: origin of replication. KanR: kanamycin resistance marker gene. CamR: chloramphenicol resistance marker gene. *ccdB*: *ccdB* gene encoding a toxic product that targets DNA gyrase and kills cells unless they have a specific mutation in this gene (“*ccdB* survival cells” are used for propagation of empty vectors).

Seventeen transcription factors were identified. Of these, eleven were TCP (Teosinte branched 1, Cycloidea, and PCF family) proteins. An example of this interaction being presented by the yeast is shown in Figure 4.12. The others were:- SCL5 (Scarecrow-like 5), HDG11(Homeodomain group 11), a HMG (high mobility group) protein, AGL3(Agamous-like 3), YAB5(Yabby5) and a DREB protein. The binding of the HMG protein can be seen in Figure 4.12. Sequences of PCR products matched database sequences by at least 93%, and the expected probability of finding a match by chance was zero in each case as determined by the NCBI Blast algorithm (Table 4.2). Most proteins bound to the fragment representing the 250 bp to 750 bp sequence upstream of the *CYCD3;1* ATG codon (Table 4.2). None bound solely to the fragment representing the first 500 bp upstream, and only two proteins: SCL5 and the DREB protein, bound solely to the 500 bp 1000 bp upstream fragment. Fragment two completely overlaps the other two fragments. Therefore, these results suggest that there are important *cis* element that either span across the boundary between fragments one and three, or interact with one another across this boundary.

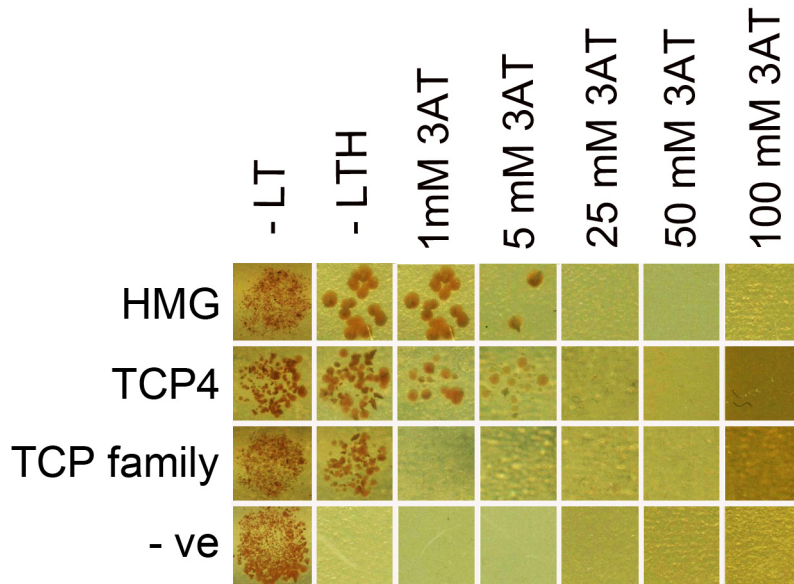


Figure 4.12: Yeast-one hybrid assay for Arabidopsis transcription factors binding to the *CYCD3;1* promoter. Four examples are shown, the last (-ve) being one that did not show any binding. Two colonies were picked from each spot for PCR and sequencing. The first column shows colonies growing on media lacking leucine and tryptophan, amino acids for which the yeast are auxotrophic. Marker genes conferring prototrophy for these amino acids are [ $\}^+$ ] the two vectors used for the assay. Positive growth in this column shows that mating of the parent strains, one containing the expression vector and the other containing the reporter vector, occurred successfully. In the next column—media was also lacking histidine. Binding of a GAL4-fused transcription factor to the *CYCD3;1* promoter was necessary for expression of  $\alpha$ -*HIS* reporter gene conferring histidine prototrophy for growth on this media. Subsequent columns show media that lacked leucine, tryptophan and histidine but contained the indicated concentrations of 3-AT. 3-AT inhibits histidine biosynthesis and therefore selects for stronger expression of the reporter gene.

Table 4.2: Arabidopsis transcription factors capable of binding to the *CYCD3;1* promoter in yeast. Results are ordered in ascending AGI number. *PCYCD3;1* fragment indicates the fragment of the *CYCD3;1* promoter that the protein bound to. Fragment one is the sequence 500 bp to 1000 bp upstream of the start codon, fragment two 250 bp to 750 bp upstream and fragment three 1 bp to 500 bp upstream. Identity indicates the percentage match of the PCR product sequence with the transcription factor sequence from the NCBI database. The e value was returned from the NCBI Blast search and represents the probability that the sequence match occurred by chance.

AGI number	Name	<i>PCYCD3;1</i> fragment	Identity (%)	e value
AT1G30210.2	<i>TCP24</i>	2	100	0
AT1G50600.1	<i>SCL5</i>	1	99	0
AT1G53230.1	<i>TCP3</i>	1, 2	98, 99	0, 0
AT1G67260.2	<i>TCP1</i>	1, 2, 3	99, 99, 97	0, 0, 0
AT1G69690.1	<i>TCPFAMILYTF</i>	1, 2	99, 99	0, 0
AT1G73360.1	<i>HDG11</i>	2	97	0
AT1G76110.1	<i>HMG</i>	2	99	0
AT2G03710.2	<i>AGL3</i>	2	100	0
AT2G26580.2	<i>YAB5</i>	2	93	0
AT2G31070.1	<i>TCP10</i>	2	97	0
AT3G02150.2	<i>PTF1/TCP13</i>	2	95	0
AT3G15030.3	<i>TCP4</i>	1, 2, 3	96/96/95	0, 0, 0
AT3G18550.1	<i>TCP18</i>	2	98	0
AT3G45150.1	<i>TCP16</i>	2	100	0
AT3G47620.1	<i>TCP14</i>	2	99	0
AT3G57600.1	<i>DREB protein</i>	1	99	0
AT4G18390.2	<i>TCP2</i>	1, 2	99, 99	0, 0

#### 4.11 The *ERECTA* gene is required for proper secondary growth

Loss of functional ANT had more of an effect on secondary growth in the *Col-0* ecotype than it did in the *Ler* ecotype (compare figures 4.5 and 4.8). The same can be said for the loss of functional *CYCD3;1* i.e. this also had more of an effect in the *Col-0* background (compare figures 4.5 and 4.8). This suggests that *ANT* and *CYCD3;1* might be interacting with some locus/loci that is/are altered in the *Ler* ecotype compared to the *Col-0* ecotype. Since the *er* mutation is well known to affect growth and development in *Ler* plants (van Zanten *et al.*, 2009), we tested the hypothesis that *ER* regulates secondary growth. The *er-105<sub>Col-0</sub>* mutant has been described previously (Torii *et al.*, 1996), and was isolated in the *Col-0* ecotype. The *er-105* allele was generated by fast-neutron irradiation. This allele consists of the *ER* gene with an insertion of ~ 4 kb DNA of unknown origin (Torii *et al.*, 1996). The *er-105<sub>Col-0</sub>* mutants display the altered inflorescence morphology associated with loss of ER function (Torii *et al.*, 1996). Full-length *ER* transcripts are absent in the *er-105<sub>Col-0</sub>* mutant (Torii *et al.*, 1996). Root cross sectional area was compared in *WT* and *er-105* loss-of-function mutant (Torii *et al.*, 1996) roots in the *Col-0* background. Whilst cross-sectional area of *WT<sub>Col-0</sub>* roots was  $71573 \pm 6473 \mu\text{m}^2$ , that of *er-105<sub>Col-0</sub>* roots was  $35926 \pm 2966 \mu\text{m}^2$  (Figure 4.13A,B). Thus a reduction in cross-sectional area of 50% was observed in *er-105<sub>Col-0</sub>* roots (Figure 4.13A,B; one-way ANOVA,  $p < 0.0001$ , d.f. = 60). To confirm that this reduction in secondary growth was indeed due to the loss of functional ER, an attempt at complementing the phenotype was undertaken. This was done using an *er-105<sub>Col-0</sub>* transgenic line ectopically expressing *ER*. The *er-105<sub>Col-0</sub>* *ER* complementation line contains a pMDC124-originating construct containing the *ER* gene and was kindly gifted by Jose Gutierrez-Marcos (Warwick, UK). Cross-sectional area in *er-105<sub>Col-0</sub>* *ER* roots was  $51474 \pm 4395 \mu\text{m}^2$ . Whilst this was still a 28% reduction from *WT<sub>Col-0</sub>* mean root cross-sectional area (Figure 4.13A,B; one-way ANOVA,  $p = 0.01$ , d.f. = 60), it was an increase of 43% from the *er-105<sub>Col-0</sub>* mutant (Figure 4.13A,B; one-way ANOVA,  $p = 0.03$ , d.f. = 60). Thus partial complementation of the phenotype was observed suggesting that the reduction in secondary growth in the *er-105<sub>Col-0</sub>* mutant is due to the absence of functional ER. The incompleteness of the complementation might be due to insufficient expression levels of *ER* in the transgenic line, or by an altered pattern of expression.

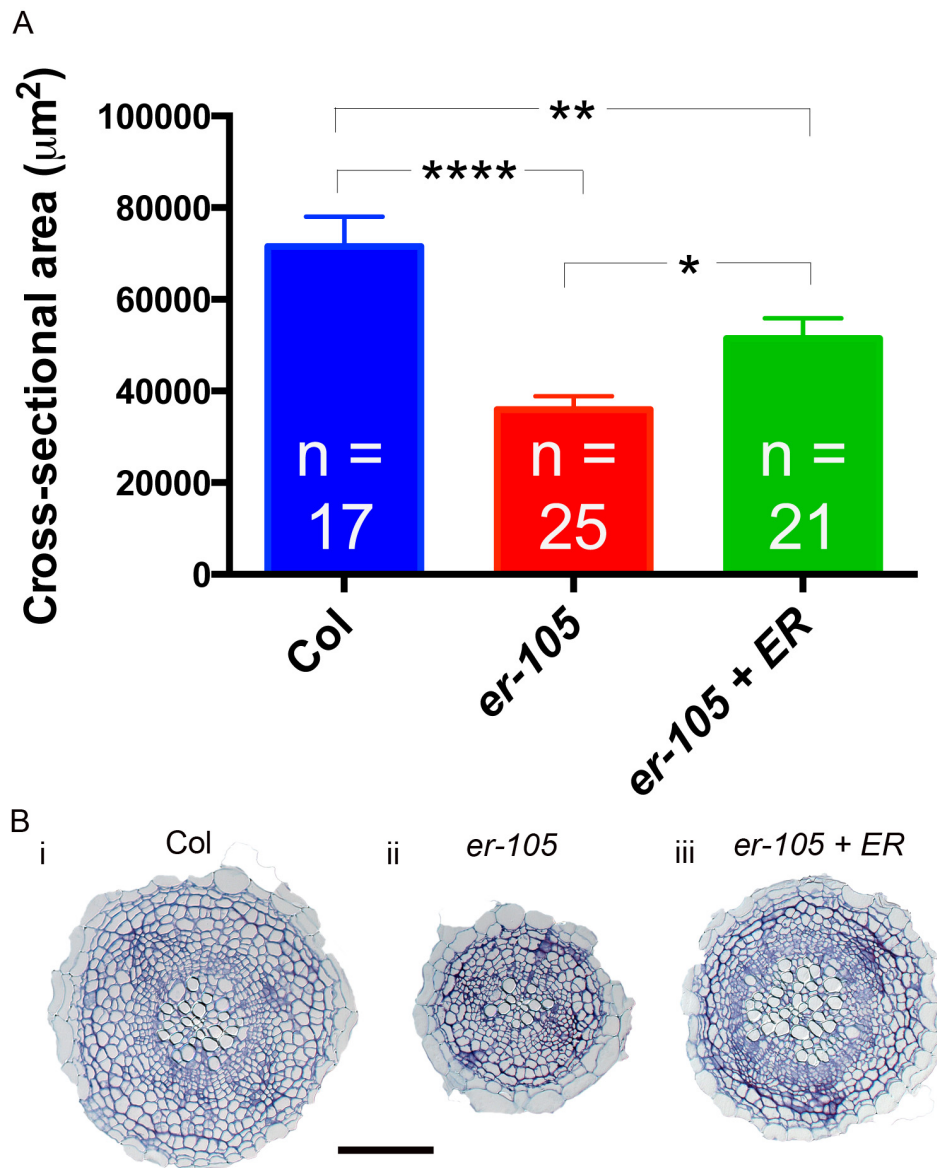


Figure 4.13: Reduced secondary growth in the *er-105* loss-of-function mutant. A) Mean cross-sectional area of *Col-0* WT and *er-105* roots and *er-105* roots ectopically expressing *ER*. Error bars represent SEM. B) Cross-sections of the roots used in the analysis in A. Cross-sections were taken within 1 cm of the root-hypocotyl junction. Scale bar represents 100 µm. \*\*\*\*: ] <0.0001; \*\*: ] <0.01; \*: ] <0.05.

## Discussion

---

Higher plants have a relatively large family of D-type cyclins to utilize in cell cycle control (Menges *et al.*, 2007). This has led to a consensus that, in higher plants, different D-type cyclins have individual if not exclusive roles to play during plant growth and development (Inze, 2008). In *Arabidopsis*, the *CYCD3* genes, of which there are three, represent the largest subgroup of *CYCDs* in this species (Menges *et al.*, 2005; Menges *et al.*, 2007). The capability of *CYCD3;1* to promote cell division has been demonstrated (Dewitte *et al.*, 2003; Menges *et al.*, 2006; Collins *et al.*, 2012). Furthermore, roles for the *CYCD3s* during the regulation of leaf and petal growth have been identified, although these genes do not appear to be required for the achievement of correct leaf/petal growth at an organ level (Dewitte *et al.*, 2007).

In this study, a novel role for *CYCD3;1* in the regulation of secondary root growth was identified. *cycd3;1<sub>Ler</sub>* roots were thinner than their *WT<sub>Ler</sub>* counterparts, showing that *CYCD3;1* is limiting for secondary growth in *Arabidopsis*. Secondary vascular tissue development involves the reinitiation of transversal cell division activity within an axillary meristem, the procambium (Miyashima *et al.*, 2013). Since secondary growth still occurred in *cycd3;1* mutants, the gene is not required for this reinitiation. It may be rate-limiting for the initiation, or it may be limiting for proliferation of cambium cells following initiation. Since some functional redundancy between the three *Arabidopsis* *CYCD3s* has been shown previously (Dewitte *et al.*, 2007), the secondary growth phenotype of the single *cycd3;1<sub>Ler</sub>* mutant was compared with that of the triple *cycd3;1-3<sub>Ler</sub>* mutant. No significant enhancement of the phenotype was observed in the triple mutant. Whilst subsequent analyses focused on *CYCD3;1*, it does remain possible that *CYCD3;2* and *CYCD3;3* play their own roles in regulating secondary growth.

Consistent with *CYCD3;1* regulating secondary growth, expression of *CYCD3;1* was detected within the stele of roots undergoing this developmental process. However, using different means of detecting *CYCD3;1* expression suggested different expression patterns at a cellular level. Whilst promoter:reporter constructs suggested expression in all of the outer tissues of the stele, *in situ* hybridisation analysis indicated that *CYCD3;1* transcripts are detected primarily in the phloem poles. This might mean that the promoter:reporter constructs do not faithfully represent the *CYCD3;1* expression

pattern. Alternatively, since no known *in situ* hybridisation analyses of Arabidopsis root tissue undergoing secondary growth have been published, it might be that detection of mRNA within the other tissues is less sensitive. Whatever the case, all methods indicated expression of *CYCD3;1* within the stele of roots undergoing secondary growth. It is nonetheless important to resolve the *CYCD3;1* expression pattern in the root, as this will provide evidence of the cells in which *CYCD3;1* functions. The *pCYCD3;1:GUS-GFP<sub>Col-0</sub>* reporter suggested expression in the pericycle cells. During the transition stage at the beginning of secondary development, these cells contribute to secondary thickening (Baum *et al.*, 2002). Perhaps, during this stage at least, it is the cell cycle activity of these cells that is stimulated by *CYCD3;1*. *CYCD3;1* might instead or also function in the phloem cells, where its expression is suggested by *in situ* hybridisation. It would be interesting to try to quantify the number of phloem cells in *cycd3;1* roots. A reduction in phloem cell number could impact on secondary growth indirectly, since several signalling molecules, including cytokinins (Bürkle *et al.*, 2003; Bishopp *et al.*, 2011b), are transported in the phloem (Turgeon and Wolf, 2009).

In this study, roots over-expressing the gene *CKX1*, which inactivates cytokinins (Schmulling *et al.*, 2003), exhibited reduced expression of *CYCD3;1*. Addition of cytokinin to roots induced expression of the *pCYCD3;1:GUS* reporter. This suggests that cytokinins regulate the expression of *CYCD3;1* in Arabidopsis roots, which is consistent with the regulation of *CYCD3;1* expression by these phytohormones in other developmental contexts (Riou-Khamlichi *et al.*, 1999; Dewitte *et al.*, 2007). This, together with the *cycd3;1* secondary growth phenotype, implicates *CYCD3;1* in the cytokinin signalling mechanism activating cell division in the cambium. To test this hypothesis, a dose response curve quantifying root diameter following treatments of cytokinins was performed for *WT* and *cycd3;1* roots. Relatively low concentrations of cytokinins that stimulated secondary growth in *WT* roots failed to stimulate secondary growth in *cycd3;1* mutants. Treatments with higher concentrations of cytokinins did induce secondary growth in *cycd3;1* roots, and with the highest concentration of cytokinin used, root diameter in *WT* and *cycd3;1* roots was similar. Therefore, the secondary growth phenotype in *cycd3;1* mutants appeared to be rescued by supplementation of roots with a high concentration of cytokinin. Taken together, these results demonstrate that *cycd3;1* mutant roots are less sensitive to cytokinins than their *WT* counterparts, and are consistent

with *CYCD3;1* acting downstream of cytokinins to induce secondary growth. They also show that *CYCD3;1* is not strictly required for cytokinin-mediated secondary growth, and highlight the importance of future studies to identify other targets of cytokinins. Cytokinins also regulate secondary growth in poplar (Nieminen *et al.*, 2008). It is possible that cytokinins additionally regulate the expression of a *CYCD3* gene in poplar, as the *CYCD3* subgroup is conserved in this species (Menges *et al.*, 2007).

To identify potential regulators of *CYCD3;1* expression, the correlation of Arabidopsis transcription factor gene expression and *CYCD3;1* expression was analysed using all available data from the Genevestigator tool. The expression of *ANT* correlated with that of *CYCD3;1* more than any other transcription factor gene explored. Prior to investigating the interaction between *ANT* and *CYCD3;1*, the roles of *ANT* in the regulation of secondary growth were investigated. Secondary growth was reduced in the *ant-GK* mutant, revealing *ANT* as a novel regulator of secondary growth. This is, to the author's knowledge, the first known role for *ANT* in the regulation of Arabidopsis root development.

*ANT* promoter activity was detected in the stele of roots undergoing secondary growth, consistent with it playing a role there. Whilst this was done with two different promoter:reporter lines, *in situ* hybridisation or immunolocalization of *ANT* protein would tell us with greater confidence whether or not *ANT* is expressed in the cambium. However, evidence of cambium-expression of *ANT* orthologues exists. Microarray analysis of *Populus tremulus* cambium cells obtained from tangential sections showed that the orthologue of *ANT* in this species was expressed relatively highly in this tissue (Schrader *et al.*, 2004). Removing bark in a ring around trees, a process termed bark girdling, causes differentiating but live secondary xylem cells to dedifferentiate to form new sieve elements, and xylem callus tissue to form so called wound cambium tissue. When this was performed on *Populus tomentosa* trees, microarray analysis showed that the orthologue of *ANT* was upregulated during the dedifferentiation of secondary xylem cells (Zhang *et al.*, 2011b). Without any published roles of *ANT* in regulating secondary vascular tissue development, it is already being treated as a molecular marker of cambium development in laboratories around the world.

qPCR expression of *ANT* in roots overexpressing the *CKX1* gene revealed that *ANT* expression is downregulated in these roots. Therefore, like *CYCD3;1*, *ANT* appears to be regulated by cytokinin signalling. This together

with the high correlation of *ANT* and *CYCD3;1* expression in root tissue suggest that either *CYCD3;1* is regulated by *ANT*, or that *ANT* and *CYCD3;1* are coregulated in response to cytokinins.

To test the hypothesis that *ANT* regulates the expression of *CYCD3;1*, two approaches were undertaken. The first was to analyse the expression of two *CYCD3;1* promoter:reporter lines in *ant* loss-of-function mutants. This was done in the *Ler* and *Col-0* backgrounds. In the *Ler* background, whilst *pCYCD3;1:GUS* expression was detected in *ANT* roots, it was not detected in *ant-9* roots. This suggests that, indeed, *ANT* regulates the expression of *CYCD3;1* in secondary growth. However, in the *Col-0* background, *pCYCD3;1:GUS-GFP* expression was detected at similar levels in *ANT* and *ant-GK* mutants. This difference between these two results has several potential explanations. *ANT* could be required for *CYCD3;1* expression in the *Ler* ecotype, but not in the *Col-0* ecotype. ER, which is present in the latter ecotype but absent in the former, could somehow promote *CYCD3;1* expression independently of *ANT*. Other possible explanations are that the two reporters are differentially regulated due to different insertion sites in the Arabidopsis genome, or that the regulation is indeed different in both ecotypes. The reporters are different at the molecular level, in the sense that the *pCYCD3;1:GUS* reporter is absent of several base pairs of sequence immediately upstream of the *CYCD3;1* ATG start codon, whereas the *pCYCD3;1:GUS-GFP* reporter is not. This could also explain the difference, although it may be unlikely that the sequence so close to the ATG start codon is regulated by *ANT*.

The second approach taken to test the hypothesis that *ANT* regulates *CYCD3;1* expression involved qPCR analyses of *CYCD3;1* mRNA levels in *ant* mutants. In the *ant-9* mutant, which is in the *Ler* background, no difference in *CYCD3;1* transcript levels was detected between *ANT* and *ant-9* mutant roots. This suggests that *ANT* does not regulate *CYCD3;1* expression. This conclusion contradicts that formed from the promoter:reporter analysis in *ant-9* roots. The *pCYCD3;1* reporter might not faithfully report *CYCD3;1* expression. This could also explain the different expression of the two reporters observed in the *ant-9* and *ant-GK* mutants. Alternatively, it could be that, whilst the levels of *CYCD3;1* mRNA are not downregulated in the *ant-9* mutant, the protein might be. The same phenomenon could then be occurring with the *pCYCD3;1:GUS* reporter in the *ant-9* mutant: the mRNA levels might not be downregulated whilst the

protein levels are. Unfortunately, attempts at quantifying *GUS* mRNA levels were unsuccessful. This hypothetical post-transcriptional regulation of the expression of the reporter and the *CYCD3;1* gene would have to occur via a sequence element present in both of the loci. The promoter is the sequence shared between the *GUS* system and the native *CYCD3;1* gene, and part of this is transcribed to form the *CYCD3;1* UTR (Menges *et al.*, 2007). A hypothesis that ANT regulated the start site of *CYCD3;1* transcription to modify this UTR was tested, but there was not evidence that ANT promoted the use of a specific start site. It therefore remains unknown whether the *pCYCD3;1:GUS* reporter is simply unfaithful, or a post-transcriptional regulatory mechanism not investigated here exists.

qPCR of *CYCD3;1* expression in the *Col-0 ant-GK* mutant revealed a 20% decrease in this mutant compared to the *WT* control. Although this might be considered a small decrease, it may represent some regulation of *CYCD3;1* by ANT in the *Col-0* background. qPCR of *pCYCD3;1:GUS-GFP* expression in the *ant-GK* mutant revealed a similar decrease in *GUS-GFP* transcript levels. Thus in the *Col-0* background, the *pCYCD3;1:GUS-GFP* reporter faithfully represents *CYCD3;1* expression at the transcriptional level. Taken together with the results in the *ant-9* mutant, it is tempting to base conclusions upon the results with the *pCYCD3;1:GUS-GFP* reporter rather than the *pCYCD3;1:GUS* reporter. Nonetheless, it remains possible that a different mechanism of regulation of *CYCD3;1* expression by ANT exists in the *Ler* ecotype.

To further explore the interaction between *ANT* and *CYCD3;1* in secondary growth, phenotypic analyses of the *ant-9 cycd3;1<sub>Ler</sub>* double mutant and the respective single mutants were performed. This showed that the *ant-9<sub>Ler</sub>* mutant, which is in the *Ler* background, did not have a detectable secondary growth phenotype. In contrast, a strong inhibition of growth was observed in the *ant-GK* mutant in the *Col-0* background. This is consistent with involvement of *ER* in secondary growth (see below). However, whilst *cycd3;1* mutants in the *Ler* ecotype displayed reduced secondary growth, this reduction was enhanced when functional ANT was also lost, confirming that ANT has a role in regulating secondary growth, and showing a synergism between *ANT* and *CYCD3;1*. Whilst a synergistic relationship does not indicate that the two genes are in a linear pathway regulating secondary growth, it does not rule out the possibility that ANT contributes to the regulation of *CYCD3;1* expression. It might be that, in the absence of functional ANT, another transcription factor that positively

regulates *CYCD3;1* is upregulated. Since *ANT* is a transcription factor, it is likely to have many targets, and consequently there will probably be many more effects than simply those due to downregulation of *CYCD3;1* expression, if *ANT* regulates *CYCD3;1*, when functional *ANT* is lost. Reciprocally, there are likely to be many factors regulating the expression of *CYCD3;1*. Ultimately, *ANT* and *CYCD3;1* are likely to fit into a regulatory network involving cytokinins regulating secondary growth. Indeed, expression of *ANT* was, like *CYCD3;1*, reduced in plants with lower levels of active cytokinins. What this data does suggest is that when functional *ANT* is absent, *CYCD3;1* might partially fulfil its roles, and that other factors regulated by *ANT* might partially fulfil the roles of *CYCD3;1* when it is absent.

A putative *ANT*-binding site in the *CYCD3;1* promoter was used to test the molecular interaction of *ANT* with this site in a yeast-one-hybrid assay. Whilst a positive control sequence demonstrated binding, no binding was detected with the site from the *CYCD3;1* promoter. No direct targets of *ANT* have been detected in *Arabidopsis*, to the author's knowledge, and therefore the mechanism/s by which *ANT* act/s remain/s to be confirmed. The *35S:ANT-GR* line described in Chapter 3 might be useful for addressing this issue. Upregulation of the *UGT85A1* gene was detected in *35S:ANT-GR* plants induced with dexamethasone (Chapter 3). This gene might therefore be a direct target of *ANT*, although this needs to be confirmed, for example by the induction of the *ANT-GR* protein along with cyclohexamide treatment to prevent the alteration of expression of indirect *ANT*-targets. Whether or not this is a direct target, it is interesting, since it regulates the levels of active cytokinins (Hou *et al.*, 2004). *UGT85A1* encodes a glucosyl-transferase that can glucosylate *trans-zeatin* and dihydrozeatin, thereby inactivating these cytokinin molecules (Hou *et al.*, 2004). *Arabidopsis* plants overexpressing *UGT85A1* are less sensitive to cytokinin treatments (Jin *et al.*, 2013). Perhaps the upregulation of this gene in the dexamethasone-induced *35S:ANT-GR* plants reveals a negative feedback loop in which *ANT*, a gene positively regulated by cytokinins, reduces cytokinin sensitivity. Overexpressing *ANT* might duplicate this phenomenon.

The hybrid aspen orthologue of *AtANT*, *PtAIL1*, has been shown to bind to the promoter of the hybrid aspen orthologue of *AtCYCD3;1*, named *CYCD3;2* (Karlberg *et al.*, 2011). Down-regulation of *AIL1*-dependent *CYCD3;2* expression was required for cessation of bud growth when plants were shifted from long- to short-days. Therefore, if the regulation of a *CYCD3* gene by an

ANT-like protein is conserved between Arabidopsis and poplar, the mechanism would appear to be different.

Since stronger secondary growth phenotypes were observed in the *ant-GK* and *cycd3;1* mutants in the *Col-0* background than in the *ant-9* and *cycd3;1* mutants in the *Ler* background, that *ANT* and *CYCD3;1* interact with some factor absent in the *Ler* ecotype was hypothesized. The obvious factor to analyse was *ER*. *ER* encodes an LRR-RLK (leucine-rich repeat receptor-like kinase), which regulates shoot organ positioning and growth (Torii *et al.*, 1996; Douglas *et al.*, 2002). Since its identification, studies have revealed diverse roles for *ER*, including regulation of stomata development and transpiration (Masle *et al.*, 2005; Shpak *et al.*, 2005), and more recently, vascular cell proliferation in shoots (Etchells *et al.*, 2013). An *er<sub>Col-0</sub>* loss-of-function mutant displayed reduced secondary growth, which was partially rescued by ectopic expression of *ER*. Thus the genetic analyses point to an interaction between *ANT* and *CYCD3;1* and *ER*. *ER* has recently been shown to regulate secondary growth in shoots and hypocotyls (Etchells *et al.*, 2013). Together with the data presented here, this suggests that *ER* might regulate secondary growth in all parts of Arabidopsis. *ER* can be added to this hypothetical regulatory network regulating secondary growth.

The evidence presented herein does not support a strong interaction between *ANT* and *CYCD3;1*. To create a list of candidate regulators of *CYCD3;1* expression, a yeast-one-hybrid screen using a library of Arabidopsis transcription factors and *CYCD3;1* promoter fragments was undertaken. Several TCP transcription factors were identified. The TCP family of transcription factors is highly conserved in plants and is present in precursors of land plants such as algae (Navaud *et al.*, 2007). In higher plants, TCP proteins regulate various aspects of plant growth and development (Martín-Trillo and Cubas, 2010). These proteins are split into two sub-groups: type I and type II TCPs (Cubas *et al.*, 1999; Kosugi and Ohashi, 2002). Whilst type-I TCPs are thought to promote cell proliferation, type-II TCPs are thought to inhibit cell proliferation (Martín-Trillo and Cubas, 2010).

In lateral aerial organ growth, TCPs repress the expression of boundary-specific genes, and repression of TCP activity can lead to ectopic shoot formation (Koyama *et al.*, 2007). For example, the type-II TCP TCP3 induces the expression of *miR164*, which represses the expression of the boundary *CUP SHAPED COTYLEDON (CUC)* genes, to promote leaf differentiation (Koyama

*et al.*, 2010). TCP3 bound to the *CYCD3;1* promoter in yeast. Since TCP3 promotes differentiation whereas *CYCD3;1* promotes meristematic identity of cells (Shen *et al.*, 2012; Scofield *et al.*, 2013), it might be that TCP3 represses *CYCD3;1*.

The influence of TCPs on meristem growth led to the proposition that TCPs somehow regulate cell division (Cubas *et al.*, 1999). This proposition is supported by the observation that TCP4, another type-II TCP, can block the G1 to S transition in yeast (Aggarwal *et al.*, 2011). In plants, TCP4 promotes plant organ maturation (Sarvepalli and Nath, 2011), and when at high levels of expression can inhibit the growth of petals and other floral organs (Nag *et al.*, 2009). TCP4 also bound to the *CYCD3;1* promoter in yeast; perhaps TCP4 also represses *CYCD3;1*.

Other type-II TCPs identified as binding the *CYCD3;1* promoter here have been implicated in the repression of meristematic competence of cells via repression of class-I *KNOX* genes (Li *et al.*, 2012a). Perhaps these genes also repress *CYCD3;1* expression. *CYCD3;1* and the class-I *KNOX* gene *STM* have been shown to have similar but partially independent roles (Scofield *et al.*, 2013).

TCPs also regulate lateral aerial organ development in other higher plants, such as *Antirrhinum* (Corley *et al.*, 2005) and *Gerbera* (Broholm *et al.*, 2008) species; it would be interesting to test for the molecular interaction between any TCPs and *CYCD3* orthologues in these species.

The class-I TCPs TCP14 and TCP16 (Danisman *et al.*, 2013) also bound to the *CYCD3;1* promoter in yeast. TCP14 promotes cell proliferation during internode, leaf and floral organ growth in concert with TCP15 (Kieffer *et al.*, 2011). Perhaps *CYCD3;1* is a target of TCP14 in some of these processes, as it was shown in this study that *cycd3;1* leaves have fewer cells than their *WT* counterparts. TCP14 also promotes seed germination (Rueda-Romero *et al.*, 2012), and is expressed in the vascular initial cells of embryos (Tatematsu *et al.*, 2008). The *CYCD3;1* promoter is active in these cells during the early stages of embryogenesis (Collins *et al.*, 2012). However, overexpression of *CYCD3;1* in embryos delays germination whilst causing extra cell division activity in the embryo (Masubelele *et al.*, 2005a). Perhaps TCP14 does not promote germination via *CYCD3;1*.

Little is known regarding the roles of TCP16. One study has shown that *TCP16* is expressed in the microspores during pollen development, and that

downregulation of *TCP16* expression leads to aberrant pollen development (Takeda *et al.*, 2006). Cell-cycle regulatory factors, including *CDKA;1*, are essential for correct pollen development (Iwakawa *et al.*, 2006; Gusti *et al.*, 2009; Wijnker and Schnittger, 2013), opening the possibility that *TCP16*-regulated *CYCD3;1* is also involved in this process.

SCARECROW-LIKE5 (*SCL5*) bound to the *CYCD3;1* promoter in yeast. *SCL* proteins are GRAS-family transcription factors, meaning that they show sequence homology with GIBERELIC ACID INSENSITIVE (*GAI*) and REPRESSOR OF THE *gai1-3* MUTANT (*RGA*) proteins (Pysh *et al.*, 1999). SCARECROW (*SCR*) and *SCL* proteins show high sequence homology with one another at the carboxyl termini (Pysh *et al.*, 1999). The *scr* mutant fails to undergo a formative periclinal cell division event in the root cortex-endodermis initial (*CEI*) cells, leading to the absence of a root cell file (Di Laurenzio *et al.*, 1996b). The remaining cell file has neither endodermis identity nor cortex identity, but has a heterologous identity (Di Laurenzio *et al.*, 1996b). *SCR* is also required for QC specification and hence stem-cell identity of cells surrounding the QC (Sabatini *et al.*, 2003). A link between *SCR* and cell division has been revealed in the form of *SCR* promoting cell proliferation and cell division in leaves (Dhondt *et al.*, 2010b). In roots, *SCR* binds the *CYCD6;1* promoter to promote asymmetric cell divisions in the *CEI* cells (Cruz-Ramirez *et al.*, 2012), demonstrating the first example of a *SCR*-family protein binding to the promoter of a D-type cyclin gene. Little is known regarding the roles of *SCL* genes, although orthologues in trees appear to be involved in auxin-induced cell division in cuttings (Sanchez *et al.*, 2007). *SCL3* is involved in gibberellic acid signalling in *Arabidopsis* (Zhang *et al.*, 2011c). To the author's knowledge, no known roles for *SCL5* exist. *SCL5* mRNA has been detected in shoots, roots and siliques (Pysh *et al.*, 1999). Perhaps *SCL5* promotes radial cell division activity in the cambium via the activation of *CYCD3;1*.

The *CYCD3;1* promoter was also bound, in yeast, by AGAMOUS-LIKE 3 (*AGL3*). *AGL3* is broadly expressed in shoots but not at all in roots (Huang *et al.*, 1995). AGAMOUS (*AG*) itself is a floral homeotic gene i.e. it is required for correct floral organ identity (Yanofsky *et al.*, 1990; Alvarez and Smyth, 1999). The roles of *AGL3* are yet to be elucidated, but perhaps a good start would be to search for any roles in the regulation of petal and leaf growth, since roles for *CYCD3;1* in the regulation of these processes were shown in this study.

The YABBY5 (YAB5) protein that bound to the *CYCD3;1* promoter is a member of a seed plant-specific transcription factor family, of which there are six in Arabidopsis (Bartholmes *et al.*, 2012). YAB proteins are involved in leaf lamina development and specifying adaxial and abaxial cell identity in these organs (Sarojam *et al.*, 2010). *YAB5* is expressed in vegetative tissues, and in contrast to some other *YAB* genes, is not required for abaxial and/or adaxial cell identity, but is involved in SAM maintenance and general leaf growth (Stahle *et al.*, 2009). Since *CYCD3;1* is also involved in SAM maintenance, (Scofield *et al.*, 2013), *YAB5* might regulate *CYCD3;1* to achieve this.

The HOMEODOMAIN GROUP PROTEIN11 (HDG11) protein that bound to the *CYCD3;1* promoter negatively regulates trichome branching (Nakamura *et al.*, 2006). *CYCD3;1* is not normally expressed in trichomes (Schnittger *et al.*, 2002), and misexpression of *CYCD3;1* in trichomes leads to cell division which does not normally occur (Schnittger *et al.*, 2003a). However, branching was unaffected in the *CYCD3;1* misexpresser (Schnittger *et al.*, 2003a). Currently there is therefore no clear link between HDG11 and *CYCD3;1* in plants.

These molecular interactions were all identified in yeast. To confirm that these interactions occur *in planta*, CHIP studies will be necessary. Genetic analyses should follow to investigate the functional links between the respective genes.

# Chapter Five: CYCD3s and ER

## Regulate Primary Development of

### the Vascular Tissue

#### **Introduction**

---

In Arabidopsis, establishment of the primary pattern of the vascular tissue occurs during embryogenesis. At the globular stage of embryogenesis, three tissues can be distinguished: the protoderm, the ground meristem and the procambium (Leyser and Day, 2007). The protoderm is the outermost layer of cells, and will form the epidermis. The next layer of tissue in the embryo is the ground meristem, which will form the cortex and endodermis. In the middle of the embryo can be found the procambium, which will form the vascular tissue. At this stage, the ground meristem and procambium can be distinguished from one another, since the cells of the ground meristem are large and heavily vacuolated, whereas the procambium cells are relatively small and have smaller vacuoles (Leyser and Day, 2007). This difference remains post-embryonically (Dolan *et al.*, 1993). The procambium cells divide, and by the torpedo stage of embryogenesis, the number of pericycle and vascular initials (aka founder cells) is similar to the number normally found post-embryonically (Scheres *et al.*, 1994). Thus the primary pattern of the vascular tissue has been established, and this same pattern of vascular initial cells exists adjacent to the QC post-embryonically (Scheres *et al.*, 1994; Mahonen *et al.*, 2000). Clonal analysis of Arabidopsis root cells during embryogenesis and post-embryonically showed that all of the post-embryonic vascular cells normally derive from these vascular initials (Scheres *et al.*, 1994). However, it has been shown via laser ablation of root meristem cells and observations of random divergences from cell division patterns that it is positional information that defines the identities assumed by root meristem cells (van den Berg *et al.*, 1995; Kidner *et al.*, 2000). This

positional information comes at least partially in the form of morphogens (van den Berg *et al.*, 1997), auxin being a key player (Uggla *et al.*, 1996; Friml *et al.*, 2002; Kramer, 2004; Santuari *et al.*).

Post-embryonically, the radial pattern of the primary vascular tissue is elaborated with further periclinal cell divisions, and this occurs within the meristem (Mahonen *et al.*, 2000). The meristem contains relatively small cells that undergo cell division (Verbelen *et al.*, 2006). This region is normally around 250  $\mu\text{m}$  long in an *Arabidopsis* root (Dolan *et al.*, 1993). The xylem initial cells appear to be the earliest initials to divide periclinally, as a primary xylem axis of four to five cells exists just 6  $\mu\text{m}$  from the QC (Mahonen *et al.*, 2000). However, phloem cells differentiate earlier than the xylem cells (Mahonen *et al.*, 2000).

One of the first mutants identified for having an effect on the vascular cell file number in the primary root tissue is the *wol* (*wooden leg*) mutant (Scheres *et al.*, 1995a). This mutant fails to undergo a cell division event in the torpedo stage of embryogenesis, resulting in a reduction in the vascular cell file number in the mature embryo (Scheres *et al.*, 1995a). Subsequent analyses identified additional roles for the gene mutated in the *wol* mutant in the post-embryonic periclinal divisions of the vascular initial cells (Mahonen *et al.*, 2000). The gene mutated in the *wol* mutant was cloned and sequenced, and was predicted to encode a two-component hybrid molecule with phosphorelay activity (Mahonen *et al.*, 2000). This gene was expressed throughout the vascular tissue (Mahonen *et al.*, 2000). It was later found that the *WOL* gene was the same gene characterized elsewhere as a novel cytokinin receptor (Inoue *et al.*, 2001; Suzuki *et al.*, 2001a; Yamada *et al.*, 2001; Spichal *et al.*, 2004). Thus cytokinin signalling appears to be important for the establishment of a primary pattern of vascular tissue with the correct number of cell files. *CYCD3* genes are regulated by cytokinin signalling under at least some circumstances (Riou-Khamlichi *et al.*, 1999; Dewitte *et al.*, 2007), and are expressed during embryogenesis when the vascular initials are derived (Collins *et al.*, 2012), suggesting possible roles in mediating cytokinin regulation of vascular cell proliferation.

## Aims & Objectives

---

To test the hypothesis that *CYCD3* genes regulate the development of the primary vascular tissue, microscopical analyses were employed to visualize vascular cell files in the primary root of *Arabidopsis* and to quantify cell file number within the stele. Optical cross-sections of the meristems of young roots were taken using confocal line-scanning microscopy. The expression of *CYCD3* genes within the primary root vascular tissue was assessed, since expression of these genes in this tissue would support the existence of roles for these genes in the tissue. Since the available *cycd3* mutant alleles are derived in different ecotypes, *cycd3* phenotypes were analysed in the *Col-0* and *Ler* backgrounds. This led to the observation that a *cycd3* phenotype existed in the *Col-0* ecotype but not in the *Ler* ecotype. To test the hypothesis that the *er* mutation in the *Ler* ecotype causes the alteration in this phenotype, vascular cell file number was visualized in the *Col-0 er-105* mutant via sectioning of plastic-embedded roots. This led to the identification of an *er-105* phenotype similar to the *Col-0 cycd3* phenotype.

## Results

---

### 5.1 Roots Lacking Functional *CYCD3* Genes Have a Reduced Number of Cell Files within the Primary Stele

To determine whether *CYCD3* genes are required for correct patterning of the primary vascular tissue, vascular cell files were quantified in the root apical meristems of 5 DAG roots lacking different combinations of functional *CYCD3* genes (Figure 5.1, Table 5.1). Confocal line scans were used to obtain optical sections at the position of the seventh cortical cell from the QC, which equates to 35 – 40  $\mu\text{m}$  from the QC, a distance at which the primary root vascular pattern is normally established (Mahonen *et al.*, 2000). Phloem and procambial cells were difficult to distinguish from one another in these images, so total numbers of phloem and procambial cells were quantified, and xylem cell files were quantified separately. *cycd3;1-3<sub>Col-0</sub>* and *cycd3;1<sub>Col-0</sub>* roots often contained four xylem cell files in the primary meristem, whereas *WT<sub>Col-0</sub>* roots invariably contained five, as did *cycd3;2-3<sub>Col-0</sub>* roots in most cases (Table 5.1), implicating *CYCD3;1* in the regulation of xylem cell number. All three of the mutants mentioned above contained fewer phloem and procambium cells than *WT<sub>Col-0</sub>* roots (Table 5.1). Whilst *WT<sub>Col-0</sub>* roots contained on average 25 phloem and procambium cell files, *cycd3<sub>Col-0</sub>* roots contained 20 on average (Table 5.1). Roots of all genotypes had an average of 13 pericycle cell files (Figure 5.1, Table 5.1), suggesting that the reduction in cell file number caused by loss of *CYCD3* function in the primary roots specifically leads to a reduction in the number of vascular cell files.

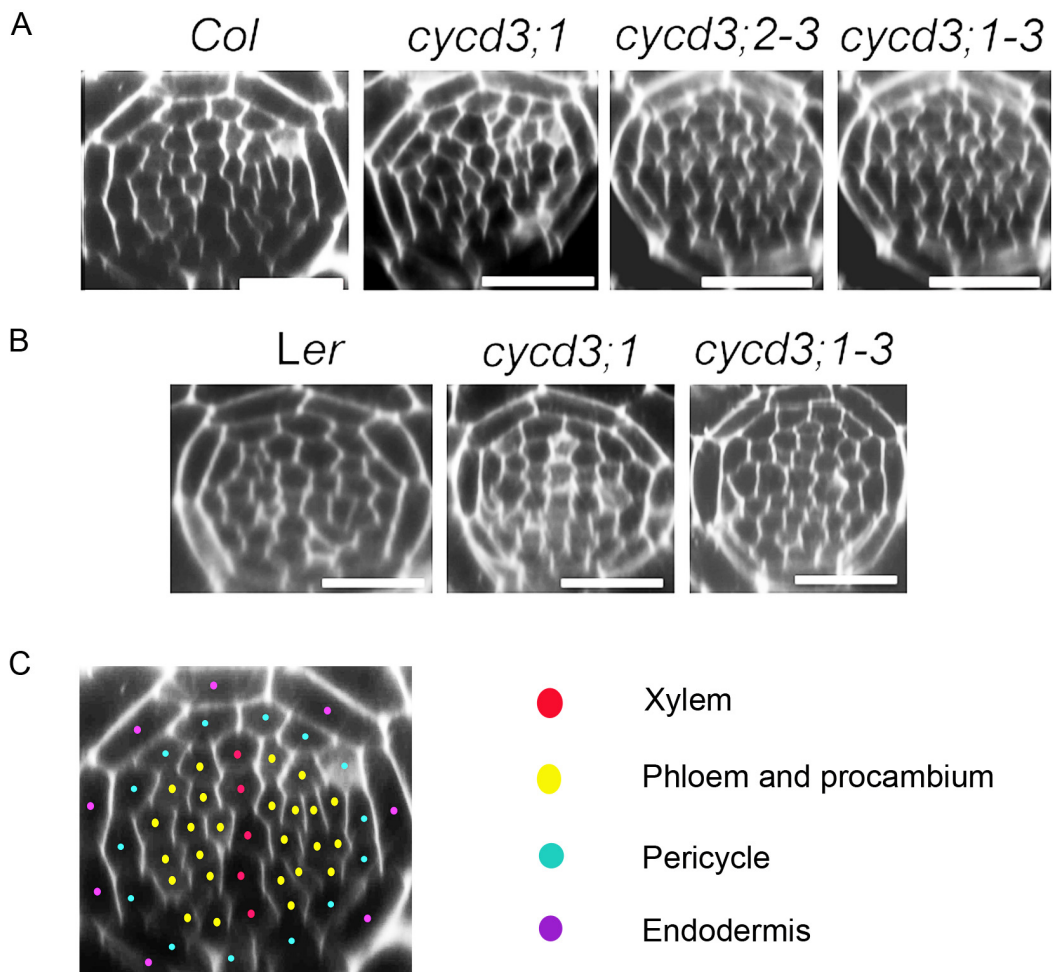


Figure 5.1: Vascular cell file number in the primary root meristem is reduced in *cycd3* mutants in the *Col-0* background, but not in the *Ler* background. A & B) Optical cross-sections at the position of the seventh cortical cell from the QC. In A, *cycd3;1* and *cycd3;3* mutants were originally isolated in the *Ler* background, but were then back-crossed twice to the *Col-0* background (Dewitte *et al.*, 2007). In B, the *cycd3;1* mutant is the original line isolated in the *Ler* background, and the *cycd3;1-3* triple mutant contains the *cycd3;1* and *cycd3;3* alleles isolated in *Ler* and the *cycd3;2* allele isolated in *Col-0* but backcrossed twice to *Ler*. Roots were analysed following the Schiff staining procedure, and this was undertaken 5 DAG. Z-stacks were created at the position of the seventh cortical cell from the QC. All scale bars represent a distance of 20  $\mu\text{m}$ . C) Annotated optical cross-section of the *Col-0* WT root shown in A.

**Table 5.1: Quantification of vascular cell number within the stele of roots undergoing primary growth (5 DAG) in the *Col-0* background. Cells were counted from sections taken at the position of the seventh cortical cell. The first row shows data from *WT. cycd3* is shortened to *d3*. Standard error is indicated.**

	Pericycle	Xylem	Phloem + procambium
<i>Col-0</i> <sup>a</sup>	13.33 ± 0.37	5.00 ± 0.00	25.00 ± 0.26
<i>d3;1-3</i> <sup>b</sup>	12.75 ± 0.48	4.25 ± 0.25	20.25 ± 1.25
<i>d3;1</i> <sup>c</sup>	12.80 ± 0.20	4.20 ± 0.20	20.00 ± 0.55
<i>d3;2-3</i> <sup>d</sup>	13.00 ± 0.26	4.83 ± 0.17	19.50 ± 0.76

<sup>a</sup> n = 6

<sup>b</sup> n = 5

<sup>c</sup> n = 4

<sup>d</sup> n = 6

Expression of the *CYCD3* genes in the vascular tissue of the primary root meristem was analysed (Figure 5.2). Expression of *pCYCD3;2:GUS-GFP* and *pCYCD3;3:GUS-GFP* promoter:reporter constructs was detected within the stele, becoming stronger closer to the QC (Figure 5.2), whereas no expression of the *pCYCD3;1* promoter:reporter could be detected in the root meristem (Figure 5.3C, right).

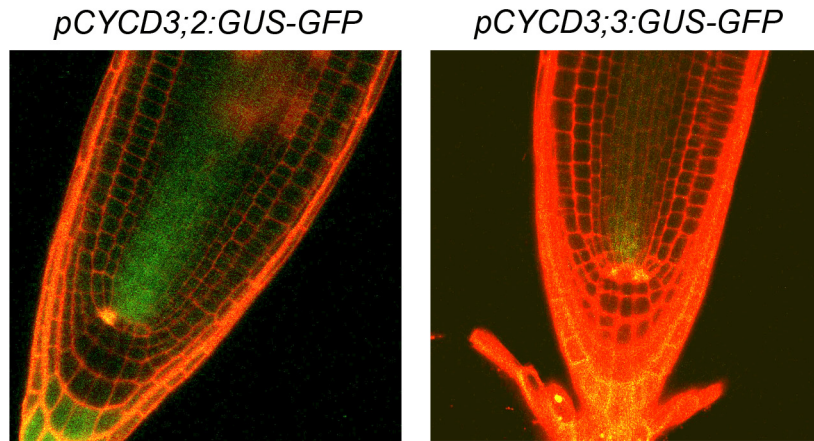


Figure 5.2: Activity of *CYCD3;2* and *CYCD3;3* promoters in the *Col-0* RAM. Roots were 5 DAG, and were stained with propidium iodide to distinguish cell walls. This can be seen in red. GFP signal can be seen in green.

### 5.2 *Ler* Roots have a Reduced Number of Vascular Cell Files, and this Reduction is not Enhanced by Loss of *CYCD3* Genes

The *cycd3;1* and *cycd3;3* alleles used to generate the above mutants were isolated in the *Ler* background, and were crossed at least twice successively to *Col-0* plants to generate mutants containing a majority of DNA sequence from the latter genetic background. *Ler* has altered growth characteristics in part due to a mutation in the *ERECTA* receptor kinase that also affects cell number and organ size (Torii *et al.*, 1996; Tisne *et al.*, 2011). Vascular cell files were also quantified in the primary meristems of *cycd3<sub>Ler</sub>* mutants in the *Ler* background (Figure 5.3, Table 5.2). The number of phloem and procambial cell files in *Ler* *WT* roots was less than that in *Col-0* roots, and this difference was similar to that between *Col-0* *WT* and *cycd3* roots (compare tables 5.1 & 5.2). *WT<sub>Ler</sub>* roots

contained five xylem cell files in most cases, as did *cycd3<sub>Ler</sub>* roots. *WT<sub>Ler</sub>* roots contained on average 18 phloem and procambium cells, as did *cycd3;1<sub>Ler</sub>* and *cycd3;1-3<sub>Ler</sub>* roots (Figure 5.3, Table 4.2). No further reduction in vascular cell file number was observed in *cycd3* roots in the *Ler* background (Figure 5.3, Table 4.2). Pericycle cell number was on average 12 or 13 in all of the genotypes analysed. These data suggest that *CYCD3s* are rate-limiting for periclinal cell divisions forming the vasculature of primary root meristems in the *Col-0* background, but not in the *Ler* background.

**Table 5.2: Quantification of vascular cell number within the stele of roots undergoing primary growth (5 DAG) in the *Ler* background. Cells were counted from sections taken at the position of the seventh cortical cell. Standard error is indicated.**

	Pericycle	Xylem	Phloem & procambial
<i>Ler</i> <sup>a</sup>	12.3 ± 0.7	4.8 ± 0.4	17.9 ± 1.2
<i>cycd3;1</i> <sup>b</sup>	12.2 ± 0.4	4.7 ± 0.5	18.0 ± 1.6
<i>cycd3;1-3</i> <sup>c</sup>	12.6 ± 0.5	4.6 ± 0.5	18.1 ± 2.1

<sup>a</sup> n = 9

<sup>b</sup> n = 9

<sup>c</sup> n = 9

### 5.3 ER is Required for the Correct Number of Vascular Cell Files in the Root Meristem

*Ler WT* roots contain a fewer number of vascular cell files in the root meristem than *Col-0* roots. This could be a phenotype caused by the loss of functional ER in *Ler* plants. In Chapter Four, the *er-105* mutant was shown to share a phenotype with the *cycd3;1* mutant, and in this chapter, the *Ler* ecotype “*WT*” roots share an aspect of the *cycd3* mutant root phenotype. Furthermore, the *Ler* phenotype was not further enhanced by loss of functional *CYCD3;1*. To test the

hypothesis that the *er* mutation in *Ler* causes the reduction in vascular cell file number when compared to *Col-0* roots, sections were taken of plastic-embedded *WT<sub>Col-0</sub>* roots and *er-105<sub>Col-0</sub>* roots (Figure 5.3A). The *er-105* mutant is a loss-of-function allele of the ERECTA kinase-encoding gene in the *Col-0* background (Torii *et al.*, 1996). The *er-105<sub>Col-0</sub>* mutant had fewer phloem and procambium cell files than the *WT<sub>Col-0</sub>* control (Figure 5.3A). *WT<sub>Col-0</sub>* roots had on average 22 phloem and procambium cells, 5 xylem cells and 13 pericycle cells (Table 5.3; Figure 5.3B). *er-105<sub>Col-0</sub>* mutant roots contained typically 17 phloem and procambium cells, 5 xylem cells and 13 pericycle cells (Table 5.3; Figure 5.3B). The endodermis cells in the *er-105<sub>Col-0</sub>* mutant appear smaller than those in the *WT<sub>Col-0</sub>* roots, probably to fit around the smaller stele (Figure 5.3B).

To analyse expression of *ER* in the root meristem at a cellular level, a *pER:GUS* promoter:reporter line was used. Roots were subjected to a GUS assay and were then cleared, embedded in plastic and sectioned perpendicular to the direction of root growth. In this cross-section (Figure 5.3C), activity of the GUS enzyme was detected within the stele, but not in the xylem. It appeared that expression of the reporter was absent in the phloem cells also, but a less sensitive GUS assay would confirm this. This suggests that *ER* is expressed in the procambium.

**Table 5.3: Quantification of vascular cell number within the stele of *WT<sub>Col-0</sub>* and *er-105<sub>Col-0</sub>* loss-of-function mutant roots undergoing primary growth (5 DAG) in the *Col-0* background. Cells were counted from sections taken 35  $\mu$ m shootward of the QC. Standard error is indicated.**

	Pericycle	Xylem	Phloem & procambial
<i>Col-0 WT<sup>a</sup></i>	12.9 $\pm$ 0.2	4.6 $\pm$ 0.2	22.1 $\pm$ 0.7
<i>er-105<sup>b</sup></i>	12.8 $\pm$ 0.2	4.6 $\pm$ 0.2	17.2 $\pm$ 0.6

<sup>a</sup> n = 11

<sup>b</sup> n = 9

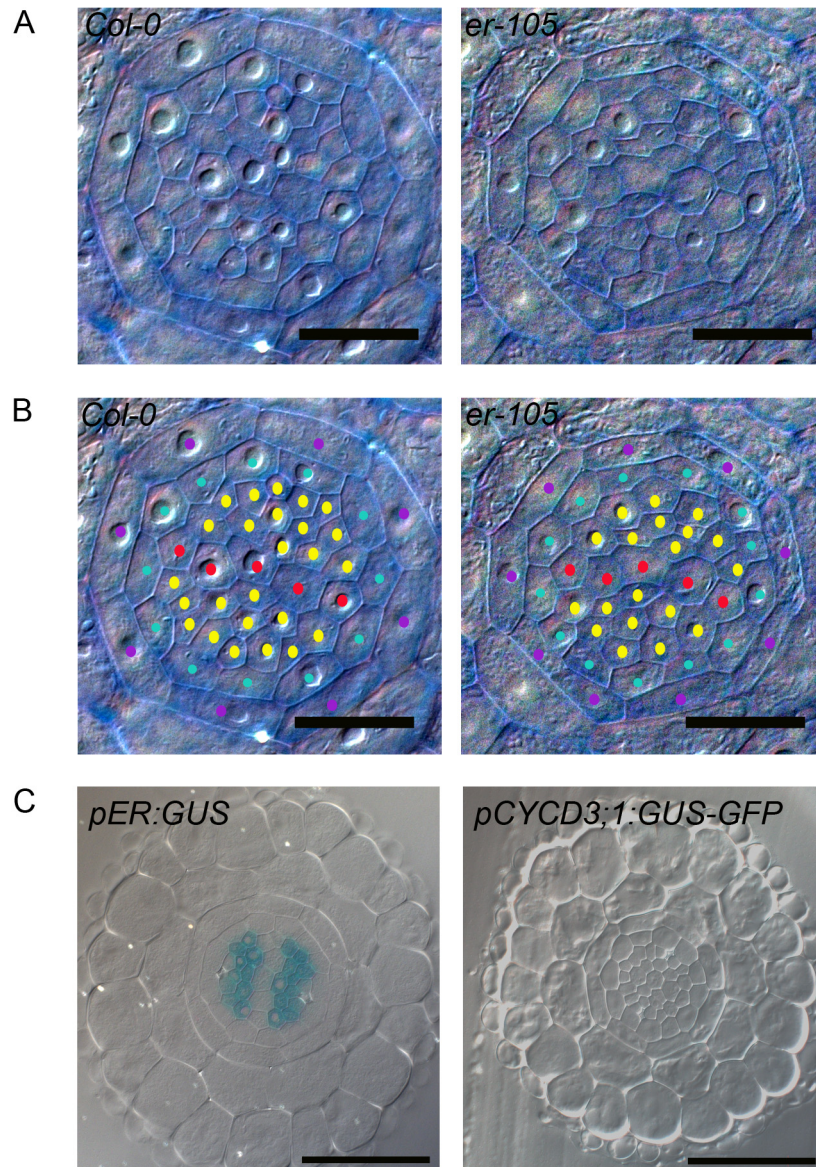


Figure 5.3: The *er-105*<sub>Col-0</sub> mutant has a reduced number of primary vascular cell files, and the *ER* promoter is active in the procambium. A) Cross-sections of 5 DAG plastic-embedded roots. Sections were taken 35  $\mu$ m shootward of the QC. A *WT*<sub>Col-0</sub> root is shown on the left, an *er-105*<sub>Col-0</sub> mutant root is shown on the right. B) Cross-sections shown in A annotated. As in figure 4.1, red spots indicated xylem cells, yellow spots indicate phloem and procambium cells, turquoise spots indicate pericycle cells and purple spots indicate endodermis cells. C) Cross-sections of 5 DAG *pER:GUS* (left) and *pCYCD3;1:GUS-GFP* (right) roots subjected to a GUS assay. Sections were taken within the primary meristem. In all pictures, scale bars represent 20  $\mu$ m.

#### 5.4 CYCD3 Expression is Unchanged in the *er-105* T utant

The *er-105<sub>Col-0</sub>* mutant has a primary stele composed of a reduced number of cell files. Roots of the *Ler* ecotype, which have a different *er* loss-of-function mutant allele, also have a reduced number of cell files compared to *Col-0* roots. This suggests that the reduction of vascular cell file number in *Ler* compared to *Col-0* is a consequence of the *er* mutation in the former ecotype. Whilst loss of CYCD3 function causes a reduction in cell file number in *Col-0* roots, it does not cause a further reduction in *Ler* roots, which have a reduced number compared to *Col-0*. This suggests that a genetic interaction between *ER* and *CYCD3s* may exist. Since the *ER* gene encodes a receptor-like kinase (Torii *et al.*, 1996), it is likely that, in any cell-signalling pathway connecting *ER* and *CYCD3s*, *ER* functions upstream of the *CYCD3s*. To test the hypothesis that *CYCD3* expression is altered in the absence of functional ER, qPCR was used to quantify *CYCD3* expression in *WT<sub>Col-0</sub>* and *er-105<sub>Col-0</sub>* seedlings (Figure 5.4). No consistent difference in *CYCD3* gene expression was observed in the *er-105<sub>Col-0</sub>* mutant when compared to the *WT<sub>Col-0</sub>* seedlings (Figure 5.4). To confirm that ER does not regulate the expression of *CYCD3* genes in the vascular tissue, qPCR should be performed with RNA extracted from root tips.

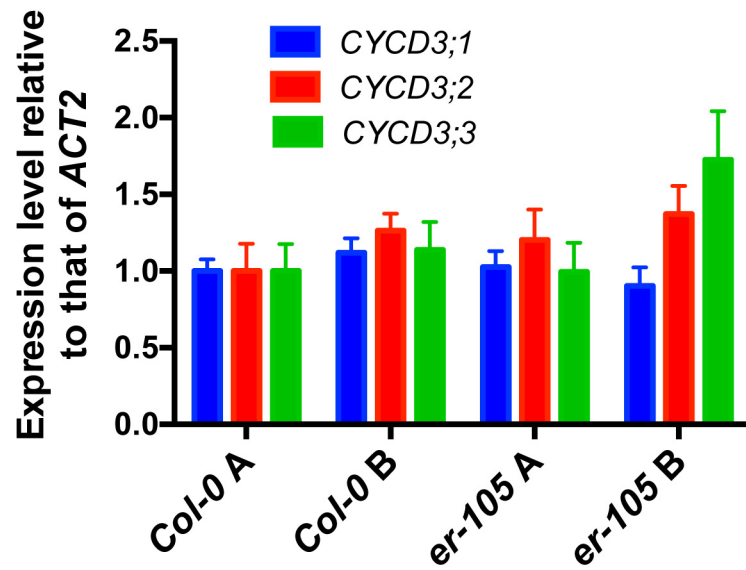


Figure 5.4: Expression of *CYCD3* genes in the *er-105<sub>Col-0</sub>* mutant. RNA was extracted from 5 DAG seedlings grown on GM media. For each sample (two are shown for each genotype), several seedlings were pooled for an extraction. Expression levels are shown for each gene relative to those in the *Col-0* A *WT* sample. Error bars represent standard deviation in three technical replicates. A & B represent biological replicates.

## Discussion

---

Plant embryogenesis is driven by a typical pattern of cellular division events (Leyser and Day, 2007). *CYCD* genes regulate cell division via the G1 to S transition during various developmental programs in Arabidopsis (Hu *et al.*, 2000; Menges *et al.*, 2006; Dewitte *et al.*, 2007; Nieuwland *et al.*, 2009; Sanz *et al.*, 2011), and expression of various *CYCD3* genes has been inferred via promoter:reporter lines in the embryo (Collins *et al.*, 2012). The *wol* mutant has demonstrated the importance for cytokinin signalling in the regulation of vascular initial cell division in the embryo (Scheres *et al.*, 1995a), and *CYCD3* genes appear to be regulated by cytokinins in several developmental contexts (Riou-Khamlichi *et al.*, 1999; Dewitte *et al.*, 2007). Thus it is possible that these genes form part of the cytokinin signalling pathway regulating primary vascular tissue development. Here, roles for the *CYCD3*s in primary vascular tissue development are shown. Primary roots lacking either *cycd3;1* alone, *cycd3;2* and *cycd3;3* or all three *cycd3*s contained fewer phloem and procambium cells than their *WT<sub>Col-0</sub>* counterparts. Whilst there also appeared to be one less xylem cell in *cycd3;1<sub>Col-0</sub>* and *cycd3;1-3<sub>Col-0</sub>* mutants, pericycle cell number appeared to be unchanged, revealing that the reduction in cell number was specific to the vascular cells. It is interesting to note that all three *cycd3<sub>Col-0</sub>* mutant combinations had similar phenotypes in terms of procambium and phloem cell file number. This suggests that when the function of a *CYCD3* gene is lost, another *CYCD3* compensates, since an additive phenotype in the triple mutant might otherwise be expected. Alternatively, some other factor that induces cell divisions might be induced once the procambium and phloem cell file number is reduced to a certain extent. This also suggests that *CYCD3* genes are not required for all vascular initial cell division events, since 80% of the vascular cell files remain in the mutants.

This data was obtained from roots post-germination, but the developmental point/s at which cell division event/s fail to occur in *cycd3<sub>Col-0</sub>* mutants remain/s unknown. Since the primary vascular pattern is initially created in the embryo (Scheres *et al.*, 1994), it might be that the phenotype becomes apparent during embryogenesis. The *wol* cytokinin signalling mutant acquires the phenotype in vascular development during embryogenesis (Scheres *et al.*, 1995a). In growing *Col-0* roots, the number of vascular cell files shootward abutting the QC is lesser than that seen slightly further away, where the full

primary pattern exists (Mahonen *et al.*, 2000). Which cells divide periclinally within this region is unclear, but assuming the initial cells adjacent to the QC do so, like other initial cells surrounding the QC do (Petricka *et al.*, 2012), post-embryonic periclinal divisions of these cells will be required for maintenance of the correct number of vascular cell files. Therefore, there are two temporal windows during which the *CYCD3s* may act to promote periclinal cell divisions in the vascular tissue. If they do so downstream of cytokinins, it might be likely that they act during embryogenesis, since the *Arabidopsis wol* mutant is defective in a periclinal cell division event essential for correct vascular tissue patterning in embryogenesis (Scheres *et al.*, 1995a).

The *CYCD3;1* promoter is active throughout the developing embryo during the globular and heart stages, but appears to be restricted to the cotyledon regions by the torpedo stage (Collins *et al.*, 2012). The number of vascular initial cells in the embryo only matches the number found adjacent to the QC post-embryonically by the torpedo stage (Scheres *et al.*, 1994). It is possible that *CYCD3;1* act prior to the torpedo stage within the procambium cells, but it might act in a non-cell-autonomous manner when it is expressed in the cotyledon regions. The latter hypothesis is supported by the observation that perturbations to cotyledon development also affect development of the root vascular tissue (Help *et al.*, 2011). However, it needs to be verified that the promoter activity of *CYCD3;1* observed by Collins *et al.* (2012) faithfully reflects native *CYCD3;1* expression in the embryo, since the faithfulness of the reporter used in these experiments is uncertain (Chapters 3 & 4). Although the establishment of the primary vascular tissue pattern occurs during embryogenesis, this pattern must be maintained post-embryonically by divisions of the vascular initial cells (Mahonen *et al.*, 2000). It is therefore also possible that *CYCD3;1* regulates these divisions. However, activity of the *CYCD3;1* promoter was not detected in the primary root meristem in this study. *In situ* hybridization analysis of *CYCD3;1* expression would be required to rule out the possibility of *CYCD3;1* expression in the primary root meristem.

The *CYCD3;2* promoter is active in the basal part of the globular-stage embryo, throughout the embryo at the heart stage, and in the cotyledon regions at the torpedo stage (Collins *et al.*, 2012). This expression pattern is concomitant with *CYCD3;2* regulating procambium cell divisions in the embryo. However, activity of the *CYCD3;2* promoter was also detected within the stele of

the primary root meristem in this study, suggesting that it may also, or instead, regulate divisions of the vascular initial cells post-embryonically.

The *CYCD3;3* promoter is active throughout the embryo during the globular and heart stages, and is restricted to the cotyledon regions and the basal part of the embryonic radical at the torpedo stage (Collins *et al.*, 2012). As for *CYCD3;2*, *CYCD3;3* promoter activity is also observed in the stele of the primary root meristem post-germination (This chapter; Forzani *et al.*, 2014). Therefore, *CYCD3;3* might also act to promote vascular initial cell division during embryogenesis and/or post-germination.

Cytokinin signalling also regulates cell differentiation in the primary vascular tissue. In the *wol* mutant, remaining vascular initial cells differentiate exclusively into protoxylem (Scheres *et al.*, 1995a), and this is phenocopied by ectopically expressing a *CKX* gene, encoding an enzyme that inactivates cytokinins (Schmulling *et al.*, 2003), in the primary stele (Mahonen *et al.*, 2006a). This suggests that cytokinins normally inhibit protoxylem differentiation. In agreement with this, cytokinins promote PIN1-mediated export of auxin from the procambium cells into the protoxylem cells, where auxins promote protoxylem differentiation (Bishopp *et al.*, 2011a; Bishopp *et al.*, 2011b). How cytokinins maintain procambium identity in the procambium cells remains unknown. Recently, *CYCD3* genes have been shown to play roles in the maintenance of STM (Shoot Meristemless) – mediated meristematic competence of SAM cells (Scofield *et al.*, 2013). Perhaps *CYCD3* genes are also involved in the maintenance of procambial cell identity, since these cells must remain capable of dividing and differentiating into different cell types later in development. Cytokinins have been shown to repress cell differentiation (Yokoyama *et al.*, 2007), as has *CYCD3;1* (Dewitte *et al.*, 2003). Therefore, perhaps cytokinins are inducing *CYCD3* expression in procambium cells. Regulation of *CYCD3* expression by cytokinins in whole roots was shown in this study, but regulation of these genes by cytokinins specifically during primary vascular tissue development remains to be confirmed.

Embryos defective in auxin signalling, like those defective in cytokinin signalling, develop with a reduced number of vascular initial cell files (Hardtke and Berleth, 1998). The auxin-response factor MONOPTEROS (MP) – encoding gene is expressed in the embryo, initially broadly, but specifically in the vascular tissue later in embryo development (Hardtke and Berleth, 1998). When functional MP is absent, fewer embryonic vascular cell files develop (Hardtke

and Berleth, 1998). Auxins might promote divisions of the vascular initial cells during embryogenesis via activation of *CYCD3s*. However, auxins control Arabidopsis embryogenesis globally (Moller and Weijers, 2009), and inhibit cytokinin signalling in the embryo (Muller and Sheen, 2008). Auxins also promote the formation of protoxylem cells post-embryonically (Bishopp *et al.*, 2011a; Bishopp *et al.*, 2011b), and one less protoxylem cell file was observed in *CYCD3* mutants in this study. It would be interesting to determine whether or not this represents a link between auxins and *CYCD3s* in protoxylem formation, perhaps involving induction of *CYCD3* by auxins in the xylem precursor cells.

The phenotypes discussed were observed in the *Col-0* ecotype, but were absent in the *Ler* ecotype. *Ler WT* roots contained fewer vascular cell files than *Col-0 WT* roots, in the absence of *CYCD3* loss. It therefore seems that, in the *Ler* ecotype, certain cell division events in the vascular lineage fail to occur, and those remaining do not depend on *CYCD3s*. This suggests that the cell divisions that fail to occur in *Ler* are the same as those that fail to occur in *cycd3<sub>Col-0</sub>* mutants. This led to the hypothesis that *ER*, which is mutated in the *Ler* ecotype (Torii *et al.*, 1996), was required for the establishment of a primary root vascular tissue pattern containing the correct number of cell files. A reduced number of phloem and procambium cell files was observed in the *Col-0 er-105* mutant. Consistent with *ER* regulating procambium and phloem transversal cell divisions, plants lacking both *ER* and its paralogue *ERL1* display perturbed procambium development in stems (Uchida and Tasaka, 2013). These results suggest that the *er* mutation in *Ler WT* roots might be the cause of the reduction in vascular cell file number. If this is the case, the *Ler cycd3* mutants display a non-additive phenotype in terms of *er* and *cycd3* mutations, leading to the hypothesis that *ER* and *CYCD3* genes regulate vascular cell divisions via the same pathway. *er* mutant pedicels are smaller than their *WT* counterparts, and this phenotype is correlated with slow cell cycle progression and reduced proliferation of cortex cells (Bundy *et al.*, 2012). Thus there does appear to be a link between *ER* and cell cycle control. Perhaps this link is via *CYCD3* genes, or the respective proteins, and perhaps it is universal in Arabidopsis vascular tissue development. Supporting this, expression of *ER* in the phloem is sufficient to suppress some *er* phenotypes (Uchida *et al.*, 2012a), including that of perturbed vascular tissue development (Uchida and Tasaka, 2013), and expression of *CYCD3;1* in the root phloem poles was detected in this study via *in situ* hybridization (Chapter 4).

Whilst no consistent difference in *CYCD3* expression was observed in the *er-105* mutant, many other mechanisms by which these genes might interact remain. It might even be the case that *CYCD3*s are upstream of *ER* in this putative cell-signalling pathway, for example by CDK-mediated phosphorylation of the *ER* protein. *cycd3 er-105* double mutants will need to be created to confirm that there is a non-additive phenotype in these mutants. If this is confirmed, the mechanism of interaction between *ER* and *CYCD3*s should be investigated.

It has been claimed that *ER* does not function in roots (Bundy *et al.*, 2012), but activity of its promoter in roots is demonstrated in this study, and *er* root phenotypes in secondary growth (Chapter 4) and primary vascular tissue patterning (this chapter) are shown. How *ER* regulates vascular tissue development will need to be investigated. In the SAM, *ER* limits the number of stem cells present (Uchida *et al.*, 2012b), and reduces cytokinin responsiveness of the SAM when cytokinin levels are high (Uchida *et al.*, 2013). In this study, root procambium cell number and secondary growth decreased rather than increased in *Ler* and *er-105* roots, suggesting that the mechanism of *ER* action in the root is different from that in the SAM.

One aspect of the *cycd3;1* phenotype was not shared by that of *Ler WT* or *er-105* mutants: the loss of a single xylem cell in the former mutant. In the *Col-0* background, *cycd3;1<sub>Col-0</sub>* and *cycd3;1-3<sub>Col-0</sub>* mutants contained four xylem cells, instead of the five in *WT<sub>Col-0</sub>* control roots. The *cycd3;2-3<sub>Col-0</sub>* double mutant contained five xylem cell files, suggesting that this phenotype was due to the loss of functional *CYCD3;1*. However, in the *Ler* ecotype, five xylem cell files were present in both *WT<sub>Ler</sub>* and *cycd3;1<sub>Ler</sub>* roots. This indicates another epistatic relationship between *CYCD3;1* and some locus/loci polymorphic between the *Col-0* and *Ler* ecotypes. However, relatively low sample sizes have been used here, so the experiment should be repeated with a larger sample size to confirm this conclusion.

It would be interesting to investigate the regulation of *de novo* primary vascular development in newly arisen lateral and axillary roots and shoots, as well as leaves and other LAOs containing vascular tissue. Inflorescence stems arise post-embryonically, and procambium tissue formation in these stems is perturbed in plants lacking two cytokinin receptor genes, *AHK2* and *AHK3* (Hejatko *et al.*, 2009). This suggests that the involvement of cytokinins in the regulation of the establishment of the primary pattern of vascular tissue might be

## *Chapter Five: Primary Vascular Tissue Patterning*

universal in the plant. Perhaps the *CYCD3* genes also regulate the development of this tissue throughout the plant.

# Chapter 6: Final Discussion

## 6.1 Novel Roles for *CYCD3;1* in Arabidopsis Development & Cytokinin Signalling

---

Despite the severe effects of over-expression of *CYCD3;1* on plant development (Dewitte *et al.*, 2003), relatively little is known regarding the roles of native *CYCD3;1*. The roles of this gene are explored further in this study. As observed previously (Dewitte *et al.*, 2007), *CYCD3;1* was found to regulate final leaf cell number and petal epidermal cell size. However, the phenotypes leading to these conclusions were subtle, supporting the idea that many other regulators of the cell cycle function to coordinate cell division and cell elongation during LAO growth. Consistent with these roles, expression of *CYCD3;1* transcriptional reporters was observed in LAO primordia.

Novel roles for *CYCD3;1* in the regulation of root vascular tissue development were identified. *cycd3;1* loss-of-function mutants displayed a reduction in the number of phloem and procambium cell files in the root meristem, as well as a reduction in radial root growth during secondary thickening. Secondary thickening is driven by radial proliferation of the cambium (Miyashima *et al.*, 2013), suggesting that *CYCD3;1* regulates cambium cell divisions. It is therefore likely that *CYCD3;1* regulates radial divisions of the procambium cells and the cambium cells that derive from these. Consistent with this, expression of a *CYCD3;1* transcriptional reporter has been observed during embryogenesis (Collins *et al.*, 2012), the process during which the procambium is established. In this study, expression of *CYCD3;1* was observed within the vascular tissue of roots undergoing secondary thickening.

*cycd3;1* mutant plants appear normal at first glance (Dewitte *et al.*, 2007), but the specific mutant phenotypes characterized suggest that *CYCD3;1* is under developmental regulation. This would explain the specific localization of *CYCD3;1* expression to the LAO primordia, root vascular tissue and root tips, as opposed to expression in all dividing tissues. To identify candidate transcription factors that might regulate *CYCD3;1* expression during plant growth and development, a yeast-1-hybrid screen was undertaken. Several TCP transcription

factors bound to the *CYCD3;1* promoter. Some of these TCPs promote cell division, whilst others inhibit it (Martín-Trillo and Cubas, 2010). It is therefore likely that *CYCD3;1* is used to coordinate cell division with growth and development by TCPs. Several other transcription factors bound to the *CYCD3;1* promoter in yeast. Of particular interest was SCL5. Paralogues of this protein have been shown to regulate radial cell division events (Di Laurenzio *et al.*, 1996b) and to directly regulate the expression of another D-type cyclin gene (Cruz-Ramirez *et al.*, 2012). SCL5 might regulate radial cell division in the vascular tissue via regulation of *CYCD3;1*. If so, this would represent the first known role for SCL5.

## 6.2 Weakening the Link Between *AINTEGUMENTA* and *CYCD3;1*

---

Mizukami & Fisher (2000) showed that over-expression of *AINTEGUMENTA* (*ANT*) led to ectopic expression of *CYCD3;1*. This single result has led to the hypothesis that *ANT* regulates *CYCD3;1*, a hypothesis that has not been further tested. Since *ANT* over-expressers have prolonged windows of cell proliferation in LAO growth, it is likely that a greater number of dividing cells will cause a relative increase in *CYCD3;1* expression in the whole organ, due to the nature of the identity of those cells. Indeed, the authors of this study were using *CYCD3;1* as a marker of cell division activity, rather than testing a hypothesis that *ANT* regulates *CYCD3;1* expression. Nonetheless, it has been proposed in several articles that *ANT* regulates *CYCD3;1* (Schruff *et al.*, 2006a; Anastasiou and Lenhard, 2007; Horiguchi *et al.*, 2009). Several approaches were taken to test this hypothesis in this study. Firstly, a genetic approach was taken to investigate the functional interaction between these two genes. To the author's knowledge, no *ant cycd3;1* double loss-of-function mutant has been created to date. This might be due to the genetic linkage of the two loci, making it difficult to create such a mutant. A technique involving backcrossing was utilized to identify plants with *ant-9* and *cycd3;1* alleles on the same chromosome, leading to obtainment of the double mutant. Like *CYCD3;1*, *ANT* was shown to regulate leaf cell number, petal cell size and root secondary thickening. However, double mutants displayed additive phenotypes i.e. mutations in both genes caused phenotypes more severe than those resulting from either single mutation. This suggests that the two genes do not lie in a linear pathway regulating the processes affected in these mutants, but act at least partially independently. Agreeing with this, the

cause of increased petal epidermal cell size appeared to be different in *ant* and *cycd3;1* mutants, since the latter displayed increased ploidy levels whilst the former did not.

qPCR analyses showed that only a small change in *CYCD3;1* expression occurred in *ant* mutants, and this change was ecotype-dependent. This change might have been due to the decrease in the proportion of cells in plants undergoing cell division, rather than a consequence of a dependence of *CYCD3;1* on ANT. Nonetheless, a small change was observed, maintaining the possibility that ANT does regulate some fraction of *CYCD3;1* expression. Strengthening this possibility, a sequence showing similarity to the optimal ANT-binding sequence is present in the *CYCD3;1* promoter. However, binding of ANT to this site in yeast could not be detected in this study. Expression of a *CYCD3;1* transcriptional reporter was downregulated in *Ler ant* mutants, but this result could not be repeated in the *Col-0* ecotype, and did not agree with qPCR analyses of expression of the native *CYCD3;1* gene. It is therefore likely that the reporter used is not faithful, or that there are ecotype-specific effects perhaps involving the ERECTA kinase.

The expression domains of *ANT* and *CYCD3;1* appeared to overlap, and correlation analyses showed a relatively high correlation of expression for these two genes in roots. This is consistent with ANT regulating *CYCD3;1* expression. However, a circumstance in which the expression of *ANT* is not strongly correlated with that of *CYCD3;1* was identified in this study: when expression of *ANT* is eliminated in a loss-of-function mutant. Both *ANT* and *CYCD3;1* appeared to be regulated by cytokinins, as transgenic plants with reduced cytokinin levels displayed severe reductions in both *ANT* and *CYCD3;1* expression. This is the first example of cytokinin-induced regulators of secondary root thickening. Furthermore, the response of roots to cytokinins in terms of secondary thickening involved *CYCD3;1* on a functional level, since *cycd3;1* roots did not respond in the same manner as *WT* counterparts. The cause for a correlation between *ANT* and *CYCD3;1* expression might be coregulation by cytokinins. Perhaps both genes are regulated by type-B ARRs, making them primary cytokinin targets.

Little evidence is identified here suggesting that ANT regulates the expression of *CYCD3;1*. On the contrary, evidence is provided supporting the hypothesis that the two genes act at least partially independently. It remains possible that ANT regulates *CYCD3;1*, but if this is the case, redundant transcription factors must also regulate *CYCD3;1* in the same step of this cell

signalling pathway. Future studies would do well to take an unbiased approach to identify targets of ANT, and regulators of *CYCD3;1*. The former is essential, since no direct evidence of ANT acting as a transcription factor regulating the expression of native Arabidopsis genes has been provided.

### 6.3 Novel Roles for ERECTA in Root Radial Cell Divisions

---

Many of the phenotypes characterized in this study were altered when they were analysed in the *Ler* ecotype instead of the *Col-0* ecotype, or *vice versa*. In particular, *Ler* appeared to have several epistatic effects on root radial growth. This highlights the importance of phenotypic analyses in different ecotypes when Arabidopsis is used as a model plant. For it to be likely for the role of a gene identified in an Arabidopsis laboratory to hold true for a wild plant, it should be the case that the phenotype is consistent in different ecotypes.

The phenotype that changed dramatically in this study when analysed in *Ler* was that of the reduction in the number of phloem and procambium cell files in *cyd3* mutants. That this phenotype occurred in *Col-0* but not *Ler* led to the hypothesis that *ER*, which is mutated in *Ler*, interacts with *CYCD3s*. It was found that, like *CYCD3s*, *ER* regulated phloem and procambium cell file number. Furthermore, an *ER* transcriptional reporter was expressed in the phloem and procambium. Thus it is possible that an interaction between *ER* and *CYCD3s* is involved in the regulation of radial cell divisions in the vascular tissue. Whilst *ER* does not appear to regulate *CYCD3* expression at the transcriptional level, other mechanisms of *CYCD3* regulation by *ER* are yet to be explored. Conversely, it might be that *ER* is downstream of *CYCD3s* in the regulation of vascular cell divisions. *ER* was also found to regulate root secondary thickening. However, the *cyd3;1* mutant in the *Ler* ecotype also had a secondary root thickening phenotype. Therefore, if an interaction between *ER* and *CYCD3;1* occurs during secondary root thickening, it is not as strong as the interaction in the root meristem vascular tissue. These are the first known roles for *ER* in the regulation of root development, and should be explored further.

## 6.4 Concluding Remarks and Future Directions

---

This study aimed to test the hypothesis that ANT regulates *CYCD3;1* expression. At present, the null hypothesis that ANT does not regulate *CYCD3;1* expression must be accepted. However, novel and exciting roles for *ANT* and *CYCD3;1* in the regulation of radial growth of roots were identified. These roles might translate to their orthologues in trees. This is of great importance, since tree biomass, a source of construction material and fuel, is largely derived from this radial growth. Common consensus is that multiple D-type cyclins exist in *Arabidopsis* for control of the cell cycle in a developmental context. The novel roles for ANT, a member of the PLT clade, identified here suggest that different *PLETHORA* genes resulting from duplication events (Galinha *et al.*, 2007) are also subject to individual developmental regulation. For example, PLT1 and PLT2 integrate instructive auxin gradients in the root (Galinha *et al.*, 2007), whereas this work places ANT in the cytokinin signalling mechanism regulating root secondary thickening.

Whilst the initial hypothesis was that *ANT* and *CYCD3;1* interact, one outcome of this study has been the formulation of the hypothesis that *ER* and *CYCD3s* interact. Whether or not this is the case, *ER* was identified as another regulator of root radial growth. Thus factors fitting into three levels of canonical signalling pathways regulating cell division during growth and development were identified: a putative receptor (*ER*), a transcription factor (*ANT*) and a cell cycle regulator (*CYCD3;1*). Whilst these factors may or may not be linked, they provide starting points for studies elucidating the signalling pathways they belong to, and are likely to fit into a regulatory network regulating radial growth of roots.

# Appendix

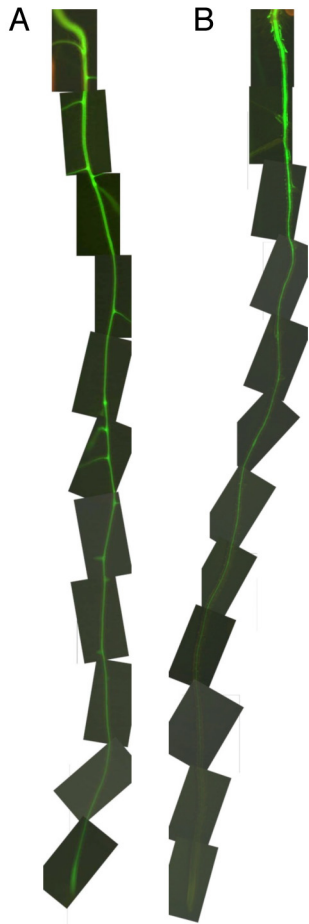


Figure 1: Expression of *ARR5* (A) and *ANT* (B) reported by *pARR5:GFP* and *pANT:GFP* reporters, respectively, in 8 DAG roots. This work was performed by Anakaisa Elo (Helsinki).

# References

- Achard, P., Gusti, A., Cheminant, S., Alioua, M., Dhondt, S., Coppens, F., Beemster, G. T. & Genschik, P.** 2009. Gibberellin Signaling Controls Cell Proliferation Rate in Arabidopsis. *Curr. Biol.* **19**: 1188-93.
- Adams, P. D., Li, X., Sellers, W. R., Baker, K. B., Leng, X., Harper, J. W., Taya, Y. & Kaelin, W. G., Jr.** 1999. Retinoblastoma Protein Contains a C-Terminal Motif That Targets It for Phosphorylation by Cyclin-Cdk Complexes. *Mol. Cell. Biol.* **19**: 1068-80.
- Aggarwal, P., Padmanabhan, B., Bhat, A., Sarvepalli, K., Sadhale, P. P. & Nath, U.** 2011. The TCP4 Transcription Factor of Arabidopsis Blocks Cell Division in Yeast at G1-->S Transition. *Biochem. Biophys. Res. Commun.* **410**: 276-81.
- Aida, M., Beis, D., Heidstra, R., Willemsen, V., Blilou, I., Galinha, C., Nussaume, L., Noh, Y.-S., Amasino, R. & Scheres, B.** 2004. The Plethora Genes Mediate Patterning of the Arabidopsis Root Stem Cell Niche. *Cell.* **119**: 109-20.
- Alonso-Blanco, C. & Koornneef, M.** 2000. Naturally Occurring Variation in Arabidopsis: An Underexploited Resource for Plant Genetics. *Trends Plant Sci.* **5**: 22-29.
- Alvarez, J. & Smyth, D. R.** 1999. Crabs Claw and Spatula, Two Arabidopsis Genes That Control Carpel Development in Parallel with Agamous. *Development.* **126**: 2377-86.
- Anastasiou, E., Kenz, S., Gerstung, M., Maclean, D., Timmer, J., Fleck, C. & Lenhard, M.** 2007. Control of Plant Organ Size by Kluh/Cyp78a5-Dependent Intercellular Signaling. *Dev. Cell.* **13**: 843-56.
- Anastasiou, E. & Lenhard, M.** 2007. Growing up to One's Standard. *Curr. Opin. Plant Biol.* **10**: 63-69.
- Autran, D., Jonak, C., Belcram, K., Beemster, G. T. S., Kronenberger, J., Grandjean, O., Inze, D. & Traas, J.** 2002. Cell Numbers and Leaf Development in Arabidopsis: A Functional Analysis of the Struwwelpeter Gene. *EMBO J.* **21**: 6036-49.
- Bartel, B.** 1997. Auxin Biosynthesis. *Annu. Rev. Plant Physiol. Plant Mol. Biol.* **48**: 51-66.
- Bartholmes, C., Hidalgo, O. & Gleissberg, S.** 2012. Evolution of the Yabby Gene Family with Emphasis on the Basal Eudicot *Eschscholzia Californica* (Papaveraceae). *Plant Biol.* **14**: 11-23.

**Bartrina, I., Otto, E., Strnad, M., Werner, T. & Schmulling, T.** 2011. Cytokinin Regulates the Activity of Reproductive Meristems, Flower Organ Size, Ovule Formation, and Thus Seed Yield in *Arabidopsis thaliana*. *Plant Cell*. **23**: 69-80.

**Baucher, M., El Jaziri, M. & Vandeputte, O.** 2007. From Primary to Secondary Growth: Origin and Development of the Vascular System. *J. Exp. Bot.* **58**: 3485-501.

**Baum, S. F., Dubrovsky, J. G. & Rost, T. L.** 2002. Apical Organization and Maturation of the Cortex and Vascular Cylinder in *Arabidopsis thaliana* (Brassicaceae) Roots. *Am. J. Bot.* **89**: 908-20.

**Beemster, G. S., Vercruyse, S., De Veylder, L., Kuiper, M. & Inzé, D.** 2006. The *Arabidopsis* Leaf as a Model System for Investigating the Role of Cell Cycle Regulation in Organ Growth. *J. Plant Res.* **119**: 43-50.

**Beemster, G. T., De Veylder, L., Vercruyse, S., West, G., Rombaut, D., Van Hummelen, P., Galichet, A., Gruitsem, W., Inze, D. & Vuylsteke, M.** 2005. Genome-Wide Analysis of Gene Expression Profiles Associated with Cell Cycle Transitions in Growing Organs of *Arabidopsis*. *Plant Physiol.* **138**: 734-43.

**Begum, S., Nakaba, S., Yamagishi, Y., Oribe, Y. & Funada, R.** 2013. Regulation of Cambial Activity in Relation to Environmental Conditions: Understanding the Role of Temperature in Wood Formation of Trees. *Physiol Plant.* **147**: 46-54.

**Belhaj, K., Chaparro-Garcia, A., Kamoun, S. & Nekrasov, V.** 2013. Plant Genome Editing Made Easy: Targeted Mutagenesis in Model and Crop Plants Using the Crispr/Cas System. *Plant Methods*. **9**: 39.

**Benkova, E., Michniewicz, M., Sauer, M., Teichmann, T., Seifertova, D., Jurgens, G. & Friml, J.** 2003. Local, Efflux-Dependent Auxin Gradients as a Common Module for Plant Organ Formation. *Cell*. **115**: 591-602.

**Berleth, T. & Jurgens, G.** 1993. The Role of the *Monopteros* Gene in Organizing the Basal Body Region of the *Arabidopsis* Embryo. *Development*. **118**: 575-87.

**Bishopp, A., Help, H., El-Showk, S., Weijers, D., Scheres, B., Friml, J., Benkova, E., Mahonen, A. P. & Helariutta, Y.** 2011a. A Mutually Inhibitory Interaction between Auxin and Cytokinin Specifies Vascular Pattern in Roots. *Curr. Biol.* **21**: 917-26.

**Bishopp, A., Lehesranta, S., Vaten, A., Help, H., El-Showk, S., Scheres, B., Helariutta, K., Mahonen, A. P., Sakakibara, H. & Helariutta, Y.** 2011b. Phloem-Transported Cytokinin Regulates Polar Auxin Transport and Maintains Vascular Pattern in the Root Meristem. *Curr. Biol.* **21**: 927-32.

**Bjorklund, S., Antti, H., Uddestrand, I., Moritz, T. & Sundberg, B.** 2007. Cross-Talk between Gibberellin and Auxin in Development of *Populus* Wood: Gibberellin Stimulates Polar Auxin Transport and Has a Common Transcriptome with Auxin. *Plant J.* **52**: 499-511.

- Bleeker, P. M., Hakvoort, H. W., Blik, M., Souer, E. & Schat, H.** 2006. Enhanced Arsenate Reduction by a Cdc25-Like Tyrosine Phosphatase Explains Increased Phytochelatin Accumulation in Arsenate-Tolerant *Holcus Lanatus*. *Plant J.* **45**: 917-29.
- Blilou, I., Xu, J., Wildwater, M., Willemsen, V., Paponov, I., Friml, J., Heidstra, R., Aida, M., Palme, K. & Scheres, B.** 2005. The Pin Auxin Efflux Facilitator Network Controls Growth and Patterning in Arabidopsis Roots. *Nature.* **433**: 39-44.
- Bowman, J.** 1993. *Arabidopsis: An Atlas of Morphology and Development*. New York, Springer.
- Bradley, D., Ratcliffe, O., Vincent, C., Carpenter, R. & Coen, E.** 1997. Inflorescence Commitment and Architecture in Arabidopsis. *Science.* **275**: 80-83.
- Brand, U., Fletcher, J. C., Hobe, M., Meyerowitz, E. M. & Simon, R.** 2000. Dependence of Stem Cell Fate in Arabidopsis on a Feedback Loop Regulated by Clv3 Activity. *Science.* **289**: 617-9.
- Broholm, S. K., Tähtiharju, S., Laitinen, R. a. E., Albert, V. A., Teeri, T. H. & Elomaa, P.** 2008. A TCP Domain Transcription Factor Controls Flower Type Specification Along the Radial Axis of the Gerbera (Asteraceae) Inflorescence. *Proc. Natl. Acad. Sci. USA.* **105**: 9117-22.
- Bundy, M. G., Thompson, O. A., Sieger, M. T. & Shpak, E. D.** 2012. Patterns of Cell Division, Cell Differentiation and Cell Elongation in Epidermis and Cortex of Arabidopsis Pedicels in the Wild Type and in Erecta. *PloS one.* **7**: e46262.
- Bürkle, L., Cedzich, A., Döpke, C., Stransky, H., Okumoto, S., Gillissen, B., Kühn, C. & Frommer, W. B.** 2003. Transport of Cytokinins Mediated by Purine Transporters of the Pup Family Expressed in Phloem, Hydathodes, and Pollen of Arabidopsis. *Plant J.* **34**: 13-26.
- Carol, R. J. & Dolan, L.** 2002. Building a Hair: Tip Growth in Arabidopsis Thaliana Root Hairs. *Philos Trans R Soc Lond B Biol Sci.* **357**: 815-21.
- Chaffey, N., Cholewa, E., Regan, S. & Sundberg, B.** 2002. Secondary Xylem Development in Arabidopsis: A Model for Wood Formation. *Physiol. Plant.* **114**: 594-600.
- Chen, F. & Bradford, K. J.** 2000. Expression of an Expansin Is Associated with Endosperm Weakening During Tomato Seed Germination. *Plant Physiol.* **124**: 1265-74.
- Cho, H. T. & Cosgrove, D. J.** 2000. Altered Expression of Expansin Modulates Leaf Growth and Pedicel Abscission in Arabidopsis Thaliana. *Proc. Natl. Acad. Sci. USA.* **97**: 9783-88.
- Ciemerych, M. A., Kenney, A. M., Sicinska, E., Kalaszczynska, I., Bronson, R. T., Rowitch, D. H., Gardner, H. & Sicinski, P.** 2002. Development of Mice Expressing a Single D-Type Cyclin. *Genes Dev.* **16**: 3277-89.

**Clough, S. J. & Bent, A. F.** 1998. Floral Dip: A Simplified Method for Agrobacterium-Mediated Transformation of *Arabidopsis Thaliana*. *Plant J.* **16**: 735-43.

**Coen, E. S. & Meyerowitz, E. M.** 1991. The War of the Whorls: Genetic Interactions Controlling Flower Development. *Nature.* **353**: 31-7.

**Collins, C., Dewitte, W. & Murray, J. A.** 2012. D-Type Cyclins Control Cell Division and Developmental Rate During *Arabidopsis* Seed Development. *J. Exp. Bot.* **63**: 3571-86.

**Cookson, S. J., Radziejowski, A. & Granier, C.** 2006. Cell and Leaf Size Plasticity in *Arabidopsis*: What Is the Role of Endoreduplication? *Plant, Cell Environ.* **29**: 1273-83.

**Corley, S. B., Carpenter, R., Copsey, L. & Coen, E.** 2005. Floral Asymmetry Involves an Interplay between TCP and Myb Transcription Factors in *Antirrhinum*. *Proc. Natl. Acad. Sci. USA.* **102**: 5068-73.

**Cruz-Ramirez, A., Diaz-Trivino, S., Blilou, I., Grieneisen, V. A., Sozzani, R., Zamioudis, C., Miskolczi, P., Nieuwland, J., Benjamins, R., Dhonukshe, P., Caballero-Perez, J., Horvath, B., Long, Y., Mahonen, A. P., Zhang, H., Xu, J., Murray, J. A., Benfey, P. N., Bako, L., Maree, A. F. & Scheres, B.** 2012. A Bistable Circuit Involving Scarecrow-Retinoblastoma Integrates Cues to Inform Asymmetric Stem Cell Division. *Cell.* **150**: 1002-15.

**Cubas, P., Lauter, N., Doebley, J. & Coen, E.** 1999. The TCP Domain: A Motif Found in Proteins Regulating Plant Growth and Development. *Plant J.* **18**: 215-22.

**Cui, H., Hao, Y., Kovtun, M., Stolc, V., Deng, X. W., Sakakibara, H. & Kojima, M.** 2011. Genome-Wide Direct Target Analysis Reveals a Role for Short-Root in Root Vascular Patterning through Cytokinin Homeostasis. *Plant Physiol.* **157**: 1221-31.

**Da Silva, E. A., Toorop, P. E., Van Lammeren, A. A. & Hilhorst, H. W.** 2008. Aba Inhibits Embryo Cell Expansion and Early Cell Division Events During Coffee (*Coffea Arabica* 'Rubi') Seed Germination. *Ann. Bot.* **102**: 425-33.

**Danisman, S., Van Dijk, A. D., Bimbo, A., Van Der Wal, F., Hennig, L., De Folter, S., Angenent, G. C. & Immink, R. G.** 2013. Analysis of Functional Redundancies within the *Arabidopsis* TCP Transcription Factor Family. *J. Exp. Bot.* **64**: 5673-85.

**De Jager, S., Scofield, S., Huntley, R., Robinson, A., Den Boer, B. W. & Murray, J. H.** 2009. Dissecting Regulatory Pathways of G1/S Control in *Arabidopsis*: Common and Distinct Targets of *Cycd3;1*, *E2fa* and *E2fc*. *Plant Mol. Biol.* **71**: 345-65.

**De Schutter, K., Joubes, J., Cools, T., Verkest, A., Corellou, F., Babiychuk, E., Van Der Schueren, E., Beeckman, T., Kushnir, S., Inze, D. & De Veylder,**

L. 2007. Arabidopsis Wee1 Kinase Controls Cell Cycle Arrest in Response to Activation of the DNA Integrity Checkpoint. *Plant Cell*. **19**: 211-25.

**De Veylder, L., Beeckman, T., Beemster, G. T. S., De Almeida Engler, J., Ormenese, S., Maes, S., Naudts, M., Van Der Schueren, E., Jacqmard, A., Engler, G. & Inzé, D.** 2002. Control of Proliferation, Endoreduplication and Differentiation by the Arabidopsis E2fa–Dpa Transcription Factor. *Embo J*. **21**: 1360-68.

**De Veylder, L., Beeckman, T. & Inze, D.** 2007. The Ins and Outs of the Plant Cell Cycle. *Nat. Rev. Mol. Cell Biol*. **8**: 655-65.

**Delgado-Benarroch, L., Causier, B., Weiss, J. & Egea-Cortines, M.** 2009. Formosa Controls Cell Division and Expansion During Floral Development in *Antirrhinum Majus*. *Planta*. **229**: 1219-29.

**Dewitte, W., Riou-Khamlichi, C., Scofield, S., Healy, J. M., Jacqmard, A., Kilby, N. J. & Murray, J. A.** 2003. Altered Cell Cycle Distribution, Hyperplasia, and Inhibited Differentiation in Arabidopsis Caused by the D-Type Cyclin *Cycd3*. *Plant Cell*. **15**: 79-92.

**Dewitte, W., Scofield, S., Alcasabas, A. A., Maughan, S. C., Menges, M., Braun, N., Collins, C., Nieuwland, J., Prinsen, E., Sundaresan, V. & Murray, J. A.** 2007. Arabidopsis *Cycd3* D-Type Cyclins Link Cell Proliferation and Endocycles and Are Rate-Limiting for Cytokinin Responses. *Proc. Natl. Acad. Sci. USA*. **104**: 14537-42.

**Dhondt, S., Coppens, F., De Winter, F., Swarup, K., Merks, R. M., Inze, D., Bennett, M. J. & Beemster, G. T.** 2010a. Short-Root and Scarecrow Regulate Leaf Growth in Arabidopsis by Stimulating S-Phase Progression of the Cell Cycle. *Plant Physiol*. **154**: 1183-95.

**Dhondt, S., Coppens, F., De Winter, F., Swarup, K., Merks, R. M., Inze, D., Bennett, M. J. & Beemster, G. T.** 2010b. Short-Root and Scarecrow Regulate Leaf Growth in Arabidopsis by Stimulating S-Phase Progression of the Cell Cycle. *Plant Physiol*. **154**: 1183-95.

**Di Lorenzo, L., Wysocka-Diller, J., Malamy, J. E., Pysh, L., Helariutta, Y., Freshour, G., Hahn, M. G., Feldmann, K. A. & Benfey, P. N.** 1996a. The Scarecrow Gene Regulates an Asymmetric Cell Division That Is Essential for Generating the Radial Organization of the Arabidopsis Root. *Cell*. **86**: 423-33.

**Di Lorenzo, L., Wysocka-Diller, J., Malamy, J. E., Pysh, L., Helariutta, Y., Freshour, G., Hahn, M. G., Feldmann, K. A. & Benfey, P. N.** 1996b. The Scarecrow Gene Regulates an Asymmetric Cell Division That Is Essential for Generating the Radial Organization of the Arabidopsis Root. *Cell*. **86**: 423-33.

**Dinh, T. T., Girke, T., Liu, X., Yant, L., Schmid, M. & Chen, X.** 2012. The Floral Homeotic Protein *Apetala2* Recognizes and Acts through an *at-Rich* Sequence Element. *Development*. **139**: 1978-86.

- Dolan, L., Janmaat, K., Willemsen, V., Linstead, P., Poethig, S., Roberts, K. & Scheres, B.** 1993. Cellular Organisation of the Arabidopsis Thaliana Root. *Development*. **119**: 71-84.
- Donnelly, P. M., Bonetta, D., Tsukaya, H., Dengler, R. E. & Dengler, N. G.** 1999. Cell Cycling and Cell Enlargement in Developing Leaves of Arabidopsis. *Dev. Biol.* **215**: 407-19.
- Douglas, S. J., Chuck, G., Dengler, R. E., Pelecanda, L. & Riggs, C. D.** 2002. Knat1 and Erecta Regulate Inflorescence Architecture in Arabidopsis. *Plant Cell*. **14**: 547-58.
- Du, J. & Groover, A.** 2010. Transcriptional Regulation of Secondary Growth and Wood Formation. *J Integr Plant Biol.* **52**: 17-27.
- Dubrovsky, J. G., Sauer, M., Napsucialy-Mendivil, S., Ivanchenko, M. G., Friml, J., Shishkova, S., Celenza, J. & Benková, E.** 2008. Auxin Acts as a Local Morphogenetic Trigger to Specify Lateral Root Founder Cells. *Proc. Natl. Acad. Sci. USA*. **105**: 8790-94.
- Dudits, D., Abraham, E., Miskolczi, P., Ayaydin, F., Bilgin, M. & Horvath, G. V.** 2011. Cell-Cycle Control as a Target for Calcium, Hormonal and Developmental Signals: The Role of Phosphorylation in the Retinoblastoma-Centred Pathway. *Ann. Bot.* **107**: 1193-202.
- Durbak, A. R. & Tax, F. E.** 2011. Clavata Signaling Pathway Receptors of Arabidopsis Regulate Cell Proliferation in Fruit Organ Formation as Well as in Meristems. *Genetics*. **189**: 177-94.
- Ecker, J. R.** 1995. The Ethylene Signal Transduction Pathway in Plants. *Science*. **268**: 667-75.
- Elliott, R. C., Betzner, A. S., Huttner, E., Oakes, M. P., Tucker, W. Q., Gerentes, D., Perez, P. & Smyth, D. R.** 1996. Aintegumenta, an Apetala2-Like Gene of Arabidopsis with Pleiotropic Roles in Ovule Development and Floral Organ Growth. *Plant Cell*. **8**: 155-68.
- Elo, A., Immanen, J., Nieminen, K. & Helariutta, Y.** 2009. Stem Cell Function During Plant Vascular Development. *Semin. Cell Dev. Biol.* **20**: 1097-106.
- Eloy, N. B., Lima, M. D., Van Damme, D., Vanhaeren, H., Gonzalez, N., De Milde, L., Hemerly, A. S., Beemster, G. T. S., Inze, D. & Ferreira, P. C. G.** 2011. The Apc/C Subunit 10 Plays an Essential Role in Cell Proliferation During Leaf Development. *Plant J.* **68**: 351-63.
- Endo, M., Nakayama, S., Umeda-Hara, C., Ohtsuki, N., Saika, H., Umeda, M. & Toki, S.** 2012. Cdkb2 Is Involved in Mitosis and DNA Damage Response in Rice. *Plant J.* **69**: 967-77.
- Etchells, J. P., Provost, C. M., Mishra, L. & Turner, S. R.** 2013. Wox4 and Wox14 Act Downstream of the Pxy Receptor Kinase to Regulate Plant Vascular

Proliferation Independently of Any Role in Vascular Organisation. *Development*. **140**: 2224-34.

**Ethells, J. P., Provost, C. M. & Turner, S. R.** 2012. Plant Vascular Cell Division Is Maintained by an Interaction between Pxy and Ethylene Signalling. *PLoS Genet*. **8**: e1002997.

**Ferjani, A., Horiguchi, G., Yano, S. & Tsukaya, H.** 2007. Analysis of Leaf Development in Fugu Mutants of Arabidopsis Reveals Three Compensation Modes That Modulate Cell Expansion in Determinate Organs. *Plant Physiol*. **144**: 988-99.

**Fisher, D. L. & Nurse, P.** 1996. A Single Fission Yeast Mitotic Cyclin B P34cdc2 Kinase Promotes Both S-Phase and Mitosis in the Absence of G1 Cyclins. *EMBO J*. **15**: 850-60.

**Fisher, K. & Turner, S.** 2007. Pxy, a Receptor-Like Kinase Essential for Maintaining Polarity During Plant Vascular-Tissue Development. *Curr. Biol*. **17**: 1061-6.

**Fobert, P. R., Gaudin, V., Lunness, P., Coen, E. S. & Doonan, J. H.** 1996. Distinct Classes of Cdc2-Related Genes Are Differentially Expressed During the Cell Division Cycle in Plants. *Plant Cell*. **8**: 1465-76.

**Forzani, C., Aichinger, E., Sornay, E., Willemsen, V., Laux, T., Dewitte, W. & Murray, J. A.** 2014. Wox5 Suppresses Cyclin D Activity to Establish Quiescence at the Center of the Root Stem Cell Niche. *Curr. Biol*. **24**: 1939-44.

**Fosket, D. E.** 1994. *Plant Growth and Development - a Molecular Approach*. London, Academic Press, Inc.

**Friml, J., Benková, E., Blilou, I., Wisniewska, J., Hamann, T., Ljung, K., Woody, S., Sandberg, G., Scheres, B., Jürgens, G. & Palme, K.** 2002. Atpin4 Mediates Sink-Driven Auxin Gradients and Root Patterning in Arabidopsis. *Cell*. **108**: 661-73.

**Friml, J., Vieten, A., Sauer, M., Weijers, D., Schwarz, H., Hamann, T., Offringa, R. & Jurgens, G.** 2003. Efflux-Dependent Auxin Gradients Establish the Apical-Basal Axis of Arabidopsis. *Nature*. **426**: 147-53.

**Fujikura, U., Horiguchi, G. & Tsukaya, H.** 2007. Dissection of Enhanced Cell Expansion Processes in Leaves Triggered by a Defect in Cell Proliferation, with Reference to Roles of Endoreduplication. *Plant Cell Physiol*. **48**: 278-86.

**Galigniana, M. D., Scruggs, J. L., Herrington, J., Welsh, M. J., Carter-Su, C., Housley, P. R. & Pratt, W. B.** 1998. Heat Shock Protein 90-Dependent (Geldanamycin-Inhibited) Movement of the Glucocorticoid Receptor through the Cytoplasm to the Nucleus Requires Intact Cytoskeleton. *Molecular Endocrinology*. **12**: 1903-13.

- Galinha, C., Hofhuis, H., Luijten, M., Willemsen, V., Blilou, I., Heidstra, R. & Scheres, B.** 2007. Plethora Proteins as Dose-Dependent Master Regulators of Arabidopsis Root Development. *Nature*. **449**: 1053-57.
- Galitski, T., Saldanha, A. J., Styles, C. A., Lander, E. S. & Fink, G. R.** 1999. Ploidy Regulation of Gene Expression. *Science*. **285**: 251-54.
- Gallagher, K. L., Paquette, A. J., Nakajima, K. & Benfey, P. N.** 2004. Mechanisms Regulating Short-Root Intercellular Movement. *Curr. Biol.* **14**: 1847-51.
- Galweiler, L., Guan, C., Muller, A., Wisman, E., Mendgen, K., Yephremov, A. & Palme, K.** 1998. Regulation of Polar Auxin Transport by Atpin1 in Arabidopsis Vascular Tissue. *Science*. **282**: 2226-30.
- Gan, S. & Amasino, R. M.** 1995. Inhibition of Leaf Senescence by Autoregulated Production of Cytokinin. *Science*. **270**: 1986-88.
- Gendreau, E., Orbovic, V., Höfte, H. & Traas, J.** 1999. Gibberellin and Ethylene Control Endoreduplication Levels in the Arabidopsis Thaliana Hypocotyl. *Planta*. **209**: 513-16.
- Gendreau, E., Traas, J., Desnos, T., Grandjean, O., Caboche, M. & Hofte, H.** 1997. Cellular Basis of Hypocotyl Growth in Arabidopsis Thaliana. *Plant Physiol.* **114**: 295-305.
- Goldberg, R. B., De Paiva, G. & Yadegari, R.** 1994. Plant Embryogenesis: Zygote to Seed. *Science*. **266**: 605-14.
- Gong, W., He, K., Covington, M., Dinesh-Kumar, S. P., Snyder, M., Harmer, S. L., Zhu, Y. X. & Deng, X. W.** 2008. The Development of Protein Microarrays and Their Applications in DNA-Protein and Protein-Protein Interaction Analyses of Arabidopsis Transcription Factors. *Mol Plant.* **1**: 27-41.
- Gonzalez, N., Vanhaeren, H. & Inze, D.** 2012. Leaf Size Control: Complex Coordination of Cell Division and Expansion. *Trends Plant Sci.* **17**: 332-40.
- Gonzalez-Garcia, M. P., Vilarrasa-Blasi, J., Zhiponova, M., Divol, F., Mora-Garcia, S., Russinova, E. & Cano-Delgado, A. I.** 2011. Brassinosteroids Control Meristem Size by Promoting Cell Cycle Progression in Arabidopsis Roots. *Development*. **138**: 849-59.
- Gopfert, U., Kullmann, M. & Hengst, L.** 2003. Cell Cycle-Dependent Translation of P27 Involves a Responsive Element in Its 5'-Utr That Overlaps with a Uorf. *Hum. Mol. Genet.* **12**: 1767-79.
- Gray, R. A.** 1957. Alteration of Leaf Size and Shape and Other Changes Caused by Gibberellins in Plants. *Am. J. Bot.* **44**: 674-82.
- Groover, A. & Robischon, M.** 2006. Developmental Mechanisms Regulating Secondary Growth in Woody Plants. *Curr Opin Plant Biol.* **9**: 55-58.

- Groover, A. & Spicer, R.** 2010. Evolution of Development of Vascular Cambia and Secondary Growth. *New Phytol.* **186**: 577-92.
- Gupta, S. & Rashotte, A. M.** 2012. Down-Stream Components of Cytokinin Signaling and the Role of Cytokinin Throughout the Plant. *Plant Cell Rep.* **31**: 801-12.
- Gusti, A., Baumberger, N., Nowack, M., Pusch, S., Eisler, H., Potuschak, T., De Veylder, L., Schnittger, A. & Genschik, P.** 2009. The Arabidopsis Thaliana F-Box Protein Fbl17 Is Essential for Progression through the Second Mitosis During Pollen Development. *PLoS One.* **4**: e4780.
- Harashima, H., Dissmeyer, N. & Schnittger, A.** 2013. Cell Cycle Control across the Eukaryotic Kingdom. *Trends Cell Biol.* **23**: 345-56.
- Hardtke, C. S. & Berleth, T.** 1998. The Arabidopsis Gene *Monopteros* Encodes a Transcription Factor Mediating Embryo Axis Formation and Vascular Development. *EMBO J.* **17**: 1405-11.
- Hase, Y., Fujioka, S., Yoshida, S., Sun, G., Umeda, M. & Tanaka, A.** 2005. Ectopic Endoreduplication Caused by Sterol Alteration Results in Serrated Petals in Arabidopsis. *J. Exp. Bot.* **56**: 1263-68.
- Heinisch, J. J., Lorberg, A., Schmitz, H. P. & Jacoby, J. J.** 1999. The Protein Kinase C-Mediated Map Kinase Pathway Involved in the Maintenance of Cellular Integrity in *Saccharomyces Cerevisiae*. *Mol. Microbiol.* **32**: 671-80.
- Heisler, M. G., Ohno, C., Das, P., Sieber, P., Reddy, G. V., Long, J. A. & Meyerowitz, E. M.** 2005. Patterns of Auxin Transport and Gene Expression During Primordium Development Revealed by Live Imaging of the Arabidopsis Inflorescence Meristem. *Curr. Biol.* **15**: 1899-911.
- Hejatko, J., Ryu, H., Kim, G.-T., Dobešová, R., Choi, S., Choi, S. M., Souček, P., Horák, J., Pekárova, B., Palme, K., Brzobohaty, B. & Hwang, I.** 2009. The Histidine Kinases Cytokinin-Independent1 and Arabidopsis Histidine Kinase2 and 3 Regulate Vascular Tissue Development in Arabidopsis Shoots. *Plant Cell.* **21**: 2008-21.
- Hejatko, J., Ryu, H., Kim, G. T., Dobesova, R., Choi, S., Choi, S. M., Soucek, P., Horak, J., Pekarova, B., Palme, K., Brzobohaty, B. & Hwang, I.** 2009. The Histidine Kinases Cytokinin-Independent1 and Arabidopsis Histidine Kinase2 and 3 Regulate Vascular Tissue Development in Arabidopsis Shoots. *Plant Cell.* **21**: 2008-21.
- Helariutta, Y., Fukaki, H., Wysocka-Diller, J., Nakajima, K., Jung, J., Sena, G., Hauser, M. T. & Benfey, P. N.** 2000. The Short-Root Gene Controls Radial Patterning of the Arabidopsis Root through Radial Signaling. *Cell.* **101**: 555-67.
- Help, H., Mahonen, A. P., Helariutta, Y. & Bishopp, A.** 2011. Bisymmetry in the Embryonic Root Is Dependent on Cotyledon Number and Position. *Plant Signal Behav.* **6**: 1837-40.

**Hirakawa, Y., Shinohara, H., Kondo, Y., Inoue, A., Nakanomyo, I., Ogawa, M., Sawa, S., Ohashi-Ito, K., Matsubayashi, Y. & Fukuda, H.** 2008. Non-Cell-Autonomous Control of Vascular Stem Cell Fate by a Cle Peptide/Receptor System. *Proc. Natl. Acad. Sci. USA.* **105**: 15208-13.

**Hirose, N., Takei, K., Kuroha, T., Kamada-Nobusada, T., Hayashi, H. & Sakakibara, H.** 2008. Regulation of Cytokinin Biosynthesis, Compartmentalization and Translocation. *J. Exp. Bot.* **59**: 75-83.

**Hofhuis, H., Laskowski, M., Du, Y., Prasad, K., Grigg, S., Pinon, V. & Scheres, B.** 2014. Phyllotaxis and Rhizotaxis in Arabidopsis Are Modified by Three *Plethora* Transcription Factors. *Curr. Biol.* **23**: 956-62.

**Holst, K., Schmulling, T. & Werner, T.** 2011. Enhanced Cytokinin Degradation in Leaf Primordia of Transgenic Arabidopsis Plants Reduces Leaf Size and Shoot Organ Primordia Formation. *J. Plant Physiol.* **168**: 1328-34.

**Horiguchi, G., Gonzalez, N., Beemster, G. T., Inze, D. & Tsukaya, H.** 2009. Impact of Segmental Chromosomal Duplications on Leaf Size in the *Grandifolia*-D Mutants of Arabidopsis Thaliana. *Plant J.* **60**: 122-33.

**Horiguchi, G. & Tsukaya, H.** 2011. Organ Size Regulation in Plants: Insights from Compensation. *Front Plant Sci.* **2**: 24.

**Horvath, B. M., Magyar, Z., Zhang, Y., Hamburger, A. W., Bako, L., Visser, R. G., Bachem, C. W. & Bogre, L.** 2006. Ebp1 Regulates Organ Size through Cell Growth and Proliferation in Plants. *EMBO J.* **25**: 4909-20.

**Hou, B., Lim, E.-K., Higgins, G. S. & Bowles, D. J.** 2004. N-Glucosylation of Cytokinins by Glycosyltransferases of Arabidopsis Thaliana. *J. Biol. Chem.* **279**: 47822-32.

**Hu, Y., Bao, F. & Li, J.** 2000. Promotive Effect of Brassinosteroids on Cell Division Involves a Distinct *Cycd3*-Induction Pathway in Arabidopsis. *Plant J.* **24**: 693-701.

**Hu, Y., Poh, H. M. & Chua, N. H.** 2006. The Arabidopsis Argos-Like Gene Regulates Cell Expansion During Organ Growth (Vol 47, Pg 1, 2006). *Plant J.* **47**: 490-90.

**Hu, Y., Xie, Q. & Chua, N. H.** 2003. The Arabidopsis Auxin-Inducible Gene Argos Controls Lateral Organ Size. *Plant Cell.* **15**: 1951-61.

**Huang, H., Tudor, M., Weiss, C. A., Hu, Y. & Ma, H.** 1995. The Arabidopsis MADS-Box Gene *Agl3* Is Widely Expressed and Encodes a Sequence-Specific DNA-Binding Protein. *Plant Mol. Biol.* **28**: 549-67.

**Hulskamp, M., Misera, S. & Jurgens, G.** 1994. Genetic Dissection of Trichome Cell-Development in Arabidopsis. *Cell.* **76**: 555-66.

**Hutchison, C. E., Li, J., Argueso, C., Gonzalez, M., Lee, E., Lewis, M. W., Maxwell, B. B., Perdue, T. D., Schaller, G. E., Alonso, J. M., Ecker, J. R. &**

- Kieber, J. J.** 2006. The Arabidopsis Histidine Phosphotransfer Proteins Are Redundant Positive Regulators of Cytokinin Signaling. *Plant Cell*. **18**: 3073-87.
- Hwang, I., Chen, H. C. & Sheen, J.** 2002. Two-Component Signal Transduction Pathways in Arabidopsis. *Plant Physiol*. **129**: 500-15.
- Imai, K. K., Ohashi, Y., Tsuge, T., Yoshizumi, T., Matsui, M., Oka, A. & Aoyama, T.** 2006. The  $\alpha$ -Type Cyclin *Cyca2;3* Is a Key Regulator of Ploidy Levels in Arabidopsis Endoreduplication. *Plant Cell*. **18**: 382-96.
- Inoue, T., Higuchi, M., Hashimoto, Y., Seki, M., Kobayashi, M., Kato, T., Tabata, S., Shinozaki, K. & Kakimoto, T.** 2001. Identification of *Cre1* as a Cytokinin Receptor from Arabidopsis. *Nature*. **409**: 1060-3.
- Inze, D.** 2008. *Cell Cycle Control and Plant Development*. Blackwell Publishing.
- Irish, V. F. & Litt, A.** 2005. Flower Development and Evolution: Gene Duplication, Diversification and Redeployment. *Curr. Opin. Genet. Dev.* **15**: 454-60.
- Ito, Y., Nakanomyo, I., Motose, H., Iwamoto, K., Sawa, S., Dohmae, N. & Fukuda, H.** 2006. Dodeca-Cle Peptides as Suppressors of Plant Stem Cell Differentiation. *Science*. **313**: 842-5.
- Iwakawa, H., Shinmyo, A. & Sekine, M.** 2006. Arabidopsis *Cdka;1*, a *Cdc2* Homologue, Controls Proliferation of Generative Cells in Male Gametogenesis. *Plant J.* **45**: 819-31.
- Ji, J., Strable, J., Shimizu, R., Koenig, D., Sinha, N. & Scanlon, M. J.** 2010. *Wox4* Promotes Procambial Development. *Plant Physiol*. **152**: 1346-56.
- Jin, S.-H., Ma, X.-M., Kojima, M., Sakakibara, H., Wang, Y.-W. & Hou, B.-K.** 2013. Overexpression of Glucosyltransferase *Ugt85a1* Influences Trans-Zeatin Homeostasis and Trans-Zeatin Responses Likely through O-Glucosylation. *Planta*. **237**: 991-99.
- Jofuku, K. D., Denboer, B. G. W., Vanmontagu, M. & Okamoto, J. K.** 1994. Control of Arabidopsis Flower and Seed Development by the Homeotic Gene *Apetala2*. *Plant Cell*. **6**: 1211-25.
- Karimi, M., Inze, D. & Depicker, A.** 2002. Gateway Vectors for Agrobacterium-Mediated Plant Transformation. *Trends Plant Sci.* **7**: 193-5.
- Karlberg, A., Bako, L. & Bhalerao, R. P.** 2011. Short Day-Mediated Cessation of Growth Requires the Downregulation of *Aintegumentalike1* Transcription Factor in Hybrid Aspen. *PLoS Genet.* **7**: e1002361.
- Kidner, C., Sundaresan, V., Roberts, K. & Dolan, L.** 2000. Clonal Analysis of the Arabidopsis Root Confirms That Position, Not Lineage, Determines Cell Fate. *Planta*. **211**: 191-9.

- Kieffer, M., Master, V., Waites, R. & Davies, B.** 2011. TCP14 and TCP15 Affect Internode Length and Leaf Shape in Arabidopsis. *Plant J.* **68**: 147-58.
- Kim, S., Soltis, P. S., Wall, K. & Soltis, D. E.** 2006. Phylogeny and Domain Evolution in the *Apetala2*-Like Gene Family. *Mol. Biol. Evol.* **23**: 107-20.
- Klucher, K. M., Chow, H., Reiser, L. & Fischer, R. L.** 1996. The *Aintegumenta* Gene of Arabidopsis Required for Ovule and Female Gametophyte Development Is Related to the Floral Homeotic Gene *Apetala2*. *Plant Cell.* **8**: 137-53.
- Kondorosi, E., Roudier, F. & Gendreau, E.** 2000. Plant Cell-Size Control: Growing by Ploidy? *Curr. Opin. Plant Biol.* **3**: 488-92.
- Koornneef, M. & Meinke, D.** 2010. The Development of Arabidopsis as a Model Plant. *Plant J.* **61**: 909-21.
- Kosugi, S. & Ohashi, Y.** 2002. DNA Binding and Dimerization Specificity and Potential Targets for the TCP Protein Family. *Plant J.* **30**: 337-48.
- Koyama, T., Furutani, M., Tasaka, M. & Ohme-Takagi, M.** 2007. TCP Transcription Factors Control the Morphology of Shoot Lateral Organs Via Negative Regulation of the Expression of Boundary-Specific Genes in Arabidopsis. *Plant Cell.* **19**: 473-84.
- Koyama, T., Mitsuda, N., Seki, M., Shinozaki, K. & Ohme-Takagi, M.** 2010. TCP Transcription Factors Regulate the Activities of *Asymmetric Leaves1* and *Mir164*, as Well as the Auxin Response, During Differentiation of Leaves in Arabidopsis. *Plant Cell.* **22**: 3574-88.
- Kramer, E. M.** 2004. Pin and Aux/Lax Proteins: Their Role in Auxin Accumulation. *Trends Plant Sci.* **9**: 578-82.
- Krizek, B. A.** 1999. Ectopic Expression of *Aintegumenta* in Arabidopsis Plants Results in Increased Growth of Floral Organs. *Dev. Genet.* **25**: 224-36.
- Krizek, B. A.** 2003. *Aintegumenta* Utilizes a Mode of DNA Recognition Distinct from That Used by Proteins Containing a Single Ap2 Domain. *Nucleic Acids Res.* **31**: 1859-68.
- Krizek, B. A.** 2009. *Aintegumenta* and *Aintegumenta-Like6* Act Redundantly to Regulate Arabidopsis Floral Growth and Patterning. *Plant Physiol.* **150**: 1916-29.
- Krizek, B. A.** 2011a. *Aintegumenta* and *Aintegumenta-Like6* Regulate Auxin-Mediated Flower Development in Arabidopsis. *BMC research notes.* **4**: 176.
- Krizek, B. A.** 2011b. Auxin Regulation of Arabidopsis Flower Development Involves Members of the *Aintegumenta-Like/Plethora (Ail/Plt)* Family. *J. Exp. Bot.* **62**: 3311-19.
- Krizek, B. A., Prost, V. & Macias, A.** 2000. *Aintegumenta* Promotes Petal Identity and Acts as a Negative Regulator of *Agamous*. *Plant Cell.* **12**: 1357-66.

- Krizek, B. A. & Sulli, C.** 2006. Mapping Sequences Required for Nuclear Localization and the Transcriptional Activation Function of the Arabidopsis Protein Aintegumenta. *Planta*. **224**: 612-21.
- Larkins, B. A., Dilkes, B. P., Dante, R. A., Coelho, C. M., Woo, Y. M. & Liu, Y.** 2001. Investigating the Hows and Whys of DNA Endoreduplication. *J. Exp. Bot.* **52**: 183-92.
- Laux, T., Mayer, K. F., Berger, J. & Jurgens, G.** 1996. The Wuschel Gene Is Required for Shoot and Floral Meristem Integrity in Arabidopsis. *Development*. **122**: 87-96.
- Lee, H. S. & Chen, Z. J.** 2001. Protein-Coding Genes Are Epigenetically Regulated in Arabidopsis Polyploids. *Proc. Natl. Acad. Sci. USA*. **98**: 6753-58.
- Lens, F., Smets, E. & Melzer, S.** 2012. Stem Anatomy Supports Arabidopsis Thaliana as a Model for Insular Woodiness. *New Phytologist*. **193**: 12-17.
- Leyser, O. & Day, S.** 2007. *Mechanisms in Plant Development*. Blackwell Publishing.
- Li, Z., Li, B., Shen, W.-H., Huang, H. & Dong, A.** 2012a. TCP Transcription Factors Interact with As2 in the Repression of Class-I Knox Genes in Arabidopsis Thaliana. *Plant J.* **71**: 99-107.
- Li, Z.-Y., Li, B. & Dong, A.-W.** 2012b. The Arabidopsis Transcription Factor AtTCP15 Regulates Endoreduplication by Modulating Expression of Key Cell-Cycle Genes. *Mol Plant*. **5**: 270-80.
- Liu, C., Thong, Z. & Yu, H.** 2009. Coming into Bloom: The Specification of Floral Meristems. *Development*. **136**: 3379-91.
- Liu, C., Xu, Z. & Chua, N. H.** 1993. Auxin Polar Transport Is Essential for the Establishment of Bilateral Symmetry During Early Plant Embryogenesis. *Plant Cell*. **5**: 621-30.
- Liu, D. F., Liu, X. J., Meng, Y. L., Sun, C. H., Tang, H. S., Jiang, Y. D., Khan, M. A., Xue, J. Q., Ma, N. & Gao, J. P.** 2013. An Organ-Specific Role for Ethylene in Rose Petal Expansion During Dehydration and Rehydration. *J. Exp. Bot.* **64**: 2333-44.
- Lloyd, A. M., Schena, M., Walbot, V. & Davis, R. W.** 1994. Epidermal Cell Fate Determination in Arabidopsis: Patterns Defined by a Steroid-Inducible Regulator. *Science*. **266**: 436-9.
- Magyar, Z., Horváth, B., Khan, S., Mohammed, B., Henriques, R., De Veylder, L., Bakó, L., Scheres, B. & Bögre, L.** 2012. Arabidopsis E2fa Stimulates Proliferation and Endocycle Separately through Rbr-Bound and Rbr-Free Complexes. *EMBO J.* **31**: 1480-93.

- Mahonen, A. P., Bishopp, A., Higuchi, M., Nieminen, K. M., Kinoshita, K., Tormakangas, K., Ikeda, Y., Oka, A., Kakimoto, T. & Helariutta, Y.** 2006a. Cytokinin Signaling and Its Inhibitor Ahp6 Regulate Cell Fate During Vascular Development. *Science*. **311**: 94-8.
- Mahonen, A. P., Bonke, M., Kauppinen, L., Riikonen, M., Benfey, P. N. & Helariutta, Y.** 2000. A Novel Two-Component Hybrid Molecule Regulates Vascular Morphogenesis of the Arabidopsis Root. *Genes Dev*. **14**: 2938-43.
- Mahonen, A. P., Higuchi, M., Tormakangas, K., Miyawaki, K., Pischke, M. S., Sussman, M. R., Helariutta, Y. & Kakimoto, T.** 2006b. Cytokinins Regulate a Bidirectional Phosphorelay Network in Arabidopsis. *Curr. Biol*. **16**: 1116-22.
- Malamy, J. E. & Benfey, P. N.** 1997. Organization and Cell Differentiation in Lateral Roots of Arabidopsis Thaliana. *Development*. **124**: 33-44.
- Mariconti, L., Pellegrini, B., Cantoni, R., Stevens, R., Bergounioux, C., Cella, R. & Albani, D.** 2002. The E2f Family of Transcription Factors from Arabidopsis Thaliana. Novel and Conserved Components of the Retinoblastoma/E2f Pathway in Plants. *J. Biol. Chem*. **277**: 9911-9.
- Martín-Trillo, M. & Cubas, P.** 2010. TCP Genes: A Family Snapshot Ten Years Later. *Trends Plant Sci*. **15**: 31-39.
- Masle, J., Gilmore, S. R. & Farquhar, G. D.** 2005. The Erecta Gene Regulates Plant Transpiration Efficiency in Arabidopsis. *Nature*. **436**: 866-70.
- Masubelele, N. H., Dewitte, W., Menges, M., Maughan, S., Collins, C., Huntley, R., Nieuwland, J., Scofield, S. & Murray, J. A.** 2005a. D-Type Cyclins Activate Division in the Root Apex to Promote Seed Germination in Arabidopsis. *Proc. Natl. Acad. Sci. USA*. **102**: 15694-9.
- Masubelele, N. H., Dewitte, W., Menges, M., Maughan, S., Collins, C., Huntley, R., Nieuwland, J., Scofield, S. & Murray, J. a. H.** 2005b. D-Type Cyclins Activate Division in the Root Apex to Promote Seed Germination in Arabidopsis. *Proceedings of the National Academy of Sciences of the United States of America*. **102**: 15694-99.
- Matsumoto-Kitano, M., Kusumoto, T., Tarkowski, P., Kinoshita-Tsujimura, K., Vaclavikova, K., Miyawaki, K. & Kakimoto, T.** 2008. Cytokinins Are Central Regulators of Cambial Activity. *Proc. Natl. Acad. Sci. USA*. **105**: 20027-31.
- Mazur, E. & Kurczynska, E.** 2012. Rays, Intrusive Growth, and Storied Cambium in the Inflorescence Stems of Arabidopsis Thaliana (L.) Heynh. *Protoplasma*. **249**: 217-20.
- Mazzoni, C., Zarov, P., Rambourg, A. & Mann, C.** 1993. The Slit2 (Mpk1) Map Kinase Homolog Is Involved in Polarized Cell Growth in Saccharomyces Cerevisiae. *J. Cell Biol*. **123**: 1821-33.
- Mcgowan, C. H. & Russell, P.** 1993. Human Wee1 Kinase Inhibits Cell Division by Phosphorylating P34cdc2 Exclusively on Tyr15. *EMBO J*. **12**: 75-85.

- Medenbach, J., Seiler, M. & Hentze, M. W.** 2011. Translational Control Via Protein-Regulated Upstream Open Reading Frames. *Cell*. **145**: 902-13.
- Menges, M., De Jager, S. M., Gruissem, W. & Murray, J. A.** 2005. Global Analysis of the Core Cell Cycle Regulators of Arabidopsis Identifies Novel Genes, Reveals Multiple and Highly Specific Profiles of Expression and Provides a Coherent Model for Plant Cell Cycle Control. *Plant J*. **41**: 546-66.
- Menges, M., Pavesi, G., Morandini, P., Bogre, L. & Murray, J. A.** 2007. Genomic Organization and Evolutionary Conservation of Plant D-Type Cyclins. *Plant Physiol*. **145**: 1558-76.
- Menges, M., Samland, A. K., Planchais, S. & Murray, J. A.** 2006. The D-Type Cyclin *Cycd3;1* Is Limiting for the G1-to-S-Phase Transition in Arabidopsis. *Plant Cell*. **18**: 893-906.
- Miyashima, S., Sebastian, J., Lee, J. Y. & Helariutta, Y.** 2013. Stem Cell Function During Plant Vascular Development. *EMBO J*. **32**: 178-93.
- Mizukami, Y.** 2001. A Matter of Size: Developmental Control of Organ Size in Plants. *Curr. Opin. Plant Biol*. **4**: 533-39.
- Mizukami, Y. & Fischer, R. L.** 2000. Plant Organ Size Control: Aintegumenta Regulates Growth and Cell Numbers During Organogenesis. *Proc. Natl. Acad. Sci. USA*. **97**: 942-7.
- Moller, B. & Weijers, D.** 2009. Auxin Control of Embryo Patterning. *Cold Spring Harb Perspect Biol*. **1**: a001545.
- Mudunkothge, J. S. & Krizek, B. A.** 2012a. Three Arabidopsis *Ail/Plt* Genes Act in Combination to Regulate Shoot Apical Meristem Function. *Plant J*. **71**: 108-21.
- Mudunkothge, J. S. & Krizek, B. A.** 2012b. Three Arabidopsis *Ail/Plt* Genes Act in Combination to Regulate Shoot Apical Meristem Function. *Plant J*. **71**: 108-21.
- Muller, B. & Sheen, J.** 2008. Cytokinin and Auxin Interaction in Root Stem-Cell Specification During Early Embryogenesis. *Nature*. **453**: 1094-7.
- Murray, A. W.** 2004. Recycling the Cell Cycle: Cyclins Revisited. *Cell*. **116**: 221-34.
- Nag, A., King, S. & Jack, T.** 2009. *Mir319a* Targeting of *TCP4* Is Critical for Petal Growth and Development in Arabidopsis. *Proc Natl Acad Sci U S A*. **106**: 22534-9.
- Nakamura, M., Katsumata, H., Abe, M., Yabe, N., Komeda, Y., Yamamoto, K. T. & Takahashi, T.** 2006. Characterization of the Class Iv Homeodomain-Leucine Zipper Gene Family in Arabidopsis. *Plant Physiol*. **141**: 1363-75.

- Nakano, T., Suzuki, K., Fujimura, T. & Shinshi, H.** 2006. Genome-Wide Analysis of the Erf Gene Family in Arabidopsis and Rice. *Plant Physiol.* **140**: 411-32.
- Nakaya, M., Tsukaya, H., Murakami, N. & Kato, M.** 2002. Brassinosteroids Control the Proliferation of Leaf Cells of Arabidopsis Thaliana. *Plant Cell Physiol.* **43**: 239-44.
- Navaud, O., Dabos, P., Carnus, E., Tremousaygue, D. & Hervé, C.** 2007. TCP Transcription Factors Predate the Emergence of Land Plants. *J. Mol. Evol.* **65**: 23-33.
- Neuhaus, G.** 2013. The Tissues of Vascular Plants. *Strasburger's Plant Sciences*. Springer Berlin Heidelberg.
- Nieminen, K., Immanen, J., Laxell, M., Kauppinen, L., Tarkowski, P., Dolezal, K., Tahtiharju, S., Elo, A., Decourteix, M., Ljung, K., Bhalerao, R., Keinonen, K., Albert, V. A. & Helariutta, Y.** 2008. Cytokinin Signaling Regulates Cambial Development in Poplar. *Proc. Natl. Acad. Sci. USA.* **105**: 20032-7.
- Nieminen, K. M., Kauppinen, L. & Helariutta, Y.** 2004. A Weed for Wood? Arabidopsis as a Genetic Model for Xylem Development. *Plant Physiol.* **135**: 653-9.
- Nieuwland, J., Maughan, S., Dewitte, W., Scofield, S., Sanz, L. & Murray, J. A.** 2009. The D-Type Cyclin Cycd4;1 Modulates Lateral Root Density in Arabidopsis by Affecting the Basal Meristem Region. *Proc. Natl. Acad. Sci. USA.* **106**: 22528-33.
- Nilsson, I. & Hoffmann, I.** 2000. Cell Cycle Regulation by the Cdc25 Phosphatase Family. *Prog Cell Cycle Res.* **4**: 107-14.
- Nilsson, J., Karlberg, A., Antti, H., Lopez-Vernaza, M., Mellerowicz, E., Perrot-Rechenmann, C., Sandberg, G. & Bhalerao, R. P.** 2008a. Dissecting the Molecular Basis of the Regulation of Wood Formation by Auxin in Hybrid Aspen. *Plant Cell.* **20**: 843-55.
- Nilsson, J., Karlberg, A., Antti, H., Lopez-Vernaza, M., Mellerowicz, E., Perrot-Rechenmann, C., Sandberg, G. & Bhalerao, R. P.** 2008b. Dissecting the Molecular Basis of the Regulation of Wood Formation by Auxin in Hybrid Aspen. *Plant Cell.* **20**: 843-55.
- Nishimura, T., Wada, T., Yamamoto, K. T. & Okada, K.** 2005a. The Arabidopsis Stv1 Protein, Responsible for Translation Reinitiation, Is Required for Auxin-Mediated Gynoecium Patterning. *Plant Cell.* **17**: 2940-53.
- Nishimura, T., Wada, T., Yamamoto, K. T. & Okada, K.** 2005b. The Arabidopsis Stv1 Protein, Responsible for Translation Reinitiation, Is Required for Auxin-Mediated Gynoecium Patterning. *Plant Cell.* **17**: 2940-53.

- Nole-Wilson, S. & Krizek, B. A.** 2000. DNA Binding Properties of the Arabidopsis Floral Development Protein Aintegumenta. *Nucleic Acids Res.* **28**: 4076-82.
- Nole-Wilson, S. & Krizek, B. A.** 2006. Aintegumenta Contributes to Organ Polarity and Regulates Growth of Lateral Organs in Combination with Yabby Genes. *Plant Physiol.* **141**: 977-87.
- Nole-Wilson, S., Tranby, T. L. & Krizek, B. A.** 2005. Aintegumenta-Like (Ail) Genes Are Expressed in Young Tissues and May Specify Meristematic or Division-Competent States. *Plant Mol. Biol.* **57**: 613-28.
- Novaes, E., Kirst, M., Chiang, V., Winter-Sederoff, H. & Sederoff, R.** 2010. Lignin and Biomass: A Negative Correlation for Wood Formation and Lignin Content in Trees. *Plant Physiol.* **154**: 555-61.
- Nowack, M. K., Harashima, H., Dissmeyer, N., Zhao, X., Bouyer, D., Weimer, A. K., De Winter, F., Yang, F. & Schnittger, A.** 2012. Genetic Framework of Cyclin-Dependent Kinase Function in Arabidopsis. *Dev. Cell.* **22**: 1030-40.
- Oakenfull, E. A., Riou-Khamlichi, C. & Murray, J. A.** 2002. Plant D-Type Cyclins and the Control of G1 Progression. *Philos Trans R Soc Lond B Biol Sci.* **357**: 749-60.
- Ohashi-Ito, K., Oguchi, M., Kojima, M., Sakakibara, H. & Fukuda, H.** 2013. Auxin-Associated Initiation of Vascular Cell Differentiation by Lonesome Highway. *Development.* **140**: 765-9.
- Palauqui, J. C. & Laufs, P.** 2011. Phyllotaxis: In Search of the Golden Angle. *Curr. Biol.* **21**: R502-4.
- Paravicini, G., Cooper, M., Friedli, L., Smith, D. J., Carpentier, J. L., Klig, L. S. & Payton, M. A.** 1992. The Osmotic Integrity of the Yeast Cell Requires a Functional Pkc1 Gene Product. *Mol. Cell. Biol.* **12**: 4896-905.
- Pauly, M. & Keegstra, K.** 2008. Cell-Wall Carbohydrates and Their Modification as a Resource for Biofuels. *Plant J.* **54**: 559-68.
- Petricka, J. J., Winter, C. M. & Benfey, P. N.** 2012. Control of Arabidopsis Root Development. *Annu. Rev. Plant Biol.* **63**: 563-90.
- Pien, S., Wyrzykowska, J., Mcqueen-Mason, S., Smart, C. & Fleming, A.** 2001. Local Expression of Expansin Induces the Entire Process of Leaf Development and Modifies Leaf Shape. *Proc Natl Acad Sci U S A.* **98**: 11812-17.
- Pinon, V., Prasad, K., Grigg, S. P., Sanchez-Perez, G. F. & Scheres, B.** 2013a. Local Auxin Biosynthesis Regulation by Plethora Transcription Factors Controls Phyllotaxis in Arabidopsis. *Proc Natl Acad Sci U S A.* **110**: 1107-12.
- Pinon, V., Prasad, K., Grigg, S. P., Sanchez-Perez, G. F. & Scheres, B.** 2013b. Local Auxin Biosynthesis Regulation by Plethora Transcription Factors Controls Phyllotaxis in Arabidopsis. *Proc. Natl. Acad. Sci. USA.* **110**: 1107-12.

**Planchais, S., Samland, A. K. & Murray, J. A.** 2004. Differential Stability of Arabidopsis D-Type Cyclins: Cycd3;1 Is a Highly Unstable Protein Degraded by a Proteasome-Dependent Mechanism. *Plant J.* **38**: 616-25.

**Prasad, K., Grigg, Stephen p., Barkoulas, M., Yadav, Ram k., Sanchez-Perez, Gabino f., Pinon, V., Blilou, I., Hofhuis, H., Dhonukshe, P., Galinha, C., Mähönen, Ari p., Muller, Wally h., Raman, S., Verkleij, Arie j., Snel, B., Reddy, G. V., Tsiantis, M. & Scheres, B.** 2011. Arabidopsis Plethora Transcription Factors Control Phyllotaxis. *Curr. Biol.* **21**: 1123-28.

**Pysh, L. D., Wysocka-Diller, J. W., Camilleri, C., Bouchez, D. & Benfey, P. N.** 1999. The Gras Gene Family in Arabidopsis: Sequence Characterization and Basic Expression Analysis of the Scarecrow-Like Genes. *Plant J.* **18**: 111-19.

**Ragauskas, A. J., Williams, C. K., Davison, B. H., Britovsek, G., Cairney, J., Eckert, C. A., Frederick, W. J., Jr., Hallett, J. P., Leak, D. J., Liotta, C. L., Mielenz, J. R., Murphy, R., Templer, R. & Tschaplinski, T.** 2006. The Path Forward for Biofuels and Biomaterials. *Science.* **311**: 484-9.

**Raven, P., Evert, R. & Eichhorn, S.** 2005. *Biology of Plants.* Freeman.

**Reinhardt, D., Mandel, T. & Kuhlemeier, C.** 2000a. Auxin Regulates the Initiation and Radial Position of Plant Lateral Organs. *Plant Cell.* **12**: 507-18.

**Reinhardt, D., Mandel, T. & Kuhlemeier, C.** 2000b. Auxin Regulates the Initiation and Radial Position of Plant Lateral Organs. *Plant Cell.* **12**: 507-18.

**Reinhardt, D., Pesce, E. R., Stieger, P., Mandel, T., Baltensperger, K., Bennett, M., Traas, J., Friml, J. & Kuhlemeier, C.** 2003. Regulation of Phyllotaxis by Polar Auxin Transport. *Nature.* **426**: 255-60.

**Ren, M. Z., Venglat, P., Qiu, S. Q., Feng, L., Cao, Y. G., Wang, E., Xiang, D. Q., Wang, J. H., Alexander, D., Chalivendra, S., Logan, D., Mattoo, A., Selvaraj, G. & Datla, R.** 2012. Target of Rapamycin Signaling Regulates Metabolism, Growth, and Life Span in Arabidopsis. *Plant Cell.* **24**: 4850-74.

**Riechmann, J. L. & Meyerowitz, E. M.** 1998. The Ap2/Erbp Family of Plant Transcription Factors. *Biol. Chem.* **379**: 633-46.

**Rigal, A., Yordanov, Y. S., Perrone, I., Karlberg, A., Tisserant, E., Bellini, C., Busov, V. B., Martin, F., Kohler, A., Bhalerao, R. & Legue, V.** 2012. The Aintegumenta Like1 Homeotic Transcription Factor Ptail1 Controls the Formation of Adventitious Root Primordia in Poplar. *Plant Physiol.* **160**: 1996-2006.

**Riou-Khamlichi, C., Huntley, R., Jacqmard, A. & Murray, J. A.** 1999. Cytokinin Activation of Arabidopsis Cell Division through a D-Type Cyclin. *Science.* **283**: 1541-4.

**Rodriguez, R. E., Mecchia, M. A., Debernardi, J. M., Schommer, C., Weigel, D. & Palatnik, J. F.** 2010. Control of Cell Proliferation in Arabidopsis Thaliana by MicroRNA Mir396. *Development.* **137**: 103-12.

**Rossi, V. & Varotto, S.** 2002. Insights into the G1/S Transition in Plants. *Planta*. **215**: 345-56.

**Rueda-Romero, P., Barrero-Sicilia, C., Gómez-Cadenas, A., Carbonero, P. & Oñate-Sánchez, L.** 2012. Arabidopsis Thaliana Dof6 Negatively Affects Germination in Non-after-Ripened Seeds and Interacts with TCP14. *J. Exp. Bot.* **63**: 1937-49.

**Sabatini, S., Heidstra, R., Wildwater, M. & Scheres, B.** 2003. Scarecrow Is Involved in Positioning the Stem Cell Niche in the Arabidopsis Root Meristem. *Genes Dev.* **17**: 354-8.

**Sanchez, C., Vielba, J. M., Ferro, E., Covelo, G., Sole, A., Abarca, D., De Mier, B. S. & Diaz-Sala, C.** 2007. Two Scarecrow-Like Genes Are Induced in Response to Exogenous Auxin in Rooting-Competent Cuttings of Distantly Related Forest Species. *Tree Physiol.* **27**: 1459-70.

**Sanger, F., Nicklen, S. & Coulson, A. R.** 1977. DNA Sequencing with Chain-Terminating Inhibitors. *Proc Natl Acad Sci U S A.* **74**: 5463-7.

**Sankar, M., Nieminen, K., Ragni, L., Xenarios, I. & Hardtke, C. S.** 2014. Automated Quantitative Histology Reveals Vascular Morphodynamics During Arabidopsis Hypocotyl Secondary Growth. *eLife*. **3**.

**Santuari, L., Scacchi, E., Rodriguez-Villalon, A., Salinas, P., Dohmann, Esther m. N., Brunoud, G., Vernoux, T., Smith, Richard s. & Hardtke, Christian s.** 2011. Positional Information by Differential Endocytosis Splits Auxin Response to Drive Arabidopsis Root Meristem Growth. *Curr. Biol.* **21**: 1918-23.

**Sanz, L., Dewitte, W., Forzani, C., Patell, F., Nieuwland, J., Wen, B., Quelhas, P., De Jager, S., Titmus, C., Campilho, A., Ren, H., Estelle, M., Wang, H. & Murray, J. A.** 2011. The Arabidopsis D-Type Cyclin Cycd2;1 and the Inhibitor Ick2/Krp2 Modulate Auxin-Induced Lateral Root Formation. *Plant Cell.* **23**: 641-60.

**Sarojam, R., Sappl, P. G., Goldshmidt, A., Efroni, I., Floyd, S. K., Eshed, Y. & Bowman, J. L.** 2010. Differentiating Arabidopsis Shoots from Leaves by Combined Yabby Activities. *Plant Cell.* **22**: 2113-30.

**Sarvepalli, K. & Nath, U.** 2011. Hyper-Activation of the TCP4 Transcription Factor in Arabidopsis Thaliana Accelerates Multiple Aspects of Plant Maturation. *Plant J.* **67**: 595-607.

**Saul, H., Elharrar, E., Gaash, R., Eliaz, D., Valenci, M., Akua, T., Avramov, M., Frankel, N., Berezin, I., Gottlieb, D., Elazar, M., David-Assael, O., Tcherkas, V., Mizrachi, K. & Shaul, O.** 2009. The Upstream Open Reading Frame of the Arabidopsis Atmhx Gene Has a Strong Impact on Transcript Accumulation through the Nonsense-Mediated Mrna Decay Pathway. *Plant J.* **60**: 1031-42.

**Scanlon, M. J.** 2003. The Polar Auxin Transport Inhibitor N-1-Naphthylphthalamic Acid Disrupts Leaf Initiation, Knox Protein Regulation, and Formation of Leaf Margins in Maize. *Plant Physiol.* **133**: 597-605.

**Scheres, B., Di Laurenzio, L., Willemsen, V., Hauser, M. T., Janmaat, K., Weisbeek, P. & Benfey, P. N.** 1995a. Mutations Affecting the Radial Organisation of the Arabidopsis Root Display Specific Defects Throughout the Embryonic Axis. *Development.* **121**: 53-62.

**Scheres, B., Dilaurenzio, L., Willemsen, V., Hauser, M. T., Janmaat, K., Weisbeek, P. & Benfey, P. N.** 1995b. Mutations Affecting the Radial Organization of the Arabidopsis Root Display Specific Defects Throughout the Embryonic Axis. *Development.* **121**: 53-62.

**Scheres, B., Wolkenfelt, H., Willemsen, V., Terlouw, M., Lawson, E., Dean, C. & Weisbeek, P.** 1994. Embryonic Origin of the Arabidopsis Primary Root and Root-Meristem Initials. *Development.* **120**: 2475-87.

**Schiessl, K., Kausika, S., Southam, P., Bush, M. & Sablowski, R.** 2012. Jagged Controls Growth Anisotropy and Coordination between Cell Size and Cell Cycle During Plant Organogenesis. *Curr. Biol.* **22**: 1739-46.

**Schmulling, T., Werner, T., Riefler, M., Krupkova, E. & Bartrina Y Manns, I.** 2003. Structure and Function of Cytokinin Oxidase/Dehydrogenase Genes of Maize, Rice, Arabidopsis and Other Species. *J. Plant Res.* **116**: 241-52.

**Schneider, B. L., Yang, Q. H. & Futcher, A. B.** 1996. Linkage of Replication to Start by the Cdk Inhibitor Sic1. *Science.* **272**: 560-2.

**Schnittger, A., Schobinger, U., Bouyer, D., Weinl, C., Stierhof, Y. D. & Hulskamp, M.** 2002. Ectopic D-Type Cyclin Expression Induces Not Only DNA Replication but Also Cell Division in Arabidopsis Trichomes. *Proc Natl Acad Sci U S A.* **99**: 6410-5.

**Schnittger, A., Weinl, C., Bouyer, D., Schobinger, U. & Hulskamp, M.** 2003a. Misexpression of the Cyclin-Dependent Kinase Inhibitor Ick1/Krp1 in Single-Celled Arabidopsis Trichomes Reduces Endoreduplication and Cell Size and Induces Cell Death. *Plant Cell.* **15**: 303-15.

**Schnittger, A., Weinl, C., Bouyer, D., Schöbinger, U. & Hülkamp, M.** 2003b. Misexpression of the Cyclin-Dependent Kinase Inhibitor Ick1/Krp1 in Single-Celled Arabidopsis Trichomes Reduces Endoreduplication and Cell Size and Induces Cell Death. *Plant Cell.* **15**: 303-15.

**Schoof, H., Lenhard, M., Haecker, A., Mayer, K. F., Jurgens, G. & Laux, T.** 2000. The Stem Cell Population of Arabidopsis Shoot Meristems is Maintained by a Regulatory Loop between the Clavata and Wuschel Genes. *Cell.* **100**: 635-44.

**Schrader, J., Nilsson, J., Mellerowicz, E., Berglund, A., Nilsson, P., Hertzberg, M. & Sandberg, G.** 2004. A High-Resolution Transcript Profile across

the Wood-Forming Meristem of Poplar Identifies Potential Regulators of Cambial Stem Cell Identity. *Plant Cell*. **16**: 2278-92.

**Schruff, M. C., Spielman, M., Tiwari, S., Adams, S., Fenby, N. & Scott, R. J.** 2006a. The Auxin Response Factor 2 Gene of Arabidopsis Links Auxin Signalling, Cell Division, and the Size of Seeds and Other Organs. *Development*. **133**: 251-61.

**Schruff, M. C., Spielman, M., Tiwari, S., Adams, S., Fenby, N. & Scott, R. J.** 2006b. The Auxin Response Factor 2 Gene of Arabidopsis Links Auxin Signalling, Cell Division, and the Size of Seeds and Other Organs. *Development*. **133**: 251-61.

**Schuppler, U., He, P. H., John, P. C. L. & Munns, R.** 1998. Effect of Water Stress on Cell Division and Cdc2-Like Cell Cycle Kinase Activity in Wheat Leaves (Vol 117, Pg 667, 1998). *Plant Physiol*. **117**: 1528-28.

**Scofield, S., Dewitte, W., Nieuwland, J. & Murray, J. A.** 2013. The Arabidopsis Homeobox Gene Shoot Meristemless Has Cellular and Meristem-Organisational Roles with Differential Requirements for Cytokinin and Cycd3 Activity. *Plant J*. **75**: 53-66.

**Sehr, E. M., Agusti, J., Lehner, R., Farmer, E. E., Schwarz, M. & Greb, T.** 2010. Analysis of Secondary Growth in the Arabidopsis Shoot Reveals a Positive Role of Jasmonate Signalling in Cambium Formation. *Plant J*. **63**: 811-22.

**Shen, Q., Wang, Y.-T., Tian, H. & Guo, F.-Q.** 2012. Nitric Oxide Mediates Cytokinin Functions in Cell Proliferation and Meristem Maintenance in Arabidopsis. *Mol Plant*.

**Shen, W. H.** 2002. The Plant E2f-Rb Pathway and Epigenetic Control. *Trends Plant Sci*. **7**: 505-11.

**Shibaoka, H.** 1994. Plant Hormone-Induced Changes in the Orientation of Cortical Microtubules - Alterations in the Cross-Linking between Microtubules and the Plasma-Membrane. *Annu. Rev. Plant Physiol. Plant Mol. Biol.* **45**: 527-44.

**Shigyo, M. & Ito, M.** 2004. Analysis of Gymnosperm Two-Ap2-Domain-Containing Genes. *Dev. Genes Evol.* **214**: 105-14.

**Shpak, E. D., McCabe, J. M., Pillitteri, L. J. & Torii, K. U.** 2005. Stomatal Patterning and Differentiation by Synergistic Interactions of Receptor Kinases. *Science*. **309**: 290-3.

**Sloan, J., Backhaus, A., Malinowski, R., Mcqueen-Mason, S. & Fleming, A. J.** 2009. Phased Control of Expansin Activity During Leaf Development Identifies a Sensitivity Window for Expansin-Mediated Induction of Leaf Growth. *Plant Physiol*. **151**: 1844-54.

**Smyth, D. R., Bowman, J. L. & Meyerowitz, E. M.** 1990. Early Flower Development in Arabidopsis. *Plant Cell*. **2**: 755-67.

- Sorrell, D. A., Marchbank, A., McMahon, K., Dickinson, J. R., Rogers, H. J. & Francis, D.** 2002. A Wee1 Homologue from *Arabidopsis thaliana*. *Planta*. **215**: 518-22.
- Spicer, R. & Groover, A.** 2010. Evolution of Development of Vascular Cambia and Secondary Growth. *New Phytol.* **186**: 577-92.
- Spichal, L., Rakova, N. Y., Riefler, M., Mizuno, T., Romanov, G. A., Strnad, M. & Schmulling, T.** 2004. Two Cytokinin Receptors of *Arabidopsis thaliana*, Cre1/Ahk4 and Ahk3, Differ in Their Ligand Specificity in a Bacterial Assay. *Plant Cell Physiol.* **45**: 1299-305.
- Stahle, M. I., Kuehlich, J., Staron, L., Von Arnim, A. G. & Golz, J. F.** 2009. Yabys and the Transcriptional Corepressors Leunig and Leunig\_Homolog Maintain Leaf Polarity and Meristem Activity in *Arabidopsis*. *Plant Cell*. **21**: 3105-18.
- Stern, B. & Nurse, P.** 1996. A Quantitative Model for the Cdc2 Control of S Phase and Mitosis in Fission Yeast. *Trends Genet.* **12**: 345-50.
- Strausfeld, U. P., Howell, M., Descombes, P., Chevalier, S., Rempel, R. E., Adamczewski, J., Maller, J. L., Hunt, T. & Blow, J. J.** 1996. Both Cyclin a and Cyclin E Have S-Phase Promoting (Spf) Activity in *Xenopus* Egg Extracts. *J. Cell Sci.* **109** ( Pt 6): 1555-63.
- Suer, S., Agusti, J., Sanchez, P., Schwarz, M. & Greb, T.** 2011. Wox4 Imparts Auxin Responsiveness to Cambium Cells in *Arabidopsis*. *Plant Cell*. **23**: 3247-59.
- Sugimoto-Shirasu, K. & Roberts, K.** 2003. "Big It Up": Endoreduplication and Cell-Size Control in Plants. *Curr. Opin. Plant Biol.* **6**: 544-53.
- Sugiyama, S. I.** 2005. Polyploidy and Cellular Mechanisms Changing Leaf Size: Comparison of Diploid and Autotetraploid Populations in Two Species of *Lolium*. *Ann. Bot.* **96**: 931-38.
- Suzuki, T., Miwa, K., Ishikawa, K., Yamada, H., Aiba, H. & Mizuno, T.** 2001a. The *Arabidopsis* Sensor His-Kinase, Ahk4, Can Respond to Cytokinins. *Plant Cell Physiol.* **42**: 107-13.
- Suzuki, T., Miwa, K., Ishikawa, K., Yamada, H., Aiba, H. & Mizuno, T.** 2001b. The *Arabidopsis* Sensor His-Kinase, Ahk4, Can Respond to Cytokinins. *Plant Cell Physiol.* **42**: 107-13.
- Szekeress, M., Nemeth, K., Koncz-Kalman, Z., Mathur, J., Kauschmann, A., Altmann, T., Redei, G. P., Nagy, F., Schell, J. & Koncz, C.** 1996. Brassinosteroids Rescue the Deficiency of Cyp90, a Cytochrome P450, Controlling Cell Elongation and De-Etiolation in *Arabidopsis*. *Cell*. **85**: 171-82.
- Taiz, L. & Zeiger, E.** 2006. *Plant Physiology*. Sinauer Associates, Inc., Publishers.

- Takeda, T., Amano, K., Ohto, M. A., Nakamura, K., Sato, S., Kato, T., Tabata, S. & Ueguchi, C.** 2006. Rna Interference of the Arabidopsis Putative Transcription Factor TCP16 Gene Results in Abortion of Early Pollen Development. *Plant Mol. Biol.* **61**: 165-77.
- Tatematsu, K., Nakabayashi, K., Kamiya, Y. & Nambara, E.** 2008. Transcription Factor AtTCP14 Regulates Embryonic Growth Potential During Seed Germination in Arabidopsis Thaliana. *Plant J.* **53**: 42-52.
- Taylor, N. G., Gardiner, J. C., Whiteman, R. & Turner, S. R.** 2004. Cellulose Synthesis in the Arabidopsis Secondary Cell Wall. *Cellulose.* **11**: 329-38.
- Teale, W. D., Paponov, I. A. & Palme, K.** 2006. Auxin in Action: Signalling, Transport and the Control of Plant Growth and Development. *Nat. Rev. Mol. Cell Biol.* **7**: 847-59.
- Tisne, S., Barbier, F. & Granier, C.** 2011. The Erecta Gene Controls Spatial and Temporal Patterns of Epidermal Cell Number and Size in Successive Developing Leaves of Arabidopsis Thaliana. *Ann Bot.* **108**: 159-68.
- Tixier, A., Cochard, H., Badel, E., Dusotoit-Coucaud, A., Jansen, S. & Herbette, S.** 2013. Arabidopsis Thaliana as a Model Species for Xylem Hydraulics: Does Size Matter? *J. Exp. Bot.* **64**: 2295-305.
- To, J. P. C., Deruère, J., Maxwell, B. B., Morris, V. F., Hutchison, C. E., Ferreira, F. J., Schaller, G. E. & Kieber, J. J.** 2007. Cytokinin Regulates Type-a Arabidopsis Response Regulator Activity and Protein Stability Via Two-Component Phosphorelay. *Plant Cell.* **19**: 3901-14.
- Tomlinson, P. B.** 2006. The Uniqueness of Palms. *Bot. J. Linn. Soc.* **151**: 5-14.
- Torii, K. U., Mitsukawa, N., Oosumi, T., Matsuura, Y., Yokoyama, R., Whittier, R. F. & Komeda, Y.** 1996. The Arabidopsis Erecta Gene Encodes a Putative Receptor Protein Kinase with Extracellular Leucine-Rich Repeats. *Plant Cell.* **8**: 735-46.
- Tran, M., Schultz, C. & Baumann, U.** 2008. Conserved Upstream Open Reading Frames in Higher Plants. *BMC Genomics.* **9**: 361.
- Tsukaya, H.** 2008. Controlling Size in Multicellular Organs: Focus on the Leaf. *PLoS Biol.* **6**: e174.
- Tuominen, H., Puech, L., Fink, S. & Sundberg, B.** 1997. A Radial Concentration Gradient of Indole-3-Acetic Acid Is Related to Secondary Xylem Development in Hybrid Aspen. *Plant Physiol.* **115**: 577-85.
- Turgeon, R. & Wolf, S.** 2009. Phloem Transport: Cellular Pathways and Molecular Trafficking. *Annu. Rev. Plant Biol.* **60**: 207-21.
- Tyers, M.** 1996. The Cyclin-Dependent Kinase Inhibitor P40<sup>sic1</sup> Imposes the Requirement for Cln G1 Cyclin Function at Start. *Proc. Natl. Acad. Sci. USA.* **93**: 7772-6.

- Uchida, N., Lee, J. S., Horst, R. J., Lai, H. H., Kajita, R., Kakimoto, T., Tasaka, M. & Torii, K. U.** 2012a. Regulation of Inflorescence Architecture by Intertissue Layer Ligand-Receptor Communication between Endodermis and Phloem. *Proc Natl Acad Sci U S A.* **109**: 6337-42.
- Uchida, N., Shimada, M. & Tasaka, M.** 2012b. Modulation of the Balance between Stem Cell Proliferation and Consumption by Erecta-Family Genes. *Plant Signal Behav.* **7**: 1506-8.
- Uchida, N., Shimada, M. & Tasaka, M.** 2013. Erecta-Family Receptor Kinases Regulate Stem Cell Homeostasis Via Buffering Its Cytokinin Responsiveness in the Shoot Apical Meristem. *Plant Cell Physiol.* **54**: 343-51.
- Uchida, N. & Tasaka, M.** 2013. Regulation of Plant Vascular Stem Cells by Endodermis-Derived Epfl-Family Peptide Hormones and Phloem-Expressed Erecta-Family Receptor Kinases. *J. Exp. Bot.* **64**: 5335-43.
- Ueguchi, C., Koizumi, H., Suzuki, T. & Mizuno, T.** 2001. Novel Family of Sensor Histidine Kinase Genes in Arabidopsis Thaliana. *Plant Cell Physiol.* **42**: 231-5.
- Uggla, C., Moritz, T., Sandberg, G. & Sundberg, B.** 1996. Auxin as a Positional Signal in Pattern Formation in Plants. *Proc. Natl. Acad. Sci. USA.* **93**: 9282-86.
- Ursache, R., Nieminen, K. & Helariutta, Y.** 2013. Genetic and Hormonal Regulation of Cambial Development. *Physiol. Plant.* **147**: 36-45.
- Vahala, T., Oxelman, B. & Von Arnold, S.** 2001. Two Apetala2-Like Genes of Picea Abies Are Differentially Expressed During Development. *J. Exp. Bot.* **52**: 1111-5.
- Van Berkel, K., De Boer, R. J., Scheres, B. & Ten Tusscher, K.** 2013. Polar Auxin Transport: Models and Mechanisms. *Development.* **140**: 2253-68.
- Van Den Berg, C., Willemsen, V., Hage, W., Weisbeek, P. & Scheres, B.** 1995. Cell Fate in the Arabidopsis Root Meristem Determined by Directional Signalling. *Nature.* **378**: 62-5.
- Van Den Berg, C., Willemsen, V., Hendriks, G., Weisbeek, P. & Scheres, B.** 1997. Short-Range Control of Cell Differentiation in the Arabidopsis Root Meristem. *Nature.* **390**: 287-9.
- Van Zanten, M., Snoek, L. B., Proveniers, M. C. & Peeters, A. J.** 2009. The Many Functions of Erecta. *Trends Plant Sci.* **14**: 214-8.
- Verbelen, J. P., De Cnodder, T., Le, J., Vissenberg, K. & Baluska, F.** 2006. The Root Apex of Arabidopsis Thaliana Consists of Four Distinct Zones of Growth Activities: Meristematic Zone, Transition Zone, Fast Elongation Zone and Growth Terminating Zone. *Plant Signal Behav.* **1**: 296-304.

**Vergani, P., Morandini, P. & Soave, C.** 1997. Complementation of a Yeast Delta Pkc1 Mutant by the Arabidopsis Proteinant. *FEBS Lett.* **400**: 243-6.

**Vernoux, T., Brunoud, G., Farcot, E., Morin, V., Van Den Daele, H., Legrand, J., Oliva, M., Das, P., Larrieu, A., Wells, D., Guedon, Y., Armitage, L., Picard, F., Guyomarc'h, S., Cellier, C., Parry, G., Koumproglou, R., Doonan, J. H., Estelle, M., Godin, C., Kepinski, S., Bennett, M., De Veylder, L. & Traas, J.** 2011. The Auxin Signalling Network Translates Dynamic Input into Robust Patterning at the Shoot Apex. *Mol. Syst. Biol.* **7**: 508.

**Weintraub, S. J., Prater, C. A. & Dean, D. C.** 1992. Retinoblastoma Protein Switches the E2f Site from Positive to Negative Element. *Nature.* **358**: 259-61.

**Werner, T., Motyka, V., Strnad, M. & Schmulling, T.** 2001. Regulation of Plant Growth by Cytokinin. *Proc. Natl. Acad. Sci. USA.* **98**: 10487-92.

**Werner, T. & Schmülling, T.** 2009. Cytokinin Action in Plant Development. *Curr. Opin. Plant Biol.* **12**: 527-38.

**White, D. W. R.** 2006. Peapod Regulates Lamina Size and Curvature in Arabidopsis. *Proc. Natl. Acad. Sci. USA.* **103**: 13238-43.

**Wijnker, E. & Schnittger, A.** 2013. Control of the Meiotic Cell Division Program in Plants. *Plant Reproduction.* **26**: 143-58.

**Woo, H. R., Kim, J. H., Kim, J., Lee, U., Song, I. J., Lee, H. Y., Nam, H. G. & Lim, P. O.** 2010. The Rav1 Transcription Factor Positively Regulates Leaf Senescence in Arabidopsis. *J. Exp. Bot.* **61**: 3947-57.

**Wright, S. P.** 1992. Adjusted P-Values for Simultaneous Inference. *Biometrics.* **48**: 1005-13.

**Yamada, H., Suzuki, T., Terada, K., Takei, K., Ishikawa, K., Miwa, K., Yamashino, T. & Mizuno, T.** 2001. The Arabidopsis Ahk4 Histidine Kinase Is a Cytokinin-Binding Receptor That Transduces Cytokinin Signals across the Membrane. *Plant Cell Physiol.* **42**: 1017-23.

**Yanofsky, M. F., Ma, H., Bowman, J. L., Drews, G. N., Feldmann, K. A. & Meyerowitz, E. M.** 1990. The Protein Encoded by the Arabidopsis Homeotic Gene Agamous Resembles Transcription Factors. *Nature.* **346**: 35-9.

**Yokoyama, A., Yamashino, T., Amano, Y., Tajima, Y., Imamura, A., Sakakibara, H. & Mizuno, T.** 2007. Type-B Arr Transcription Factors, Arr10 and Arr12, Are Implicated in Cytokinin-Mediated Regulation of Protoxylem Differentiation in Roots of Arabidopsis Thaliana. *Plant Cell Physiol.* **48**: 84-96.

**Zhang, J., Elo, A. & Helariutta, Y.** 2011a. Arabidopsis as a Model for Wood Formation. *Curr. Opin. Biotechnol.* **22**: 293-9.

**Zhang, J., Gao, G., Chen, J. J., Taylor, G., Cui, K. M. & He, X. Q.** 2011b. Molecular Features of Secondary Vascular Tissue Regeneration after Bark Girdling in Populus. *New Phytol.* **192**: 869-84.

**Zhang, Z. L., Ogawa, M., Fleet, C. M., Zentella, R., Hu, J., Heo, J. O., Lim, J., Kamiya, Y., Yamaguchi, S. & Sun, T. P.** 2011c. Scarecrow-Like 3 Promotes Gibberellin Signaling by Antagonizing Master Growth Repressor Della in Arabidopsis. *Proc Natl Acad Sci U S A.* **108**: 2160-5.

**Zhao, X., Harashima, H., Dissmeyer, N., Pusch, S., Weimer, A. K., Bramsiepe, J., Bouyer, D., Rademacher, S., Nowack, M. K., Novak, B., Sprunck, S. & Schnittger, A.** 2012. A General G1/S-Phase Cell-Cycle Control Module in the Flowering Plant Arabidopsis Thaliana. *PLoS Genet.* **8**: e1002847.

**Zhou, J., Wang, X. & Lee, J. Y.** 2013. Cell-to-Cell Movement of Two Interacting at-Hook Factors in Arabidopsis Root Vascular Tissue Patterning. *Plant Cell.* **25**: 187-201.